Gene Therapy Approaches to Disease of the Cornea and Anterior Chamber

Mark David Anthony Basche

A thesis submitted for the degree of

Doctor of Philosophy (PhD)

2014

Department of Genetics

Institute of Ophthalmology

University College London

Declaration

I, Mark David Antony Basche confirm that the work presented in this thesis is my own. Where information has been derived from other sources, I confirm that this has been indicated in the thesis.

..... Date: .....

Mr Mark Basche. BSc

Abstract

The field of ocular gene therapy has become one of the most developed areas within the wider gene therapy field, however most work to date has focused upon the retina with the cornea, by comparison, having seen relatively little application of gene therapy.

This thesis describes a program of work to further develop viral gene therapy approaches to the three cellular layers of the cornea, with particular emphasis upon the application of novel vector technologies and overcoming the various challenges presented by each layer.

Gene therapy of the corneal endothelium has to date largely aimed to increase or maintain endothelial cell density to improve the quality of donor corneas for engraftment. Such a strategy however carries an inherent risk of oncogenesis and this study has therefore aimed to improve the safety profile of endothelial gene delivery methods.

The transduction profile of various AAV serotypes within the corneal stroma was also investigated, and the most promising results applied in an augmentation gene therapy approach to prevent corneal neovascularisation. The selected methodology is shown to mediate high level transgene expression and, when delivering the antiangiogenic factor sFlt1, was highly effective in preventing haem (but not lymph) angiogenesis in a murine model of induced corneal neovascularisation.

If long term gene delivery to the corneal epithelium is to be achieved it must be targeted to the limbal epithelial stem cells (LESCs) responsible for the continuous regeneration of the layer. This study has convincingly demonstrated gene delivery to these cells *in vivo* for the first time, with the methodology developed leading to a lasting transgene expression throughout the LESC daughter cell lineages that comprise the epithelium. In addition to potential application in the treatment of congenital epithelial dystrophies this technique may also provide new insights into LESC biology and the cellular dynamics of epithelial renewal.

Table of Contents

List of Figures and Tables

Acknowledgments

Firstly I would like to thank my supervisors, Professor Robin Ali for giving me the opportunity to undertake this PhD and for supporting me throughout my time working within his lab, and Mr Frank Larkin for his regular input from a more clinical perspective.

I was fortunate enough to undertake this work within a lab possessing a strong spirit of mutual support and co-operation and thus I have received assistance of some form or another from almost every member of the group at some point, so thank you all! However there are also a number of individuals who deserve particular recognition:

Firstly Sander Smith, the lynch pin upon which all of us rely for his almost daily support, advice, assistance and patience, the go-to guy for almost anything! Secondly Ulrich Luhmann for always being there (at almost any hour!) to provide further advice, support and direction.

Also, Scott Robbie who work closely with me upon the corneal neovascularisation study, and of whose surgical skills I took ample advantage, and Daniel Kampik for his solidarity and support as the only other member of the two man cornea sub-group within a retina obsessed lab! Lastly Dr Satoshi Kawasaki with whom we began a collaboration to look into the possibility of transducing LESCs *in vivo*, work which generated some excellent and exciting results.

Most importantly however I would like to thank the one person without whom I would not be where I am today, and whose continuous love, support and belief in me was invaluable in helping me make it through the trials and tribulations of this PhD, the love of my life, my partner Clare who I'm ecstatic to say became my wife during the course of this PhD.

Finally I would like to dedicate this work to my father, Mr Clive Basche who sadly passed away in 2012. Thanks for everything Dad, and I'm sure you'd be proud of what I've achieved here.

1. Introduction

1.1 The Cornea - Overview

The Cornea is a domed, multi-layered, structure located at the front of the eye that in combination with the sclera forms the outer “shell” of the eyeball. Due to this shared structural role both the cornea and sclera are primarily composed of dense interwoven fibrous collagen providing strength and rigidity, beyond this however the two tissues have little in common. The primary functions of the cornea are optical; firstly it forms the transparent outer “window” through which light can enter the eye and secondly it acts as the eye’s primary refractive tissue accounting for approximately two thirds of the eye’s total optical power (43/60 dioptres). Maintenance of the optimal optical properties of the cornea required for vision requires fine regulation of thickness, structure and hydration of the cornea all of which are mediated by the cells of the cornea.

The cornea is one of the most densely innervated tissues in the body (3-600x more so than skin) [1,2] with the majority of these neurons being sensory. This is due in part to the requirement of maintaining high sensitivity of the corneal (or blink) reflex which keeps the eye moist and protects it from damage.

The cornea is also one of the relatively few completely avascular tissues in the body, with most somatic cells never being more than 200µm from the blood supply. The cells of the cornea therefore do not rely heavily upon the circulation to provide their metabolites, but instead chiefly rely upon diffusion or active transport from adjacent sources. Glucose and other nutrients are provided from the aqueous humour and the majority of the tissue’s oxygen derives from the atmosphere via the tear film. Direct exposure of the tear film to atmospheric oxygen is therefore vital to maintain adequate oxygenation of the cornea and any impairment of free diffusion (for example by prolonged contact lens wear) may lead to corneal hypoxia and associated pathology.

Structurally the cornea is composed of five layers, three of them cellular: the epithelium, stroma and endothelium; and two forming basement membranes that separate the cellular layers from one another: Bowman’s Layer and Descemet’s Membrane. The work presented in this thesis is focused upon the transduction of the corneal cells by gene therapy viral vectors so this introduction will focus upon the cellular layers of the tissue, the various features of which will be further expounded in the subsections that follow.

1.2 The Corneal Endothelium

The endothelium is the most posterior of the corneal layers and consists of a monolayer of squamous endothelial cells packed into a regular hexagonal array covering the cornea's entire rear surface. The cells of the endothelium are tightly adhered to one another via apically located tight junctions / gap junctions and are separated from the stroma by Descemet's membrane to which they adhere via hemidesmosomes. Descemet's is an exceptionally thick (5-10μM) basement membrane which is secreted by the endothelium [3]. In common with the keratocytes of the stroma corneal endothelial cells are derived from the neural crest cells located at the periphery of the presumptive cornea, this is in contrast to the majority of the body's endothelial cells (such as vascular endothelium or endocardium) which derive from the mesoderm. The corneal endothelium therefore displays none of the cell surface markers that typify other endothelial cells.

The primary function of the endothelium is in the control of corneal hydration and nutrition [4]. With the exception of oxygen which enters the cornea via multiple routes the vast majority of the corneas nutrients are derived from the aqueous humour and therefore must pass through the endothelium [5]. For example the glucose transporter GLUT1 is expressed on both the apical and basal sides of endothelial cells to allow transcellular glucose flow [6]. Hydration of the stroma is controlled via the so called "Pump–Leak" mechanism and is vital to maintain the fine ultrastructure of the stoma required for transparency. The pump side of this mechanism is an active, ATP dependent process that results in the generation of a net efflux of $NaHCO_3^-$ and/or NaCl from the cornea into the aqueous humour; this ion flux constitutes the osmotic driving force for water movement out of the stroma. The exact mechanism of the pump however is highly complex, involving the regulation of ion / fluid flow by many different ion transporters / channels as well as other processes, and the pump function's precise molecular nature remains only partially understood (Reviewed in [7]). The leak side of the mechanism merely refers to fluid re-entry into the cornea via passive mechanisms. In balance these two forces act to maintain corneal hydration at approximately ~78% in humans.

A key feature of the human endothelial cells that is of considerable clinical relevance is that they only very rarely undergo mitotic division in a normal eye after foetal development [8], they are thus largely considered to be completely non-replicative. Endothelial cells however have not left the cell cycle via entry in G_0; analysis of the expression and subcellular localisation of various cell cycle proteins regulating G_1/S phase transition indicates that endothelial cells exist in a state of early G_1 growth arrest [9]. Endothelial cells can thus be

induced to replicate when cultured *in vitro* isolated from the monolayer and stimulated with mitogens [10,11], many of which are also present in the aqueous humour *in vivo* [12]. This might imply that endothelial proliferation *in vivo* might be primarily suppressed by the presence of a strong contact inhibition effect [13]. Indeed in the context of an intact monolayer *ex vivo* it has been shown that EDTA can promote endothelial cell division by the loosening of cell / cell contacts [14].

One emerging means by which the endothelial proliferation has been effectively induced *in vivo* is by the application of small molecule Rho-kinase (ROCK) inhibitors [15]. It has been proposed by the authors that these act upon the cell cycle directly but it is equally possible that they mediate their effects via contact inhibition, as Rho-kinase activity is also intimately linked to the maintenance of cell contacts such as tight junctions [16].

1.2.1 Endothelial cell density

The non-proliferative natural state of the endothelium is of particular concern as endothelial cell density is known to gradually decrease throughout adult life with an average rate of cell loss of 0.3 to 0.6 % per year [17,18]. Once lost, cells are not replaced by cell replication and loss must be compensated for by enlargement and spreading of the remaining cells. The human endothelium begins with sufficient cells so that despite this loss endothelial function is usually maintained for life [19,20]. Various abnormal conditions however can cause endothelial cell density to fall to a level where the function of the endothelium is compromised and corneal decompensation invariably occurs when the cell density drops below 300 to 500 cells/mm^2, leading to loss of vision and eventual blindness [21,22]. The only available treatment for endothelial decompensation is corneal transplantation. This key role of endothelial cell density to corneal function has led to the development of two forms of partial thickness corneal transplant; Descemet's stripping / membrane endothelial keratoplasty, (DSEK / DMEK) that aim to replace only the endothelium whilst leaving the majority of the host cornea in place.

Several genetic dystrophies can lead to endothelial decompensation of which Fuchs' endothelial dystrophy is the most common [23,24]. A far more common cause of decompensation however is mechanical trauma to the endothelium. Corneal transplantation (keratoplasty) itself is invariably accompanied by endothelial cell loss [22] and late endothelial failure (LEF) is the primary cause of graft failure within 5 years of surgery and accounts for over 90% of the failures between 5 and 10 years after keratoplasty [25,26]. A repeat keratoplasty with similar or worse prognosis is the only treatment for a failed graft.

Grafts that eventually fail due to low endothelial cell density do not appear to suffer a greater rate of endothelial cell loss than grafts that do not fail, but rather have fewer endothelial cells pre transplantation [22]. In theory therefore it may be possible to prevent or delay graft failure by increasing the number of endothelial cells in donor tissue pre-transplantation.

1.3 The Corneal Stroma

The corneal stroma is the middle of the three cellular layers of the cornea separated from the endothelium by Descemet's membrane and from the epithelium by Bowman's layer. The stroma is the most substantial layer of the cornea comprising around 80-85% of total corneal thickness in humans. The stroma's primary functions are structural and thus around 90% of the layer by volume consists of extracellular matrix (ECM) largely in the form of collagen fibres. Unlike other such structural collagenous tissues however the cornea is required to be transparent and this unique property results from a precise organisation of the collagen fibres and other ECM components. The collagen within the stroma is formed into very small fibrils (25–30 nm diameter) packed tightly into a regular array and formed into 300-500 layers termed lamellae. The individual collagen fibrils are composed of both type I and V collagen in the adult with each fibril being heterotypic and thus containing both types. Type V collagen has been shown to have key roles in the initiation of fibril assembly and regulation of their diameter [27,28].

In addition to the collagenous component the adult stromal ECM also contains four proteoglycans: decorin, keratocan, lumican and mimecan. All these proteoglycans have a very similar (possibly homologous) core protein component of approximately the same size. All contain leucine rich motifs spaced at regular intervals which upon folding of the proteins into their the final coiled 3D conformations leads to the alignment of these motifs down one side of the molecule [29]. By contrast most of the asparagine residues that form the attachment sites for glycosaminoglycan side chains are located on the other side of the molecule and it is thought these highly polarised proteins act to regulate the spacing and formation of the collagen fibrils [30].

The glycosaminoglycan side chains of corneal proteoglycans primarily consist of keratan sulphate although dermatan sulphate is also present; these side chains are thought to play a role in regulating corneal hydration. It is vital that the stroma is kept in state of relative dehydration in order to maintain the precise ECM structure required for transparency. The hydration of the cornea is primarily regulated by actions of the epithelium and endothelium;

however, it has been shown that whilst dermatan sulphate is almost fully hydrated in the normal cornea keratan sulphate is not, leading to the hypothesis that the remaining hydration capacity of keratan sulphate forms a dynamic buffer for corneal hydration [31].

The stroma's primary cell population consists of corneal keratocytes which occupy ~3% of the stroma by volume. Developmentally these cells derive from the embryonic neural crest. and their primary role is the synthesis and maintenance of the stromal ECM [32]. Morphologically corneal keratocytes are broad and flattened with numerous lamellapodia through which they connect to one another via gap junctions creating a cellular network [33]. Additionally this compact morphology combined a minimal number of organelles and the fact that corneal keratocytes express crystallines all act to minimise any light scattering by these cells [34], aiding transparency. Other cell types present within the stroma include resident macrophage and dendritic cell populations [35] and a very small population of "corneal stromal stem cells" localised to the limbal stroma which may act a source of keratocytes for repopulation if cells are lost [36]. Unless the cornea is wounded, mammalian corneal keratocytes will remain quiescent throughout adulthood [37].

1.3.1 Wound healing response of the stroma

Corneal wound healing within the stroma is largely mediated through the predominant cell population: the corneal keratocytes. Broadly these cells respond to injury in one of two ways, they either undergo apoptosis or transition to various activated repair phenotypes [37]. The first response to corneal wounding is rapid apoptosis of the keratocytes immediately underlying or adjacent to the wound site, with the majority of cell loss occurring within hours of wounding [38]. There is some evidence the keratocytes undergo apoptosis in response to secreted signals from the overlying epithelium such as Interleukin 1 (IL1) and tumour necrosis factor alpha (TNFα) which mediate apoptosis via induction of Fas ligand production within keratocytes [39]. However this finding has not been replicated in cultured cells *in vitro* and thus the exact causative mechanism remains somewhat unclear [37]. The apoptotic response is variable in degree depending upon the severity of the inflicted wound and species differences. The response can be extremely sensitive and can be triggered by even very mild epithelial damage [40].

Following and triggered by this cell loss, keratocytes adjacent to the wounded area lose their quiescence and begin the process of switching to a more fibroblast-like repair phenotype, the initial steps in this process such as increase in nucleoli number (a sign of increased bio-synthetic activity) are observable ~6 hours after injury. These activated cells begin to express α5β1 integrin which in combination with fibronectin deposition at the wound site

enables their migration towards the wound [32]. Keratocytes also proliferate in response to injury as shown by Zieske et al. [41] who followed the time course of keratocyte proliferation following a limited epithelial debridement wound by tracking the cell cycle progression marker Ki67. Proliferation was first detectable 24 hours after wounding and was largely restricted to the posterior stroma close to the area of wounding, the number of Ki67 positive cells then increased, peaking at 44 hours post wound, and remaining localised to the areas immediately adjacent or posterior to the wound. No proliferating cells were observed in the anterior stroma until 5 days after wounding and from this point onwards the overall number declined until by day 10 the stroma appeared to have regained quiescence.

Keratocytes also display a second repair phenotype in response to wounding being able to reversibly transdifferentiate into myofibroblast-like cells in response to signalling via transforming growth factor beta (TGFβ) [42]. These cells are characterised by a larger size and expression of smooth muscle actin and it is thought these myofibroblasts contribute to healing process by mediating wound contraction [43] and the reorganisation and deposition of stromal ECM. In excess however this process has been shown to be pathogenic with extensive myofibroblast differentiation in response to surgical injury being associated with loss of corneal transparency and scarring [44]. It was discovered relatively recently however that keratocytes are not the only source of myofibroblasts in the context of stromal wound healing. In common with the myofibroblasts of many other tissue types they are also formed from bone marrow derived cells which have been shown to infiltrate the cornea in large numbers upon wounding [45].

1.4 The Corneal Epithelium

The epithelium is the outermost layer of the cornea and thus forms the most anterior surface of the eye. As might be expected from this location one of the primary functions of the epithelium is that of a barrier protecting the cornea from infiltration by tears (or other fluid) and pathogenic material [46,47]. This barrier function is mediated by the formation and maintenance of multiple tight junctions between epithelial cells. A healthy epithelium is also vital to maintain the optical properties of the cornea. In combination and with the tear film it provides a smooth outer surface to the cornea minimising light scatter, and by preventing fluid infiltration the epithelium also functions to keep the stroma dehydrated and transparent [48,49].

The cells of the epithelium are broadly organised into 5-7 layers; a basal monolayer of columnar cells adhered tightly to the underlying basement membrane via hemidesmosomes, and several layers of supra-basal cells [47,50,51]. The cells within the supra-basal layers closest to the basal layer are termed wing cells due to their alar cross-sectional shape, and the cells of more apical layers become increasingly more differentiated, larger, flatter and more tightly adhered to one another. These are usually referred to as superficial or squamous cells.

1.4.1 Limbal Epithelial Stem Cells (LESCs)

Unlike the other two cellular layers of the cornea the cells of the epithelium are actively replicative due to the tissue as a whole suffering continuous cellular attrition in the form of desquamation from the corneal surface and thus requiring constant renewal and regeneration. Whilst the cells of the basal layer have long been known to be mitotic, this activity alone is insufficient to maintain the layer [52]. An extrinsic source of new epithelial cells must therefore exist and for many years it was thought that the conjunctiva fulfilled this role, generating new corneal epithelial cells by the transdifferentiation of conjunctival epithelial cells which migrated into the cornea [53,54]. This was largely based upon studies of corneal injury in which both the involvement of the conjunctiva and epithelial renewal apparently proceeding from the direction of the corneal periphery inward [55] was observed. This hypothesis however could not fully explain clinical observations of failed epithelial healing in which the layer became conjunctivalised due to the ingrowth of untransdifferentiated conjunctival epithelial cells.

The alternative explanation of epithelial renewal proceeding from the limbal epithelium itself was first proposed by Davanger & Evensen in 1971 [56] and gained substantial support

when it was shown by Schermer et al. in 1986 [57] that the corneal specific keratin K3 was not expressed in the most basal limbal cells of the epithelium in contrast to the rest of the tissue in which this protein is highly expressed. It was also demonstrated that this specific keratin was one of the earliest to be expressed during the process of epithelial cell maturation thus indicating that the cells resident in the basal limbus were maintained in a less differentiated state than the majority of the cornea. These cells were therefore suggested to be *"Corneal epithelial stem cells"*, and subsequently became known widely within the field as *"Limbal epithelial stem cells"* (LESCs). The identity of these basal limbal cells as stem cells rapidly gained a large body of supporting evidence. Cells from this location where shown to retain nucleoside labels [58], displayed an increase proliferative capacity compared to the rest of the epithelium [59], and be capable of colony formation [60]. Additionally the cells of the basal limbus were also shown to express the ATP binding cassette transporter protein ABCG2 [61] which is also expressed by hematopoietic stem cells and has been proposed to have a role in the protection and isolation of stem cells from extrinsic chemicals [62].

Within the various animal models (chiefly rabbits) used in most studies of epithelial renewal there does not appear to be any specific macroscopic anatomical structure that is associated with LESCs, with the niche commonly being described as located at the basal corneoscleral junction. Within humans however there is such a structure located at the limbus in the form of radially-oriented fibrovascular ridges present around the circumference of the limbus called the palisades of Vogt. These structures were in fact proposed as a putative site of epithelial cell renewal in the same paper that first suggested the limbal epithelium as the source for this process [56]. The palisades of Vogt possess many features that might encourage cell growth and maturation such an extensive vascular supply, structural / physical protection, and pigmentation acting to protect against light damage. It has been suggested that specialised substructures called *"limbal epithelial crypts"* that extend out from palisades of Vogt beneath the conjunctiva might be especially enriched in LESCs [63] .
There is also substantial evidence of other anatomical structures constituting the LESC niche. Two such structures were identified in a study by Shortt et al. [64] in which the structure of the human limbus was examined at a very high level of detail by *in vivo* confocal microscopy. The features identified were invaginations of the epithelium into the limbal stroma associated with a blood supply termed *"limbal crypts"* (distinct from the *"limbal epithelial crypts"* in the palisades of Vogt although this similarity in terminology is confusing) and a similar reversed structure in which the stroma projected into the epithelium termed *"Focal Stromal Projections"*. Both these structures were associated with what appeared to be a high number of LESC's on the basis of the cells morphology and *in vitro* analysis of

biopsied tissue. Recently it was also proposed that a population of corneal epithelial stem cells resides outside the limbus, distributed throughout the epithelium [65]. This suggestion however has generated some controversy [66] and has not been widely accepted.

The basement membrane (BM) of the epithelium in the limbal LESC niche has also been shown to incorporate a large number of extracellular matrix components not found more widely across the BM which likely constitute a tightly controlled and highly specific microenvironment for the maintenance of LESCs [67]. Of particular note were osteonectin and tenancin C which appeared especially closely associated with putative stem cell clusters. It should be noted that despite extensive effort and many candidates having been proposed [68] that there is no single molecular marker that defines the LESC population. LESCs are therefore usually defined on the basis of the co-expression of multiple markers combined with the non-expression of others and specific cellular morphology [69]. This lack of a precise, incontrovertible definition has often made it difficult for definitive conclusions to be drawn relating to LESCs biology.

The identification and increasingly complex characterisation of both LESCs and the microenvironment of their niche has led to extensive clinical application and development. Shortly after the cells were first identified the concept of a limbal epithelial cell transplant was proposed and shown to be more effective in the treatment of disorders resulting from limbal aplasia than the similar transplantation of the bulbar conjunctiva previously performed for such conditions [70,71]. The first such transplants performed were autografts for the treatment of unilateral limbal deficiency. In bilateral cases autologous material is unavailable for engraftment and thus allografts from cadaveric sources are used and shown to be effective in such cases [72]. Since this initial development LESC transplantation has become a relatively standardised surgical procedure [73].

A further refinement of LESC transplantation technique was made by Pellegrini et al. in 1997 [74] who cultivated autologous graft material *ex vivo* pre-transplantation to expand LESCs and minimise the size of the donor biopsy required. Since this initial proof of concept a substantial body of further work has focused upon the culture and expansion of LESCs *ex vivo* and techniques for their engraftment (reviewed in: [75]). Much of the development of *ex vivo* culture techniques has aimed to provide as biomimetic an environment as possible for LESC expansion whilst maintaining “stemness”. In attempting to mirror the highly specific structural and chemical nature of natural LESC niche the bioengineering involved in such cultures has also become increasingly complex [76].

Whilst transplantation of *ex vivo* cultured LESCs can be undeniably effective in restoring the ocular surface, the means by which this beneficial effect is mediated maybe somewhat

ambiguous. It was initially (logically) assumed that the observed treatment effect of epithelial regeneration and subsequent maintenance was due to the successful engraftment of the transplanted cells into the LESC niche providing sustained restoration of normal LESC function. Whilst this assumption has been supported by analysis of the restored epithelium post transplantation [77], there is also some evidence to suggest that this may not happen in every engraftment. In some cases at least the transplanted cells do not appear to remain engrafted over the long term, with no donor derived DNA sequences being detected after 9 months post-transplantation [78,79] within the host epithelium. The clinical outcome of a much longer lasting restoration of an apparently normal host-derived epithelium is therefore hard to explain. It has been postulated that the transplanted cells may stimulate the remaining host LESC or that bone marrow derived stem cells may be recruited to the cornea to function as LESCs [50,78], but further studies are required to more fully explain this anomalous finding.

1.4.2 Epithelial maintenance and renewal

The limbal epithelial stem cells are vital to epithelial maintenance and their loss leads to complete epithelial failure. However, the LESCs themselves remain resident within their niche at the limbus and only function as the source of cells for epithelial renewal. In this capacity they are able to undergo either symmetric division to expand themselves or asymmetric division to both self-renew and produce differentiated daughter cells. It is the behaviour and dynamics of these daughter cell lineages therefore that form the fine detail of the processes by which the epithelium is maintained.

The driving force for epithelial renewal is the continuous desquamation of cells from the corneal surface during normal wear and tear which in turn drives a requirement for cell division, migration and differentiation of cells for the purposes of replacement. The *"X,Y, Z Hypothesis of Corneal Epithelial Maintenance"* proposed by Thoft & Friend in 1983 [80] has formed the basic theory behind most investigations of this renewal cycle and has become very well supported. The hypothesis proposes that the epithelial cell volume is likely to be near constant and that a balance of three forces (all previously observed) is responsible for maintaining this homeostasis of the layer.

1) The proliferation of the basal cells of the epithelium (X)
2) The centripetal movement of epithelial cells (Y)
3) The loss of cells from the corneal surface (Z)

To maintain homeostatic equilibrium X+Y = Z.

Thoft & Friend however did not define within X LESCs as the source of new cells stating only "peripheral tissues" of either the cornea or conjunctiva as such a source. This was due to the fact that at the time the involvement of the bulbar conjunctiva had not been ruled out. Subsequent mathematical modelling of the system by Sharma & Coles [52] indicated that the replication of the LESCs should be solely sufficient to account for the regeneration without any conjunctival involvement.

The daughter cells of LESCs are termed transient amplifying cells (TACs) on the basis that whilst they maintain some capacity to replicate they have lost the near indefinite replicative potential that defines a stem cell. These TACs appear to compose the entirety of the most basal columnar cell layer of the epithelium with cell division being almost exclusively restricted to this layer [55]. As they migrate centripetally they divide and progressively lose replicative capacity as shown by Lehrer et al. [81] who proposed that TACs were limited to ~3 divisions (although Lehrer et al. also acknowledged that this figure was "likely an underestimate") and that under normal homeostatic conditions cell cycle time was around 60 hours. Lehrer et al. also hypothesised that not all TACs realised their full replicative potential before differentiating into post-mitotic cells.

It is clear from multiple studies that when wounded the epithelium is able to profoundly change its usual regenerative profile, becoming far more active in order to rapidly respond to the insult and facilitate wound closure and healing [47]. It is thought that the replicative aspects of this wound healing response proceed via the shortening of cell cycle times for both LESCs and TACs (to <18 hours in the case of TACs), and all TACs fully utilising their "replicative reserve" by dividing the maximum of three times [81]. It is important to note however that any observations of epithelial behaviour made under such circumstances are almost certainly inapplicable to the normal homeostasis of the tissue.

The more superficial layers of the epithelium are generated by the differentiation of TACs into more mature post-mitotic cell types which then become increasingly mature as they move apically before being lost from the corneal surface. Once they have left the basal layer and begun this process the cells of the epithelium have an average lifespan of around 4-5 days [55]. Using the incorporation of nucleoside labels Beebe & Masters [82] studied the profile of TAC division with regard to daughter cell fate in some detail. They found that following division both daughter cells either remained within the basal layer (and thus remained TACs) or simultaneously migrated into the immediately apical wing cell layer. Segregation of daughter cells between the basal and wing cell layers post division was not observed, indicating that TAC division is always symmetric. More long term follow up of these experiments revealed that this synchronicity between the daughter cells of the last TAC division was maintained throughout their subsequent apical migration and

differentiation, always appearing to do the same thing at the same time. This may indicate that the final TAC division constitutes a key regulatory point after which there is little deviation from a pre-set “program” under normal homeostatic conditions. Later it was shown that upon leaving the basal layer the cells do indeed become committed to terminal differentiation and begin to express specific markers such as Keratin K12.

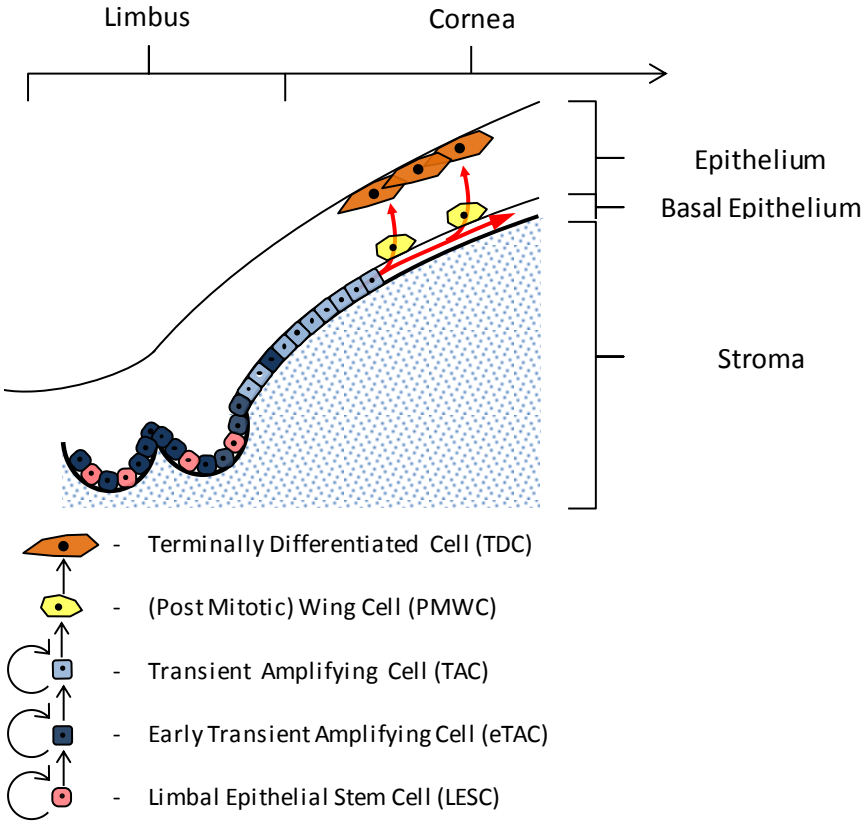

Figure 1. Schematic of epithelial renewal proceeding from the limbus
LESCs residing in the limbus give rise to eTACs which migrate centripetally, continuing to divide generating the TACs which form the basal layer of the epithelium.
Upon their terminal symmetrical division the TACs give rise to post-mitotic wing cells and leave the basal layer. The wing cells then migrate anteriorly becoming more differentiated before being lost from the corneal surface.

The centripetal migration that forms the Y component of epithelial maintenance has been extensively observed. The very first such observation was made by Mann in 1944 [83] who observed the centripetal movement of limbal pigmented cells in response to epithelial injury. The exact mechanisms driving centripetal movement remain unclear although population pressure from the periphery due to the increased proliferative capacity of LESCs / early TACs, increased loss of cells from the central cornea and chemotaxis have all been proposed [81,84,85]

There have been few direct measurements made of the rate of centripetal migration in the unwounded state. Work by Buck in 1985 [84] provided the first such direct measurement; murine epithelial cells were injected with india ink enabling their migration to be tracked over 7 days, in which time they moved ~94µm, equating to 17µm per day. The rate of centripetal

migration in the mouse was also evaluated by Nagasaki & Zhao in 2003 [86] using a transgenic model ubiquitously expressing GFP. A rate of cell movement of 26µm per day was calculated, although cell tracking relied on the ability to distinguish cell lineages based upon variable expression levels of the transgene.

The use of such transgenic models has formed the primary source of insight into the patterning of the epithelium resulting from centripetal migration of cells and streak-like patterns of labelled of cells stretching from limbal to central cornea are typically observed. One such transgenic model in which much of this work has been performed is based upon the X-inactivation of a Lac-Z gene resulting in a clonal mosaic of marker expression throughout the adult animal. Observations made in this model include:

- Time for total epithelial turnover estimated to be ~3-4 weeks [87].
- Whorl like patterns being formed when multiple streaks meet in the central cornea that are reminiscent of effects seen in certain pathological human conditions thought to be patterned by epithelial migration [88].
- An apparent decrease in the number of labelled streaks with age [89]. This might indicate a reduction in the number of active LESCs with age, but is not conclusive.

There is also evidence from such murine models that epithelial renewal via centripetal migration of cells from the limbus is not a mechanism that is present from birth. For a period extending up to 10-12 weeks postnatally the streak-like patterns typical of centripetal migration are not seen to develop, with more random mosaic patterns being present instead [87,90]. It has been hypothesised therefore that during this period an alternative embryonic mechanism of epithelial renewal remains in place proceeding from corneal epithelial stem cells present throughout the basal layer of the epithelium, a mechanism that is eventually replaced by the adult program of centripetal migration of cells derived from LESCs [90,91].

Unfortunately there is very little quantitative data available for the final aspect of epithelial maintenance and renewal: The desquamation of cells from the epithelial surface (Z). Two studies by Ren & Wilson [92,93] attempted such quantification in a rabbit model and established a range for rate of loss of between 5-100 cells/min/cornea depending on the methodology used. This large range results from difficulty in controlling for normal processes such as blinking.

It is worth mentioning that combining all of the various published data regarding the dynamics of epithelial turnover in such a way that it all fits together into a coherent model of the system is difficult, and some contradictions are apparent. It is likely therefore that some of this data is inaccurate and that the cellular dynamics of epithelial turn over remains only partially understood.

1.4.3 Inherited disorders of the epithelium

One of the most common applications of gene therapy is to the correction of an inherited genetic defect and a number of such conditions have been described affecting the epithelium. All of them, however, are extremely rare and are thus often only described in the form of case / familial reports with no broader prevalence data available. When the molecular genetics of various dystrophies was elucidated it was revealed that the degree of heterogeneity in causative genes / loci was lower than might have been implied by the number of conditions described. This was due to different conditions often being shown to be associated with the same gene or locus. For example both Reis-Bücklers and Thiel-Behnke dystrophy have been linked to mutations in *TGFBI,* and Meesmann and Stocker-Holt dystrophies to *KRT12* mutations. This perhaps implies that rather than being entirely separate these are in fact the same condition presenting with (usually small) variations in phenotype.

As a rule epithelial dystrophies generally follow an autosomal dominant pattern of inheritance with only two exceptions to date; Lisch epithelial dystrophy, which appears to follow an X-linked recessive pattern and Gelatinous drop-like corneal dystrophy (GDLD) which is inherited via an autosomal recessive pattern. This latter condition is also the most prevalent of the epithelial dystrophies (although still rare) and forms the primary research focus of our collaborator Dr Satoshi Kawasaki (Kyoto Prefectural University of Medicine). For these reasons the epithelial work presented here was primarily directed towards developing a therapy for this condition and it will thus be described in more detail below.

1.4.4 Gelatinous drop-like epithelial dystrophy

Gelatinous drop-like corneal dystrophy (GDLD) is a congenital disorder following an autosomal recessive pattern of inheritance. It is globally rare but more prevalent within the Japanese population with an estimated rate of occurrence of between 1 in 30,000 [94] and 1 in 300,000 [95] within this demographic. The disease is characterised by the development of sub-epithelial amyloid deposits which eventually lead to opacification of the cornea and visual impairment [96].

The gene locus linked with GDLD was established in the late 1990's as being located upon chromosome 1 [97] with further work establishing the disease to be caused by loss of function mutations within the gene *TACSTD2* (aka *M1S1* or *Trop2*) which lead to truncation of the gene product and cellular mislocalisation [98].

Clinical presentation of the disorder is variable with several subtypes characterised, named for their appearance: Typical mulberry type, Kumquat-like type, Band keratopathy type and Stromal opacity type (Figure 2). There does not seem to be an association however between the specific *TACSTD2* mutation present and the subtype presented, as shown by the most commonly occurring mutation (Q118X) having been associated with all 4 clinical subtypes. [99]

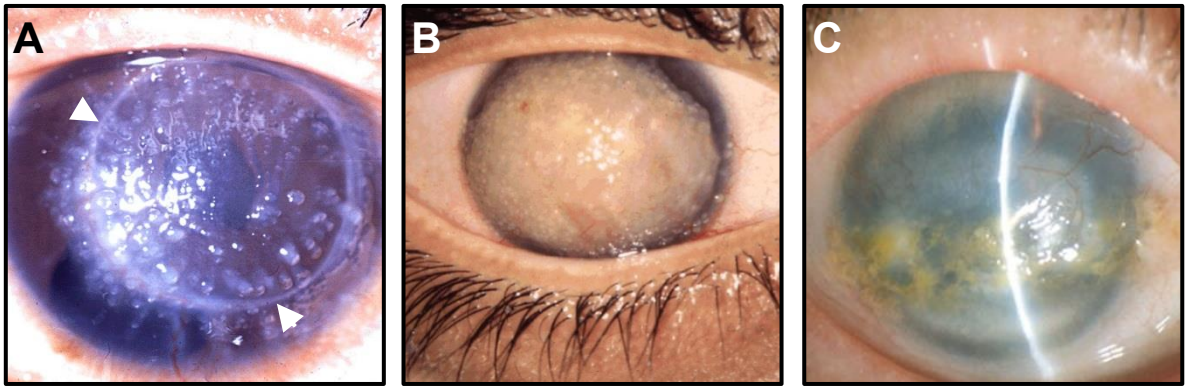

Figure 2. ***The variable phenotypes of Gelatinous drop-like corneal dystrophy***
A: Typical mulberry type, in this patient a keratoplasty has clearly been performed (incision line highlighted by white arrow heads) and the condition has recurred covering the graft.
B: Kumquat-like type
C: Band keratopathy type
Images in this figure adapted from references: [100,101]

The pathological mechanism of GDLD has been partially elucidated. Epithelial permeability to chemicals such as fluorescein [102] or horse radish peroxidase [103] is increased in the condition indicating that epithelial barrier function is impaired. Immunohistological data obtained from GDLD corneal samples also tend to support this conclusion [104]. The expression and localisations of various tight junction related proteins have been shown to be disrupted in the GDLD epithelium. ZO-1 and occludin are entirely absent from the most superficial epithelial cells and claudin-1 and desmoplakin are abnormally expressed and localised in both superficial and basal cells. The localisation patterns of various integrins, collagen types and laminin-5 are also abnormal in the GDLD epithelium with many of these patterns indicating a thickened, involuted basement membrane.

The mechanism by which mutations in *TACSTD2* leads to impairment of epithelial barrier function has been determined. In 2010 Nakatsukasa et al. [105] showed that the TACSTD2 protein is present throughout the normal corneal epithelium but is entirely absent from GDLD corneas. The protein is able to bind directly to tight junction related proteins, claudins 1 and 7 and colocalises with these proteins *in vivo*. Knock down of TACSTD2 mediated via shRNA *in vitro* leads to a drop in transepithelial resistance and a reduction in levels of claudin 1 and

7 at both the mRNA and protein level. Additionally other tight junction related proteins such as claudin 4 and occludin became mislocalised to the cytoplasm.

The exact mechanism by which TACSTD2 loss mediated disruption of tight junctions and the resulting impairment of epithelial barrier function leads to the primary phenotype of sub epithelial amyloid deposition is not well understood however. It has been hypothesised the deposits consist of lacoferrin [106] or apolipoprotein [107] which may have infiltrated from the tear film.

The only currently available treatment for GDLD is a corneal allograft, although this procedure does not resolve the disease permanently. Corneal grafts only replace the central portion of the cornea whilst leaving the host's more peripheral corneal tissue in place. The host's limbal stem cells therefore remain *in situ* and the transplanted healthy donor epithelium is replaced over time by the host's diseased epithelial cells via the process of normal corneal renewal. Recurrence of the condition thus usually occurs within 1-2 years. Re-engraftment is then required, although due to the risk of graft failure increasing with each subsequent engraftment [108], treatment by repeated corneal transplantation has a very poor long term prognosis.

1.5 Corneal Neovascularisation

The healthy cornea is maintained in an avascular state due to the functional requirement for optical transparency and minimal light scatter. This avascularity is maintained by a complex balance of both pro and anti-angiogenic factors present within the cornea [109] with soluble VEGF receptor 1 (sVEGFR1 / sFlt1) in particular having been shown to play a key role. Conditional knockout of this factor alone is sufficient for murine corneas to lose their avascularity and the only species known to have a vascular cornea, the Florida manatee, lacks sFlt1 in the cornea [110].

The cornea's closest contact to the circulation is located at the corneal limbus where it is ringed by a vascular arcade formed of an episcleral anastomotic circle, the arterial supply of which derives from the anterior ciliary arteries extending from the rectus muscles. Extending from this ring are looping arterioles that supply many structures located in or close to the limbus such as the palisades of Vogt, the conjunctiva, the ciliary muscle and anterior uvea. The limbal arcade is drained by an almost directly parallel venous system which exits the limbal region via the anterior ciliary veins.[111]

It is from this vascular plexus that pathological corneal neovascularisation proceeds via the sprouting of new vessels and can fall into one of three categories based upon the extent and depth of neovascular growth [112]. Vascular pannus is limited to the peripheral cornea and is usually associated with disorders of the ocular surface, superficial vascularisation extends only through the epithelium and, as its name implies, stromal invasion involves the penetration of neovascular vessels into the stroma. The generation of pathological blood vessels is clearly the result of an unregulated and misdirected process, and this is reflected in the resulting blood vessels themselves which are functionally immature and lacking in structural integrity. Therefore in addition to their own negative impact upon corneal transparency they are also often associated with lipid keratopathy, a condition in which lipid leaks from the vessels to forms opaque deposits within the cornea.

Pathological corneal neovascularisation is present within an extremely wide range of different conditions such as: extended contact lens wear, trauma, alkali burns, infections (bacterial or viral), parasitosis, or immunological conditions. Within the developed world the extended wear of soft hydrogel contact lenses is the most common cause, although the vascularisation observed is these cases is usually very mild, non-sight threatening and treatable merely by modification of the regime of contact lens use. Far more serious is the corneal neovascularisation / inflammation that results from corneal injury or infection. In the

developed world the most common corneal infection is herpes simplex keratitis although prevalence is relatively low; however in the developing world a bacterial infection associated with corneal neovascularisation, trachoma, constitutes the primary cause of corneal blindness and is prevalent to such a degree that this condition is also the leading cause of corneal blindness worldwide.

With the exception of contact lens wear (in which corneal hypoxia is thought to be the responsible) corneal neovascularisation is almost always a secondary disease phenotype resulting from a primary inflammation. The inflammatory response to injury or infection is associated with the cascading activation of numerous cytokine pathways within the cornea initiated by IL1 secretion from the cells of the corneal epithelium and infiltrating innate immune cells [113,114]. Many of these cytokines are potent pro-angiogenic factors themselves (IL1-β for example has been shown to comparable to VEGF-A as an angiogenic factor in the cornea [115]) and also lead to the widespread downstream up-regulation of the VEGF pathway [116]. This prolific cytokine activation therefore strongly disregulates the angiogenic homeostasis of the cornea leading to neovascularisation. In most cases inflammation related pathogenesis is not limited to neovascularisation with the up-regulation of TGF-β in particular often also resulting in the activation of stromal keratocytes which can lead to stromal fibrosis and scarring [42].

If the pathology in these conditions progresses to the point of becoming blinding often the only means to restore vision is via corneal transplantation, and it is in reference to this procedure that corneal neovascularisation is of particular relevance.

Under ideal conditions the prognosis of penetrating keratoplasty is excellent with 5-year graft survival rates of up to 95-99% achievable in conditions such as keratoconus which present with no inflammatory complications [117]. As discussed however corneal transplantation may be indicated for the treatment of a condition in which the host cornea is inflamed and / or vascularised at the point of transplantation, and the presence of neovascular vessels in two or more quadrants of the cornea is one of several factors leading to a corneal engraftment being classified as “high risk”. Another major risk factor is the regrafting of a previously failed transplant. This classification is due to the very well characterised negative impact of pre-existing corneal vascularisation on long term graft survival [117–120]. Probably the most extensive study demonstrating this association was a meta-analysis of nearly 25,000 penetrating keratoplasty procedures [121] in which the presence of pathological corneal neovascularisation at the point of surgery was shown to increase the risk of graft failure or rejection with pooled risk ratios of 1.32 and 2.07 respectively, with the data also indicating that risk increased in proportion to degree of neovascularisation.

The high success rate of corneal transplantation under ideal conditions without the need for tissue typing and only minimal immune suppression is due to the immune privilege enjoyed by the cornea [122,123], and it is thought that corneal neovascularisation increases the probability of graft failure by compromising this privileged status [124,125]. The neovascular vessels facilitate a greater exposure of the grafted tissue to the host immune system by providing conduits for both the egress of alloantigens for presentation to the peripheral immune system and ingress of immune effector cells such as T-cells into the graft.

Whilst the clinical focus upon corneal neovascularisation has very much been upon the clearly visible blood vessels, such haemangiogenesis has been shown to almost invariably be accompanied by lymphangiogenesis [126] and there is a growing body of evidence to suggest that these vessels may in fact be of greater relevance in the context of immune mediated graft rejection [127–129], a logical assertion due to the key role of the lymphatic system in antigen presentation.

Treatments for neovascularisation are highly varied and at the point of initial insult are usually focused upon the suppression of the inflammatory response via the topical application of steroids, which are often most effective when applied shortly after the onset of inflammation before neovascularisation has become established. In the case of infections drugs targeted towards inhibition of the pathogen are also applied although in such cases a careful balance must be struck with regard to steroid application as excessive inhibition of the immune system may act to aid the pathogen.

Once neovascularisation is more established more direct treatments can be applied including the direct ablation or occlusion of vessels by means of lasers, fine needle diathermy [130] or photodynamic therapy [131]. More recently the extensive clinical use of VEGF binding based therapeutics for the treatment of choroidal neovascularisation in wet AMD has led to these drugs also being directed towards corneal neovascularisation both in the clinic and in animal models (reviewed in [132]). Initial results from these studies are promising overall but treatment regimens often involve repeated administration at relatively high doses.

1.6 Gene therapy

Gene therapy is the term applied to any treatment that mediates its primarily therapeutic effect via application of a nucleic acid based product, be it DNA, RNA or various synthetic analogues such as morpholinos. The technique usually aims to modify the gene expression within a target cell, either to directly correct a deleterious mutation or to mediate a more general beneficial effect such as the promotion of cell survival. Perhaps the most promising aspect of gene therapy as a methodology is that it allows the gene defects that constitute the underlying causes of congenital disorders to be targeted directly and thus the approach has the potential to be curative. Other treatment methodologies can only aim to target and alleviate the symptoms of such conditions.

For a gene therapy approach to be effective a number a conditions must be met:

- The nucleic acid products must be efficiently delivered to the target cells, ideally whilst avoiding transduction of non-target cells.
- The nucleic acid must then mediate its effects at a physiologically appropriate therapeutic level.
- Immune mediated reactions to the therapy, which can be directed at either vector components or transgene product should be avoided or minimised.

Additionally in most cases it is desirable for the treatment effect to be effective over the long term without the need for re-administration of the therapeutic construct.

Gene therapy methodologies to date can be broadly split into two categories, non-viral and viral and each has its advantages and disadvantages in relation to these conditions for efficacy.

Non-viral methods (reviewed in [133,134]) can constitute the simplest approaches to gene therapy, in many cases involving direct physical delivery of nucleic acids to cells. The nucleic acids themselves are usually unable to cross the cell membrane of the target cells due to the cells themselves not tending to actively take up naked nucleic acids and the negative charge of acids leading to their inability to cross the hydrophobic interior of the plasma membrane. This latter limitation however is overcome by some modern synthetic DNA/RNA analogues which are uncharged. Physical non-viral techniques usually aim to transiently disrupt the target cell's plasma membrane to allow entry of the nucleic acid and such disruption has been induced by the application of energy in the form of electric currents, ultrasound, ballistics or lasers.

Many chemical non-viral methods to mediate cellular nucleic acid uptake have also been developed including the coupling of nucleic acid to cationic polymers, or their encapsulation within engineered liposomes or other forms of nanoparticle. This latter approach in particular has become advanced with the nanoparticles design often being highly structurally complex or incorporating ligands to promote endocytosis via a specific cell surface receptor [135].

The chief advantage to non-viral methods is that they are usually completely non-immunogenic, however they also present with several substantial disadvantages most significant of these being their limited efficacy *in vivo*. Effective gene delivery by non-viral methods is hampered by many factors including vector instability *in vivo*, loss of vector to interaction with non-target tissues, intra-cellular processing leading to mislocalisation or destruction of the transgene and loss of transgenic construct upon cell division [134]. Whilst much progress has and continues to be made, non-viral methods currently lag behind the alternative of virally mediated gene therapy [136], with inspiration for improvements of non-viral systems often being gleaned from viruses themselves [137].

The majority of work in the gene therapy field (especially in regard to clinical application) has utilised viral methods of gene delivery, in which the natural ability of various viruses to deliver DNA/RNA to cells has been co-opted and exploited for use in therapeutic gene delivery, achieved via the replacement of viral genomes with transgenic constructs. The main advantage of this approach is that the natural history of viral evolution has led to the genesis of wide variety of viral species all of which are highly optimised to mediated gene transfer to their target cell of choice and which have developed complex and often elegant mechanisms to overcome many problems that have limited the efficacy of non-viral gene therapy. A large “toolkit” is therefore available for use in gene therapy which has in many cases been further refined towards specific therapeutic application.

A natural viral infection is of course often pathogenic and thus all organisms have evolved both systemic and intracellular defences against viral infections which constitute the chief disadvantage of the use of viruses as gene therapy vectors, their immunogenicity, which can both limit efficacy or induce pathology [138,139]. Whilst most gene therapy vectors are heavily modified to prevent any possibility of pathogenesis and reduce immunogenicity as far as possible, due to the coevolution of viral virulence and host immunity it is likely that any modification that promotes immune tolerance might also reduce the vector’s efficacy. A number of specific viral vectors of particular relevance to this thesis will be further discussed in 1.6.2

1.6.1 Gene Therapy Strategies

Once effective transgene delivery to the target cell has been achieved there are a number of means by which a therapeutic effect might be mediated, either upon the transduced cell itself or the wider tissue or system of which it is a part. Some of these will be briefly outlined below.

1.6.1.1 Gene Supplementation

This constitutes one of the simplest and most widely utilised approaches to gene therapy and is generally applied in the context of a recessively inherited disease causing loss of function mutation. The strategy aims to restore the lost function and correct the defect by the delivery of functional wildtype copies of the mutated gene. This strategy might also be effective in the correction of dominant disorders resulting from haploinsufficiency and has been shown to be effective in a hypomorphic mouse model of retinal disease [140].

Once the gene delivery to the target cells has been achieved the transgene should then be expressed in such a way that the normal wildtype function is mimicked as closely as possible for the best chance of therapeutic effect. This is not always desirable however, in some conditions patients are protein null and thus completely immunologically naïve to the wildtype transgene product. In these cases it is best to aim for the minimal effective dose of transgene delivery to avoid adverse immune responses. Many supplementation strategies are relatively crude in regard to fine regulation of transgene expression level, often utilising a virally derived promoter sequence able to induce a very high level expression but in a relatively uncontrolled, non-specific or ubiquitous fashion [141]. This is often effective but has the potential to cause toxicity resulting from overexpression or disregulation of a finely controlled processes [142].

More controlled expression is often achieved placing the transgene under the control of a cell or tissue-specific promoter, ideally the endogenous promoter of the gene in the wildtype context [143]. In addition to more physiological control of transgene expression within target cells this also acts to limit or prevent transgene expression within any non-target cells that may also be infected by the vector. Such promoter driven control is often not possible however as an appropriate promoter may not be known, only partially defined, or too large to be contained within the vector's packaging capacity. Additionally even the use of the transgenes exact endogenous promoter is unlikely to result in a precise recapitulation of the wildtype expression pattern due to the transgenic copy not being present within the same complexly regulated genomic context as the endogenous gene.

In recent years this distinction has led to a subtle change in the terminology applied to this approach. Gene **supplementation** is now the term of choice for the traditional approach that leaves the defective host gene in place and adds functional copies either episomally or at other sites within the host genome. The formerly used term of gene **replacement** is now more accurately applied to various attempts to mediate a physical replacement of the defective gene copy within the host genome via approaches based on combination of homologous recombination with engineered nucleases targeting specific sites. This approach whilst far more complex presents with multiple advantages such as:

- Removal of any possible deleterious function of the defective copy.
- Transgene being regulated in the precise endogenous genomic context.
- Transgene being copied upon cell replication and thus maintained in replicating cell types

This technology is still however at a very early stages of development and has not yet seen extensive application [144], especially *in vivo*.

1.6.1.2 Gene suppression

Gene supplementation is likely to be ineffective for the treatment of dominant disorders resulting from gain of function or dominant negative mutations. For gene therapy to be effective in such cases the expression of the mutated gene product must be supressed.

This approach is usually mediated via the gene therapy vector delivering a nucleic acid construct designed to act via RNA interference (RNAi). This system works by co-opting an endogenous system in all mammalian cells which enacts post transcriptional gene silencing via the enzymatic destruction of RNA species. This silencing is mediated by a large multicomponent RNA/protein complex called the RNA induced silencing complex (RISC). RISC functions by processing dsRNA species into small (19-21bp) ssRNA species which are then incorporated into the structure of the complex in order to act as a template for the recognition of larger ssRNA species by complimentary base pairing. Upon such recognition an RNAase component of the complex becomes active and the target molecule is degraded. It was initially thought that this system may have evolved as a host defence against viral infection which seems to be the case in plants and invertebrates, however support for this idea in the mammalian context has recently been challenged as relatively weak and the discovery of endogenous microRNAs (miRNAs) that act through RISC forming a vital post transcriptional gene regulatory mechanism suggests that mammals may have repurposed RNAi/RISC to a different primary function [145].

Gene suppression constructs are often based upon a short hairpin RNA structure (shRNA), in which two inverted repeat sequences are separated by a short sequence designed to fold into a hairpin loop and thus the whole construct is capable of folding into dsRNA by a self-complimentary base pairing of the inverted regions, designed to be specific to the gene to be silenced. The dsRNA transgenic construct is processed by RISC which then mediates the destruction of endogenous target gene mRNA resulting in reduced translation. As the shRNA transgene is required to be delivered in the form of a very short RNA molecule without a poly A tail the promoters used in such constructs bind RNA polymerase III as these enzymes are designed to transcribe such RNA species. Commonly used promoters are U6 and H1 although these induce a ubiquitous expression profile and thus control is limited.

There is evidence however that in the case of RNAi based gene knockdown the effects of overexpression may be of greater concern than is the case for gene supplementation. This appears to be due to the relatively limited capacity of the RISC complex as artificial short interfering RNAs and expressed shRNAs have both been shown to inhibit both each other and the endogenous miRNAs by competition for access to RISC components [146]. This competition results in combinatorial shRNAs approaches proving less effective than either component in isolation and overexpression potentially causing toxicity via the deregulation of endogenous miRNA function. Another study showed that such shRNA overexpression mediated miRNA dysfunction can prove fatal in a murine model and identified a nuclear dsRNA exporter (karyopherin exportin-5) as a particular bottleneck prone to saturation within the system [147]. Dosing within shRNA based gene knockdown approaches is therefore of critical importance.

Some modulation of dosing might be achieved by the use of gene silencing constructs based upon miRNA structure. These do not appear to be expressed as highly as more traditional shRNA-based designs and do not result in as substantial a gene knockdown when compared under tightly controlled conditions [148]. Whilst this may act to limit their efficacy it also reduces their toxicity, and it has been shown that such miRNA mediated RNAi can result in an effective gene knockdown whilst showing no signs of competitive interference with other constructs [146].

1.6.1.3 Gene Augmentation

Augmentation gene therapy is an approach whereby gene transfer does not aim to directly address a genetic defect by replacement or inhibition of the mutated gene product. Augmentation approaches instead aim to express factors which might be able to mediate a

beneficial effect on a pathological process via direct modulation of the process itself or stimulation of other endogenous systems or responses to act antagonistically to the pathology. This approach is therefore not limited to application solely to congenital disease, as pathological processes that may be amenable to amelioration via such a mechanism are present in almost every disease state.

The target systems of augmentation gene therapy approaches have therefore been incredibly varied and include: promotion of cell survival [149], induction of cell death [150], induction of cell proliferation [151], inhibition of neovascular growth [152], neuroprotection [153], inhibition of immune responses [154], retargeting of cytotoxic T-cells to specific epitopes[155] and the prevention of amyloid deposition [156] to name but a few.

In common with every other gene therapy approach appropriate regulation of the transgene expression is key and indeed such control may be especially vital in the case of augmentation-based approaches. Off-target transgene expression in the context of a gene supplementation may have little pathogenic effect as the transgene is often highly specific only functioning within the target cell type. The target systems of augmentation-based approaches however are usually far more widely applicable and off-target or excessive expression could be highly deleterious, for example in cases where the approach aims to induce cell death or immunosuppression.

Therefore in addition to the transgene regulation afforded by tissue or cell-specific promoters or vector tropisms, augmentation approaches have also seen the development of promoter sequences designed to be able to modulate transgene expression in direct response to the severity of the pathology in effect. For example NFκB responsive promoter sequences have been used to drive transgene expression specifically in response to inflammation [157] and the GFAP promoter has been used to up-regulate transgene expression at the site of CNS lesions.[158]

A commonly employed approach in augmentation gene therapy is often not to target directly the cell type (or even tissue or organ) which is most affected by the pathology but instead aim to act at a distance via a secreted product, providing said product can be delivered to the target site in sufficient quantity by normal physiological processes. Such an approach may be of particular benefit if for example:

- Transduction of the affected cells themselves would not result in the production of physiologically relevant amounts of secreted transgene product.
- The affected area has been rendered especially sensitive to further damage (such as that which might result from gene delivery itself) by the ongoing pathology.

- The cells or tissues directly affected are physically difficult to access.
- The cells in question cannot be currently be transduced by any available gene delivery system.
- The site of disease itself is especially exposed to the immune system leading to a high probability of vector or transgene directed immune responses.

It should be noted however that whilst this secretion based approach is more common in augmentation approaches, supplementation gene therapy can also share this mechanism of action. For example the gene defects in factor IX that are causative of haemophilia B result in a systemic dysfunction and supplementation of factor IX does not have to be directed to the natural site of production in the liver with other tissues such a muscle having been targeted instead [159].

1.6.2 Vectors for viral gene therapy

1.6.2.1 Adenoviral vectors

Adenoviruses are non-enveloped viruses with a linear double stranded 37kb DNA genome contained within an icosahedral capsid with fibres extending from each vertex of the capsid structure. There are 57 distinct serotypes identified and in their wildtype forms are associated most commonly with mild respiratory infections.

Infection is primarily mediated via interactions between the fibre knob domain with the coxsackie and adenovirus receptors [160]. Internalisation of virions then proceeds by binding of cellular integrins to an RGD motif in the adenovirus penton base protein, and subsequent endocytosis [161]. Adenoviruses became a popular gene therapy vector based upon a number of factors. They display a wide tropism to both quiescent and proliferating cell types, have a relative large genomic packaging capacity of between 8 and 38Kb for transgenic inserts, are stable [162] and are relatively easy to both genetically manipulate and produce. Adenovirus serotype 5 in particular has emerged as the adenoviral vector of choice and is used in the majority of approaches employing adenoviral vectors.

Adenoviruses do present with a significant disadvantage however, they have been shown to mediate extensive innate immune responses [163]. This issue was tragically highlighted by death of a patient taking part in a gene therapy trial for ornithine transcarbamylase (OTC) deficiency due to a massive systemic immune response to the adenoviral vector [138]. Even in the absence of such an extreme response the transgene expression mediated by adenovirus is often lost due to adaptive immune responses eliminating transduced cells [164,165], a response directed towards either viral antigens or transgene product with the latter potentially having been potentiated by the former.

Modification of adenoviral vectors in order to reduce or mask their immunogenicity is therefore an area that has received some significant attention [166] with improvements in production techniques and a greater understanding of the virology of adenovirus leading to the development of 2nd and 3rd generation vectors. These newer generations have been engineered to package an increasingly minimal set of adenoviral gene sequences within the final vector and thus have minimised immune responses directed at these sequences and their products. Such an approach however does little to reduce the immunogenicity induced by the capsid proteins themselves and thus a significant immune response can still be induced [167].

Adenoviral vectors have not seen widespread use within the eye due to both concerns over their immune profile and the fact that they do not generally display tropism to photoreceptors, the cell type most commonly targeted within the eye [168]. More recently adenoviruses have been generated with modifications made to the capsid which appear to mediate a more extensive retinal transduction [169] but these have not yet seen application. Adenoviruses do effectively transduce corneal endothelial cells however and this will be further discussed in 1.7.2.

Adenoviruses continue to see widespread use within the field of cancer gene therapy, in which rather than being deleterious to gene expression any adaptive immune response generated is likely to be advantageous as such gene therapy usually aims to destroy the target cells; innate responses however remain a concern.

1.6.2.2 Adeno-associated viral vectors (AAVs)

Adeno-associated viruses (AAV) are members of the family Parvoviridae which are all non-enveloped viruses with a single-stranded DNA genome contained within an icosahedral capsid; collectively the Parvoviridae also constitute some of the smallest, simplest eukaryotic viruses. The AAV's are the sole members of the Dependovirus genus within the family, a genus so named due to the inability of its members to independently replicate. Dependoviruses are dependent for replication upon gene functions provided in *trans* by the co-infection of a so called "Helper virus". This role is most commonly fulfilled by adenoviruses (leading to the group's species name) although helper function can also be fulfilled by herpes or vaccinia virus.

AAV displays multiple features that make it highly attractive as a gene therapy vector. Firstly and in common with the rest of its family, AAV is an exceptionally small, deceptively simple virus, allowing relatively easy genetic manipulation and production. A single AAV virion is around 22nm in diameter and is formed of 60 protein subunits, consisting of three individual capsid proteins, VP1-3 in the ratio 5:5:50 [170]. Genomically AAV is equally economical, its genome being 4.7kb long containing only two open reading frames, the genes *Rep* and *Cap*. As their names imply *Rep* encodes proteins required for AAVs replication and other cellular functions whilst *Cap* encodes the structural capsid proteins. Both genes are extensively alternative spliced meaning that 3 cap and 4 rep protein products are produced. Genomic packaging is mediated by short (145 base) inverted terminal repeat sequences (ITR) flanking the genome and all sequences lying between these ITRs will be effectively packaged meaning the design of transgenic constructs for packaging into AAV is extremely easy.

Infection with wildtype AAV is generally not associated with any form of pathogenesis and although they do induce humoral immunity, innate and cellular responses are limited, possibly due to AAVs limited antigen presentation [139]. As a vector these characteristics lead to an excellent safety profile although the presence of neutralising antibodies may limit the efficacy of both repeated applications and treatment of those individuals already seropositive.

Upon infection wildtype AAV is capable of proceeding down either lysogenic or lytic routes depending upon the presence or otherwise of its helper virus [171]. If present, infection will proceed via the lytic pathway but in the absence of helper virus AAV is able to integrate its genome into the host's and establish a latent infection. The integration of AAV is unique amongst all known eukaryotic viruses, in that it integrates only at a single highly specific site (a 4kb region) on human chromosome 19 and is mediated by either Rep78 or Rep68. Recombinant AAV (rAAV) vectors however do not generally encode the *Rep* gene, with the entirety of the genome save the ITRs having been replaced with transgenic construct for reasons of both maximising packaging capacity and safety. Recombinant AAVs are therefore incapable of this site specific integration and do not integrate to any substantial degree, maintaining their genomes episomally. Such integration however could be of great utility in a vector, potentially allowing the stable infection of a replicative cell type with minimal risk of insertional mutagenesis. Unfortunately the mechanisms by which AAV mediates this unique integration are currently too poorly understood to be applied.

To date twelve different human serotypes of AAV and more than 100 serotypes from nonhuman primates have been isolated and identified. Of these, the human serotypes AAV 1-9 have been the most extensively characterised and adapted for use as vectors and between them display tropism to a very wide variety of different tissue / cell types leading to potential utility in the treatment of an equally wide range of genetic disorders [172].

AAV9 is of particular note in regard to tropism having been shown to be able to mediate transduction in many different tissues throughout the entire murine soma when delivered systemically [173] opening the intriguing possibility that treatment of syndromic conditions or gene delivery to widely distributed organ systems (such as muscle) might be possible by such means. Whilst such widespread transduction has only thus far proven possible at embryonic stages, transduction of the retina via this route in the adult has also been demonstrated [174].

When produced as vectors, AAV particles are usually composed of a genome based upon the AAV2 ITR sequences combined with the capsid best suited to the application. The convention for vector nomenclature is therefore: AAV genome / capsid, e.g. AAV2/8

AAV does however have two major disadvantages for use as a vector. Firstly AAV is unable to package much more than its wildtype genomic capacity, limiting the size of the transgenic constructs that can be packaged to 4.7 - 5.0kb. Relatively recently it had been reported this limit may not be as absolute as previously assumed, with larger genomic packing possible albeit at reduced efficiency [175]. These results however could not be replicated and may have been artifactual [176]. Secondly as already mentioned rAAV is not able to integrate its genome within the host's, and whilst this might reduce any potential for genotoxicity via insertional mutagenesis it also results in dilution of episomal transgenic constructs upon cell division and eventual loss of expression in dividing cells. Application of AAV has therefore been largely limited to non-dividing cell types.

Use of AAV within the context of gene therapy has been extensive and it has rapidly become the vector of choice within the field, especially for gene supplementation approaches. At the time of writing AAV vectors are in use in at least 38 clinical trials for conditions as diverse as haemophilia, muscular dystrophy, Alzheimer disease and arthritis [177]. Additionally in 2012 the first (and thus far only) gene therapy based pharmaceutical (Glybera), which is based upon an AAV1 vector, was approved for use in the treatment of familial lipoprotein lipase deficiency [178].

AAV is also by far the most commonly used vector in ocular gene therapy due to multiple serotypes (2, 8, 5 and 9) having been shown to mediate a substantial, and long lasting gene delivery to both photoreceptors and retinal pigment epithelium (RPE) following injection into the subretinal space (reviewed in [179,180]). AAV-based vector technology has now improved to the point where a near 100% transduction of these cell types is achievable in mice.

Clinically, four trials have begun aiming to treat Leber's congenital amaurosis (LCA) due to RPE65 deficiency via an AAV2/2 or AAV2/4 based gene supplementation. These trials have progressed to Phase I / II and have thus far demonstrated safety and some initial indications of efficacy [141,143,181].

Due the fact that AAV based gene therapy has enjoyed so much success there have also been multiple attempts made to improve AAV vectors through modification of their capsids and genomes to further expand their utility. Self-complimentary AAV vectors (scAAV) are one such modification. These vectors carry inverted repeat genomes which are capable of folding upon themselves to form double stranded DNA. Upon infection this allows the rate limiting step of second strand synthesis to be circumvented leading to more rapid onset of transgene expression [182,183]. This however comes at the cost of halving the already

limited packaging capacity of the vector. Two capsid modifications of AAV will be discussing in greater detail in 1.6.2.3 & 1.6.2.4.

1.6.2.3 Engineered capsid mutants of AAV (tyrosine mutants)

The work that lead to the inception of the various tyrosine mutant AAVs was initially based upon the finding that the cellular chaperone protein FKBP52, when phosphorylated by epidermal growth factor receptor protein tyrosine kinase (EGFR-PTK), inhibits second strand synthesis of the AAV genome [184] which constitutes a major rate-limiting step accounting for the inefficient transduction of certain cell types by AAV vectors [185].

This finding led Zhong et al. [186] to examine the role of this signalling pathway upon AAV transduction in greater detail. As a first step in the investigation of this pathway's role in second strand synthesis the effects of its pharmacological inhibition upon both normal single stranded (ssAAV) and self-complimentary (scAAV) AAV2 vectors was assessed *in vitro*. It might have been expected that the scAAV would be unaffected by such inhibition as this modification of the AAV genome eliminates the need for second strand synthesis. Surprisingly however this was found not to be the case, inhibition of the EGFR-PTK pathway was shown to improve the transduction efficiency of both ssAAV and scAAV2 significantly, with the effect upon scAAV being only marginally reduced. This therefore implicated the EGFR-PTK pathway in a substantial additional role in AAV transduction beyond that of inhibiting second strand synthesis.

Zhong et al. then examined the role of the EGFR-PTK pathway in intracellular trafficking of AAV. Inhibition of the EGFR-PTK pathway *in vitro* was shown to increase the proportion of AAV sequences localised to the nucleus to a similar degree as treatment with a proteasome inhibitor. Additionally the effects of EGFR-PTK pathway inhibition and proteasome inhibition were shown not to be additive and inhibition of the EGFR-PTK pathway also decreased the ubiquitination of AAV2 capsid proteins. It was therefore hypothesised that in addition to its role inhibiting second strand synthesis the EGFR-PTK pathway also mediates phosphorylation of the capsid proteins at tyrosine residues of AAV particles that have escaped the late endosome, resulting in their ubiquitination and subsequent degradation in the proteasome.

To test this hypothesis Zhong et al. [187] identified seven exposed tyrosine residues on the AAV2 capsid and generated an equal number of mutant AAV2 vectors in which each tyrosine was conservatively substituted with phenylalanine (Y to F). All seven mutant vectors displayed transduction *in vitro* significantly improved over wildtype although this varied widely from < 2-fold to >11-fold depending on which residue was mutated. When tested *in*

vivo on mouse hepatocytes broadly the same pattern was apparent with an even further enhanced efficacy over wildtype AAV2. It was also shown that for the two most promising mutants (Y730F and Y444F) *in vitro* translocation of vector DNA to the nucleus was increased and ubiquitination of the capsid was reduced.

Since this initial development work, application of capsid tyrosine mutations to improve transduction efficacy or modify viral tropism has been applied to a number of different AAV serotypes with varying degrees of success [188–190]. The majority of these studies have been directed towards application within the eye, likely due to the large volume of AAV based gene therapy approaches to retinal dystrophies published to date [191].

Petrs-Silva et al. [192] examined the retinal transduction efficacy of the two most effective mutants identified from previous work (Y44xF and Y73xF) in scAAV serotypes 2, 8 and 9 following intravitreal administration in mice. In all cases ganglion cell transduction by the mutant was superior to the equivalent wildtype vector and it was claimed expression was visible across the entire retina although direct evidence of this was not shown convincingly. They also showed that AAV2/2(Y444F) was capable of mediating expression in all layers of the retina following an intravitreal injection, although again it was not made clear how widespread this transduction was. Following sub-retinal injection AAV2/8(Y733F) was shown to result in the strongest and most widespread transduction of the serotypes/mutants tested and following this route of administration both this mutant and the AAV2/2(Y444F) were shown to transduce cells in all layers of the retina, although it would appear that expression beyond the outer nuclear layer did not extend throughout the whole retina.

Kay et al. [193] further examined the potential of combined tyrosine mutant scAAVs to transduce the retina following an intravitreal injection in mice and showed a quadruple tyrosine + T491V scAAV2/2 to be by far the most effective both in terms of retinal penetration and spread of transduction, with scAAV2/5 and scAAV2/8 based mutants only mediating transduction near the optic nerve head. This led them to hypothesise that the inner limiting membrane (ILM) and the differential ability of the different serotypes to bind to it was of crucial importance. It is worth noting that these results from Kay et al. [193] are generally far less impressive than the comparable data presented by Petrs-Silva et al. [192]. Kay et al. do however include the following statement: “Due to the small size of the mouse eye, it is not uncommon for trans-scleral, intravitreal injections to result in damage to the retina that might allow delivery of some vector directly to the subretinal space” perhaps hinting at a possible explanation for this disparity.

Delivered subretinally AAV2/8(Y733F)-mediated gene delivery has also been demonstrated to rescue two mouse models of retinal degeneration. Firstly the *rd10* model of autosomal

recessive retinitis pigmentosa (RP), which carries a spontaneous mutation in the β subunit of rod cGMP-phosphodiesterase (PDEβ) [194] and secondly in a RetGC1/RetGC2 double knockout mouse model of Leber congenital amaurosis [195].

To date there is only one example of published data regarding application of these tyrosine mutants AAV vectors to the cornea, a mention in a review by Mohan et al. [196] who show a single image of extremely limited transduction of the mouse corneal endothelium *in vivo* with AAV2/8(Y733F). This data has not been subsequently published in a more comprehensive format.

1.6.2.4 Engineered capsid mutants of AAV (AAV2/6[ShH10])

This serotype of AAV is a one of the newest engineered serotypes to have been developed having been first generated and published in 2009 by Koerber et al. [197] . Rather than approaching capsid engineering from a perspective of rational design founded upon insights from AAV virology (such as that utilised to generate the Tyrosine mutants), Koerber et al. employed an approach that combined such design principles with directed evolution.

The authors first generated five highly diverse libraries (10^7) of mutant AAV capsids produced by different methodologies:

1) Random mutations within the AAV2 *cap* gene mediated by error prone PCR with staggered extension steps (AAV2-EP library).
2) Random shuffling of the *cap* genes from AAV serotypes 1, 2, 4–6, 8, and 9 resulting in hybrid *cap* genes (ShH library).
3) Insertion of a random 7 amino acid polypeptide within the heparin sulphate binding motif of AAV2 (7mer library).
4 & 5) Semi random replacement of 4 important surface loops present on the surface of AAV2.

Recombinant AAV was then generated in such a way that each virion packaged a transgene encoding its own capsid, thus allowing for linkage of successful infection with the genomic *cap* mutations responsible. The AAV libraries were subjected to 4 rounds of selection focused upon the identification of AAV mutants that favoured the transduction of glial cells by positively selecting those capsids able to mediate transduction of primary human astrocytes *in vitro*. Those capsid mutations that made it through these initial 4 rounds of selection then under went further diversification by shuffling and random mutagenesis before 1 final round of selection.

The approach generated several novel capsids that demonstrated improved levels of glial transduction both *in vitro* and *in vivo*. Some of the most promising of these capsid mutants were then specifically assessed for their ability to transduce the resident glial cell type within the eye, the Müller glia, via an intravitreal administration route [198]. Somewhat surprisingly none of the most promising candidates from the selection proved especially effective when administered via this route leading the authors to conclude that transduction was being limited by additional physiological extracellular barriers present within the retina which these variants were not selected to overcome.

A partial rescreening of the library in this new context then revealed a capsid variant (ShH10) that displayed both efficient and highly specific transduction of Müller glia from an intravitreal injection. Mutational analysis of this capsid mutant revealed ShH10 to be extremely similar to wildtype AAV2/6, differing from this parent at only 4 residues which were shown to act largely synergistically to produce the transduction observed.

At no point during this work was the capacity of any of these variants to transduce the anterior segment of the eye assessed, a perhaps logical oversight as there are no glia present within the non-neural tissues of the eye.

Due to its relative novelty, application of ShH10 to date has been extremely limited; it has thus far been utilised to promote the survival of retinal neurons via secretion of the neurotropic factor GDNF from Müller glia [153], and as a Müller cell-specific means of cytotoxic gene delivery in a study of the effects of optogenetic ablation of Müller cells upon the retina [199].

1.6.2.5 Lentiviral vectors

The lentiviruses are a genus of retroviruses characterised by and named for their long incubations periods. Uniquely among the retroviruses the lentiviruses are able to infect non-dividing cell types in addition to the tropism for mitotically active cells displayed by the rest of the family. Lentiviruses are able to transduce cells within target organs including the eye, heart, pancreas, and liver [200].

Structurally lentiviruses are one of the more complex viruses to have been utilised as a vector. The lentiviral genome constitutes two positive strand RNA molecules of between of 7 – 12 kb in length associated in a dimer. The capsid is dual layered consisting of an inner cone-shaped nucleocapsid enclosing both the genome and various proteins required post infection for replication, and an outer spherical matrix which interacts with the final component of the virion, a lipid bilayer envelope derived from the host cell's plasma

membrane and containing virally encoded glycoproteins. A single complete lentiviral virion measures around 100-120nm in diameter [201].

Genomically lentiviruses are organised around three key genes, *gag*, *pol* and *env* which encode all the major structural (*gag* and *env*) and replicative (*pol*) aspects of virus. Additionally the genome contains two regulatory genes (*tat* and *rev*) and four accessory genes (*nef*, *vif*, *vpr* and *vpu*). The genome is flanked by two long terminal repeat sequences (LTRs) which are key mediators of many aspects of the lentiviral life cycle. Other key genomic sequences are the packaging signal (ψ) and the central polypurine tract (cPPT) which is implicated in both DNA synthesis and nuclear import.

The lentivirus life cycle proceeds by the following steps:

1. **Virion binding and entry**: Mediated by interactions between viral envelope glycoproteins and receptors exposed on the host cell's surface.
2. **Reverse transcription**: Due to the requirement for DNA synthesis to be primed reverse transcription occurs via an extremely complex sequence of repeated self-priming. The following features of this process are of particular relevance:
    a. Firstly that the RNA genome packaged within the virion is in a pre-primed state, with the transfer RNA $tRNA_{lys}$ derived from the host cell bound to a specific primer binding site. Without this interaction reverse transcription cannot be initiated.
    b. During the cascade of self-priming the U3 sequence of the 3' LTR is copied to the 5' end as the original 5' proviral U3 sequence was lost during virus production. In wildtype virus the two LTRs are identical so this is of little functional significance but this feature is exploited in lentiviral vector design.
3. **Provirus trafficking and nuclear import**: Reverse transcription results in a linear dsDNA version of the lentiviral genome termed the provirus, which is then trafficked to the nucleus.
4. **Integration**: The provirus is integrated into the host gene by the viral enzyme integrase which was delivered to the host cell packaged within the capsid in association with the genome. Integration occurs semi-randomly within the genome, showing preference for genomic areas undergoing active transcription [202] and certain sequence motifs [203].
5. ***De novo* expression of virally encoded genes**: In a wildtype infection this process proceeds from the promoter activity of the 5' LTR and results in virus replication. In vectors transgene expression is under the control of an exogenous promoter forming part of the transgenic construct.

This ability of lentiviruses to integrate into the host genome is key to their utility as a vector allowing them to yield a high level, stable and long term transgene expression within actively dividing cells. Lentiviruses are the only viruses commonly used as vectors for which this is the case. Use of non-integrating vectors in dividing cell lines leads to loss of transgene expression over time due to dilution of the non-replicative transgenic construct.

Many different lentiviruses have been adapted for use as vectors including equine infectious anaemia virus (EIAV), simian immunodeficiency virus (SIV), caprine arthritis encephalitis virus (CAEV), and both bovine and feline immunodeficiency viruses (BIV / FIV). Predominant in the field however is human immunodeficiency virus type1 (HIV1).

The development of HIV1 as a vector has progressed through three main vector generations with each subsequent iteration primarily focused upon improvement of the vector's safety profile. Each generation has both removed as many viral sequences as possible from transgenic genomic constructs and provided an increasingly minimal set of viral genes in trans (via helper constructs) during production, whilst maintaining efficiency of production and vector infectivity.

All generations of lentivirus packaging systems have included the genes *gag* and *pol* as these genes encode indispensable structural and assembly functions. During vector production these functions however are provided in *trans* upon a "helper" construct which lacks the packaging signal (ψ) to ensure no HIV sequences were packaged within the vector. First generation lentivirus systems did not include the HIV1 *env* gene upon the helper plasmid but this was the only gene deleted. The second generation further improved upon biosafety by the deletion of all accessory genes from helper constructs but preserved regulatory functions provided by *tat* and *rev*, which in the third generation were separated from *gag* and *pol* being provided upon a second trans acting plasmid, in order to further minimise the risk of inadvertent packaging of complete viral functionality via unintentional recombination between a helper construct and a ψ containing plasmid [204].

As mentioned earlier, the process of reverse transcription duplicates the U3 element of 3' LTR in such a way that this sequence flanks both ends of the DNA provirus; this feature of the lifecycle has been exploited to further improve lentivector safety [205]. Transgenic vector genomic constructs carry a 3' LTR in which the U3 region has been deleted. Whilst this has no effect on the first round of viral infection or *in vitro* production once integrated into the target cell this modification eliminates the promoter activity of the 5' proviral LTR. Transcription can only therefore be initiated from a transgenic promoter inserted downstream of the ψ signal, meaning that even in the unlikely event of superinfection with wild type HIV1

the transgenic construct can never be mobilised and repackaged. Most generations of lentivirus carry this modification and are termed self-inactivating (SIN).

Few lentiviral vectors utilise the wildtype envelope genes encoded by *env*, partly for reasons of safety but also because these envelope glycoproteins would restrict vector tropism to the natural target of HIV1, CD4+ T-cells. Vectors are therefore pseudotyped with envelope proteins from other viruses and by such modification tropism can (within limits) be restricted or broadened as desired. The most commonly used envelope (VSV-G) derives from vesicular stomatitis virus as this results in a vector with a broad tropism to almost any cell type [206].

As a result of this extensive safety orientated vector engineering HIV1 based lentiviruses are in use in phase I clinical trials aiming to treat systemic disorders such as X-linked adrenoleukodystrophy [207], β-thalassaemia [208], adenosine deaminase severe combined immunodeficiency (ADA-SCID) [209], and Wiskott Aldrich Syndrome (WAS) [210].

One major concern regarding the clinical use of retroviral vectors was however highlighted within another trial for X-linked SCID utilising a gamma retroviral vector. A number of patients developed leukaemia as a result of treatment due to the malignant transformation of vector transduced cells [211]. This oncogenesis was caused by integration of the provirus into the LMO2 proto-oncogene resulting its upregulation via the promoter activity of the proviral 3' LTR. Whilst oncogenesis by this exact mechanism could not have occurred with a SIN lentivector (and no lenti related oncogenic events have thus far been reported [212]) it is still possible that disruption of the host genome by integration could lead to such deleterious effects [213].

This possibility has led to the development of a Lentiviral generation in which the integrase gene used for vector production has been rendered defective [214]. The genomes of these vectors therefore do not integrate and are maintained episomally. Although this reduces the risk of genotoxicity it also eliminates the ability of the vector to stably transduce dividing cell types and would therefore have been inapplicable to any clinical approach to date.

1.7 Gene therapy of the cornea

1.7.1 The eye as a target for gene therapy

The eye has long been considered an extremely attractive target for gene therapy [191]. Firstly the organ is eminently accessible with vector delivery to all parts of the eye being possible via minimally invasive techniques, many of which are already routine within ophthalmic surgery. This accessibility also allows for easy, non-invasive observation of the phenotypic effects of therapy *in vivo* and, due to the optical properties of the eye enabling direct observation, such assessments are often possible at a high level of detail and resolution. Indeed recent advances in imaging technology such as adaptive optics have allowed the live imaging of individual cells within the living eye [215]. The highly compartmentalised anatomy of the eye also facilitates tissue-specific vector targeting with the added advantage that several compartments of the eye such as the anterior chamber and subretinal space are also considered to be immune privileged sites [216,217]. This privilege is highlighted by remarkable success rate of corneal allografts which are both the most commonly performed transplant surgery [120] and the only such procedure that is routinely performed without graft tissue typing or systemic immunosuppression. This privileged status is the result of a combination of features such as the blood retinal barrier, a relative lack of lymphatic and/or haematic vascularisation in some ocular tissues and the presence of secreted immunomodulatory factors, all features promoting immune tolerance.

These qualities, combined with the fact that a large number of inherited retinal dystrophies have been identified and characterised, has led to the posterior segment of the eye becoming one of the predominant target tissues within the gene therapy field, with some such approaches having progressed to clinical trial [218]. Gene therapy directed at the cornea however has not seen nearly such extensive development in part due to the success enjoyed by corneal transplantation surgery for the treatment of many corneal pathologies. Transplantation is not however applicable to all disease states and graft outcomes also have the potential to be further improved by gene therapy. A substantial number of gene therapy-based approaches to the cornea have thus been developed and the subsections that follow will outline some of the notable work within the field to date.

1.7.2 Endothelium directed gene transfer

The majority of corneal endothelium-directed gene therapy approaches to date have been based upon transduction mediated by viral vectors. Certain non-viral approaches such as electroporation [219], liposomal vectors [220], polyamidoamine dendrimers [221] and synthetic peptides [222] have all been shown to transduce the endothelium although in all cases the transgene expression achieved was both of limited duration and inefficient, only transducing a very small proportion of the endothelium.

Of the commonly used viral gene therapy vectors AAV on balance appears unable to efficiently transduce the endothelium *ex vivo* [223,224], despite a single report to the contrary [225]. One study reported that whilst AAV might transduce the rabbit corneal endothelium *in vivo,* significant transgene expression was only seen in the context of severe ocular anterior segment inflammation induced by injection of lipopolysaccharide [226]. So the efficacy of gene delivery to the endothelium via AAV is somewhat unclear and has seen no application in functional transgene delivery.

Herpes simplex virus-based vectors also have not seen widespread application in gene delivery to the corneal epithelium. The level of gene delivery they can mediate in the endothelium is superior to that of AAV but is still relatively low at around 5% of cells *ex vivo* [223]. Additionally HSV based vectors are often highly immunogenic and this may be of particular concern in the cornea which is a known site of naturally pathogenic herpes simplex infections.

The majority of endothelium directed gene therapies of the cornea have therefore utilised either adenovirus or lentivirus based vectors both of which have been shown to transduce corneal endothelial cells with high efficiency. Adenoviral vectors were first demonstrated to transduce rabbit corneal endothelium with 75-100% efficiency [227] *in vivo* and later human endothelium with a similar level of efficiency *ex vivo* [151,228,229]. Similar efficacy of endothelial transduction mediated by adenovirus has also been shown almost every other animal system tested, including large animal models such as the sheep [230].

Lentiviral vectors appear equally effective having been shown to efficiently transduce the endothelium across an equally wide range of species both *in vivo* [231] and *ex vivo* [232]. Critically in regard to clinical application lentiviruses appear able to mediate a near 100% transduction of human corneal endothelium *ex vivo* [228].

Beyond demonstrating simple transduction efficacy, endothelial gene therapy has also seen application in functional gene delivery. Most such studies have constituted augmentation gene therapy approaches aiming to improve corneal graft survival, this focus being due both to the high level of clinical relevance of such a strategy and the fact that donor corneas are

commonly stored in organ culture pre-transplantation providing an ideal window of opportunity for gene therapy to be applied *ex vivo*.

Promotion of graft survival has been attempted by the direct modulation of immune mediated rejection of the graft by the gene delivery of various factors promoting immune tolerance such as IL10 [230], soluble TNF receptor [233], NGF [234] and others. Such approaches have seen some success in animal models and perhaps the most promising results having been obtained in the following studies. Klebe et al. [230] delivered the anti-inflammatory cytokine IL10 to the endothelium of donor tissue with an adenoviral vector pre-transplantation in an ovine corneal allograft model and demonstrated an improvement in the median graft survival time from 21 to 55 days with two animals demonstrating exceptional survival times of >150 days. Beutelspacher et al. [235] achieved a similar level of improvement in median graft survival time from 11 to 21 days in a murine allograft model in which indoleamine 2,3-dioxygenase, a well-known mediator of immune tolerance via the inhibition of T-cells, had been delivered via a lentivirus to the donor endothelium one hour before transplantation.

In these immune modulatory gene therapy approaches acting via secreted factors the endothelium is simply serving as an accessible, transducible site for production of transgene product, a role that could likely be equally well served by other potentially less critical or sensitive cells of the cornea such as stromal keratocytes. Of more direct relevance to the endothelium itself however are approaches that aim to improve the quality of graft tissue or prevent graft failure via gene delivery aiming to maintain or increase endothelial cell density. As discussed in 1.2.1 endothelial cell density is of critical importance to corneal transplant survival as post-operative endothelial cell loss represents a major cause of graft failure and insufficient endothelial cell density is the primary reason donor tissue is rejected for transplantation. Whilst there is general agreement that endothelial cell density decreases during organ culture, it is less clear by what mechanism the cell loss proceeds. A study by Albon et al. [236] concluded that apoptosis constituted the primary mechanism of endothelial cell loss, however a separate study by Crewe et al. [237] (which utilised a similar methodology) conversely found very little evidence of endothelial apoptosis during organ culture.

However, despite this uncertainty a number of studies have nonetheless focused upon apoptosis and thus aimed to preserve endothelial cells in donor tissue by the delivery of anti-apoptotic factors. Lentiviral delivery of one such factor, Bcl-xL to the endothelium has been shown to both inhibit experimentally induced apoptosis and improve graft survival at 8 weeks from 40% to 90% when delivered pre-transplantation in a murine allograft model [238]. Potentially even more effective than Bcl-xL when delivered by the same methodology is the

baculovirus caspase inhibitor P35 which was shown to mediate a greater anti-apoptotic effect in endothelial cells than Bcl-xL [239] and prevented experimentally induced apoptosis more effectively in human tissue stored under eyebank conditions [240].

Rather than trying to prevent cell death an alternative approach is to increase endothelial cell density directly, inducing cell replication by modulation of the cell cycle. This is possible since the naturally non-replicative endothelial cells have not completely left the cell cycle via G_0 and exist in a state of early G_1 arrest, thus retaining some proliferative potential [8]. Several studies have attempted such induction of endothelial proliferation via gene therapy and have largely focused upon overexpression of the transcription factor E2F2 which is known to regulate the transition from G_1 to S phase. Such overexpression in rabbit corneas *ex vivo* via a lipid based non-viral vector showed some signs of cell cycle progression but any increase in cell density was masked by a substantial toxic effect of the vector [241]. Subsequent studies therefore utilised an adenoviral vector for E2F2 delivery to human tissue *ex vivo* and observed a significant increase in cell density without any apparent toxicity [151].

An alternative approach to E2F2 overexpression is the RNAi mediated knockdown of p21 and p16, negative regulators G_1 progression. When tested *in vitro* upon primary endothelial cultures with small interfering RNAs delivered by electroporation cells showed signs of cell cycle progression such as Ki67 expression but as in the case of previous non-viral methods no increase in cell density could be noted due to a very high level of transfection induced cell death [242].

Gene therapy to promote endothelial cell survival or induce their replication clearly holds promise for the improvement of corneal graft quality however all such gene delivery by its very nature carries with it a substantial risk of oncogenic transformation, especially if delivered with an integrating viral vector such as lentivirus. Therefore before such an approach can see clinical application, mechanisms must be developed to substantially reduce the inherent risk.

1.7.3 Stroma directed gene transfer

Effective gene delivery to the cells of the corneal stroma has been demonstrated with a wide range of gene therapy vectors both non-viral and viral. Non-viral techniques such as electroporation [243,244], ultrasonication [245], direct injection of plasmid DNA [245,246] or nanoparticles [247] have all been shown to mediate transgene expression within the stroma, although as is often the case for such methods, transgene expression is relatively short lived in all cases. Non-viral transduction of the stroma might therefore be of useful application to

very acute conditions but is likely to be less effective in treatment of any more chronic pathology.

Adenovirus has been shown to mediate a very substantial transduction of the stroma in the mouse when delivered by intrastromal injection [248], however transgene expression was relatively short lived. Loss of expression is probably due to the immune-meditated clearance that is commonly seen with transgene delivery via adenovirus and this is likely the reason this vector has seen limited further application to the stroma.

There is only one example to be found within the literature of lentivirus mediated transduction of the stroma, Bemelmans et al. [249] compared two modes of delivery, intrastromal injection and injection into a corneal pocket created by a femtosecond laser. They showed that whilst both methods resulted in transgene expression sustained up to three weeks post injection, the corneal pocket method appeared more effective. Lentiviruses are therefore a potentially effective vector for stromal gene delivery and may merit further investigation.

Transduction of the stroma by AAV appears to be heavily serotype and context dependent. Sharma et al. examined the transduction efficacy of AAV 2/6, 2/8 and 2/9 on corneal keratocytes both *in vitro* [250] and *in vivo* [251]. The *in vitro* study on human cells found that AAV2/6 was by far the most effective mediating up to 50-fold greater transgene expression than either 2/8 or 2/9. However this finding was not translated to their *in vivo* study in which the same serotypes were applied topically to the murine stroma after epithelial debridement. In this context the order of transfection efficacy appeared to be 2/9 >2/8 > 2/6 with all serotypes exhibiting an increase in expression over time up to 30 days post injection. Sharma et al. explained this difference largely in terms of the *in vitro* vs *in vivo* although it is worth noting that a species difference was also present between the two studies.

The same group also examined the effect of stromal drying on AAV vector solution uptake and transgene expression in murine and rabbit corneas *in vivo* and human corneas *ex vivo* [252]. The technique applied was as follows: The epithelium was surgically removed and the underlying stroma was then subjected to increasingly long periods of hot air mediated drying before topical application of AAV2/8 to the stroma. It was shown that vector solution absorption and subsequent expression of transgene (14 days post vector delivery) were both increased in proportion to the period of drying; however the technique also increased the amount of inflammatory cells present in the cornea. Mohan et al. logically attributed the increase in expression to the increased absorption; however, work by Hippert et al. [253] has also shown that inflammation within the stroma can act to transiently hyper-activate AAV2/8 expression, indicating this too may have played a role. This work by Hippert et al. also

represents the longest follow-up of an AAV mediated transduction of the stroma to be found in the literature showing some level of transgene expression to be sustained for up to 17 months *in vivo* in mice.

Gene therapy of the stroma has been applied most widely to modulation of corneal keratocytes to reduce corneal scarring and opacification / haze during the process of corneal wound healing, and McDonnell et al. appear to have progressed the furthest with such an approach. Following work in which they demonstrated that herpes simplex virus (HSV) was able to transduce corneal keratocytes both *in vitro* and *in vivo* at an efficiency of around 20%-40% [254], they developed a strategy utilising a gammaretrovirus, murine leukaemia virus (MLV), to inhibit keratocyte proliferation in response to phototherapeutic keratectomy (PTK)-associated injury. The MLV vector was applied topically to the stroma after the PTK procedure had ablated the overlying epithelium. The transgene delivered was a mutant cyclin G1 designed to act in a dominant negative fashion on the endogenous protein and thus inhibit cell cycle progression. Pre-clinical work in a rabbit model showed this approach to be effective in reducing the development of corneal haze, preventing keratocyte proliferation / subepithelial fibrosis and reducing extracellular matrix protein deposition [255]. This technique subsequently progressed to a phase I/II clinical trial [256] the results of which have not yet been published.

Other gene therapies directed at the stroma (and elsewhere [257]) to ameliorate corneal scarring / fibrosis have targeted the TGF-β pathway due to the well characterised role of TGF-β1 in the differentiation of corneal keratocytes into myofibroblasts in the stromal wound healing response [42]. Mohan et al. [258] achieved a significant reduction in corneal haze and stromal structural improvement via topical stromal application of AAV2/5 delivering decorin, a small, leucine-rich proteoglycan endogenous to the stroma that has been shown to inhibit TGF-β. The same group has more recently demonstrated similar results targeting the TGF- β pathway via a different route: the delivery to the stroma of a BMP7 transgene, a factor thought to act antagonistically to TGF- β, using a non-viral nanoparticle based vector system [259].

Corneal neovascularisation is a pathology that has more commonly been targeted by gene transfer to other tissues such as the conjunctiva [260–263]. Several studies however have targeted gene transfer to the stroma to ameliorate this condition including Mohan et al. [264] who utilised exactly the same decorin based approach they previously applied to reduction of corneal fibrosis. This study demonstrated some significant inhibition of corneal

angiogenesis although the effect appeared highly localised, likely due to the means of corneal neovascular induction via a VEGF secreting implant also being highly localised.

Two studies have directly targeted the stroma for gene delivery via intrastromal injection of either naked plasmid DNA or nanoparticles. Stechschulte et al. [265] showed that the injection of plasmid DNA alone was able to rapidly lead to transgene expression across up to 50% of the stroma (as assessed by area) although this transduction was short lived having dropped to half this level by 48 hours post injection and being almost undetectable by 10 days. This gene delivery was shown to significantly inhibit angiogenesis induced by VEGF pellet implantation; however given that the therapeutic transgene's (sFlt1) mechanism of action is VEGF sequestration this result is perhaps to be expected and its relevance to more physiological neovascularisation is somewhat questionable.

Qazi et al. [266] delivered a shRNA construct targeting VEGF via intrastromal injection in the form of both naked RNA and incorporated into a poly(lactic co-glycolic acid) based nanoparticles. Angiogenesis was induced via an alkali burn and vector delivered 4 weeks later. Both methods of transgene delivery were shown to significantly reduce neovascular area although as might be expected the nanoparticle appeared the more effective. The regression of vascularisation was relative mild although critically substantial improvement was noted in the central area of the cornea most vital for vision.

Finally Yu et al. [267] did not appear to target the stroma directly in their study in which they injected adenovirus encoding the anti-angiogenic factor sFlk1 into the anterior chamber; the target tissue for gene delivery via this combination of vector / delivery route was likely the corneal endothelium. Transduction of the stroma was however claimed on the basis of immunohistological staining showing transgene product to be present within the stroma. As the transgene in question encodes a soluble factor, transduction of the stroma in this case is questionable.

1.7.4 Epithelium directed gene transfer

Gene therapy approaches directed towards the corneal epithelium to date have thus far been extremely limited with almost all such studies having limited themselves to demonstrating the transduction efficacy achievable with various vectors when delivering a marker gene, while only a very few have attempted any kind of functional gene delivery [268]. This relative lack of application in epithelial gene therapy is possibly due to the rarity of genetic diseases of the epithelium and the difficulties involved in mediating a stable gene delivery to such a highly dynamic tissue.

dIn order to effect any long term or permanent transduction of the corneal epithelium it will clearly be necessary to target limbal epithelial stem cells (LESC) for gene delivery as it is from these cells that all other epithelial cells are derived. Gene transfer to any other epithelial cell type would eventually be lost as a result of normal cell turnover. Despite its accessibility the epithelium has proven difficult to transduce due to its natural function as a barrier designed to prevent the infiltration of material such as gene therapy vectors. Many attempts to transduce the corneal epithelium have utilised non-viral vectors (reviewed in [269,270]) and very few have demonstrated any *in vivo* transduction. Most studies that have shown some level of gene delivery *in vivo* have utilised ballistic delivery via a "gene gun" [268,271] perhaps indicating the efficacy of the epithelial barrier function against less traumatic means of gene delivery. Other non-viral methods utilising a carrier peptide [272] or engineered nano-polymeric micelles [273] have also demonstrated gene delivery to the epithelium *in vivo;* in all cases however the degree of gene transfer could be characterised as relatively low.

The ability of many different viral gene therapy vectors to transduce the epithelium has also been assessed and many have demonstrated some transduction efficacy. However almost all such approaches have either been conducted *ex vivo* or utilised some means of disrupting epithelial barrier function prior to vector delivery *in vivo*. Most of the *in vivo* data shows only very limited transduction: *Herpes simplex* virus has been shown to mediate a very isolated transduction around areas of epithelial scarification made to facilitate vector access [274]. Adenovirus when applied topically to an unwounded cornea only transduced the occasional epithelial cell although gene delivery to the conjunctiva was more substantial [275]. Both adenovirus and AAV have also been applied topically to the epithelium in the context of epithelial wounding and have been found to either only infect the edges of the wound [276], or mediate a more widespread transduction [224] although in the latter case the GFP transgene was only visible upon signal amplification. The transduction of the epithelium shown *ex vivo* with both adenovirus and AAV is far more convincing with extensive epithelial transduction visible in this context without the need for any signal amplification [224]. This difference is likely due to both the increased exposure of the tissue to the vector present in the culture medium and impairment of the epithelial barrier function under organ culture conditions due to tissue oedema and the absence of the tear film.

Probably the best results to date regarding viral vector transduction of the epithelium have been achieved using lentiviral vectors. Wang et al. showed efficient gene transfer to all layers of human cornea in the context of an isolated fragment of the corneal rim *ex vivo* [277]. The duration of expression achieved is a little unclear; however, the following statement implies 60 day duration of epithelial transduction:

"Fluorescent microscopy reveals eGFP expression in endothelial and epithelial cells by 3 post- transduction days in situ*. This pattern of expression was undiminished for the duration of organ culture (60 days)."*

Whilst the figures included do show endothelial transduction at the 60 day time point the figures shown for the epithelium state they were taken at 3 days in the legend (7 days in the text). The claim of lasting transduction of the epithelium is therefore somewhat dubious. More convincing data was presented by Igarashi et al. who after inflicting an epithelial wound at the limbus applied topically adenoviral, AAV or lentiviral vectors encoding eGFP. Whilst transgene expression from adenovirus and AAV was lost within 2 weeks, lentiviral transduction was shown to be sustained for up to 6 weeks.

Igarashi et al. claim that a 6 week duration of expression is sufficient to indicate LESC transduction although we feel this is an insufficient period of follow-up to rule out the possibility of transduction being limited to transient amplifying cells (TACs) as it has been shown to take up to 10 weeks for labelled cells to migrate from the limbal to central cornea [90]. Igarashi et al. also did not show any evidence of such centripetal migration of labelled cells that would be expected to result from either LESC or TAC transduction over a 6 week period. Irrespective of the interpretation of their results though Igarashi et al's study does represent the sole example of any form of sustained epithelial gene delivery via any method shown to last beyond the very short term.

1.8 Overall aims

This thesis will describe a program of work aiming to further develop viral gene therapy approaches to the three cellular layers of the cornea, with particular emphasis upon the application of novel vector technologies.

- In regard to the endothelium work will be directed toward improving the safety profile of gene transfer with potential application to increase endothelial cell density via cell cycle manipulation.
- In the stroma work will be undertaken to develop and characterise an AAV based gene augmentation approach to prevent corneal neovascularisation.
- To date no effective method exists by which to mediate a long lasting gene transfer to the epithelium, work here will aim to develop such a method based upon transduction of LESCs with an integrating lentiviral vector.

2. Materials and Methods

2.1 Molecular biology

2.1.1 General cloning strategy

Wherever possible cloning was achieved by excising the insert fragment and opening the backbone vector with restriction enzymes that created mutually compatible “sticky ends” to facilitate easy ligation in the correct orientation. If this was not possible one following alternative approaches was taken:

- More suitable sites introduced using site directed mutagenesis.
- Blunting of digestion products using Klenow DNA polymerase to fill in 5’ overhangs.

All cloning products were validated by both diagnostic restriction enzyme digests and sequencing. Concentration of all DNA was measured by photospectroscopy at 260 nm using a NanoDrop ND1000 Spectrophotometer (LabTech Int.)

2.1.2 Restriction digests

To characterize DNA plasmids or fragments, or to isolate fragments of interest, DNA was selectively cut using restriction enzymes (Promega, or New England Biolabs,). The following digestion mix formulation was typical:

0.5 – 1 µg of DNA

0.5 µL of each restriction enzyme (10 U/µL)

1.6 µL of appropriate 10x Buffer

1.6 µL of 10x BSA

Sterile, deionized water added to a total volume of 16 µL

The mix was incubated for 2-4 hours at the recommended temperature.

In the case of double digests using enzymes requiring different buffer conditions a sequential digest was performed. The first digest was performed as above and following digestion ethanol precipitation was performed by addition of 3.2 µL of 3M sodium acetate (in dH_2O) and 40 µL of 100% Ethanol. This was thoroughly mixed before being spun in a microcentrifuge at 20,000g for 30 minutes. Supernatant was discarded and pellet washed

with 50 µL of 70% ethanol before being respun at 20,000g for 10 minutes. Supernatant was discarded and pellet resuspended in 10 µL of dH_2O. This was used as the DNA for digestion by the next restriction enzyme.

2.1.3 DNA electrophoresis and gel extraction of DNA

DNA fragments resulting from restriction enzyme digests were separated by size as follows:

Samples of 16 µL had 4 µL of loading dye (Blue/Orange Loading Dye, 6x: Promega) added to them before being loaded on to a 1-2 % (w/v) agarose gel prepared in 1 x TBE buffer containing ethidium bromide (1 µL of 10 mg/mL EtBr per 50 mL of gel). A 1 kb or 100 bp DNA ladder (Promega) was run alongside to evaluate the size of the fragments.

For a 200-250 mL gel volume, a voltage of 180 V was applied across the gel for 30 to 120 min, according to the expected size of the DNA bands. Gels were photographed digitally on an ultraviolet transilluminator (BioRad).

When required for cloning DNA fragments were excised from the gel and extracted using a using silica gel based purification kit (QIAquick Gel Extraction Kit: Qiagen) according to the manufacturer's instructions.

2.1.4 DNA ligation

Ligation of the gel purified DNA fragments into the appropriate vector backbone was performed using 1:5 – 1:20 molar ratio of backbone to insert. DNA was first heated to 45 °C for 5 minutes to melt any annealed cohesive ends, and then rapidly cooled on ice.

Ligations were performed in a mix formulated as follows:

4 µL of DNA (insert and backbone in appropriate ratio)

5 µL of 2x Ligation Buffer (LigaFast: Promega)

1 µL of T4 DNA Ligase (3U/mL, LigaFast: Promega)

Ligations were then incubated overnight at 4 °C after which the ligase was heat inactivated for 10 minutes at 65 °C. The entire ligation mixture was then used to transform competent bacterial cells.

2.1.5 Transformation of bacteria with DNA

All plasmids used contained one or more antibiotic resistance genes as a selection marker for successfully transformed bacteria.

For transformation, chemically competent DH5α cells (α-Select, Bioline) from -80 °C were thawed on wet ice. 50 µL of cells were incubated with 5 -10 µL DNA to be transformed for 30 min. on ice. Cells were heated shock for 60 seconds at 42 °C in a heat block then returned to ice for 5 min. 1 mL SOC medium (Invitrogen) was added and cells were incubated for 1 hour at 37 °C to allow sufficient expression of the resistance gene. Bacteria were then plated on lysogeny broth (LB) 10 cm agar plates containing the appropriate antibiotic(s) and incubated at 37 °C overnight.

Bacterial colonies were then picked using a sterile pipette tip and DNA was amplified and extracted at the mini-prep scale for analysis by diagnostic restriction enzyme digests and sequencing. Clones containing the desired plasmid products were prepared as Glycerol stocks for long term storage at -80 °C

2.1.6 Amplification of plasmid DNA in bacteria

When required, all plasmids were amplified from frozen transformed bacterial stock in LB medium (supplemented with appropriate antibiotic(s)) at a variety of scales depending on application. Scales and kits used are listed below; all kits used according to manufactures instructions.

5-10 mL of bacterial culture - GenElute Plasmid Miniprep Kit, Sigma-Aldrich

50-200 mL of bacterial culture - GenElute Plasmid Maxiprep Kit, Sigma-Aldrich

500-1000mL of bacterial culture - EndoFree Plasmid Megaprep Kit, Qiagen

2.1.7 Sequencing of plasmid DNA

Plasmid DNA prepared at the mini scale was used for sequencing.

All primers were designed by hand and synthesized by Sigma-Aldrich. Enough primers were designed/used so as to give a complete sequencing read (with sizable overlaps) through the entire region of interest within the plasmid. Regions of interest ranged in size from an entire viral genome to a single ligation site. Sequencing reactions were formulated as below:

1µL of Primer (3 µM)

1µL of Big Dye3.1 dNTP mixture (Applied Biosystems)

3.5 µL of Sequencing Buffer (Applied Biosystems)

6 µL of DNA (10-300ng / µL)

8.5 µL of dH_2O

Sequencing reaction was performed in a PCR machine on the following cycle:

96°C 1 min.

96°C 10 sec.
50°C 10 sec. } x35 cycles

60°C 4 min.

4°C Hold until clean up.

After this reaction the labelled DNA was cleaned up as follows:

To each sample was added:

0.5 µL of 0.5mM EDTA pH8

2 µL of 3M CH_3COONa pH5.2

50 µL of 100% Ethanol

This was incubated at room temperature, covered with foil for 15 min. before spinning down the DNA in a microcentrifuge at 20,000g for 30 min. Supernatant was discarded and 70 µL of 70% EtOH added. This was then spun down again at 20,000g for 15 min. Supernatant was discarded as before and the pellet dried at 65°C for 30 minutes covered with foil before resuspension in 13 µL of deionised formamide and loading onto a sequencing plate.

Sequencing was then run on a 3730 DNA Analyser (Applied Biosystems), traces analysed and contigs constructed using CodonCode Aligner.

2.1.8 Site directed mutagenesis

All site directed mutagenesis of plasmid DNA was performed using the Quikchange Lightening Kit (Agilent Technologies) according to the manufacturer's instructions. Primers used with this kit were designed by hand and synthesized by Sigma-Aldrich.

2.1.9 Polymerase chain reaction (PCR)

Primers for PCR reactions were designed either by using by PrimerSelect software, version 7.0.1 (DNAStar) or by hand. All primers used shown in (2.1.10). A standard PCR reaction mix (25 µL total volume) consisted of the following components:

2.5 µL 10x buffer

2.5 µL MgCl2 (25 mM)

1 µL dNTP mix (10 mM)

1 µL of each forward and reverse primer (10 µM)

0.5 – 1 µL polymerase enzyme (GoTaq DNA polymerase, 5 U/µL, Promega),

10 – 20ng template DNA from plasmid (50 – 100ng for genomic DNA)

dH_2O to make up 25 µL.

For all reactions a negative control with dH2O instead of the template was run alongside. Typical PCR cycling conditions were:

95°C	1 min.	-	Initial Denaturation
95°C	30 sec.		
50-60°C	30 sec.	x35 Cycles	
72°C	1 min.		
4°C		-	Hold until analysis

For use in cloning products of PCR were split, with a sample being analysed and validated by electrophoresis (2.1.3) and the remainder being purified by ethanol precipitation before use in cloning steps.

2.1.10 Primers used in PCR, sequencing and site directed mutagenesis

Name	Sequence 5' to 3'	Intended use
MB-MidLUC2-F	GCATGTACACCTTCGTGAC	Sequencing Primer binding to LUC2
MB-MidLUC2-R	GTCACGAAGGTGTACATGC	Sequencing Primer binding to LUC2
MB-StaLUC2-R	CTTCATGGCTTTGTGCAGCTGC	Sequencing Primer binding to LUC2
MB-SFFV-R	GTCATTTCAGGTCCTTGG	Sequencing Primer binding to SFFV
MB-SFFV-F	CCAAGGACCTGAAATGAC	Sequencing Primer binding to SFFV
MB-SFFV2-F	CTTCCCGAGCTCTATAAAAG	Sequencing Primer binding to SFFV
MB-WPRE-1F	GACAATTCCGTGGTGTTG	Sequencing Primer binding to WPRE
MB-WPRE-1R	CAACACCACGGAATTGTC	Sequencing Primer binding to WPRE
PBKOMUTGEN01	GACCCTTTTAGTCAGTGTGGAAAATCTCTAGCTTGAAAGCGAAAGGGAAACAAGAGGAG	Mutagenesis Primer to remove lenti Primer binding site.
PBKOMUTGEN01-RC	CTCCTCTTGTTTCCCTTTCGCTTTCAAGCTAGAGATTTTCCACACTGACTAAAAGGGTC	Mutagenesis Primer to remove lenti Primer binding site.
SALIKOMUTGEN	GCGACTCTAGAGTCAACCTGCAGGCATGCAAG	Mutagenesis Primer to remove SalI site.
SALIKOMUTGEN-RC	CTTGCATGCCTGCAGGTTGACTCTAGAGTCGC	Mutagenesis Primer to remove SalI site.
PCRRRE-F1	CAGTCGACGATAGAGGAAGAGCAAAACAAAAGTAAG	PCR Primer to amplify lenti RRE
PCRRRE-F2	CAGTCGACCAAGCGGCCGCTGATCTTC	PCR Primer to amplify lenti RRE
PCRRRE-R	CAGTCGACGTCCCACTCCATCCAGGTCG	PCR Primer to amplify lenti RRE
END-R2	CACATACGATTTAGGTGAC	Sequencing Primer binding to lenti backbone

2.2 Cell culture and virus production, purification and validation

2.2.1 Cell culture

All cells used *in vitro* were either HEK-293T (293T) or HeLa cells both of which were grown and maintained as follows. Cells were maintained in DMEM supplemented with 10 % FCS, 100 U/mL penicillin G, 100µg/mL streptomycin, and 0.25µg/mL amphotericin B (all Invitrogen). This medium will be referred to henceforth as "D10". To keep cells healthy and their transfection efficacy high cells were split frequently three times a week at a ratio of 1:3 to 1:5, and were not grown above 90% confluency.

All viruses were produced by transient transfection of 293T cells and for virus production purposes cells were only used between passages 10 and 24 and grown on 150cm^2 plates (Nunclon Surface, Nunc), for other purposes growth format varied.

2.2.2 Adeno-associated virus production (all serotypes)

All serotypes of adeno-associated virus (AAV) were produced by transient transfection of 293T cells using a three plasmid system and then purified by FPLC. Plasmids where as follows:

Viral Genomic plasmid based upon pd10 backbone. This plasmid contains the viral genome to be packaged sandwiched between AAV2 based inverted terminal repeat sequences. Providing this plasmid in *trans* to the replication and packaging genes minimizes the risk of generating replication competent viral particles.

Packaging Plasmid. This plasmid contains the AAV2 Rep78 gene and Viral Capsid gene. The viral capsid gene will depend upon the serotype of AAV being produced. Different packaging plasmids are used to produce different AAV serotypes.

Helper Plasmid (pHGTI-Adeno1). This plasmid contains 3 large chunks of the Adenovirus 4 genome ligated together. This plasmid provides all the adenovirus genes that AAV requires to package and assemble.

The day before transfection, cells in 150cm^2 plates at 80-90% confluency were split 1:2 in 20 mL of D10. A typical AAV production batch consisted of 10-20 x 150cm^2 plates.

Cells were transfected using polyethylenimine (PEI) at a PEI to DNA ratio of 2.25 : 1 (w/w). Linear PEI (MW 40,000, Polysciences) was prepared at 2 mg/mL in H_2O, adjusted to pH 7.4 with HCl, and stored at -80 °C.

Per 150 cm^2 plate the following transfection mix was made:

> A total of 50 µg of total plasmid DNA with the 3 plasmids in the ratio 1:1:3, Genome : Packaging : Helper.
>
> PEI in the ratio of 2.25:1, PEI : DNA by µg
>
> 2.5 mL of DMEM (no supplements)

Transfection mix was mixed and incubated at room temperature for 15 min to allow DNA/PEI complex formation. This mix was then added to the plates drop-wise.

Transfections were left for a minimum of 4hrs to a maximum of overnight, medium was then replaced with 15 mL of fresh D10.

Cells were physically detached from the plates 72hrs after transfection by scraping and collected suspended in their growth medium. Cells were then pelleted at ~1000g for 10 minutes in a centrifuge. Supernatant medium was then discarded and the cell pellet resuspended in Tris density buffer at a concentration of 0.5-1 plates of cells / mL.

Cells were then lysed to release the AAV virions, by 4 cycles of Freeze / Thaw / Vortex as follows:

Freeze – 20 min. in Dry Ice / Isopropanol Bath at -77°C

Thaw – 20 min. in Water Bath at 37°C

Vortex – 10 min. at full speed

Any non-packaged DNA remaining in the cell lysate was destroyed by digestion with Benzonase (Sigma-Aldrich) which was added to the lysate to a working concentration of 50U/mL and incubated at 37°C for 30 minutes.

Before purification by FPLC cell lysate was clarified by centrifugation and filtration as follows:

Spun at 3220g for 10 minutes, pellet discarded.

Spun at 7500g for 15 minutes, pellet discarded.

Syringe filter 5µM dead-end.

Spun at 7500g for 15 minutes, pellet discarded.

Syringe filter 0.45µM dead-end.

Syringe filter 0.22µM dead-end.

Spun at 20,000g for 30 minutes, pellet discarded.

Clarified Lysate was then purified by a 2 step FPLC procedure performed on an AKTA Pure (GE Healthcare) FPLC machine using pre-programmed protocols.

The lysate was first run upon a large (~400 mL column volume) size exclusion column (Sephacryl S300HR, GE Life Sciences) and the first peak collected, this contains all material larger than $1.5x10^6$ Da including the AAV virions.

This peak was them loaded upon a (10 mL column volume) strong anion exchange column (Poros HQ50, Invitrogen) and the material that eluted from this column at a NaCl concentration between 0.045M and 0.18M was collected.

This eluate was them concentrated down to a volume of 200 µL by centrifugation at 5000g in a 10,000 MW cut off Vivaspin 4 centrifugal concentrator (GE Healthcare), 2 mL of PBS-MK was then added (to dilute out high salt elution buffer) and the eluate re-concentrated back to ~200µL using the same concentrator.

This material constituted the purified AAV virus and was aliquoted as appropriate and stored at -80°C

2.2.3 Titering of AAV

Purified AAV was titered using a genomic dot blot. Different amounts of purified virus (1 µL and 3 µL were typical) were first digested with Proteinase K to release the viral genomes from the capsid. Digests formulated as follows and incubated at 56°C for ~2 hours

100 µL – 2x Proteinase K Buffer

1 or 3 µL – Virus

98 or 96 µL – dH_2O

1 µL – Proteinase K (10mg/mL)

The released genomes were then precipitated by addition of 0.1 volume 3M NaOAc and 2.5 volumes of ethanol and pelleted by centrifugation at 20,000g for 30 minutes. DNA pellet was then resuspended in 200 µL of 0.4M NaOH + 10mM EDTA.

A 10-fold standard series was also prepared from the genomic plasmid used to produce the virus. The highest standard was calculated to contain 10^{12} copies of the plasmid; each standard was also prepared in 200 µL of 0.4M NaOH + 10mM EDTA.

Both samples and standards were then denatured at 95°C in a heat block for 10 minutes and then stored on ice before being blotted onto a Hybond N+ membrane (Amersham) using the dotblot apparatus (Bio-Rad). The membrane was then dried, before being wetted with Hybridisation Buffer (Church mix) and incubated in a hybridisation oven at 65°C with a biotinylated DNA probe specific for a sequence contained within the genome for at least 16hrs. Probe was made using NEBlot Phototope labelling kit, used according to manufacturer's instructions.

Probe binding was then visualised by chemiluminescence using a NEBlot Phototope detection kit according to manufacturer's instructions and quantified using densometery (using Image-J, NIH) of images taken using a FujiFilm Intelligent Dark Box 2. Virus titre was then calculated by comparing integrated density of samples against standards.

2.2.4 Lentivirus (VSV-G envelope) production

HIV1 based lentiviral vectors were produced using a second generation system, to minimize the risk of generating replication competent viral particles. Plasmids where as follows:

1) As packaging (helper) plasmid, pCMVR8.74 (11.921 bp) was used delivering *gag, pol, tat,* and *rev* (HIV accessory genes having been deleted or inactivated).

pCMVR8.74 is a derivative of pCMVR8.91, in which a splice donor site has been deleted from the CMV derived region upstream of the HIV sequences to optimize expression.

2) The envelope plasmid pMD2.G (5824 bp) was used to pseudotype the virus with the vesicular stomatitis virus G envelope (VSV-G).
3) The standard genome vector was based on the self-inactivating lentiviral vector, pHR'SIN-cPPT. It contains the 5' and 3' LTR sequences and central polypurine tract (cPPT) fragment from wild type HIV1 virus. To mediate self-inactivation (SIN), the U3 region of the 3' LTR is deleted. The transgene delivered by the vector was under the control of a promoter based upon the U3 region of the spleen focus forming virus (SFFV) long terminal repeat sequence. The transgene was flanked downstream by the enhancer, woodchuck hepatitis virus posttranscriptional regulatory element (WPRE).

Three days before transfection, cells were seeded at a density of 2.5×10^6 cells per 150 cm^2 plate in 25 mL of D10 medium. This is roughly equivalent to a 1:7 split of a near confluent 150 cm^2 plate. A typical production consisted of 16 x 150cm^2 plates.

Medium was changed one hour before transfection. Cells were transfected using polyethylenimine (PEI) at a PEI to DNA ratio of 2.25 : 1 (w/w). Linear PEI (MW 40,000, Polysciences) was prepared at 2 mg/mL in H_2O, adjusted to pH 7.4 with HCl, and stored at -80 °C

Per 150 cm^2 plate the following transfection mix was made:

A total of 80µg of plasmid DNA with the 3 plasmids in the ratio 50 : 17.5 : 32.5, Genome : Envelope : Helper.

PEI in the ratio of 2.25:1, PEI : DNA by µg

1.3 mLs of OPTIMEM (no supplements)

Transfection mix was mixed and incubated at room temperature for 15 min. to allow DNA/PEI complex formation and was added drop wise to the 150cm^2 plates containing the cells in 20 mLs of D10.

After 4-6 hours of transfection, medium was replaced with 22 mL of fresh D10. Culture medium was harvested 48 hours post transfection and immediately replaced with fresh medium for a second harvest at 72 hours.

Virus was purified and concentrated from supernatant medium by centrifugation and filtering. First the medium was spun 3500g for 10 min. to pellet larger cell debris before supernatant

was passed through a vacuum driven 0.45µm filter (Stericup-HV PVSF 500mL, Millipore) to remove finer contaminants.

Filtrate was then transferred into polyallomer ultra-centrifuge tubes (UltraClear, 38.5 mL, Beckman Coulter) and ultra-centrifuged at 23,000 rpm for 1 hour 45 min. (rotor SW 32 Ti, Beckman Coulter), corresponding to an average relative centrifugation force of ~90,000 g. In the safety cabinet the supernatant was decanted off and the tubes maintained upside down on tissue paper to drain the remaining supernatant. The last drops around the rim were dried with tissue paper. 100 µL of OptiMEM were added to each tube (6 tubes was usual for a 16 plate prep), pipetted up and down carefully ten times to dislodge the pellet. Tubes were sealed with parafilm and left on ice for 45 min. to allow virus resuspension. After pipetting another ten times, all tubes were pooled and mixed. A final clarifying centrifugation step (10 min at 3220g) was only done when a higher purity of virus was required, as this resulted in a lower yield.

Aliquots of concentrated virus were stored at –80 °C. The average yield of a 16 plate virus preparation was approximately 600 µL of concentrated virus of 10^7 to 10^8 infectious particles per mL.

For production of LeGO lentiviruses this procedure was identical but transformed bacterial stocks of the three LeGO genomic plasmids was purchased from Addgene.

2.2.5 Titering and validation of lentivirus

All lentiviral vectors produced contained a reporter gene by which the virus' infectivity could be assessed.

For vectors containing fluorescent proteins, the infectious titre (infectious viral particles per mL of virus preparation) was determined by counting fluorescent protein positive cells post infection. 293T cells were seeded at 50,000 cells per well in a 24 well plate one day before infection. In duplicate, a 10 fold dilution series of concentrated virus was prepared in D10 and added to the cells in such a way that the highest dilution was equivalent to 1 uL Virus / well (containing cells and 1 mL of D10).

Virus dilutions were incubated with the cells for 3 days. Medium was then replaced with 2% PFA and the number of fluorescent protein positive cells per well counted under an inverted microscope (Axio Observer.Z1, Zeiss, 10x objective). As lentivirus is integrating multiple cells in contact with each other were counted as a single infection event. Counts for duplicate dilutions were averaged and the infectious titre was calculated.

For vectors containing Luciferase a similar methodology was used. Instead of counting fluorescent protein positivity, cells in each well were instead lysed with 150 uL of GloLysis Buffer (Promega). This lysate was then assessed for presence of Luciferase using BrightGlo (Promega) substrate mixed 1:1 with the lysate. Emission of Light was quantified 6 minutes after addition of the substrate using a TD20/20 Luminometer (Promega).

The last dilution at which the Luciferase was detectable above background was used to calculate infectious titre.

2.3 Animal experiments and surgery

2.3.1 Animals (mice)

All mice used were of the strain C57Bl/6J and were housed in University College London facilities. All animal experiments were conducted according to the ARVO Statement for the Use of Animals for Vision and Ophthalmic Research.

2.3.2 Anaesthesia

Animals were anaesthetised using a mixture of medetomidine hydrochloride (1 mg/mL, Domitor, Pfizer Pharmaceuticals) and ketamine (100 mg/mL, Fort Dodge Animal Health) and sterile water in the ratio 5:3:42. Adult mice weighing 20g received an intraperitoneal injection of 0.2 mL. After the surgical procedure, anaesthesia was reversed with 0.2 mL of intraperitoneal atipamezole hydrochloride (0.10 mg/mL, Antisedan, Pfizer Pharmaceuticals).

2.3.3 Intrastromal injection of vectors (mouse, *in vivo*)

Intrastromal injections were performed under general anaesthesia under an operating microscope. The eye was held in place by holding extraocular muscle or conjunctiva with corneal notched forceps (Acrofine). Vector or control solution was injected with a 34 gauge hypodermic needle mounted on a 5 µL Hamilton syringe (Hamilton).

The tip of the needle (bevel up) was positioned about a half, to quarter of the corneal radius in from limbus and penetrated the cornea in this position. The needle was then carefully pushed into the cornea (taking care not to penetrate through the cornea into the anterior chamber) towards the centre of the cornea (Schematic of injection route shown in Figure 3B). Once the needle tip was positioned centrally within the stroma 2µL of purified virus or control solution was injected. Upon injection the cornea became opaque in the area of the injected bleb (usually extending over the whole cornea), this was completely resolved 48hrs post injection. After treatment, 1 % chloramphenicol ointment (FDC International) was carefully applied topically to the cornea and anaesthesia reversed.

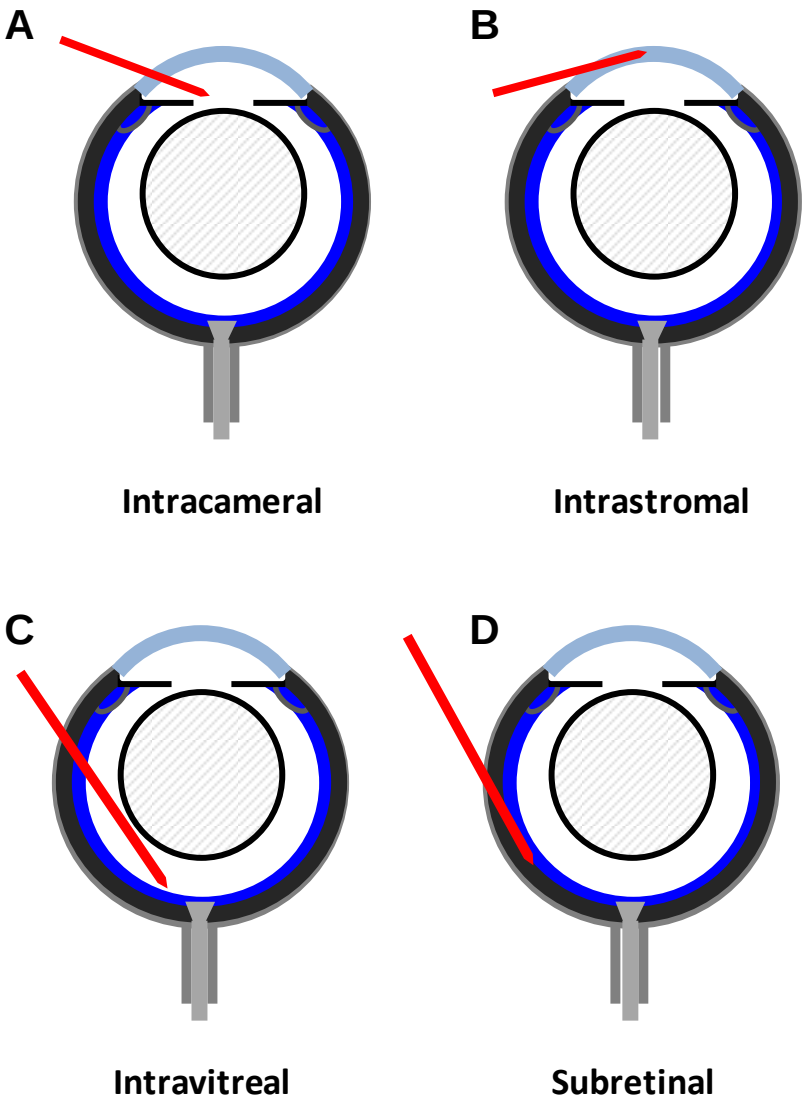

Figure 3. ***Schematic representation of different routes of injection used* in vivo *upon the murine eye***

2.3.4 Intrastromal injection of vectors (human, *ex vivo*)

Intrastromal injections were performed upon human corneal tissue obtained from Moorfields eye bank, for this procedure only cultured donor corneas (as described in 2.4.2) could be used. Corneas were stored in Culture Medium I w/o dextran T500 (BiochromAG) at 37°C until use.

The procedure was undertaken using a plastic artificial anterior chamber (Barron) to secure the cornea for injection. These devices are designed as a disposable, sterile medical device but for this purpose reuse of the same device was deemed to be acceptable. Between uses the device was stored disassembled and submerged in 70% IMS.

The device was prepared as follows. It was removed from storage under 70% IMS and sterile MilliQ dH_2O was used to both rinse it thoroughly and flush out the two injection ports in the base. Syringes (2mL) containing sterile dPBS were then attached to the two injection ports and both lines were filled with dPBS they formed a continuous circuit via a droplet on the top of the base. A small blob of Viscotears (Novartis Pharmaceuticals) was then placed on top of the dPBS droplet. The cornea was then placed on top of the device taking care to form a connection with the liquid droplets that excluded any air bubbles. The tissue retainer was then placed in position and the locking ring attached and secured.

With both clips in the injection tubes unfastened dPBS was slowly injected through one of the ports to check for leaks, if the circuit was sealed then depressing one syringe would result in fluid flowing into the other. If the system leaked then cornea's position was adjusted until it did not. Once a sealed circuit was established one of the injection tube clips was fastened and the opposing syringe used to carefully inject dPBS into the device increase the pressure within and "inflating" the cornea. Pressure was monitored by assessing resistance upon gentle depression of the corneal surface. Once an approximately physiological pressure was obtained dPBS injection was stopped and the remaining injection tube clip was fastened.

Intra stromal injection of vector or control solution was then performed using a ½ cc Tuberculin syringe with permanently attached 27G x ½ in. needle and an operating microscope. The tip of the needle (bevel up) was positioned about a half, to quarter of the corneal radius in from limbus and penetrated the cornea in this position. The needle was then carefully pushed into the cornea (taking care not to penetrate through the cornea into the artificial anterior chamber device) towards the centre of the cornea. Once the needle tip was positioned centrally within the stroma 50 µL of purified virus or control solution was injected. Upon injection the cornea became opaque and in the area of the injected bleb and this was completely resolved 48hrs post injection.

After injection the cornea was returned to Culture Medium I and incubated at 37°C / 5% CO_2 until further use / analysis. The artificial anterior chamber was thoroughly washed and flushed out with sterile MilliQ dH_2O and then stored under 70% IMS.

2.3.5 Limbal intrastromal and subepithelial injection of vectors (mouse, *in vivo*)

Limbal intrastromal and subepithelial injections were performed under general anaesthesia using an operating microscope. The eye was mildly prolapsed and secured in position with an elasticated Vinyl drape.

Virus or control solutions were injected using a glass needle pulled from borosilicate glass capillaries (1.0mm O.D. x 0.78mm I.D. – Harvard Apparatus) and an injection holder set (IM-H1 Narishige). The exact specifications of the needle varied between experiments. Flow of solution to be injected was continuous through the needle, driven by air pressure applied from a 50 mL Luer Lock Syringe compressed to the 5 mL position. For this reason no exact volume per injection could be recorded. Whilst solution was flowing the multiple injections were performed (~30-50) around the entire limbal region of the cornea. To achieve this, the mouse was rotated whilst the needle remained in essentially the same position. The needle tip was placed at different depths within the cornea to vary between limbal intrastromal and subepithelial injection, assessment of depth was guided by the feel and resistance of the tissue to the needle tip. All injections of this type were performed by Dr Satoshi Kawasaki (Kyoto Prefectural University of Medicine). After injections were complete, 1 % chloramphenicol ointment (FDC International) was carefully applied topically on the cornea and anaesthesia reversed.

2.3.6 Subretinal injection of vectors (mouse, *in vivo*)

Subretinal injections were performed under general anaesthesia using an operating microscope. The eye to be injected was dilated by topical application of tropicamide 1% (Chauvin Pharmaceuticals). Corneal refractive power was neutralized by placing a 5 mm coverslip on the cornea covered with a coupling medium solution (Viscotears, Novartis Pharmaceuticals) and the fundus brought into focus. The eye was secured in position by grasping the conjunctiva using corneal notched forceps (Acrofine). A 10mm, 34 gauge needle mounted on a 5 µL Hamilton syringe (Hamilton) was used to inject material subretinally. The tip of the needle was placed underneath the cover slip and penetrated the eye tangentially through the sclera below the equator of the globe into the subretinal space. The needle tip could be observed entering the eye and guided into position in the subretinal space using the microscope (Schematic of injection route shown in Figure 3D). Material was then injected and a retinal detachment could be observed to develop. The needle was then withdrawn and any reflux of material out through the needle tract was noted, although this was a rare occurrence. After injection, 1 % chloramphenicol ointment (FDC International) was carefully applied topically on the cornea and anaesthesia reversed.

2.3.7 Intravitreal injection of vectors (mouse, *in vivo*)

Intravitreal injections were performed under general anaesthesia using an operating microscope. The eye to be injected was dilated by topical application of tropicamide 1%

(Chauvin Pharmaceuticals). Corneal refractive power was neutralized by placing a 5 mm coverslip on the cornea covered with a coupling medium solution (Viscotears, Novartis Pharmaceuticals) and the fundus brought into focus. The eye was secured in position by grasping the conjunctiva using corneal notched forceps (Acrofine). A 10mm, 34 gauge needle mounted on a 5 µL Hamilton syringe (Hamilton) was used to inject material intravitreally. The tip of the needle was placed underneath the cover slip and penetrated the eye tangentially through the sclera just below the limbus just above the edge of peripheral retina. The needle tip could be observed entering the eye and guided into a position as close as possible to the optic nerve head within the vitreous, whilst taking care not to touch the lens at any point (Schematic of injection route shown in Figure 3C). Material was then injected and the needle withdrawn. After injection, 1 % chloramphenicol ointment (FDC International, UK) was carefully applied topically on the cornea and anaesthesia reversed.

2.3.8 Intracameral injection of vectors (mouse, *in vivo*)

Intracameral injections were performed under general anaesthesia using an operating microscope. The eye to be injected was dilated by topical application of tropicamide 1% (Chauvin Pharmaceuticals). The eye was secured in position by grasping the conjunctiva using corneal notched forceps (Acrofine). A 10mm, 34 gauge needle mounted on a 5 µL Hamilton syringe (Hamilton) was used to inject material intracamerally. The tip of the needle was positioned on the cornea about a third of the cornea's radius in from the limbus. The needle penetrated the anterior chamber tangentially through the cornea in this position. The needle tip could be observed entering the anterior chamber and guided into a central position beneath the cornea, taking care not to touch the iris (Schematic of injection route shown in Figure 3A). Material was then injected and the needle was then withdrawn. Reflux of liquid out of the injection tract was a relatively common occurrence. After injection, 1 % chloramphenicol ointment (FDC International, UK) was carefully applied topically on the cornea and anaesthesia reversed.

2.3.9 Induction of corneal neovascularisation by placement of corneal sutures (mouse, *in vivo*)

Corneal sutures were placed under general anaesthesia using an operating microscope. The eye to be sutured was dilated by topical application of tropicamide 1% (Chauvin Pharmaceuticals) and mildly prolapsed and secured in position with an elasticated Vinyl drape. Suturing was performed using a 6.5mm, 3/8 circle, spatula, advanced micro-point

double needle with attached 11-0 nylon (non-absorbable) thread (Ethilon), the needle being held with a needle holder. Sutures were placed by penetrating the full thickness of the cornea as close to the limbus as possible with the needle. The needle tip was then moved within the anterior chamber, taking care not to damage the iris, until positioned beneath the central cornea. Once in position the needle was pushed back through the cornea and out of the eye. Nylon thread was then drawn through the tract created by the needle until only a small length (2 – 3 cm) was left protruding from the limbal entrance to the suture tract.

Suture was then tied and secured with a 2-1-1 knot taking care not to over tighten and deform the cornea. Sutures were not buried and a small length (3-5mm) protruding from the knot was left to aid with suture removal at a later date if required.

The following factors were revealed as critical to inducing a high level of neovascularisation.

- Initial penetration of the cornea as close to the limbus as possible.
- Full thickness penetration of the cornea. During initial test phase of the procedure the needle tract passed within the cornea and not penetrate the anterior chamber. This approach did not induce neovascularisation reliably.
- Sutures should be as long as possible; from limbus to central cornea. Shorter sutures did not induce neovascularisation reliably.

Figure 4 below illustrates how sutures (in red) were placed:

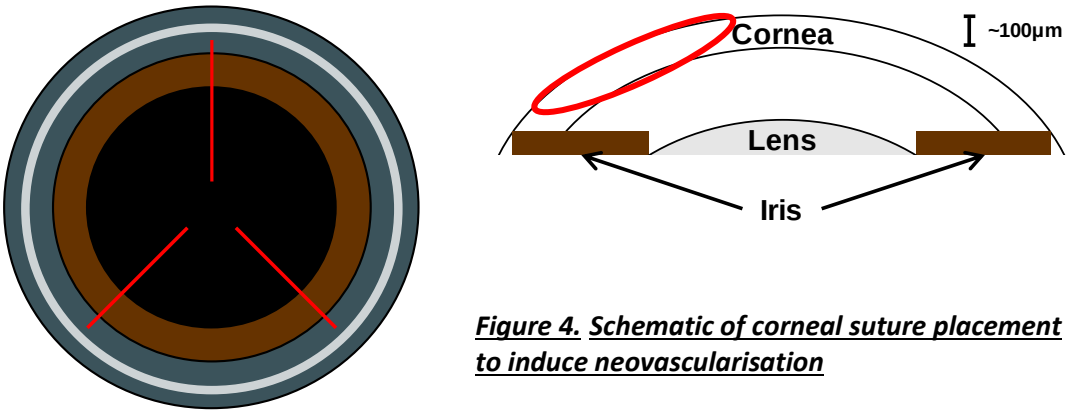

Figure 4. Schematic of corneal suture placement to induce neovascularisation

After suturing, 1 % chloramphenicol ointment (FDC International) was carefully applied topically on the cornea and anaesthesia reversed. Over the following 2 weeks corneal neovascularisation should develop. By one week post induction neovascularisation was visible but not fully developed, by 2 weeks post induction neovascularisation was well developed and this time point was usually chosen for analysis. By 5 weeks post induction

the sutures were usually no longer present in the cornea (having worked their way out) and little to no neovascularisation was visible.

If removal of sutures was required at any point it this was undertaken as follows. The animal was placed under general anaesthesia and an operating microscope was used. The length of suture protruding from the knot was grasped with fine forceps and gently pulled a small distance away from the eye to expose the loop of the suture. The tip of a 25G needle was then positioned within the loop of the suture and the sharp edge of the needle tip used to sever the suture, which could then easily be withdrawn from the tissue.

2.3.10 Imaging of corneal GFP fluorescence by fundoscopy (mouse, *in vivo*)

Fundoscopy was performed under general anaesthesia to ensure the animal remained still throughout the procedure. The instrument used was a slit lamp (SC-16, Keeler) modified as follows. The chin rest designed for human patients was replaced with a flat platform upon which to place the animals. The filter wheel was modified so that the incident light could pass through a 475±25nm filter, a wavelength range optimised to excite GFP. Images were taken using an attached DC500 digital camera and its software (Leica).

Once anaesthetized, pupils were dilated with 1 % topical tropicamide (Chauvin Pharmaceuticals). Corneal refractive power was neutralized by placing a 5 mm coverslip on the cornea covered with a coupling medium solution (Viscotears, Novartis Pharmaceuticals).

Under bright light the instrument was adjusted and the animal positioned so that the retina was in sharp focus and the optic disk was centred in the field of view. The focus was then adjusted to bring the cornea into sharp focus and an image taken under bright light (200ms exposure). Immediately after this the light source was filtered with the 475±25nm filter, all other light sources extinguished and the GFP image was taken (30s exposure). After the procedure the animal was either culled or allowed to recover.

2.3.11 In vivo imaging of corneal GFP fluorescence by Scanning Laser Ophthalmoscopy (SLO) (mouse, *in vivo*)

SLO was performed under general anaesthesia to ensure the animal remained still throughout the procedure. The instrument used was a Spectralis HRA2 with a 55° lens (Heidelberg engineering) modified as follows. The chin rest designed for human patients has been replaced with a flat platform upon which to place the animals. The 488 excitation laser has been modified to increase its power.

Once anaesthetized, the animal was positioned and the machine adjusted so that:

- The eye filled the majority of the image
- The pupil was centred
- As far as possible the axis of the eye and camera were directly aligned.

All images were taken using 25° angle setting. Infrared (790nm) images were taken using a power setting of 76% and 30 images were averaged and normalized. GFP (488nm) images were taken using a power setting of 95% and 30 images were averaged and normalized. For each eye a single infrared image was taken in order to visualise the positioning of the entire eye. To visualise GFP expression between one and five 488nm images were taken. This was because the focal plane of the instrument does not allow the entire cornea to be simultaneously in focus; therefore multiple images are required to build a composite of the entire cornea if expression is widespread. After the procedure the animal was either culled or allowed to recover.

2.3.12 Fluorescein angiography of cornea imaged by SLO (mouse, *in vivo*)

The initial stages of this procedure with regard to anaesthesia, instrumentation and alignment of the animal's eye are identical those described in 2.3.11.

Once the animal was positioned with one eye aligned to the machine it was injected intra-peritoneally with 0.2mL of 2% Fluorescein in sterile water for injection. As soon as injection began the SLO's in built timer function was started.

Once imaging of one eye was complete the animal was repositioned to image the other eye. This was done as quickly as possible but due to the extremely rapid spread and leakage of the dye through the tissues it was inevitable that the second eye to imaged would always appear brighter with vessels less well defined. The order in which the eyes were images was therefore randomised on a per animal basis in an attempt to ensure this inherent property of the technique did not affect the results.

All images were taken using 25° angle setting. Infrared (790nm) images were taken using a power setting of 76% and 30 images averaged and normalized.

Fluorescein (488nm) images were taken using various power settings. This was due to the increasing brightness and leakage of the fluorescein visible with increasing time after injection. Generally speaking the longer after injection the lower the power setting used. Power setting ranged between 70 – 90%. Again 30 images were taken and averaged but not normalized. For each eye a single infrared image was taken in order to visualise the positioning of the entire eye. To visualise fluorescein expression between one and five

488nm images were taken. This was because the focal plane of the instrument does not allow the entire cornea to be simultaneously in focus; therefore multiple images are required to build a composite of the entire cornea if vascularisation is widespread. After the procedure the animal was either culled or allowed to recover.

2.3.13 BrdU / EdU administration

Incorporation of these 2 thymidine analogues into genomic DNA is used to label cells undergoing cell division. BrdU solution for injection was made up to 10mg/mL in sterile PBS and animals received a dose of 100ug/g of body weight. EdU solution for injection was made up to 2.5mg/mL in sterile PBS and animals received a dose of 25ug/g of body weight. Both BrdU and EdU were administered via intra-peritoneal injection daily for a maximum period of 4 consecutive days.

2.4 Histology, immunohistochemistry and microscopy

2.4.1 Ethical requirements

Approval by the local NHS Research Ethics Committee was obtained to use human corneal samples for research. Samples were treated according to the Human Tissue Act (2004) and the Human Tissue Authority's codes of practice (2009, see http://www.hta.gov.uk/policiesandcodesofpractice/codesofpractice.cfml). All samples were disposed of by incineration at the end of each experiment. Samples from living donors were anonymised through the Human Research Tissue Database of the pathology department of the Institute of Ophthalmology. For corneas of deceased donors, the anonymisation process was already performed by the eye bank. A consecutive number was allocated to each corneal specimen.

2.4.2 Types of human corneal samples available

Three types of corneal tissue were available, each type displaying different advantages and disadvantages.

Fresh corneal specimens. During corneal transplantation surgery, the patient's diseased central cornea is cut out at a diameter of 7 to 8.5 mm. This "button" would normally be discarded or, if the diagnosis was unclear, fixed in formalin for further histopathological examination and testing. Before surgery, written informed consent was obtained from the patient after the purpose of this study had been explained to them. None of the patients approached during the course of this work declined to give consent. Under sterile conditions in the operating room the buttons were usually de-epitheialised by brief exposure of the anterior surface to ethanol, before being immediately transferred into a vial with room temperature medium (DMEM + 2% FCS, or Culture Medium I (Biochrom AG)) and then stored in the tissue culture incubator at 37°C / 5% CO_2 until use.

Cultured donor corneas. Whole corneas with the surrounding scleral rim were obtained from deceased eye donors via Moorfields Eye Bank. These corneas were always those that had been deemed unsuitable for transplantation for a number of reasons. Common exclusion causes were:

- Insufficient donor medical history
- Missing serology tests
- Donor receiving chemotherapy, high dose steroid medication.
- Patient having received brain surgery before 1990.

- Tissue having spent too long in organ culture.
- Tissue having being rejected due to low endothelial cell density.

Tissues rejected due to these last two criteria were generally avoided for this work due to the high probability that the tissue would be of low quality. Consent for use of tissue in research was obtained from relatives before eye retrieval.

Corneoscleral donor rims. For corneal transplantation, only the central cornea with a diameter of 7 to 8.75 mm is punched out from the donor cornea and engrafted. The remaining corneoscleral rim comprised the peripheral cornea of ~ 3 mm width with the adjacent trabecular meshwork is not used and is usually discarded. This tissue whilst obviously compromised can still be of use in research.

2.4.3 Preparation of corneal flatmounts (mouse)

Mice were killed using an approved Schedule 1 method (usually cervical dislocation) and the eyes enucleated. The globe of the eye was then punctured at the posterior pole using a 25G needle and the eye was placed in 1-4% (depending on the intended antibody staining) PFA in PBS pH 7.4. The cornea was dissected away from the rest of the globe with an orbital cut just posterior to the limbus. Any non-corneal tissue that came away attached to the cornea was carefully removed. Dissection was performed under PFA using corneal notched forceps (Acrofine) and Vannas Capsulotomy Scissors (Albert Waeschle). Once dissection was complete the cornea was further fixed for 30 minutes. Throughout the procedure, great care was exercised to touch the corneal layer of interest as little as possible. Before immunostaining (see 2.4.3), four radial cuts were made in the 3, 6, 9 and 12 o'clock positions using a scalpel (No.15 Swann-Morton) to allow the cornea to be flattened. After any staining had been performed the sample was placed in a drop of PBS upon a microscope slide. It was then manipulated so the layer of interest was upper most, the PBS removed and the cornea carefully flattened. The cornea was then allowed to very briefly dry (to adhere to the slide) before a 20-50µL drop of fluorescent mounting medium (DAKO) was placed upon the sample. A coverslip was then carefully placed upon the tissue and flattened on to the cornea by a combination of capillary action and gentle pressure. The slide was then incubated at 4°C for 30minutes to allow the mounting medium to partially harden before edges of the cover slip were sealed with nail polish.

2.4.4 Preparation of corneal flatmounts (human)

Tissue samples were washed briefly in dPBS before fixation in 1–4% (depending on the intended antibody staining) PFA in PBS, pH 7.4, for 30 min. Throughout the procedure, great care was exercised to touch the corneal layer of interest as little as possible. Before immunostaining (see 2.4.3), radial cuts were made using a scalpel (No.15 Swann-Morton) to flatten corneoscleral rims or corneal buttons.

After staining was complete the sample was attached to a glass microscopic slide endothelium side up using a small drop of cyanoacrylate glue at the edge. A long cylinder of 1 mm diameter was prepared from a pressure sensitive adhesive (BluTac) and used to encircle the tissue sample. Further small balls of BluTac were placed in the corners of the slide. A drop of fluorescent mounting medium (DAKO, UK) was added on the endothelium and a glass coverslip pressed down on to the sample with even pressure, sticking to the BluTac.

Human corneas swell during 37°C culture, resulting in folds and an irregular surface. To flatten the cornea, mounted samples were placed under a 5 kg weight for a minimum of 4 hours to overnight. A spacer between weight and base surface limited the compression to the physiological thickness of the cornea.

2.4.5 Staining of corneal blood vessels by DiI perfusion

This method is described in detail in application to the retina in reference [278]. Described here is a simplification / modification of the protocol applied to the cornea.

DiI solution stock solution was made to ~6 mg/mL in ethanol, this was protected from light and stored at room temperature. Once made this solution was considered stable for up to a year. Immediately before use this stock solution was diluted 1:50 in diluent with the following formulation: PBS (pH7.4) + 5% w/v glucose in dH_2O, mixed in the ratio 1:4. This constituted the working DiI solution.

Mice were euthanized via terminal anaesthesia with pentobarbital (Euthatal, Merial Animal Health) before intracardiac perfusion was performed. During the surgery preparing the animal for perfusion the descending aorta was clamped so as to limit the perfusion to the upper body. Each animal was perfused with the following three solutions in the following order.

1) ~5-6mLs of PBS (pH7.4)
2) ~5-6mLs of working DiI solution
3) ~5-6mLs of 4% PFA

Perfusion of all three solutions was performed at a rate of ~2.5 mLs/min controlled by a syringe driver, smooth switch over between solutions was achieved by use of a device very similar to that shown in Figure 1 of reference [278].

Once perfusion was complete eyes were enucleated and cornea dissected from the rest of the globe with an orbital cut significantly posterior to the limbal vascular arcade (essentially around the eyes equator) and the anterior pole further fixed in 4% PFA for 1 hour. The tissue was then further stained and / or flat mounted (2.4.3).

Note: The entire method post perfusion was performed taking care to place an absolute minimum of mechanical stress upon the perfused tissues, the DiI is NOT rigidly fixed within the endothelial membranes of the vasculature and physical damage to stained vessels can cause it to "leak" into surrounding cells. For the same reason heavy permeabilisation is not recommended, the maximum that was well tolerated was 1% Triton X-100 for 10 minutes.

2.4.6 Cryosections

Tissue fixed in 4 % PFA for 1 hour was embedded in O.C.T. medium (R.A. Lamb) and frozen in isopentane, which had been precooled in liquid nitrogen. Specimens were stored at - 20 °C and 18 µm thick sections were cut using a Bright cryostat. Slides were stored at -20 °C. Sections were air dried for 10 min and marked with a hydrophobic pen before immunostaining.

2.4.7 Homogenisation of ocular tissue

All tissues that were homogenised were later used as samples for ELISA (2.4.8) and thus were homogenised in ELISA reagent diluent (1x PBS + 1% BSA), the volume of which varied. Murine tissue was homogenised using a plastic pestle with matched microcentrifuge tube (Anachem). Human corneas were homogenised using a glass pestle and matched test tube. All tissues were homogenised using a stroke and twist motion which was repeated until no pieces of tissue large enough to be visible to the naked eye remained.

Corneal tissue (human in particular) often proved extremely difficult to completely homogenise and often a large fibrous mass remained despite extremely aggressive homogenisation. This was accepted as a limitation of the tissue.

Homogenate was then spun at 200 x g for 5 minutes in a microcentrifuge and the supernatant treated as the sample for ELISA.

2.4.8 DuoSet ELISA kits for murine IL10 and sFlt1

Both these ELISA's were carried out using DuoSet kits (R&D Systems). These kits are supplied as three components required for the specific ELISA: Capture antibody, detection antibody and recombinant protein standard. All the reagents further required for the colorimetric quantification reaction are supplied separately and can be used interchangeably with any DuoSet kit.

Upon arrival the specific reagents (antibodies and standards) were diluted from stock aliquots as shown in the table below. All aliquots were designed to be sufficient for one 96 well plate reaction and stored at -80°C until use:

	Recommended working conc.	**Stock conc. made**	**Dilution of stock to working**
Mouse IL10 DuoSet (Cat. #DY417)			
Capture antibody.	4 µg / mL	720 µg / mL 55.5 µL Aliquots	1:180 55.5 µL / 10 mL
Standard.	2 ng / mL as highest standard	16.6 ng / mL 60 µL Aliquots	1 : 8.3 60 µL / 500 µL
Detection antibody.	300 ng / mL	54 µg / mL 55.5 µL Aliquots	1:180 55.5 µL / 10 mL
Mouse sVEGFR1 / Flt1 DuoSet (Cat. #DY471)			
Capture antibody.	1.6 µg / mL	320 µg / mL 50 µL Aliquots	1 : 200 50 µL / 10 mL
Standard.	10 ng / mL as highest standard	73.3 ng / mL 68 µL Aliquots	1 : 7.35 68 µL / 500 µL
Detection antibody.	0.5 µg / mL	100 µg / mL 50 µL Aliquots	1 : 200 50 µL / 10 mL

Before the procedure was started the following buffers were made up fresh

Reagent Diluent: 1x dPBS + 1% BSA, stored at 4°C

Wash Buffer: 1x dPBS + 0.05% Tween 20, stored at room temperature

The capture antibody was diluted to working concentration in dPBS, and 100 µL was pipetted into each well of a 96 well plate (MaxiSorp, Nunc) before being covered and left overnight at room temperature.

The following day the capture antibody solution was removed and each well was then washed. All washes in this procedure were performed by filling each well with 400 µL wash buffer using a squirt bottle, immediately discarding the wash and removing any liquid remaining from the wells by concussively blotting the plate against clean paper towels. All washes were performed in triplicate.

Each well was then blocked with 300 µL of reagent diluent for a minimum of 1 hour at room temperature. During this time the standards were thawed and diluted to working concentration in reagent diluent. From working concentration a 2 fold dilution series was then made (250 µL in 250 µL) down to 1:64. If dilutions of sample was required these were made either in reagent diluent or another appropriate buffer (e.g. the same buffer as the undiluted sample was in). Block was then removed and wells washed before 100 µL of either standard, NTC or sample was added to each well as required. All standards, NTC's and samples were run in at least duplicate, higher numbers of replicates were performed if the amount of sample available allowed. Samples / standards were incubated on the plate for two hours at room temperature.

Samples / standards were then removed and wells washed. Detection antibody was then thawed and diluted to its working concentration in reagent diluent before 100 µL was added to each well and incubated on the plate for two hours at room temperature.

Detection antibody was then removed and wells washed. Streptavidin HRP (Part # 890803) was then diluted to working concentration (either 1:100 or 1:200 depending on the bottle supplied, correct dilution is always indicated on the label) in reagent diluent before 100 µL was added to each well and incubated on the plate for 20 minutes at room temperature.

Streptavidin HRP was then removed and wells washed. Substrate solution was then made up (1:1 Mixture of mixture of Colour Reagent A (H_2O_2) and Colour Reagent B (Tetramethylbenzidine) (R&D Systems Cat. # DY999) and 100 µL was added to each well. Plate was covered so exposure to light would be minimised. Development of colour was then monitored by eye and the reaction stopped by addition of 50 µL of 2 molar H_2SO_4 to each well. Development usually took between 5 and 20 minutes.

The optical density of each well was then determined immediately, using a microplate reader and associated software (Emax Microplate reader and SoftMax Pro software, Molecular Devices). Plate was read at 450 nm with a reference reading taken at 650nm subtracted.

Data was analysed and quantified against the standards using the software's HRP+TMB setting.

2.4.9 Immunostaining of corneal flatmounts and cryosections

Tissue was briefly washed in TBS and the cell membranes were permeabilised with 1% Triton X100 in TBS for 10-15 minutes. After another brief wash with TBS the tissue was placed in block solution (2% normal goat serum (or serum of the species the secondary antibody was raised in) + 2% foetal calf serum in TBS) for 1 hour. Primary antibody was diluted in blocking solution and incubated with the sample overnight at 4 °C. A complete list of antibodies and their staining conditions can be found in (2.4.10).

After washing 5 times in TBS for 5 minutes, secondary antibody (usually raised in goat, Alexa Fluor Secondary Antibodies, Invitrogen, UK) diluted 1:500 in block solution was added and incubated for 2h at room temperature. Finally the tissue was washed a further 5 times in TBS for 5 minutes. Some stains were also included in the 3rd of these washes, if used the wash was extended to 15 minutes. A list of these is also found in (2.4.10).

2.4.9.1 To-Pro-3 Iodide Staining

To-Pro-3 (Invitrogen) is a carbocyanine monomer nucleic acid stain that is commonly used as a high sensitivity nuclear counterstain that fluoresces in the far red. Upon testing it was found that this stain also stains cytoplasmic RNA leading to high background. In order to minimise this the following step in the staining protocol was added before the final wash steps in which the To-Pro-3 was present

- Incubation in 1 mg / mL RNAse A (Sigma-Aldrich) @ 37°C for 30 mins

Additionally To-Pro-3 requires the staining step to last for 30 minutes rather than 15.

2.4.10 Antibodies and stains

Name / Epitope	Supplier / Cat #	Source	Target Species	Dilution	Application Notes
F4/80	Abcam / Ab16911	Rat Monoclonal	Mouse, Human	1:100	None
LYVE1	Affymetrix eBioscience / 53-0443	Rat Monoclonal	Mouse	1:200	1° Conjugated Alexa 488, no 2° required.
CD34	Affymetrix eBioscience / 14-0431	Rat Monoclonal	Mouse	1:200	None
BrdU	Abcam / Ab6326	Rat Monoclonal	N/A	1:100	Denature DNA / HCL wash required
Phalloidin TRITC	Sigma / P1951	*Amanita phalloides*	F Actin Human, mouse and others	Used at 1 µg / mL	Include either with 2° antibody or in TBS wash
DAPI (4',6-Diamidino-2-phenylindole dihydrochloride)	Sigma / D9542	n/a	All DNA	Used at 5 µg / mL	Include either with 2° antibody or in TBS wash
To-Pro-3 Iodide	Invitrogen / T3605	n/a	All DNA, RNA at lower efficiency.	Used at 10 µM in TBS	Include either with 2° antibody or in TBS wash. Requires additional steps described in 2.4.9.1

2.4.11 Click-iT EdU detection

EdU incorporation was stained using the Click-iT® EdU Alexa Fluor® 647 Imaging Kit (Invitrogen) used according to the manufacturer's instructions after any other immunostaining had been performed. The kit is designed for use upon cells in culture but was adapted without difficulty for use with corneal flat mounts with 60 µL of the Click-iT reaction cocktail used per corneal flat mount.

2.4.12 TUNEL Staining

Samples for TUNEL staining were cryosectioned as described in 2.4.6 but unfixed. Once sectioned the tissue was very lightly post fixed upon the slide by coving with 1% PFA for 10 minutes.

TUNEL labelling was then performed using an ApopTag Red *in situ* Apoptosis Detection Kit (Chemicon International), used largely according to the manufacturer's instructions although with the following modifications made to the protocol which have been found to increase the kits efficacy and utility.

- Within the manufacturer's instructions the volumes of all reagents to be applied to the tissue are given as volumes to be applied per 5 cm^2 of area. This was modified so that the same volumes were instead applied per slide (an area of ~13cm^2)
- Equilibration buffer was applied to the tissue for 60s rather than the 10s specified in the manual

2.4.13 Microscopy

Microscopy of most specimens was performed using an upright confocal laser scanning microscope (Leica TCS SPE DM5500 Q, Leica Microsystems) and the manufacturer's software (Leica LAS AF, Version 2.4.1). Large specimens such as whole corneal flat mounts where imaged using the microscopes tiling function to combine multiple fields of view.

Alternatively, an inverted fluorescence microscope with phase contrast was used (Zeiss Axio Observer.Z1, Zeiss), which also allowed imaging of live cells grown in 6 or 24-well plates.

2.5 Image analysis and statistics

2.5.1 Statistical Analysis

In all case where statistics were applied no more than two groups were compared. The test applied in all cases to determine the probability of obtaining the observed (or more extreme) results if there was no relationship / difference between the two groups (p-value) was the Mann-Whitney U test. This test is non-parametric and thus does not assume the data being analysed is normally distributed. The statistical and graphing software package Prism 5 (Graphpad) was used for most statistical analysis.

2.5.2 Quantification by integrated density of eGFP expression observed by slitlamp fundoscopy.

The camera attached to the slitlamp fundoscope takes images in full RGB colour mode. As a first step the image was opened in GNU Image Manipulation Program (GIMP, open source) and converted to greyscale mode (Image tab) and inverted (Colours tab). This image was then saved in .tif format which was then reopened in ImageJ (NIH, open source). The globe of the eye selected as the region of interest (ROI) using the elliptical selection tool. The "Area" and "Integrated density" values were then recorded using the measure tool.

For each image a data value was generated using the following equation:

(Integrated density / Area) – Mean (Control integrated density / Area)

Dividing by the area controls for the fact the ROI is likely to be a different size for each image. Subtracting the mean value for all the relevant control images essentially sets the control values as a baseline at zero. The images below illustrate the process:

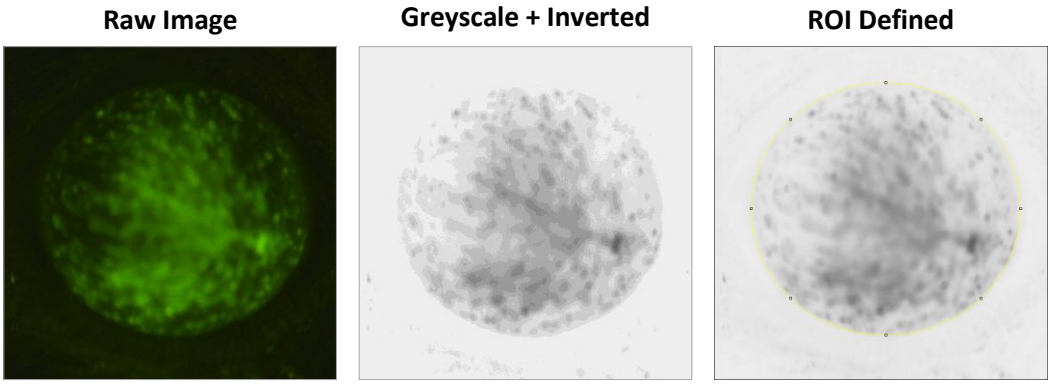

2.5.3 Compilation of SLO images taken in different focal planes

The SLO's 55° angle lens has too limited a focal plane to get the entire murine cornea from limbus to centre in focus at the same time. Therefore, in order to obtain an overview image of the entire cornea multiple images had to be combined. Usually between 3 and 5 images were required to cover the entire depth of the cornea.

The images were then compiled using GIMP. First the separate images were opened as layers within one image, layers were ordered from top to bottom as follows: Limbal cornea focused → Central cornea focused. The uppermost (Limbal) layer's mode was then changed to "screen" which renders darker areas more transparent. In this case this rendered areas of no signal transparent whilst leaving the signal (in white) solid. If the uppermost layer and the layer below it were obviously out of alignment for reasons such as mouse movement or variations in focus then the move layer tool was used to align them correctly by hand. The two aligned layers were then merged to one layer and the process repeated down the layers until all layers were merged as one image. The images below illustrate the process.

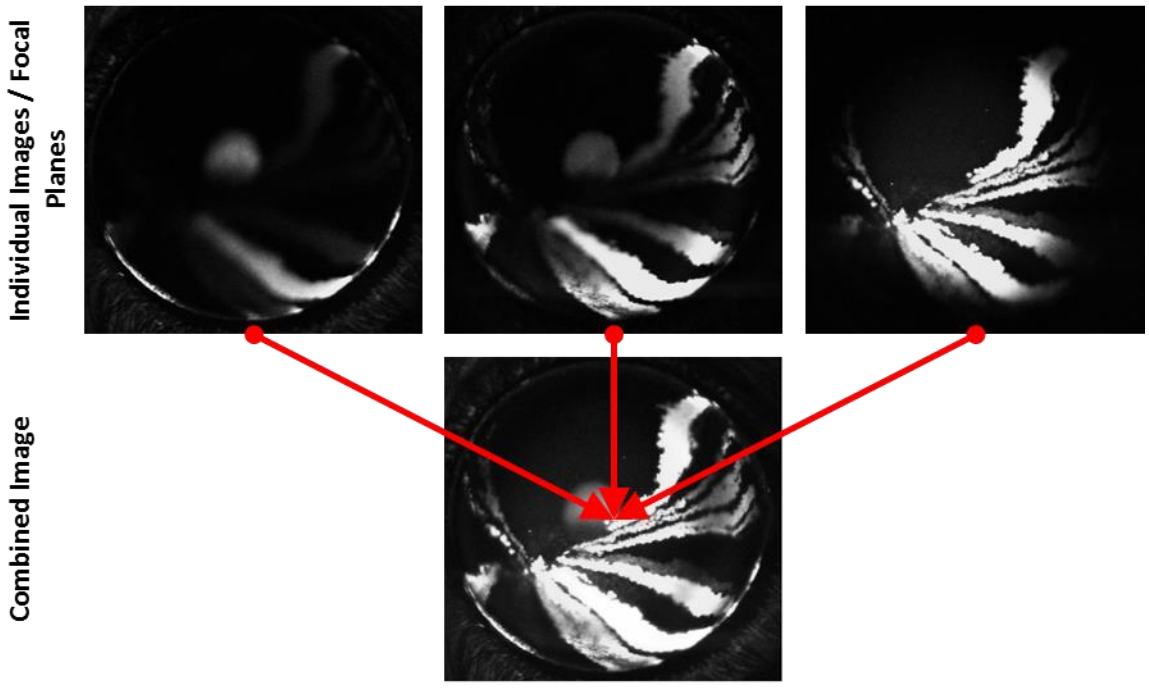

2.5.4 Quantification by area of regions of interest

This analysis technique (with minor variations) was applied to images obtained from both fluorescein angiography (SLO) and immunohistological staining.

For images of fluorescein angiography taken by SLO, images were usually combined as described in the previous section (2.5.3). For quantification the process was as follows. The image to be quantified was opened in GIMP, and a circular selection tool was used to

highlight the region of interest (ROI), usually the whole globe of the eye. Stroke selection (Edit tab) was used to permanently mark the area. All further manipulations will only apply to the ROI. The mode (Image tab) of the image was then switched to “Grayscale” as the mode most suitable for the monochrome SLO images. The levels tool (Colour tab) was then used to remove all pixels with a value below 40, this helped to de-noise the image and make the background an even black (value 0).

The threshold tool (Colour tab) was then used to highlight only the pixels with a value between 100 – 255. This range was chosen as in all images it seemed to nicely separate signal from background and also dampened down the signal resulting from leakage of fluorescein from vessels seen in late stage fluorescein angiography images. The histogram dialogue (Windows tab) was then used to quantify both the total pixels within the ROI and the number of pixels within the threshold. The images below illustrate the process.

Raw Image **ROI Defined** **Leveled and Thresholded**

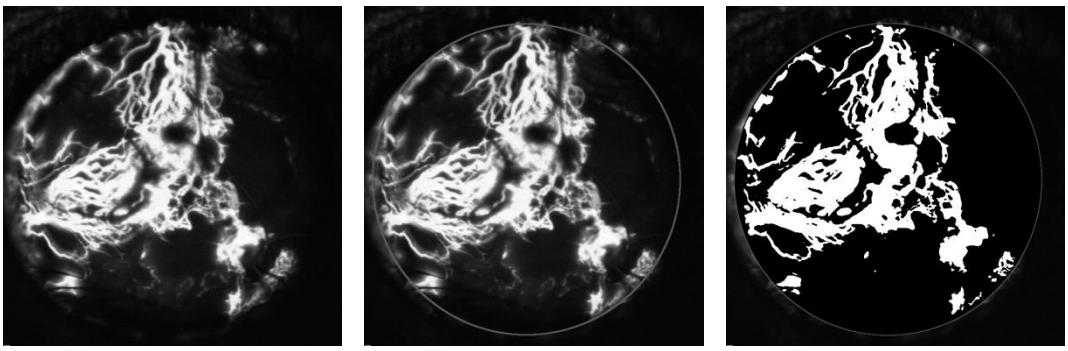

Histogram for pixel quantification

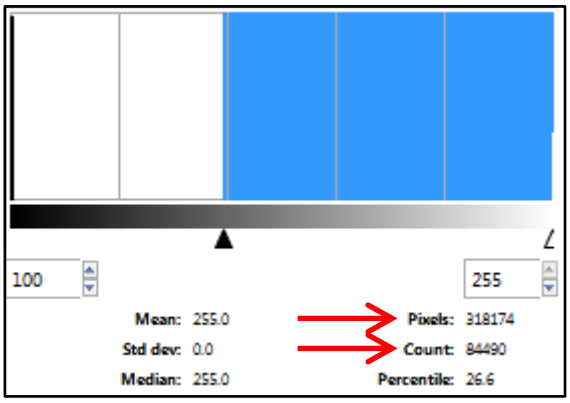

A very similar process was used upon images of immunohistological staining. In this case each channel was treated as a separate greyscale image for analysis. No fixed threshold values were used due to the greater variability in the staining and signal strength between samples. The best threshold settings to separate background from signal were assessed on an image by image basis.

Due to the images being confocal z-projections and certain stains being extremely high signal (causing bleed through) it was not uncommon to observe pixels in the image that were shared between channels once they had been thresholded. These were also defined as a third channel as follows. All the thresholded pixels from one channel were selected using the magic wand tool, the inverse of this selection was then applied to the other channel and all pixels within this inverse selection were deleted. The remaining pixels are those shared between the channels. All three channels could then be overlaid as layers, a circular region of interest selected (usually the central cornea, i.e. area inside the limbal vascular cascade) and the non-black pixels in each channel quantified. After quantification the channels were false coloured back to the colours appropriate to the channel. Shared pixels between the red and green channels were coloured yellow. The images below illustrate the process.

Raw Confocal z-projection (2 channels)

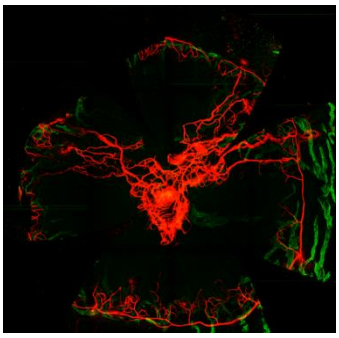

Green channel thresholded (20-255)

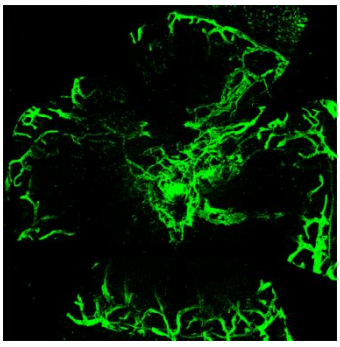

Red channel thresholded (80-255)

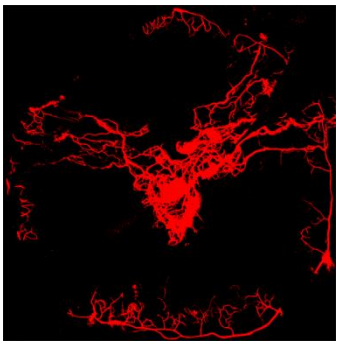

Pixels shared between thresholded channels

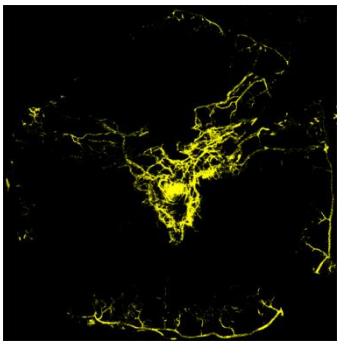

Thresholded channels overlaid and ROI defined

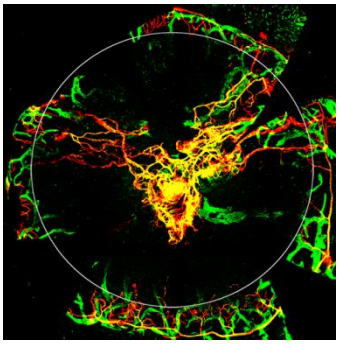

3. Development of novel vectors and application to the corneal endothelium.

3.1 Introduction

Viral gene therapy of the corneal endothelium to date has largely utilised either adeno or lentiviral vectors, these being the only two viruses reliably shown to mediate a substantial transduction of this tissue. Reports within the literature regarding the efficacy of adeno-associated virus (AAV) for endothelial transduction are limited and somewhat mixed, although on balance the published work indicates that AAV is only able to mediate an extremely limited transduction of the endothelium. This would also reflect our own experience within the lab.

The use of both adeno and lentivirus present concerns for application in a clinical context, adenovirus virus is well known to be highly immunogenic and transgene expression is often lost over a relatively short timescale due to the immune mediated destruction of transduced cells. In the context of a non-replicative cell type critical to maintaining the optical transparency of the cornea any possibility of such an immune reaction would constitute an unacceptable clinical risk.

Lentivirus as a retrovirus is able to integrate into the host genome in a semi-random fashion; the process of integration displaying a preference for actively transcribed DNA regions and certain genomic sequence motifs. Integration has the potential therefore to result in insertional mutagenesis and past use of a retroviral gene therapy vector in the clinic has resulted in the malignant transformation of transduced cells. Due to the critical effect of endothelial cell density in maintaining corneal transparency and endothelial decompensation being a major cause of graft failure, many gene therapy approaches to the endothelium have attempted to increase or maintain endothelial cell density and such an approach presents an additional inherent risk of oncogenesis.

If such gene therapy of the endothelium is ever to be translated to the clinic the safety profile of gene transfer must be improved, potentially by ensuring transduction is temporary and self-limiting. Thus work in this chapter will focus upon developing means by which this might be achieved via the modification of lentivirus and the application of novel recombinant AAV serotypes.

3.1.1 Aims

The aim of work presented in this chapter was, firstly, to develop a lenti-based vector modified in such a way as to render it incapable of undergoing the reverse transcription portion of the retroviral lifecycle. The vector would be expected to be unable to integrate and only to mediate an extremely limited gene transfer both in terms of expression level and duration and should therefore minimise any risk of oncogenic transformation

Secondly in recent years there have been great developments made in the field of capsid engineering of AAV; however, none of these engineered serotypes have thus far been applied to the cornea. This work will therefore aim to assess the capacity of these vectors to transduce the corneal endothelium, with a view to application in gene therapy based treatment of corneal endothelial disease.

3.2 Methods and results

3.2.1 Molecular cloning to produce a lentiviral construct designed to be incapable of undergoing reverse transcription

In order to produce a lentivirus genome incapable of undergoing reverse transcription post infection a number of modifications to the standard 2nd generation backbone will be required. First and foremost the elimination of reverse transcription will be primarily achieved by the deletion of the primer binding site that is required to initiate reverse transcription, however a number of other modifications can also be made to further optimise transgene expression.

The ssRNA genome of the modified lentivirus will be required to act directly as mRNA. Thus ribosome binding will take place at the end of the capped 5' LTR. In order to maximise the likelihood of initiation of translation of the transgene the distance between ribosome binding at the 5' end of the genome and the start codon of the transgene sequence will be minimised. The following sequences are present in this region:

Primer Binding Site – This sequence is to be removed.

Psi (ψ) – This is the lentiviral packaging signal and must be preserved if the modified genome is to be packaged.

Rev response element – This sequence functions to aid the export of viral RNA sequences from the nucleus [279]. Whilst this function will not be required post infection with a reverse transcription defective virus, it is likely to be useful during the virus production process *in vitro* and should be preserved.

Central poly purine tract (cPPT) – This sequence both acts as a secondary site of initiation of 2nd strand synthesis and plays an important role in the import of DNA provirus into the nucleus [280]. It would therefore be desirable to remove this sequence from our modified vector.

Spleen focus forming virus (SFFV) promoter – If functioning as designed the viral genome will never form a DNA provirus and will never be trafficked to the nucleus, thus the promoter sequence will never have a chance to function and is therefore expendable.

It would not be expected that a reverse transcription incompetent lentivirus would mediate a very high level of transgene expression and indeed in the context of the intended application high levels would be undesirable. Thus a highly sensitive reporter gene may be required to detect any expression and for this reason firefly luciferase was selected.

Below are described the steps undertaken to produce such a construct. At each step that generated a new plasmid, sequencing (2.1.7) was undertaken to ensure the identity of the product. A schematic of the process is shown in Figure 5. The sequences of all primers used are shown in 2.1.10.

The two starting plasmids used for this cloning were:

pGL4.10[Luc2] – A commercially available (Promega) construct encoding firefly luciferase.

LNT-SFFV-MCS – The 2nd generation lentiviral backbone in use within the lab. It has no transgene and a multiple cloning site positioned immediately after the promoter to allow ease of transgene insertion.

Maps of both plasmids are available in Appendix 1 (9.1)

The first cloning step was to excise the luciferase gene (Luc2) from pGL4.10 and clone it into the lentiviral backbone. This was achieved by first cutting pGL4.10 with BamHI and XbaI, before blunting with Klenow and religating the larger 3980bp fragment. This step excised the SV40 PolyA from pGL4.10 and thus moved a SalI site into a position immediately downstream of the Luc2 gene. The resulting construct was named “Product 1”.

Product 1 was cut with SalI and BglII excising the Luc2 gene in a 1721bp fragment. LNT-SFFV-MCS was then cut with BamHI and XhoI, opening the back bone. The Luc2 fragment was ligated into the lentiviral backbone using the compatible sticky ends of BamHI & BglII and XhoI & SalI. The resulting construct was a 2nd generation lentiviral backbone delivering a firefly luciferase transgene under the control of the SFFV promoter. This construct was named “LNT-SFFV-Luc2”.

LNT-SFFV-Luc2 was cut with NruI and PflFI. These enzymes required different buffer conditions and thus a sequential digest was performed. The 8766bp fragment resulting from this digestion was then blunted with Klenow and religated. This step has the effect of removing much of the sequence upstream of the Luc2 transgene, including the rev response element (RRE), the central poly purine tract and SFFV promoter. The resulting contract was named “Product 3”

The next step was to reintroduce the RRE in a different position downstream of the transgene. As a first step in this procedure Product 3 underwent site direct mutagenesis to remove a SalI site located immediately downstream of the Luc2 gene. This made the remaining SalI site downstream of the woodchuck hepatitis virus regulatory element (WPRE) a unique site. The resulting construct was named “Product 3a”.

The RRE was then amplified by PCR (using original LNT-SFFV-MCS plasmid as the target) using primers modified to include SalI sites on their 5’ ends. Both the PCR product and

Product 3a were cut with SalI and the PCR product ligated into Product 3. The resulting construct was named “Product 4” and was sequenced to ensure correct orientation of the RRE.

Product 4 then underwent site directed mutagenesis to remove all 20 bp of the Primer Binding Site. The resulting final construct was named “LNT-*d*PBS-Luc2”

The result of sequencing of LNT-*d*PBS-Luc2 to confirm its identity is shown in Figure 6. The extent of the sequencing was sufficient to cover the entire genomic construct from mid 5’ LTR to end of 3’ LTR. Sequencing confirms the cloning procedure has been successful. All rearrangements are exactly as predicted *in silico* and the primer binding site has been removed. Only a single base pair mismatch was revealed in the sequence of the Luc2 transgene although this point mutation should be silent (AAG → AAA, both Lysine).

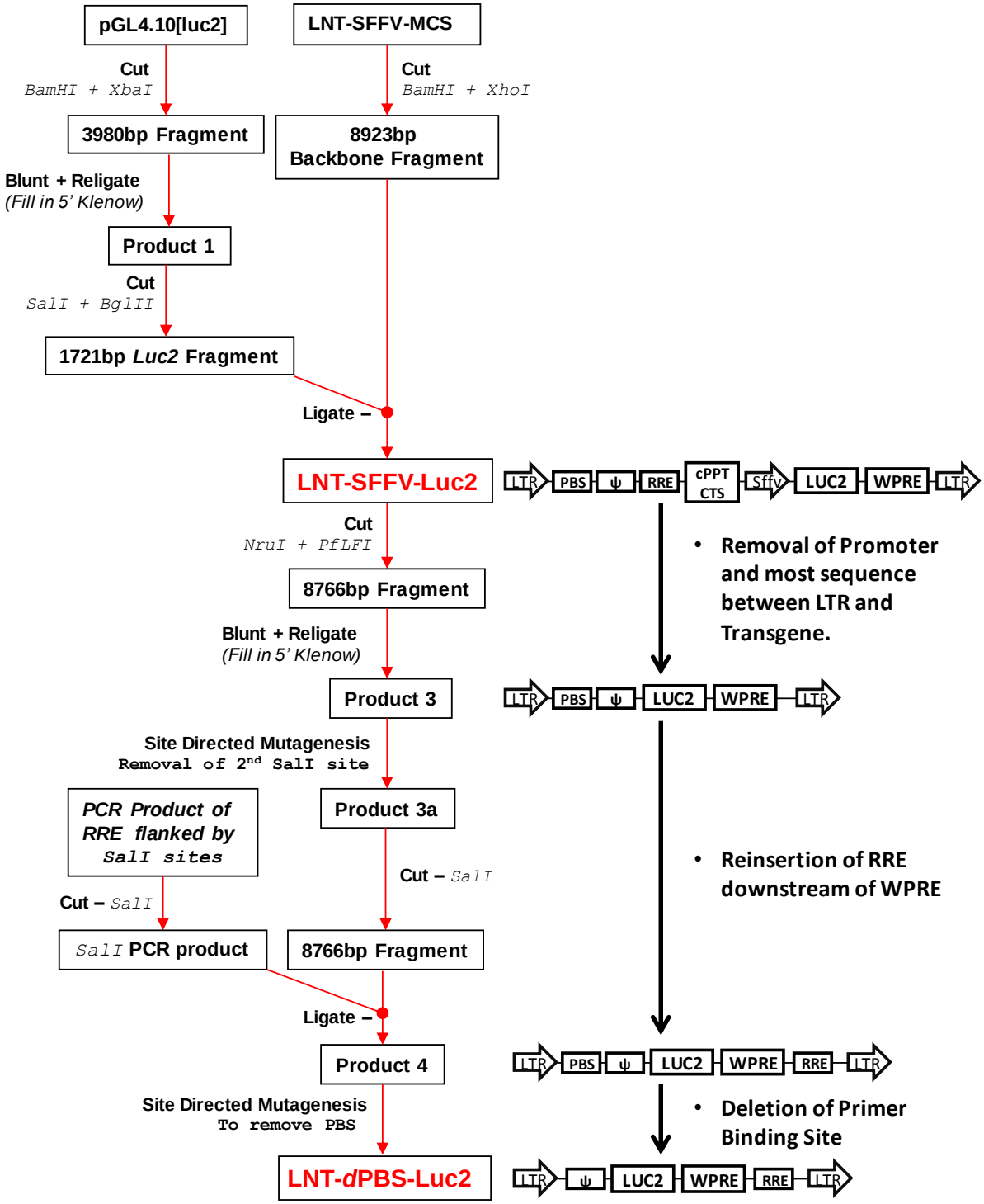

Figure 5. Schematic plan of cloning steps performed in order to produce a lentivirus genomic construct in capable of undergoing reverse transcription post-infection

Key:

Sequencing features:

ATCG = Sequence confirmed by one sequencing pass

ATCG = Sequence confirmed by >1 sequencing pass

ATCG = Binding site of sequencing primer

ATCG = Mismatch of sequencing result with expected sequence

==== = Site of lenti primer binding site removal

Genes / regulatory elements:

ATCG = Lentivirus long terminal repeat sequences (LTR's)

ATCG = Psi sequence

ATCG = Luciferase gene (LUC2)

ATCG = Woodchuck hepatitis virus posttranscriptional regulatory element (WPRE)

ATCG = Rev response element (RRE)

Figure 6. Sequencing result confirming the identity of the final product (LNT-dPBS-Luc2) of cloning described in 3.2.1

3.2.2 Testing of reverse transcription defective lentiviral vector on 293T cells *in vitro*

In order to prove the reverse transcription defective lentivirus was functioning as designed it was tested *in vitro* on HEK293T cells. The expression of the transgene (luciferase) would be assessed at regular time points post infection to monitor the infection profile of the virus. Initially time points at 4, 8, 19, 24, 28, 52 and 68 hours post infection were selected.

A total of six 24-well plates were seeded with $2x10^5$ 293T cells / well and the cells were left to attach to the plate for a total of 19 hours before being infected with virus.

For each of the 7 time points a total of 19 wells were required which were treated as follows:

6-wells were infected with 1 µL of unmodified lentivirus delivering luciferase under control of the SFFV promoter (LNT-SFFV-Luc2) – Titre of $1x10^7$ vg / mL. These will act as a positive control

6-wells were infected with 1 µL of reverse transcription incompetent lentivirus (LNT-*d*PBS-Luc2) – Titre of $1x10^7$ vg / mL

6-wells were left uninfected to act as a negative control / background.

1 additional well was also left uninfected so the cells could be counted at each time point

At each time point the 12 lentivirus infected and 6 uninfected wells were assayed for the presence of firefly luciferase activity. The cells in each well were lysed in 150 µL of GloLysis Buffer (Promega) and a third of these lysates (50 µL) was assayed for presence of luciferase by addition of an equal volume of BrightGlo substrate (Promega). Emission of light was then quantified in a TD20/20 Luminometer (Promega) 6 minutes after addition of substrate. At each time point the cells in 1 well were trypsinised and counted with a haemocytometer.

Figure 7 shows the results of the luciferase activity assessment. For the time points initially assessed (darker points and lines) it was apparent that at the first time point at 4 hours post infection the luciferase activity for both reverse transcription incompetent and unmodified virus was significantly raised above the controls, and the unmodified virus was also significantly raised above the reverse transcription incompetent. This resulted in a gap in the data set in which the initial deviation in infection profile between the reverse transcription competent and unmodified virus may have occurred. It was therefore decided that earlier time points were required. The experiment was thus repeated for the following time points 0.5, 1, 2, 4, 6, 8 hours post infection, these are shown as paler points and lines in Figure 7.

Infection with the positive control unmodified virus (LNT-SFFV-Luc2) resulted in luciferase activity detectable significantly above background again from the first time point at 0.5 hours

post infection. Luciferase activity then increased exponentially until it rose above the upper detection limit of the assay at 24 hours post infection.

Infection with the reverse transcription defective virus (LNT-*d*PBS-Luc2) resulted in luciferase activity rising significantly above background at 1 hour post infection and continued to rise to a maximal level at 19 hours post infection at which point the level was ~400 fold lower than the positive control. The level of luciferase activity remained above background until the end of the experiment at 70 hours post infection but between 19 and 70 hours declined approximately 2.3 fold.

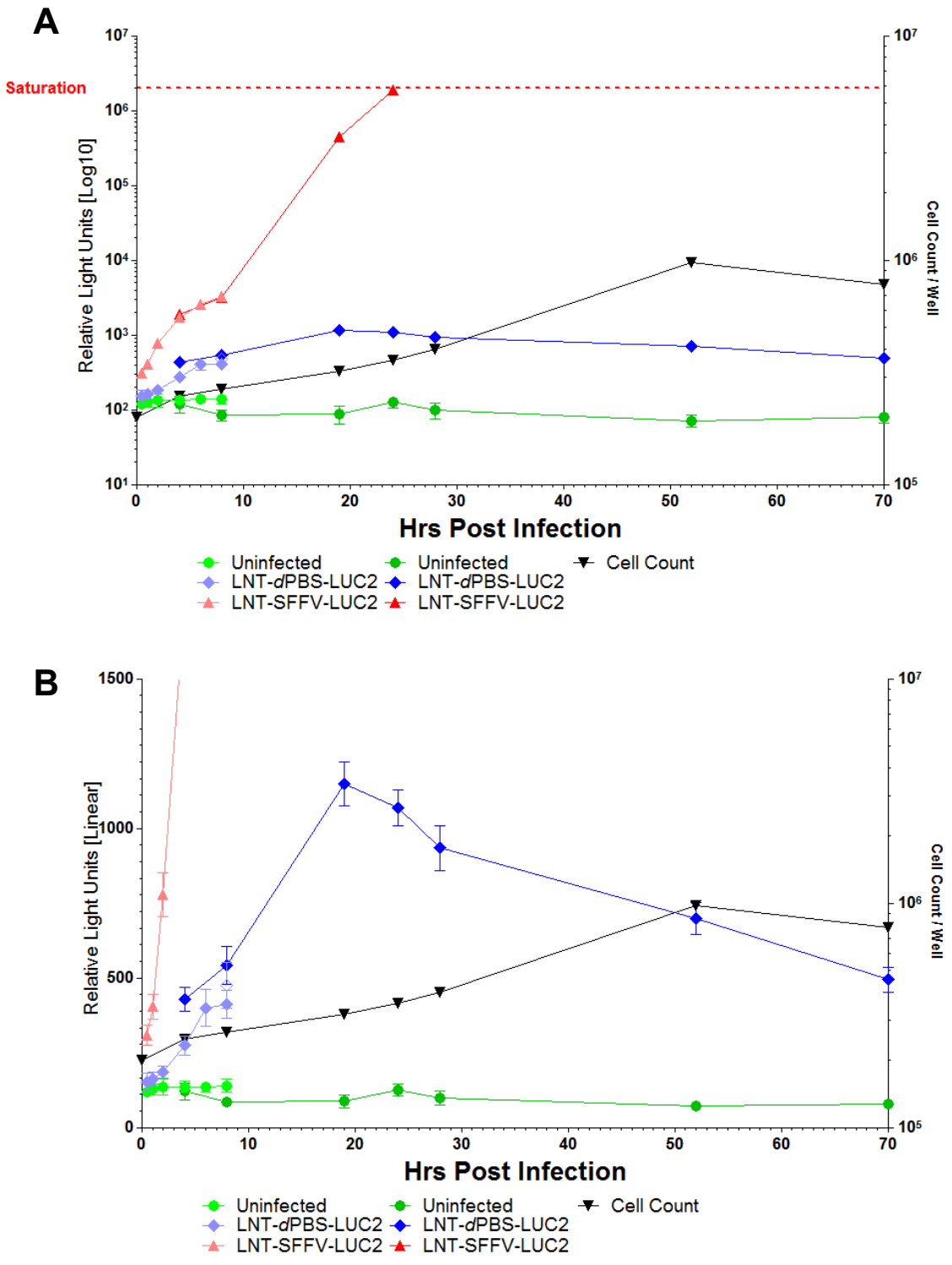

Figure 7. ***Time course of luciferase expression in vitro post infection with LNT-SFFV-Luc2 and LNT-dPBS-Luc2***

A – Data shown on log scale

B – Data shown on a linear scale (most LNT-SFFV-Luc2 data out of range)

Both graphs show 2 repeats of the experiment.

Paler lines: 0.5, 1, 2, 4, 6, 8 hrs post infection

Darker lines: 4, 8, 19, 24, 28, 52, 70 hrs post infection

3.2.3 Assessment of corneal endothelial transduction by AAV2/6(ShH10) following intravitreal and intracameral injection in the mouse

Recombinant adeno-associated viruses (rAAV) have not been widely reported to transduce the corneal endothelium, with the majority of gene therapy directed towards the endothelium having utilised Adenoviral [151] or Lentiviral [232,281] vectors for gene delivery.

What has been published regarding AAV transduction of the endothelium is confusing and sometimes contradictory. AAV has been variously reported to transduce the endothelium; poorly [223,224], “highly efficiently” [225] or only in the presence of ocular inflammation [226].

In our hands no serotype of AAV in common use within the lab (2/2, 2/8, 2/8(Y733F) and 2/9) has ever shown any significant transduction of the corneal endothelium in murine tissue (*in vivo*) or human tissue (*ex vivo*).

A large library of AAV capsid mutations was recently generated by Koerber et al. who used an artificial selection technique to isolate those mutants displaying a tropism towards glial cells. [197]. The serotype AAV2/6(ShH10) was one of those developed by this technique and has been shown to mediate extensive Müller glia transduction following intravitreal injection into the eye [198].

We received this serotype as a kind gift from Professor John Flannery (University of California, Berkeley) and evaluated its ability to transduce the corneal endothelium.

Four mice were injected bilaterally with 2 µL of AAV2/6(ShH10)-CMV-eGFP, vector titre was 4×10^{12} vg/mL (total vector dose: 8×10^{9} vgs) one eye was injected by the intravitreal route and the other by the intracameral route, giving a total of 4 eyes injected per route.

After 9 days all animals were culled and 2 eyes per route of injection were prepared for corneal flat mounting whilst the other two were prepared for cryosectioning.

Figure 8 shows the result of intravitreal injection. Extensive endothelial transgene (eGFP) expression is visible across the entire endothelium in all 4 eyes injected intravitreally.

Figure 9 shows the result of intracameral injection. Some endothelial eGFP expression is visible although it appears weaker and less widespread than that following intravitreal injection. Additionally there is extensive transduction of stroma and epithelium by this route of injection, although from the flat mount it is apparent that all transduction appears limited to an area near the site of injection (Figure 9D).

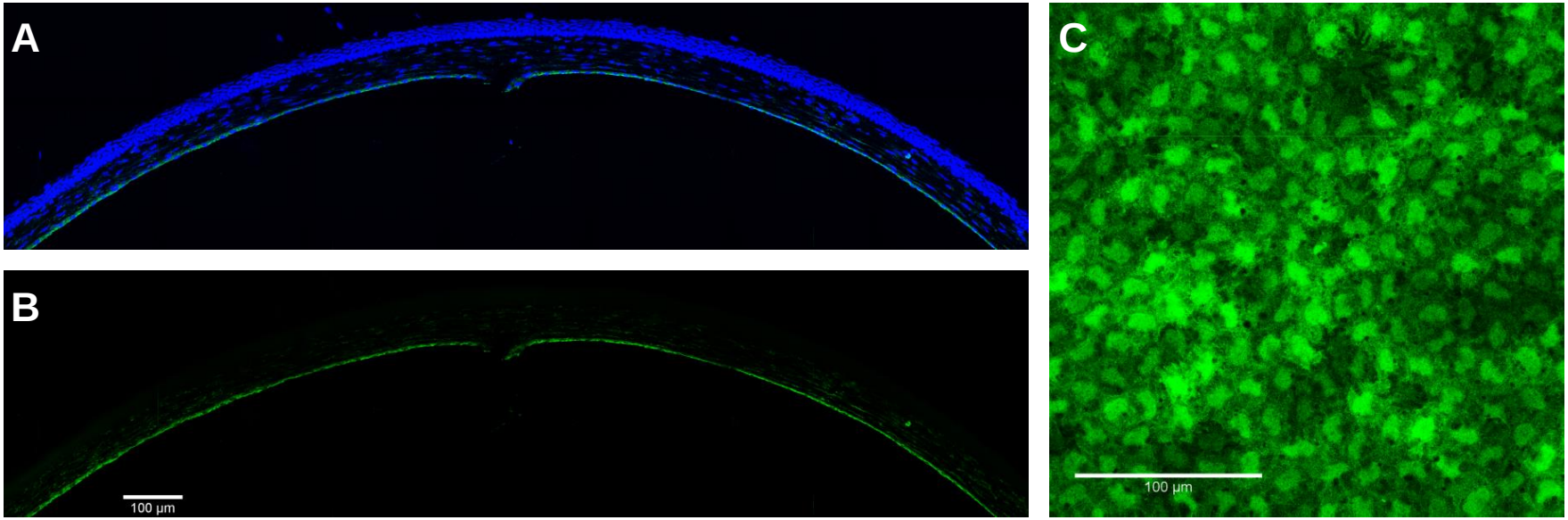

Figure 8. ***Representative histology showing endothelial eGFP expression in the murine cornea 9 days post intravitreal injection of AAV2/6(ShH10)-CMV-eGFP***

A: Transverse cryosection (18µm), confocal z-projection at 10x magnification.

B: Green (eGFP) channel only of image presented in **A**

C: Corneal flat mount of murine cornea showing endothelial transgene (eGFP) expression. Confocal z-projection at 40x magnification.

In all images: Blue = DAPI, Green = Vector mediated eGFP

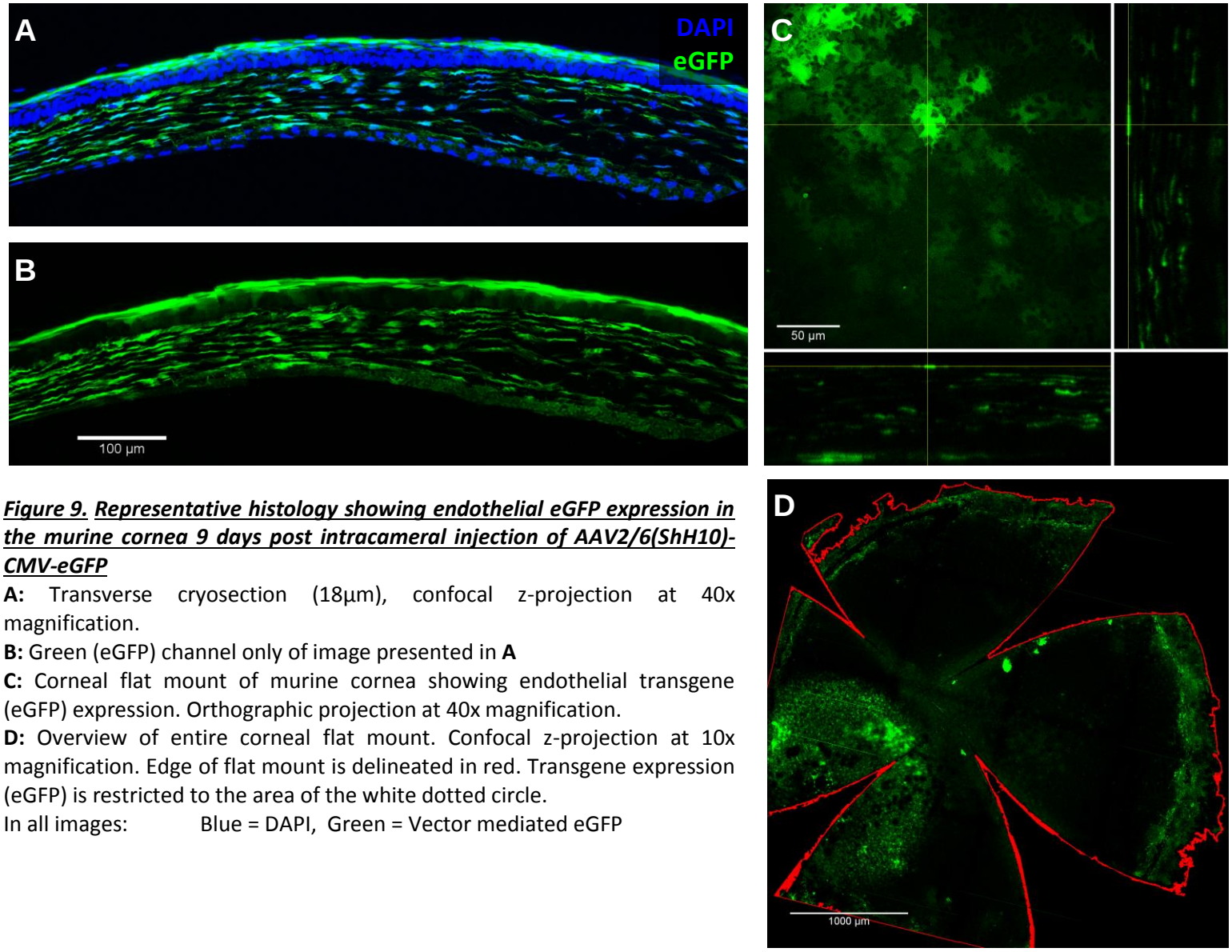

Figure 9. Representative histology showing endothelial eGFP expression in the murine cornea 9 days post intracameral injection of AAV2/6(ShH10)-CMV-eGFP

A: Transverse cryosection (18µm), confocal z-projection at 40x magnification.

B: Green (eGFP) channel only of image presented in **A**

C: Corneal flat mount of murine cornea showing endothelial transgene (eGFP) expression. Orthographic projection at 40x magnification.

D: Overview of entire corneal flat mount. Confocal z-projection at 10x magnification. Edge of flat mount is delineated in red. Transgene expression (eGFP) is restricted to the area of the white dotted circle.

In all images: Blue = DAPI, Green = Vector mediated eGFP

3.2.4 Assessment of corneal endothelial transduction by AAV2/6(ShH10) in human tissue *ex vivo*

Following the observation of widespread transduction of the murine corneal endothelium by AAV2/6(ShH10) following intravitreal injection the capacity of this serotype to transduce human corneal endothelial cells was assessed. A fresh de-epithelialised corneal button was obtained from the operating room and bisected using a razor blade. Each half was placed in 300 µL of culture medium I (Biochrom AG). To one half an additional 300 µL of medium was added supplemented with 4 µL AAV2/6(ShH10)-CMV-eGFP, (total vector dose: 1.6×10^{10} vgs) to the other half 300 µL of medium alone was added to act as a negative control.

Both halves of the corneal button were then incubated at 37°C + 5% CO_2 for 48 hours, before a further 1 mL of culture medium I was added to each half. Button halves were then incubated at 37°C + 5% CO_2 for a further 5 days, before being fixed, flat mounted and assessed for transgene (eGFP) expression by confocal microscopy.

Figure 10 shows the confocal images. In the AAV treated half of the corneal button a large number of eGFP positive endothelial cells were seen in areas where endothelium was present. (Figure 10A & B).

Any further analysis proved difficult as the cornea used for this experiment proved to be of a very poor quality. Endothelium was extremely patchy over both halves and in areas where cells were present their density was low. Many pyknotic nuclei (white arrow heads) were also visible in both the infected (Figure 10B) and uninfected (Figure 10C) halves. Such a level of deterioration would not be expected from a 1 week culture period and is likely indicative of a poor initial quality.

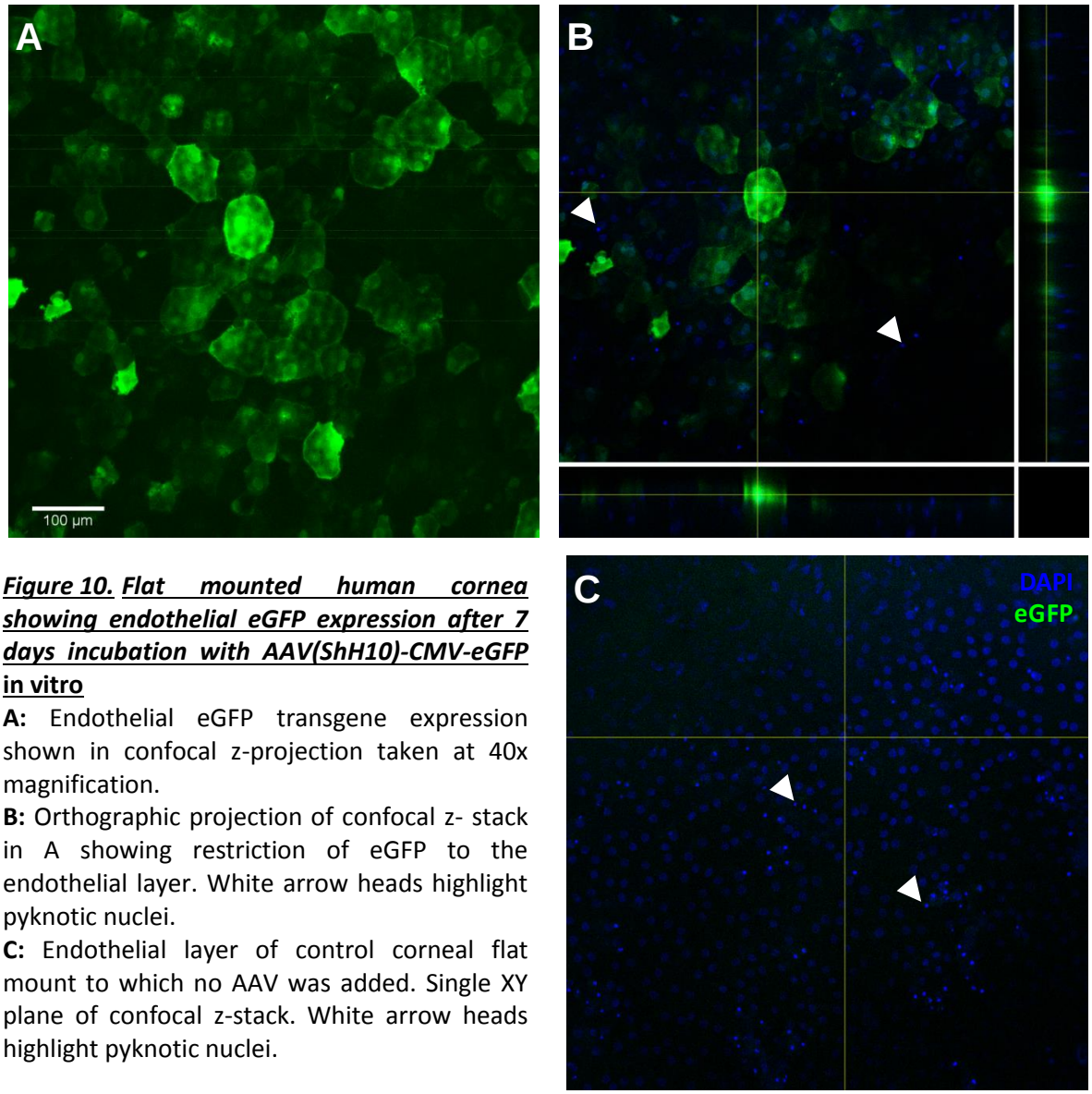

Figure 10. Flat mounted human cornea showing endothelial eGFP expression after 7 days incubation with AAV(ShH10)-CMV-eGFP in vitro

A: Endothelial eGFP transgene expression shown in confocal z-projection taken at 40x magnification.

B: Orthographic projection of confocal z- stack in A showing restriction of eGFP to the endothelial layer. White arrow heads highlight pyknotic nuclei.

C: Endothelial layer of control corneal flat mount to which no AAV was added. Single XY plane of confocal z-stack. White arrow heads highlight pyknotic nuclei.

3.3 Discussion

3.3.1 Reverse transcription defective lentivirus

The development of this vector was initially undertaken with the intention of utilising it to improve the safety profile of the potentially oncogenic gene transfer that would be required to trigger corneal endothelial cell replication.

Specifically it was to be used in the context of work undertaken within the lab to adapt over expression of the cell cycle control factor E2F2 shown to induce endothelial cell replication via adenovirus [151,241] to a lentiviral vector platform. In 2007 Haberichter et al. [282] calculated by mathematical modelling of their observations of G1 cell cycle progression that some cell cycle regulatory factors (especially E2F2) may trigger cell cycle progression even if only present at extremely low levels (<10 molecules / cell). For this reason we believed that the limited transduction achievable by the reverse transcription defective lenti vector may be sufficient for this purpose.

This prediction was not borne out by experiment however. Work by Dr Daniel Kampik (unpublished) revealed that even E2F2 gene delivery by an unattenuated lentivirus was not always effective in triggering endothelial cell replication but was in fact dependent upon virus titre. Only high MOI's of unattenuated lentivirus were successful in triggering endothelial cell replication and it was therefore deemed extremely unlikely that the up to 1000-fold lower expression levels mediated by the RT defective vector would ever be effective in triggering endothelial cell replication via E2F2. The work to develop and characterise this vector was therefore suspended before fully complete.

Nonetheless the progress that was achieved will be discussed below including areas that require further development or characterisation, and it is possible that the low level, transient gene delivery mediated by the reverse transcription defective vector might prove of future utility in an alternative application.

The cloning strategy designed and presented in this chapter has successfully produced a lentiviral genomic construct that should be unable to undergo the reverse transcription portion of the retroviral lifecycle due to the deletion of the primer binding site required to initiate reverse transcription. Reverse transcription is essentially the very first step in the retroviral lifecycle post cell entry and uncoating, and thus if eliminated all subsequent steps should also be prevented. It has not been conclusively demonstrated here however that this vector undergoes **no** reverse transcription although the vastly reduced transgene expression

level mediated by the vector is certainly indicative of a substantial impairment. More conclusive proof could be obtained by performing PCR upon the DNA of infected cells to determine the presence or absence of proviral DNA.

Even if proviral DNA were shown to be experimentally undetectable it remains unlikely that prevention of reverse transcription will ever be 100% complete so the vector designed here has been additionally modified to attenuate any downstream processing in case of any residual reverse transcription.

In common with most other 2nd generation lentiviral vectors the defective vector generated here has been rendered self-inactivating (SIN) by the deletion of the U3 sequence in the 3' long terminal repeat (LTR). During normal lentivirus reverse transcription this portion of the 3' LTR is copied to the 5' end of the provirus from which position it acts as a promoter driving the expression of viral genes in the nucleus [283]. Recombinant lentiviral vectors are usually designed to include an additional non-lentiviral promoter to drive transgene expression in the nucleus. The reverse transcription defective vector contains no known promoter of any kind and thus even if a residual level of provirus is produced and trafficked to the nucleus then transgene expression should be minimal.

As a further modification the central polypurine tract (cPPT) has also been removed from the reverse transcription defective vector's genome. The cPPT acts as a second initiation site of reverse transcription and 2nd strand synthesis [284] and thus its removal was vital in rendering the vector fully incapable of undergoing reverse transcription. The function of this second initiation site is primarily to generate what has been termed the "central DNA flap" which has been shown to be an important feature facilitating the nuclear import of provirus [285]. Its removal therefore should act to both prevent any alternative initiation of reverse transcription that might result in proviral forms and attenuate any nuclear trafficking of this DNA.

When the transduction profile of the defective vector was assessed *in vitro* by luciferase transgene expression (3.2.2) it was found that as expected the defective virus mediated a level of expression several orders of magnitude below an unmodified vector. This low level was still however easily detectable above background (uninfected), and the level of expression remained above background until the end of the experiment at 70 hours post infection. Between 19 and 70 hours post infection the luciferase level dropped approximately 2.3 fold, indicating a possible genome half-life of around 44 hours. This is somewhat longer than average [286] for an mRNA but still well with in normal range [287]. Unfortunately it was not possible to extend the experiment to witness the complete extinction of the signal due to the cells in culture reaching confluency and losing viability as a result.

The experiment presented in 3.2.2 does not eliminate the possibility that the lentiviral genome had in fact degraded and continued "expression" of luciferase was due to stable luciferase protein rather than *de novo* translation. The half-life of luciferase *in vitro* (in the absence of live cells) at 37°C / 5% CO_2 was therefore determined by incubation and assessment of (highly expressing) LNT-SFFV-Luc2 infected cell lysate over time. Half-life was determined to be ~40 minutes (see Figure 11 below). Such a half-life would lead to the complete decay of the reverse transcription defective vector mediated signal in approximately 2 hours 40 minutes and it is therefore unlikely that residual luciferase is responsible for the signal.

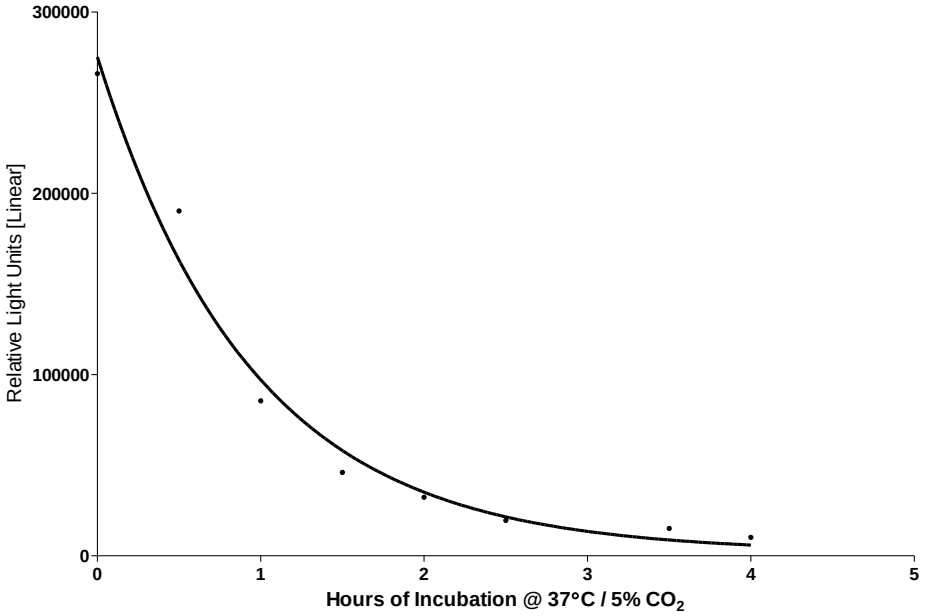

Figure 11. Stability of Luc2 at 37°C / 5% CO_2

The results obtained characterising the reverse transcription defective lentivirus are in general agreement with work by Galla et al. [288] in which a murine leukaemia virus was modified in a very similar manner to eliminate reverse transcription. Direct comparison of the two data sets is difficult due to variation in the cell type, transgene, and multiplicity of infection (MOI) between the two experiments. There is a clear difference however in the level of transgene detected over background. The work presented here detected a maximal expression of approximately 12-fold over background whereas Galla et al. demonstrated a 2-fold difference at best. This is likely to be due to the increased sensitivity and decreased background of the luciferase detection over eGFP fluorescence rather than reflective of any difference between the two viruses themselves, although this possibility cannot be discounted.

3.3.2 Adeno-associated virus

The adeno-associated virus serotype ShH10 has only very recently been acquired by the lab (a kind gift from Prof. John Flannery) and this work has demonstrated that this serotype is able to mediate significant levels of transgene expression in the corneal endothelium in both murine and human tissue. We believe this transduction to be far more convincing than any previously seen from any other AAV serotype in this tissue, either in our hands or in the literature [223–226].

The far lower endothelial transduction efficiency resulting from an intracameral injection when compared to intravitreal administration was initially surprising. An intracameral injection should have resulted in delivery of vector closer to the endothelium and thus a better transduction profile may have been expected. Instead a transduction of the whole thickness of the cornea was noted which was limited to an area close to the site of injection. This is likely due to the fact that the intracameral injection route involves a full thickness penetration of cornea. We believe that following intracameral injection the majority of the vector likely refluxed back up the injection tract driven by the force of the increased ocular pressure resulting from the injection. This both limited the spread of transduction and exposed the stroma and epithelium to the vector. The transduction observed, whilst off-target, is nonetheless interesting, demonstrating the capacity of the ShH10 vector to transduce other corneal cell types.

Whilst the transduction demonstrated in murine endothelium *in vivo* following intravitreal injection was both widespread and caused no obvious pathology or reduction in endothelial cell density the same cannot be concluded with certainty from the data obtained for incubation of human tissue with vector *ex vivo*. Analysis of this data was complicated by the poor quality of the corneal tissue available for this experiment. Large numbers of pyknotic nuclei indicative of cell death were observed in both the ShH10 treated and the untreated control sample, and in both cases the endothelium was patchy and of low density. From the small number of images obtained it may appear that both abnormalities may be worse in the AAV infected tissue but no firm conclusion can be drawn. It is possible that such damage may have been caused by the high MOI used in these experiments, which was selected to maximise the chances of observing transduction. Now that AAV2/6(ShH10) has been shown to transduce the corneal endothelium the MOI can be reduced in future experiments. This experiment should be repeated with better quality of corneal tissue in order to confirm whether or not any damage is indeed caused by the vector. Unfortunately this has not been

possible to date due to the limited availability of human tissue and its use in higher priority experiments.

3.3.3 Conclusions

Genetic manipulation of the lentiviral genomic backbone has been successful in producing a vector from which transgene expression is heavily attenuated, although still detectable significantly above background. Characterisation of this vector is however incomplete and further work is required to establish if it is indeed functioning as designed.

The novel AAV serotype AAV2/6(ShH10) has been found to be able to transduce both murine and human corneal endothelial cells, a quality not convincingly demonstrated for any other serotype of this vector.

4. AAV transduction profile in the corneal stroma following intrastromal injection

4.1 Introduction

The stroma comprises the largest compartment within the cornea with the primary role of its largest cell population, the corneal keratocytes, being biosynthetic in the production of stromal extra cellular matrix; under normal conditions these cells are considered to be largely quiescent. This cell population is therefore potentially the best suited of any corneal cell type for transduction in an augmentation gene therapy approach aiming to act upon corneal pathology via a secreted transgene product. The cells of both the epithelium and endothelium are likely ill-suited to such an approach as they act either to exclude or remove material from the cornea. Previous such approaches to alleviate corneal pathology have often targeted tissues adjacent to the cornea such as the conjunctiva and whilst some promising results have been demonstrated in animal models it is likely that the production of transgene product within the affected tissue itself might prove more efficacious.

Based upon the work published to date adeno-associated virus (AAV) based vectors appear to represent the optimal means by which to transduce the stroma due to their relative lack of immunogenicity and various serotypes of AAV (AAV2/8 in particular) having been shown to be able to effectively transduce the stroma. In this study therefore AAV2/8 will represent the current gold standard to which other serotypes will be compared.

In recent years AAV-based vectors have been the subject of a substantial body of work aimed at further increasing their utility. As a result of this research a number of capsid mutant AAV serotypes have been produced which have been shown to mediate improved gene delivery to many tissues. These capsid mutants however have not yet been applied to the cornea and this study will assess one such mutant (Y733F) shown to be especially promising within other ocular tissues for its ability to transduce the stroma.

4.1.1 Aims

Work in this chapter aims to determine the profile of AAV mediated gene transfer to the corneal stroma following vector administration by intrastromal injection, in particular for the Y733F tyrosine mutant of AAV2/8.

Vector transduction profile will be assessed for suitability in application in an augmentation gene therapy approach to corneal pathology in which the stroma acts as a site of production for a secreted transgene product. Primarily therefore this work aims to effect a long lasting AAV mediated gene transfer to the stroma capable of producing physiologically useful levels of soluble transgene product.

4.2 Methods and results

4.2.1 Comparison of corneal transduction by three different AAV serotypes following 2µL intrastromal injection

As a basis for further work this experiment aimed to determine which of the AAV serotypes in use within the lab could induce the highest and most widespread gene expression within the corneal stroma.

The three serotypes chosen for comparison were:

AAV2/8 and AAV2/9 – Two serotypes in common use within the lab both noted to mediate a high level of transgene expression within other ocular tissues such as retina and retinal pigment epithelium. AAV2/8 has also been previously shown to be effective in the stroma [253]

AAV2/8(Y733F) – A relatively novel serotype carrying a tyrosine to phenylalanine mutation in the viral coat protein VP3 which is reported to result in increased expression level and broadened tropism.

Each serotype was prepared using the same viral genomic plasmid (pd10-pst2.2, see Appendix 1 (9.1)) encoding eGFP under the control of the CMV promoter and titre matched to $4x10^{12}$ vg/mL for injection.

For each serotype tested two mice received bilateral intrastromal injections of 2µL of vector, resulting in viral dose per injection of $8x10^{9}$ vgs. A time point of fourteen days post injection was chosen for analysis. Based upon previous experience of retinal transduction this should be sufficient time for AAV8 and AAV9 to reach near maximal expression level. AAV8(Y733F) had not previously been tested by ourselves in ocular tissue its onset of expression was assumed to be either similar AAV8 or more rapid.

At fourteen days post injection all animals were assessed for corneal eGFP expression using slitlamp fundoscopy (Figure 13A-C'). After this procedure the mice were sacrificed and eyes prepared for either corneal flatmounting (Figure 13D & E) or cryosectioning (Figure 12). A total of 4 eyes were available per vector serotype so two were prepared for each post mortem analysis.

Figure 12 shows that all three serotypes tested mediate expression of transgene (eGFP) throughout the entire thickness of the corneal stroma. In addition AAV2/8 and AAV2/8(Y733F) appear to have mediated some limited transduction of the more anterior portions of the epithelium.

Of the three vector serotypes tested AAV2/9 appears to mediate the lowest level of corneal transduction as shown by all means of assessment. What transduction there is however appears relatively widespread across the entire cornea although perhaps stronger in one hemisphere, likely close to the injection site. (Figure 12A, Figure 13A-A' & D).

AAV2/8 and AAV2/8(Y733F) both mediate a higher and relatively comparable level of transgene expression as shown by all means of assessment. (Figure 12B/B' & C/C', Figure 13 B, C and E).

AAV2/8 mediated expression however appeared to be slightly less widespread than that of AAV2/8(Y733F) as shown by fundoscopy (Figure 13B/B' vs C/C'). To a less obvious degree this result was also duplicated in the cryosections (Figure 12B vs C).

AAV2/8 mediated expression was the only one of the three that showed any variability between replicates, for example the two replicate fundoscopy results shown in Figure 13B & B', although as the n number for this pilot experiment was rather low (4) this is perhaps not significant.

Unfortunately due to a tissue processing error a representative flatmount of an AAV2/8 transduced eye cannot be shown in Figure 13

Based on the combination of its high transgene expression level, widespread stromal transduction and apparent reproducibility, AAV2/8(Y733F) was chosen for further investigation.

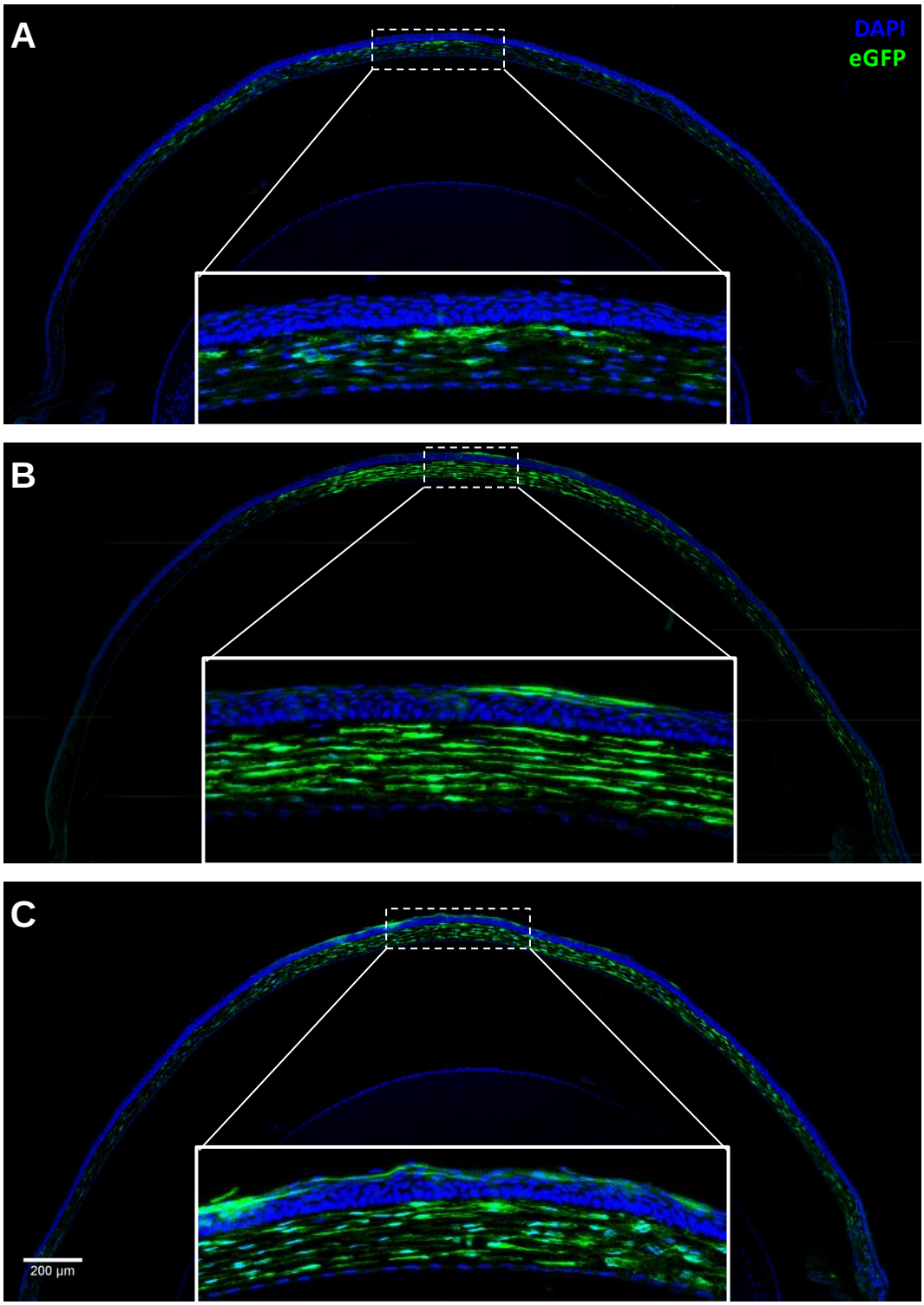

Figure 12. Transverse sections (18µm) through murine corneas showing eGFP expression 14 days after intrastromal injection of 2µL of three AAV serotypes. Total virus dose matched at $8x10^9$ vgs

A: Transduction with AAV2/9-CMV-eGFP

B: Transduction with AAV2/8-CMV-eGFP

C: Transduction with AAV2/8(Y733F)-CMV-eGFP

All images: Projection of confocal z-stacks taken at 10x magnification (insert 40x magnification) Blue = DAPI, Green = Vector mediated eGFP

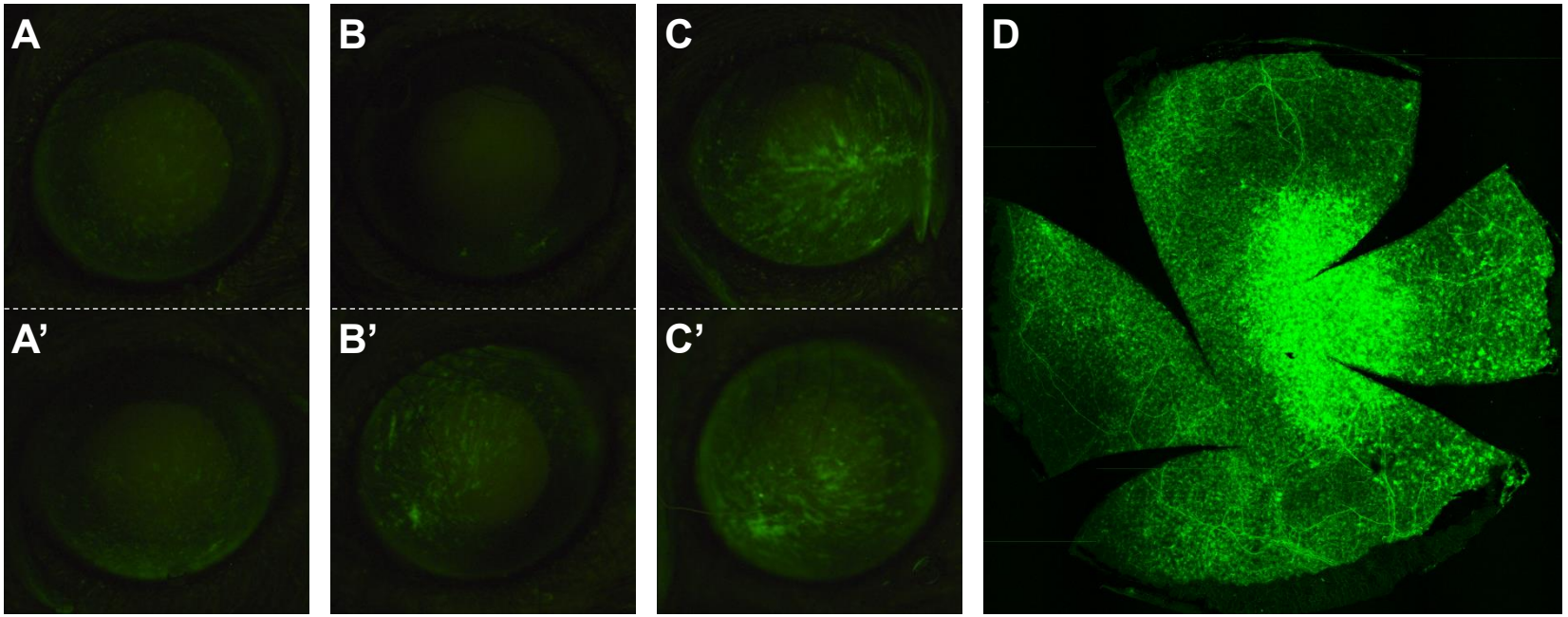

Figure 13. ***Fundoscopy in vivo and corneal flatmounts showing vector mediated eGFP expression in murine cornea 14 days after intrastromal injection of 2µL of three AAV serotypes. Virus dose matched at $8x10^9$ vgs***

A & A': Fundoscopy of 2 eyes injected with AAV2/9-CMV-eGFP
B & B': Fundoscopy of 2 eyes injected with AAV2/8-CMV-eGFP
C & C': Fundoscopy of 2 eyes injected with AAV2/8(Y733F)-CMV-eGFP
D: Flatmount of Cornea injected with AAV2/9-CMV-eGFP
E: Flatmount of Cornea injected with AAV2/8(Y733F)-CMV-eGFP

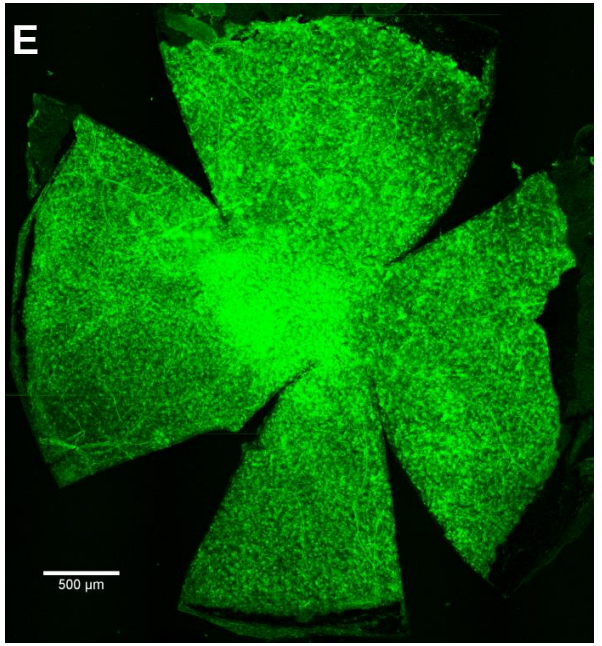

4.2.2 Time course of AAV2/8(Y733F) mediated expression following 2µL intrastromal injection, up to 37 days post injection

To establish the temporal profile of transgene expression mediated by intrastromal injection of AA2/8(Y733F) a vector encoding eGFP under the control of the CMV promoter was injected and fluorescence assessed longitudinally at regular time points by slitlamp fundoscopy.

A total of 4 animals received bilateral intrastromal injections of 2µL vector, resulting in viral dose per injection of $7x10^9$ vgs. As a sham control a single animal was injected in one eye with 2 µL of PBS-MK, the other eye being left uninjected.

All animals / eyes were assessed by fundoscopy at 2, 7, 9, 12, 22 and 37 days post injection. 0A-F shows the fluorescence observed at each time point in the 8 vector injected eyes, whilst 0G-L shows the PBS-MK injected control. The uninjected control is not shown as the sham is more relevant.

Figure 15 shows the level of fluorescence above background observed quantified by integrated density as described in 2.5.2.

Transgene expression increases rapidly from 2 to 7 days post injection reaching a peak at around the 7 day time point. Between this point and day 22 post injection expression falls rapidly to around a third the level seen at day 7. This basal level was then maintained significantly above control (defined by 0 on the y axis) until the end of the experiment at day 37 post injection.

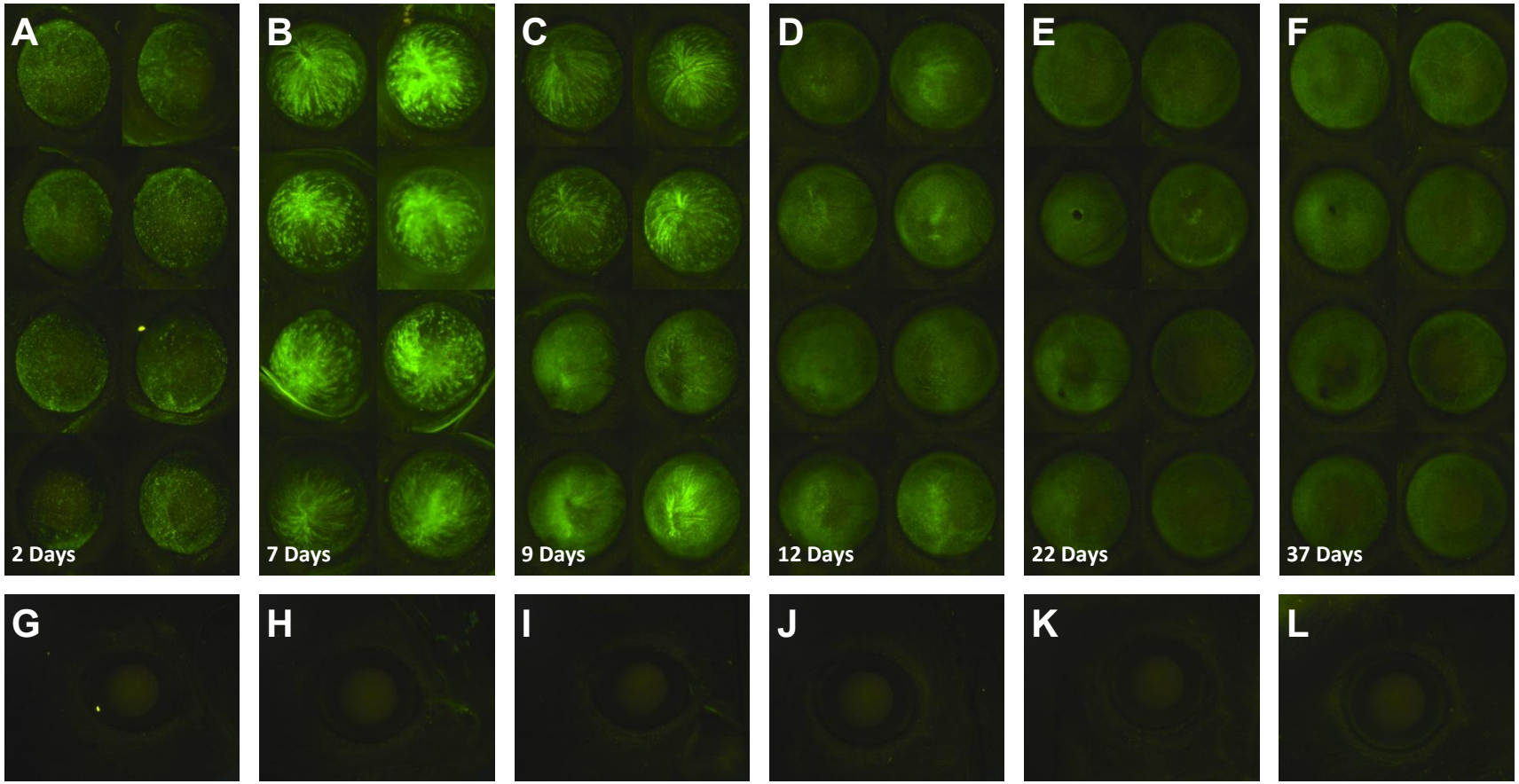

Figure 14. ***Fundoscopy in vivo showing time course of vector mediated eGFP expression in murine cornea after intrastromal injection of 2µL of AAV2/8(Y733F)-CMV-eGFP. Total virus dose: $7x10^9$ vgs***

A-F: Time course of 8 virus injected eyes. Time points are 2, 7, 9, 12, 22 and 37 days post injection respectively.

G-L: Time course of 1 PBS-MK injected eye as a control. Time points are 2, 7, 9, 12, 22 and 37 days post injection respectively.

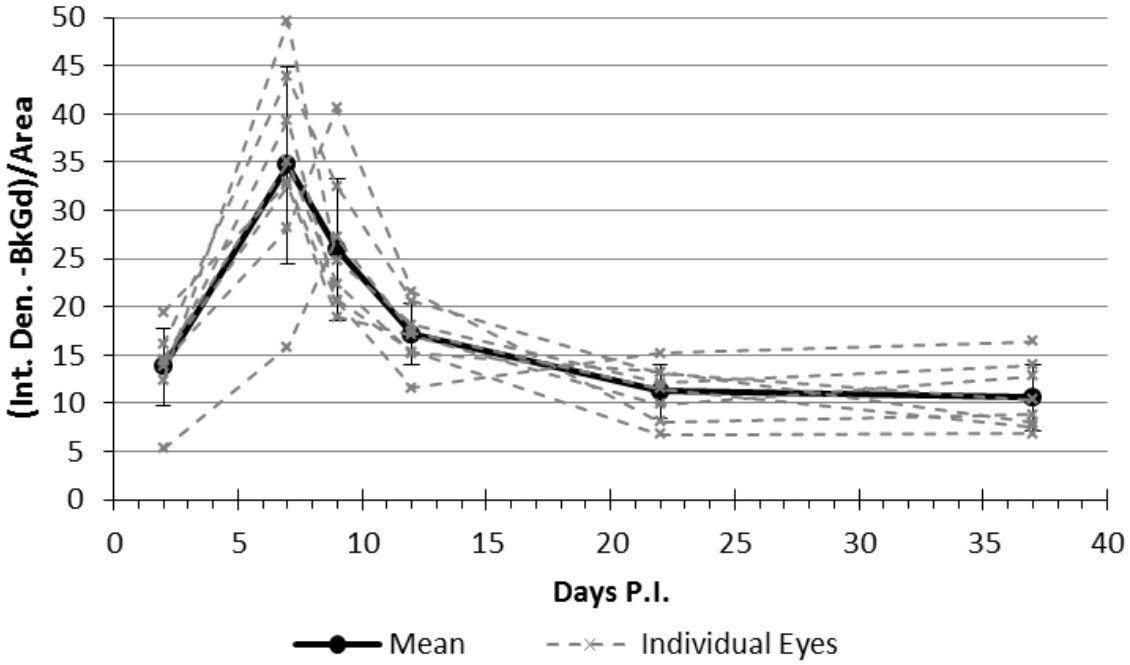

Figure 15. Quantification of eGFP expression in AAV injected eyes based upon densitometry of images shown in 0A-F

Densitometry was performed as described in 2.5.2, with relevant control eye (0G-L) used for baseline subtraction.

4.2.3 Time course of AAV2/8(Y733F) mediated expression following 0.5µL intrastromal injection, up to 148 days post injection

Following on from the data presented in 4.2.2 the time course was essentially repeated with the following modifications:

- The volume of virus injected was reduced from 2µL to 0.5µL. This was in attempt to reduce the tissue trauma associated with the injection and perhaps ameliorate the loss of transgene expression observed.
- The time course was extended with the final time point taken at 148 days (~5 months) post injection in order to gain a more extensive insight into the duration of transgene expression.
- A greater number of control eyes were included. In this experiment a total of 8 eyes were injected, 5 with vector and 3 with PBS-MK

All animals / eyes were assessed by fundoscopy at, 7, 12, 18, 28, 61, 90 and 148 days post injection.

Figure 16B-H shows the fluorescence observed in the 5 vector and 3 control injected eyes at each of the time points

Figure 17 shows the shows the level of fluorescence over background observed quantified by integrated density as described in 2.5.2. The data from the previous experiment (4.2.2) is also presented on the same graph for comparison.

The pattern of transgene expression over time appears to mirror the results obtained in 4.2.2 although the earliest time point was not repeated in this experiment.

The drop in transgene expression observed between 7 and 12 days post injection in 4.2.2 is replicated between days 7 and 18 in this experiment. The reduced injection volume has had no effect to reduce this loss.

The level of expression at 7 days in this experiment is considerably lower than that observed at the same time point in the previous experiment (4.2.2).

Once the decline in expression was over by 28 days post injection a basal residual level of expression was maintained until the end of the experiment at 148 days post injection. The variability in the data did seem to increase over time which would seem to be due to the basal level being better maintained in some eyes, for example those highlighted by white asterisks in Figure 16H.

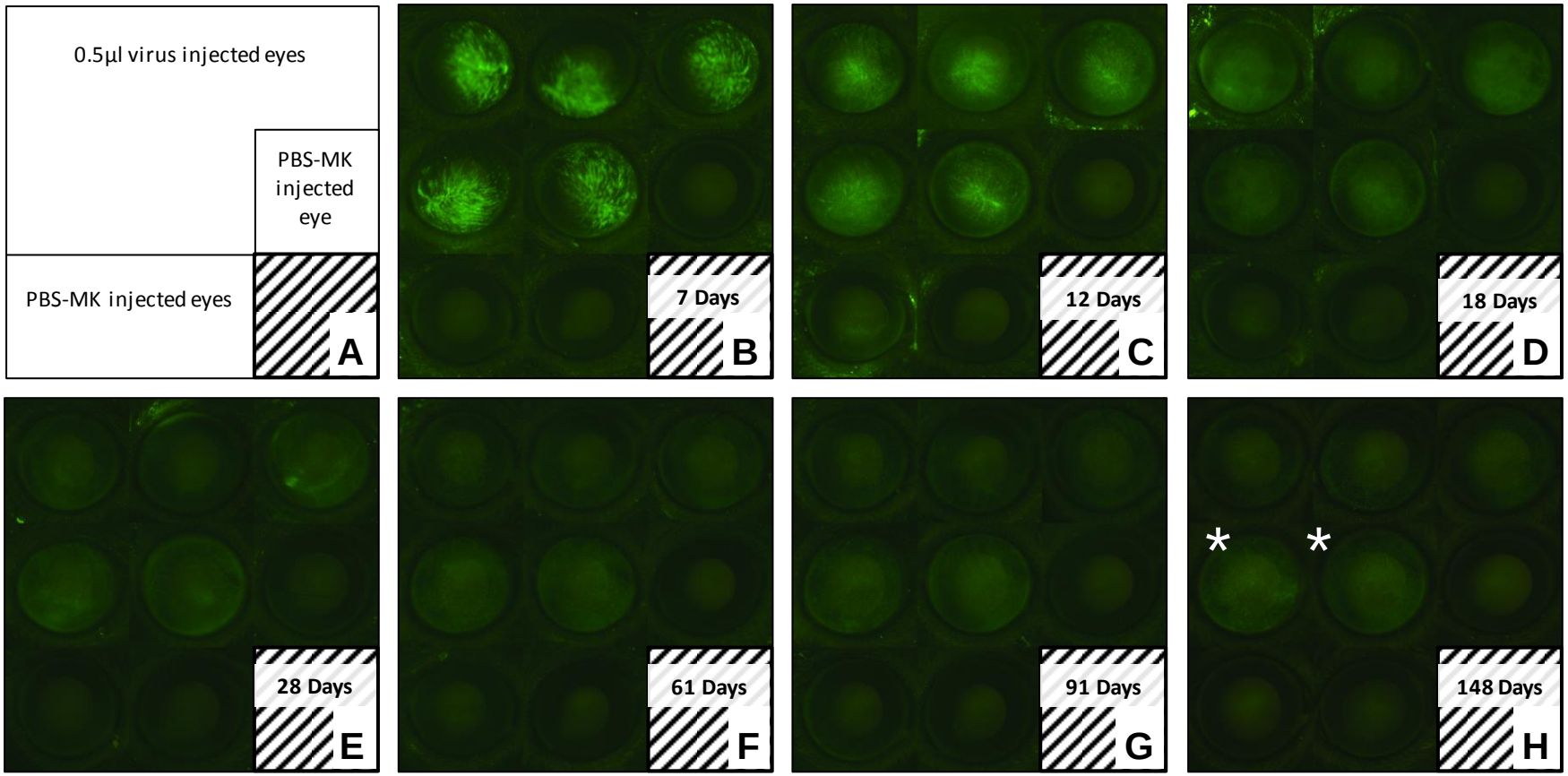

Figure 16. Fundoscopy in vivo showing time course of vector mediated eGFP expression in murine cornea after intrastromal injection of 0.5µL of AAV2/8(Y733F)-CMV-eGFP. Total virus dose: 1.75x10^{9} vgs

A: Schematic showing the position of virus and PBS-MK (control) injected eyes in panels **B-H.**

B -H: Time course after injection, time points are 7, 12, 18, 28, 61, 90 and 148 days post injection respectively.

The two white asterisks in **H** highlight two eyes in which the eGFP fluorescence appears highest.

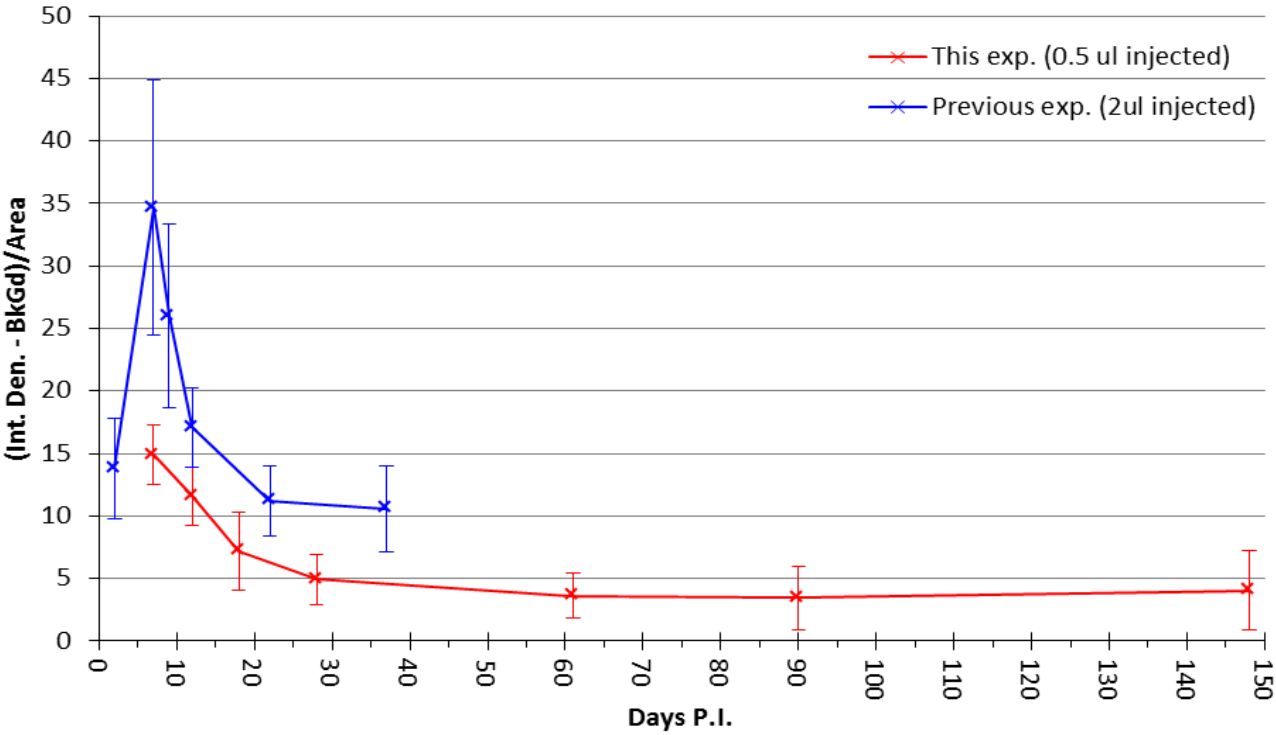

Figure 17. Quantification of eGFP expression in AAV injected eyes based upon densitometry of images shown in Figure 16A-H (red line)

Densitometry was performed as described in 2.5.2, with relevant control eyes used for baseline subtraction. For comparison, the blue line representing data from experiment (4.2.2) shown in Figure 15 is also included.

4.2.4 Histological assessment of basal level of transgene expression remaining at 148 days post intrastromal injection of AAV2/8(Y733F)

The eGFP fluorescence observed in the final time point in 4.2.3 (Figure 15) appeared extremely low. Slit lamp fundoscopy however is not an especially sensitive technique so eyes from animals injected in the previous experiment (Figure 15) were sacrificed after the final time point and their eyes prepared for analysis by cryosectioning and stained for DAPI.

Figure 18B shows eGFP expression within the stroma at 148 days post intrastromal injection of 0.5µL of eGFP encoding vector. For the sake of comparison Figure 18A shows a section of an eye taken at 14 days post injection although this eye received the higher injection volume of 2µL.

At 148 days post injection a relatively high level of eGFP expression can still be observed by histology. No especially high gain settings etc. were required to record this image; those used were broadly similar to that used to record the image in Figure 18A. The eGFP expression also appears to be restricted to the posterior stoma closest to the endothelium as shown in Figure 18C, in contrast to the full thickness stromal transduction seen at 14 days post injection in Figure 16A.

A large area of corneal scarring is also apparent (highlighted by an asterisk in Figure 18B); however this is likely unrelated to the vector injection. Such scarring is commonly observed in the eyes of mice that have undergone repeated anaesthetics and ocular imaging even if otherwise unprocedured.

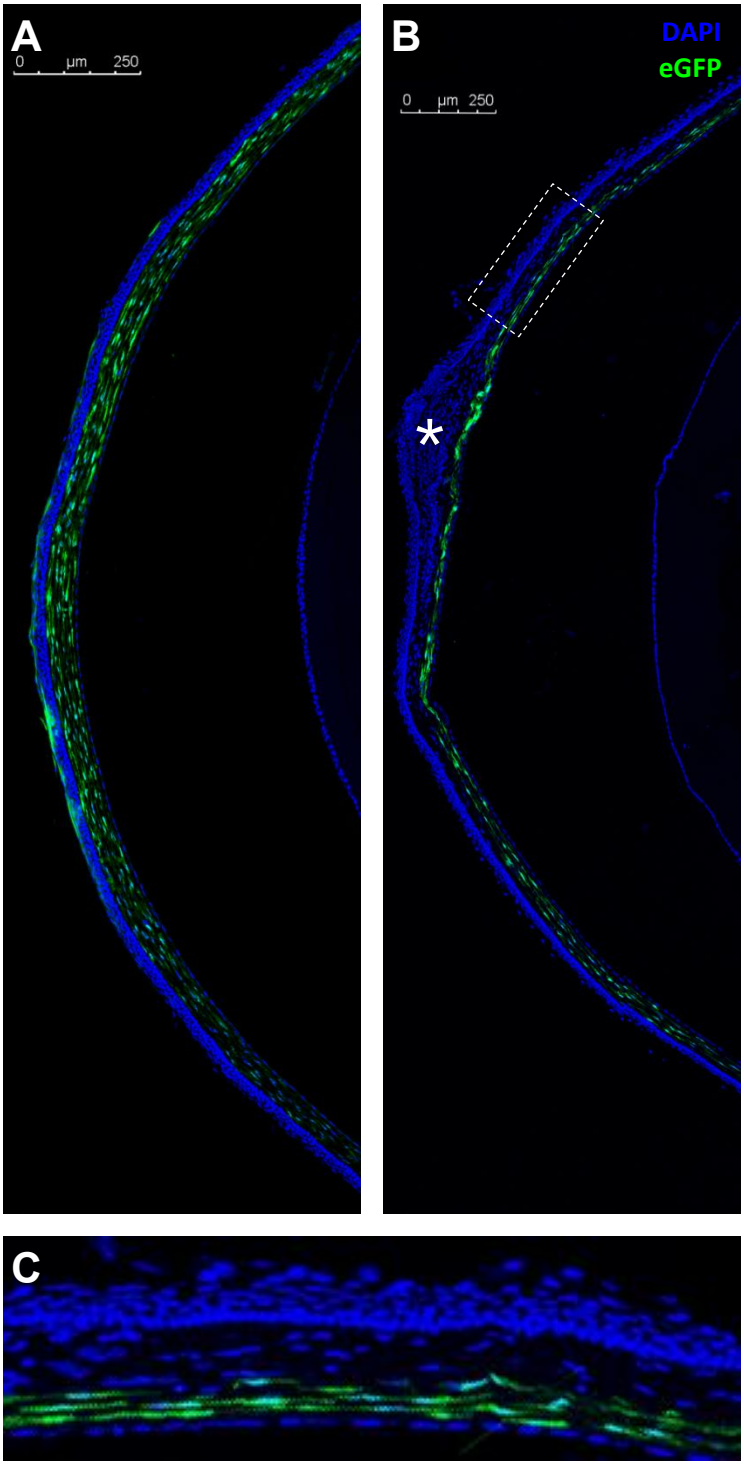

Figure 18. ***Transverse sections (18µm) through murine corneas showing eGFP expression 14 days after intrastromal injection of AAV2/8(Y733F)-CMV-eGFP***

A: 14 days post injection

B: 6 months post injection, white asterisk highlight area of fibrotic scarring associated with repeated anaesthetic and ocular imaging.

C: Highlighted area of B shown in more detail.

All images: Projection of confocal z-stacks taken at 10x magnification.

Blue = DAPI, Green = Vector mediated eGFP

4.2.5 Immunohistochemistry to determine whether corneal keratocytes are the cells transduced by AAV2/8(Y733F)

Corneal keratocytes represent the primary cell population of the stromal and it is therefore highly likely that the extensive transgene expression observed after intrastromal injection of AAV2/8(Y733F)-CMV-eGFP is the result of keratocytes transduction, however this could be confirmed by co-localisation of transgene with a keratocyte marker.

The antigen CD34 has been found to be expressed by corneal keratocytes [289] and is now commonly used as a marker of quiescent keratocytes [253]. It is important to note however that CD34 is also associated with the haematopoietic cell lineage and thus may also stain certain cell types from this lineage that may be present within the stroma [290]. Keratocytes however will constitute the vast majority of CD34+ cells in the stroma.

Three mice were injected intrastromally with 2 µL of AAV2/8(Y733F)-CMV-eGFP (viral dose $7x10^9$ vgs) bilaterally. At 7 days post injection all animals were culled and their eyes prepared for cryosectioning and staining.

Figure 19 shows a representative example of the staining. Widespread eGFP transgene expression is visible throughout the stroma and is also extremely bright within the corneal epithelium. This level of epithelial transduction had not thus far been observed at any later time point sectioned and this discrepancy is likely due to transduced epithelial cells being lost to normal epithelial turnover of the layer between 7 days post injection and later time points.

Within the stroma almost every eGFP positive cell is also CD34 positive. Due to variability in the level of eGFP transgene expressed on a cell by cell basis not all cells are a uniform yellow colour, however upon close examination the co-localisation is near 100%. This indicates that corneal keratocytes are the primary stromal cell type transduced.

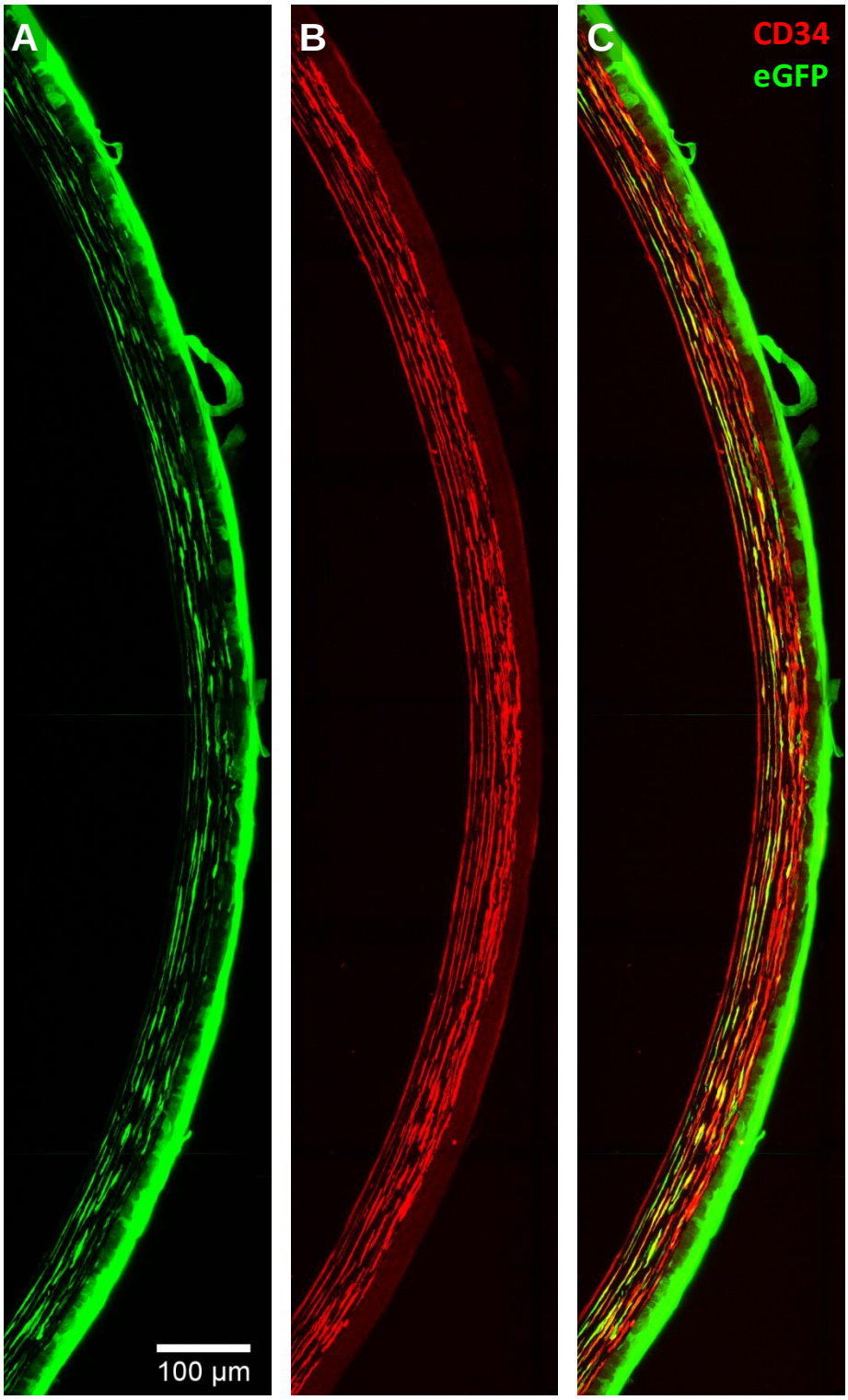

Figure 19. ***Transverse sections (18µm) through murine corneas showing co-localisation of eGFP transgene expression with CD34+ cells 7 days after intrastromal injection of AAV2/8(Y733F)-CMV-eGFP***

A: eGFP channel only
B: CD34 channel only
C: Merged image eGFP + CD34 channel
All images: Projection of confocal z-stacks taken at 40x magnification.
Green = Vector mediated eGFP, Red = CD34 staining.

4.2.6 Assessment of cell turnover in the corneal stroma following intrastromal injection of AAV2/8(Y733F)

Based upon the observed results so far the large drop off in transgene expression between days 7 and 18 post intrastromal injection in experiments 4.2.2 and 4.2.3 is likely largely due to the loss of transduced corneal epithelium due to the normal turnover of this layer. This is shown by comparison of the epithelial transgene expression in Figure 19A (7 days post injection) and Figure 18A (14 days post injection). The transduction of the epithelium in these experiments was off-target and its loss due to turnover is to be expected. However transduction of the stroma was expected to be more stable and thus any loss of expression from keratocytes is more significant as this would negatively impact the long-term efficacy of gene transfer.

Whilst quiescent under normal conditions, stromal keratocytes can become proliferative as part of the stromal wound healing response so it is possible this process may also be contributing to the observed loss of transgene expression. Replicating keratocytes will not be lost from the cornea in the same manner as the epithelial cells but due to recombinant AAV's inability to integrate into the host cell's genome replication of transduced cells will lead to loss of expression via dilution of AAV episomes.

To assess this potential cause of stromal transgene expression loss keratocyte cell turn over following intrastromal injection was assessed by uptake of the thymidine analogues BrdU and EdU. These were administered to mice via intra-peritoneal injection in 4 day pulses at various time points post intrastromal injection of 2µL of AAV2/8(Y733F)-CMV-eGFP resulting in a vector dose per injection of $7x10^9$ vgs.

Four cohorts of 4 mice (8 eyes) were injected as follows:

5 x Eyes – 2µL AAV2/8(Y733F)-CMV-eGFP

2 x Eyes – 2µL PBS-MK control

1 x Eye – Uninjected control

Each cohort received 4 day pulses of both BrdU and EdU separated by 8 days. The experiment was designed so that a 25 day time period post injection was covered. A schematic of BrdU and EdU administration is shown in Table 1

At the end of experiment 28 days post intrastromal injection all animals were culled and their corneas fixed, stained for BrdU and EdU, flat mounted (endothelium uppermost) and imaged by confocal microscopy.

The area of each cornea imaged had x/y dimension of ~3mm x 71.58µm and was located upon the flatmount as shown in Figure 22A'. The area was imaged in the z-axis to a depth of the entire corneal thickness.

Unfortunately due to a defective batch of PFA fixative in the vast majority of eyes analysed the BrdU staining did not work. A small number of eyes (3 out of a total of 32) were fixed using a different batch of PFA. Figure 20 shows BrdU staining in the corneal epithelium (which is replicative under normal conditions) compared between the two batches of PFA fixative, illustrating this issue.

Additionally for reasons unknown (possibly also related to the defective fixative) all the corneas imaged displayed a high level of autofluorescence in the red and green channels in both the corneal epithelium and endothelium. This is shown in Figure 21. Note that the green autofluorescent signal is unrelated to the virus mediated eGFP expression as it also occurs in the PBS-MK injected control (Figure 21B).

Fortunately neither of these issues affected the EdU staining in the blue channel, although due to the loss of all the BrdU data there is a gap in the data set between 6 and 13 days post injection.

Representative images for EdU for 4 periods post injection are shown in Figure 22. These images shown have been rotated 90° around the x-axis and projected in the y axis to produce pseudo transverse sections through the cornea. This image manipulation was performed using Leica LAS AF software. These pseudo sections have the advantage over cryosections that a greater depth (y axis in original image) can be visualised.

There is little to no incorporation of EdU in the corneal stroma when.it was administered 2-5 and 14-17 days post intrastromal injection of AAV (Figure 22B & C). There is however some significant incorporation of EdU in the corneal stroma when administered 18-21 days post injection (Figure 22D) This EdU uptake appears to be localised to the posterior stroma. There is also incorporation of EdU in the corneal stroma when administered 22-25 days post injection of AAV although less than at 18-21 days. This too appears to be localised to the posterior stroma. No uptake of EdU was observed in any of the PBS-MK injected or uninjected controls (Figure 22F-I).

Figure 23 shows the eGFP expression resulting from the transduction at the end of the experiment (28 days). Stromal Transgene expression was always widely observed throughout the entire x/y axis of every injected cornea although there was some variation in the strength of fluorescent signal observed. In the z-axis however it appears that virus

mediated eGFP is restricted to the posterior stroma closest to the endothelium. This result is in agreement with that the similar restriction observed at 148 days post injection in the previous experiment (4.2.4) and shown in Figure 18

As a point of interest Figure 24 shows long fibre like structures that have been transduced by the vector highlighted by white arrow heads. These are likely to be corneal nerve axons.

Days P.I.	Cohort 01	Cohort 02	Cohort 03	Cohort 04
0	All Cohorts injected with AAV2/8(Y733F)-CMV-eGFP			
1				
2	BrdU			EdU
3	BrdU			EdU
4	BrdU			EdU
5	BrdU			EdU
6		BrdU		
7		BrdU		
8		BrdU		
9		BrdU		
10			BrdU	
11			BrdU	
12			BrdU	
13			BrdU	
14	EdU			BrdU
15	EdU			BrdU
16	EdU			BrdU
17	EdU			BrdU
18		EdU		
19		EdU		
20		EdU		
21		EdU		
22			EdU	
23			EdU	
24			EdU	
25			EdU	
26				
27				
28	All Animals Culled			

Table 1. Schematic of experiment to evaluate turnover of cells in the corneal stroma following Intrastromal injection of 2µL AAV2/8(Y733F)-CMV-eGFP
All animals were injected Intra-peritoneally with 4-day pulses, separated by 8 days of both BrdU and EdU according to the schedule shown above.

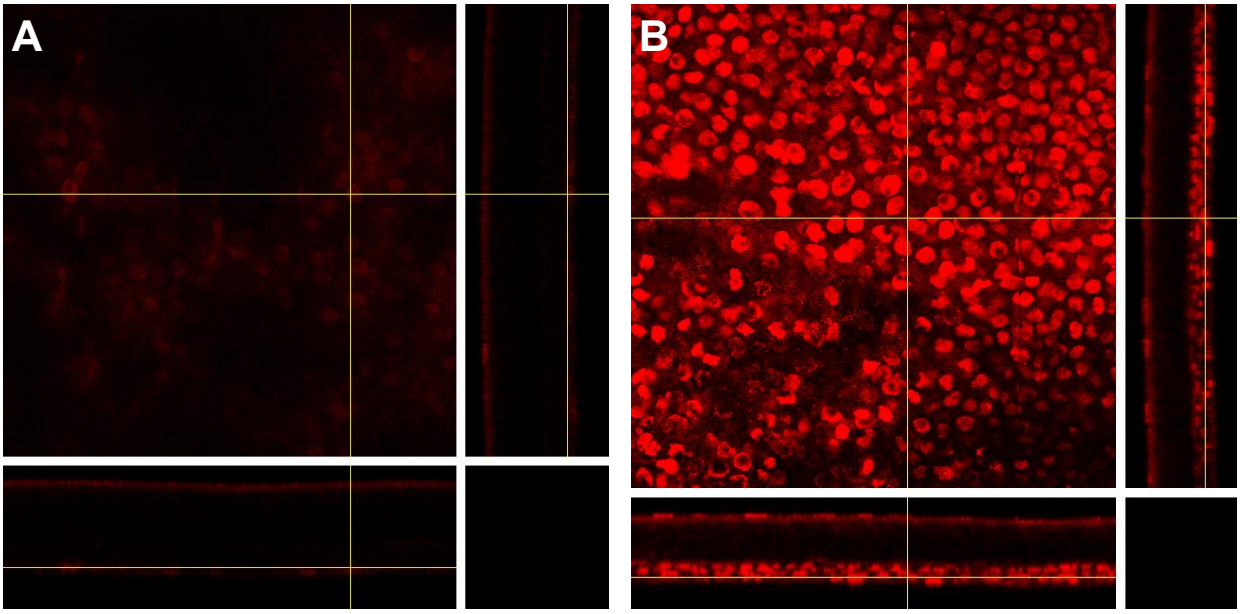

Figure 20. ***Images to illustrate the effect of variable fixation upon BrdU staining in the murine cornea obtained during experiment to assess cell turnover in the corneal stroma following intrastromal injection of AAV2/8(Y733F)-CMV-eGFP***

A: Orthographic projections of confocal z-stack through the cornea with x/y plane focused upon the proliferative basal epithelium. Tissue fixed with pre-made 4% PFA (Santa Cruz) which was used for the majority of tissue in this experiment.

B: Orthographic projections of confocal z-stack through the cornea with x/y plane focused upon the proliferative basal epithelium. Tissue fixed with lab-made 4% PFA which was used for only 3 corneas in this experiment.

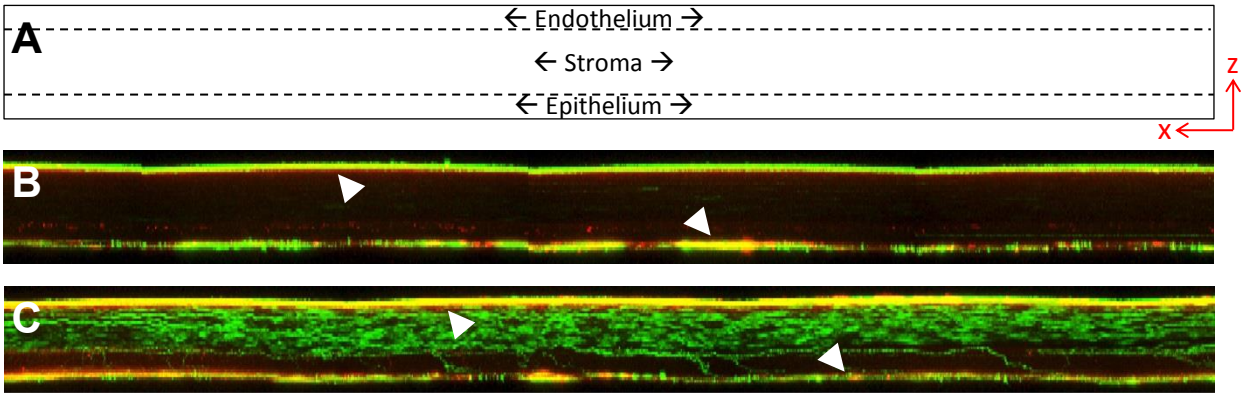

Figure 21. ***Images to illustrate the autofluorescence observed during experiment to assess cell turnover in the corneal stroma following intrastromal injection of AAV2/8(Y733F)-CMV-eGFP***

A: Schematic showing the orientation of images presented in B&C, which are x/z images projected in the y-axis.

B: Representative image of a PBS-MK injected eye, white arrow heads show high levels of signal in the red and green channels (yellow) in the Endo and Epithelium.

C: Representative image of a vector injected eye, white arrow heads show high levels of signal in the red and green channels (yellow) in the Endo and Epithelium.

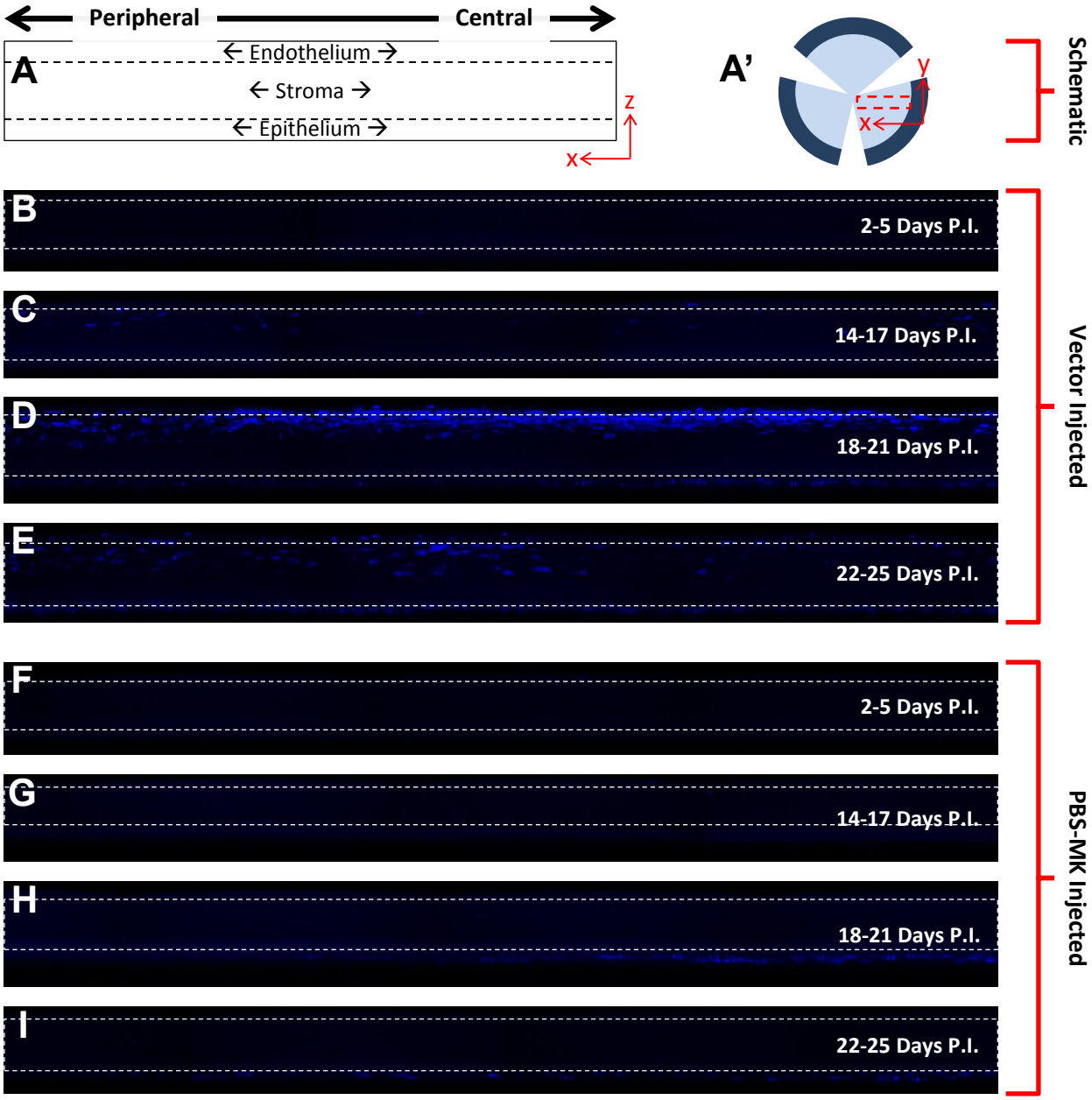

Figure 22. ***Representative images showing EdU uptake in the corneal stroma following intrastromal injection of 2µL of either AAV2/8(Y733F)-CMV-eGFP or PBS-MK at various time points post injection***

A: Schematic showing the orientation of images presented in B-I, which are x/z images projected in the y-axis.

A': Schematic showing x/y area imaged on confocal. Z-depth was the whole thickness of the cornea.

B-E: Representative images showing EdU uptake at the following time points post injection of vector respectively: 2-5 days, 14-17 days, 18-21 days and 22-25 days.

F-I: Representative images showing EdU uptake at the following time points post injection of PBS-MK respectively: 2-5 days, 14-17 days, 18-21 days and 22-25 days.

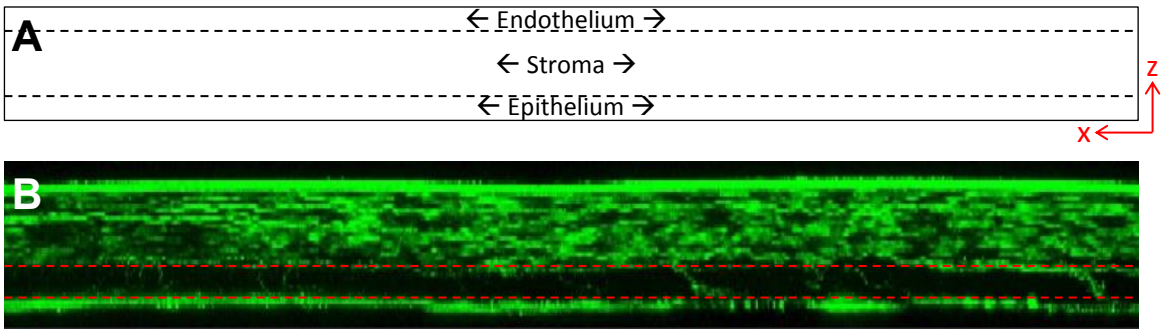

Figure 23. ***Representative image to illustrate restriction of stromal transgene expression to the posterior stroma at the end of experiment 28 days after intrastromal injection of AAV2/8(Y733F)-CMV-eGFP***

A: Schematic showing the orientation of image in B, which is an x/z image projected in the y-axis.

B: Image showing eGFP transgene expression in the stroma 28 days after intrastromal injection of AAV2/8(Y733F). Note the lack of expression in the anterior stroma between the red dotted lines.

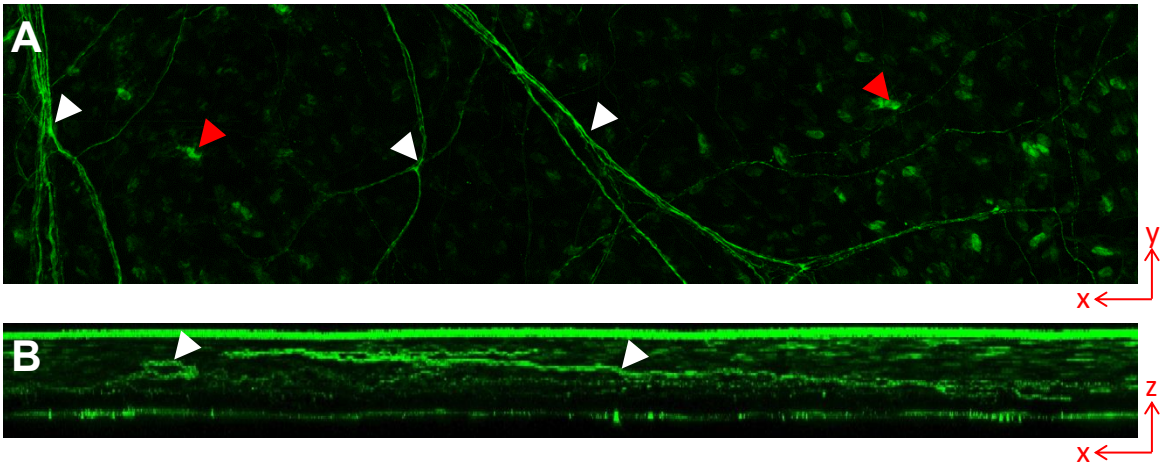

Figure 24. ***Images to illustrate corneal nerve /axon transduction in the corneal stroma following intrastromal injection of AAV2/8(Y733F)-CMV-eGFP***

A: Confocal z-projection in the x/y plane through the stroma of a vector injected eye. White arrow heads highlight fibrous structures observed; red arrow heads highlight transduced stromal cells.

B: Representative images of vector injected eyes as x/z projection, white arrow heads highlight fibrous structures observed.

4.2.7 Assessment of cell death in the corneal stroma by TUNEL assay 10 days after intrastromal injection of AAV2/8(Y733F)

There is evidence from both 4.2.4 and 4.2.6 that eGFP transgene expression is becoming restricted to the posterior stroma over time. It is possible that this might be due to the death of transduced cells in the anterior stroma by apoptosis, possibly as part of the corneal wound healing response. It is also possible that this cell death might be a contributing factor to the loss of transgene expression observed over time.

Apoptosis within the stroma was assessed by TUNEL staining within the cornea at 10 days post injection. This time point was chosen as it is:

a) Approximately half way between the peak of transgene expression at 7 days post injection and beginning of the basal plateau at 14 days post injection so any contribution to loss of transgene expression can be assessed.
b) Before the wave of posterior stromal proliferation at 18-21 days post injection observed in 4.2.6, which may have been triggered by the apoptosis of more anterior cells.

Four mice were injected intrastromally with 2 µL of AAV2/8(Y733F)-CMV-eGFP (viral dose $7x10^9$ vgs) whilst the contralateral eye was left uninjected. Uninjected was chosen as the control state for this experiment as it is highly likely that some apoptosis will be triggered by the process of injection itself in addition to any vector related process. For this initial study this complicating factor was not examined, the effects of vector + injection being examined in combination. At 10 days post injection all animals were culled and their eyes prepared for cryosectioning without fixation (as required by the TUNEL assay).

The TUNEL assay proved to be highly unreliable with even similar tissues processed entirely in parallel not always producing comparable levels / quality of staining. Good quality staining was rare. The experiment was therefore repeated several times in an attempt to achieve acceptable staining in a reasonable number of eyes. The apical corneal epithelium has been shown to undergo apoptosis prior to desquamation of mature cells from the corneal surface [291]. This area was therefore chosen to act as an internal control for the unreliable staining; only in tissue where this was clearly visible was the staining deemed to have worked.

Figure 25 shows examples of the best staining achieved in both an injected and uninjected corneas. Whilst staining in the uninjected controls was reasonably reproducible staining was less consistent in injected eyes. The staining shown in the injected condition therefore whilst indicative may not be truly representative. In the uninjected control condition the only TUNEL staining visible is in apical epithelial cell nuclei as would be expected. In the vector injected condition TUNEL staining is visible in apical epithelial cell nuclei and extensively within

stromal nuclei. Additionally some level of background in which TUNEL stain does not colocalise with the nuclear marker DAPI is also visible; although this is less extensive than properly colocalised staining. No eGFP transgene expression is visible due to TUNEL requiring only very light fixation conditions which does not fix the eGFP.

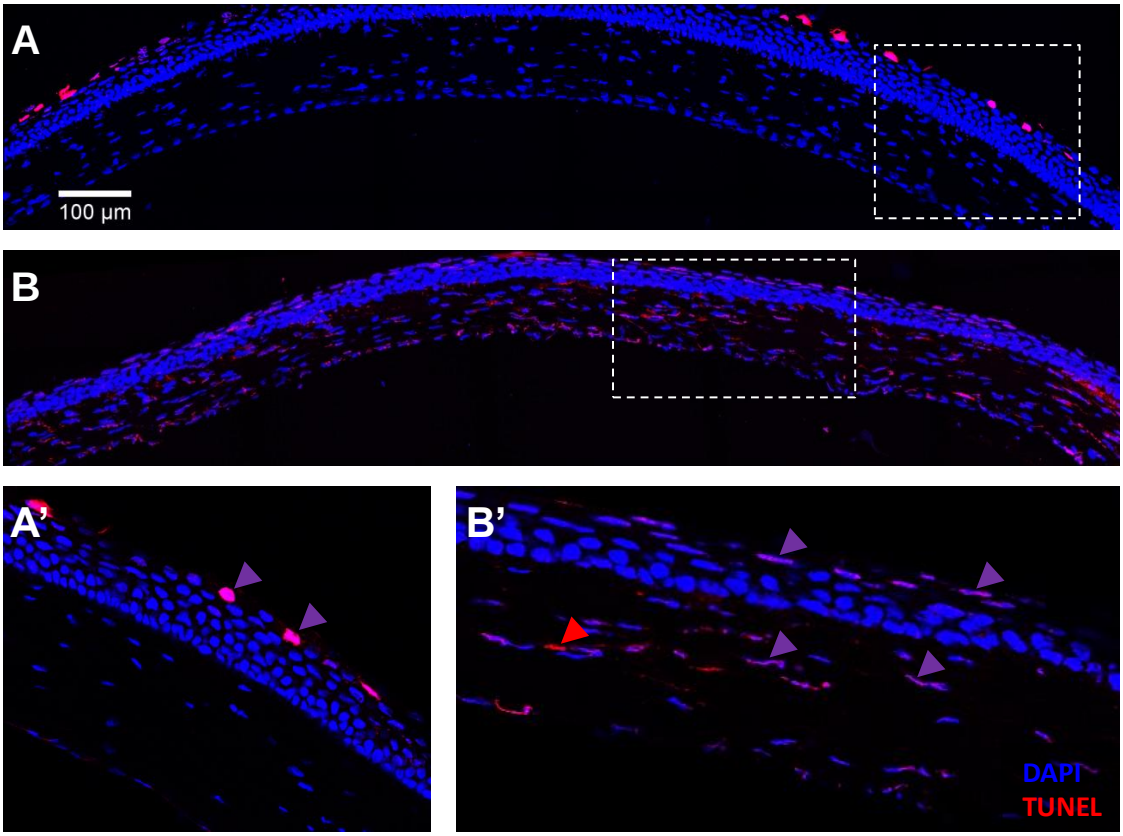

Figure 25. Transverse sections (18µm) through murine corneas showing TUNEL positive (apoptotic) cells in the stroma 10 days after 2µL intrastromal injection of AAV2/8(Y733F)

A: Uninjected cornea. Confocal z-projection at 40x magnification.

A': Highlighted area in A shown in greater detail. Single confocal image in z-plane at 40x magnification.

B: Injected cornea Confocal z-projection at 40x magnification.

B': Highlighted area in B shown in greater detail. Single confocal image in z-plane at 40x magnification.

In all: Purple arrows highlight DAPI/TUNEL colocalisation, Red arrow show non-colocalised TUNEL.

4.2.8 Immunohistochemistry to determine whether macrophages are present in the corneal stroma at 10 days post intrastromal injection of AAV2/8(Y733F)

The data thus far indicates that a corneal wound healing response may have been triggered by the intrastromal injection of vector as shown by an increase in stromal apoptosis (4.2.7), the subsequent proliferation of stromal cells (4.2.6) and the restriction of transgene expression to the posterior stroma over time (4.2.4 & 4.2.6). This is unlikely to be the result of the acute injury of injection itself the responses have only become apparent long after this initial insult. Thus the observed responses may be driven by a vector induced inflammation.

To further examine this possibility immunohistological staining for F4/80 was performed upon corneal tissue at 10 days post injection. F4/80 is well established as a specific marker of activated macrophages [292], and as a critical cell type in both innate and adaptive immunity the presence of activated macrophages would act as a good indicator of any inflammatory process or immune response that may be occurring.

Three mice were injected intrastromally with 2 µL of AAV2/8(Y733F)-CMV-eGFP (viral dose $7x10^9$ vgs), the contralateral eye was injected with 2 µL of PBS-MK to act as a negative control. At 10 days post injection all animals were culled and their eyes prepared for cryosectioning and staining.

Figure 26 shows representative examples of the staining for both an AAV and control injected corneas. In the PBS-MK injected control tissue (Figure 26A) very few F4/80 positive cells can be seen, whereas in the AAV injected cornea (Figure 26B) a large number of cells stain positive for F4/80 indicating the presence of activated macrophages. The eGFP transgene was not imaged in this experiment.

.

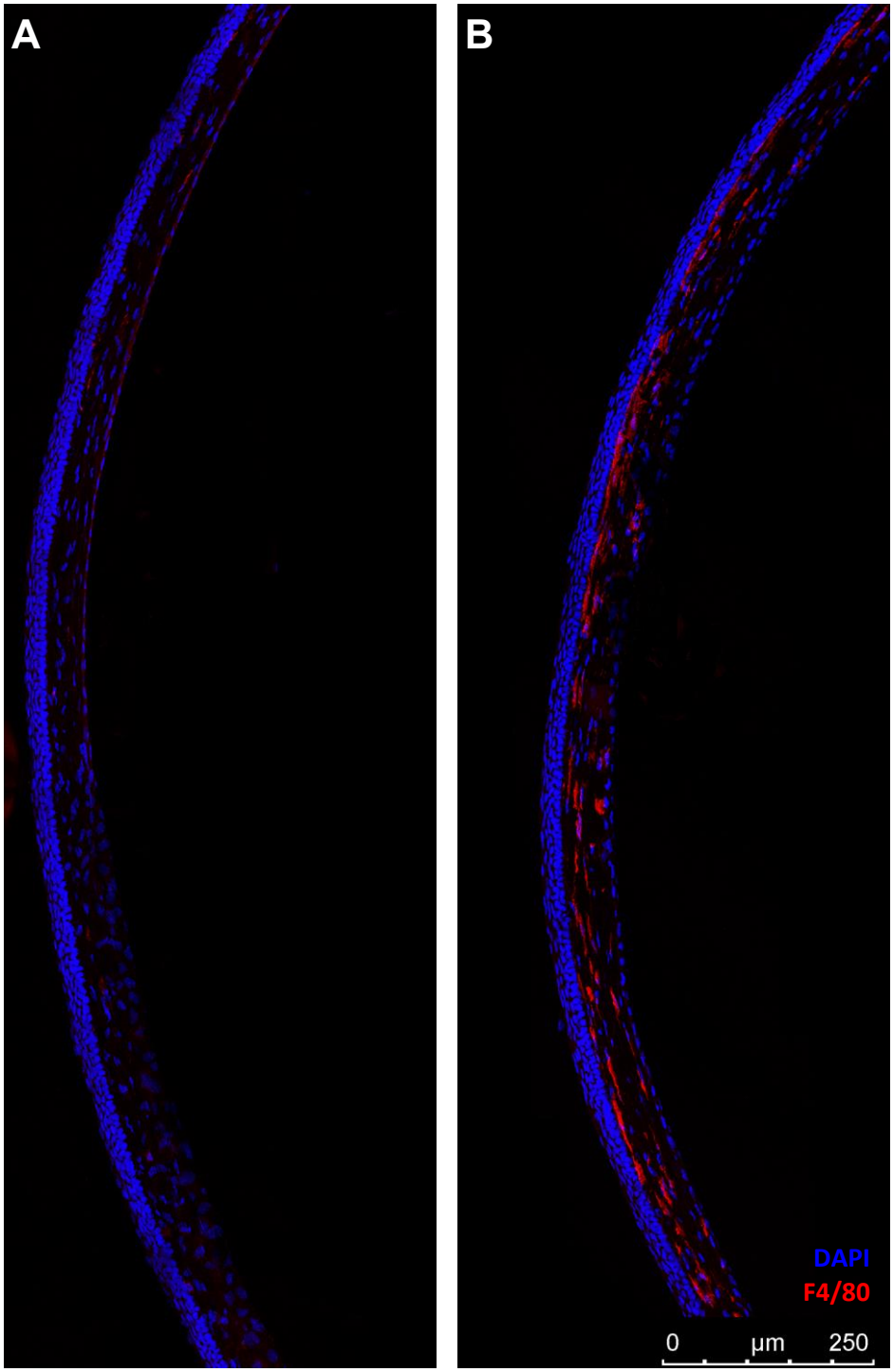

Figure 26. ***Transverse sections (18µm) through murine corneas showing F4/80 positive cells (mature macrophages) in the stroma 10 days after 2µL intrastromal injection***

A: Post injection with PBS-MK as a control.

B: Post injection with AAV2/8(Y733F)-CMV-eGFP.

All images: Projection of confocal z-stacks taken at 10x magnification.

Blue = DAPI, Red = F4/80

4.2.9 Amounts of soluble protein resulting from transgene translation within the murine eye (*in vivo*) at 7 days post intrastromal injection of AAV2/8(Y733F) as assessed by ELISA

The intended application of gene delivery to the corneal stroma via AAV2/8(Y733F) in this study is for transduced cells to act as production sites for continuous expression of soluble factors to ameliorate corneal disease.

Interleukin 10 (*IL10*) was chosen as a test transgene firstly because it is a potential therapeutic gene, shown by some studies to have beneficial effects in the cornea for the amelioration of corneal allograft rejection [230] and herpetic keratitis [293]. Secondly murine *IL10* encoding vector constructs already existed within the lab and a reliable ELISA assay for murine IL10 had been well established.

To establish the levels of soluble protein that might be produced by this approach the amount of transgene product (muIL10) present in the murine eye 7 days post intrastromal injection was assessed by ELISA. As a positive control and for purposes of comparison the vector was also injected subretinally. As a negative control eGFP encoding virus was also injected both intrastromally and subretinally.

A total of 6 mice (12 eyes) were injected as follows

3 eyes – 2µL Intrastromal AAV2/8(Y733F)-CMV-IL10-IRES-eGFP

3 eyes – 2µL Subretinal AAV2/8(Y733F)-CMV-IL10-IRES-eGFP

3 eyes – 2µL Intrastromal AAV2/8(Y733F)-CMV-eGFP

3 eyes – 2µL Subretinal AAV2/8(Y733F)-CMV-eGFP

At 7 days post injection all animals were sacrificed and all eyes enucleated. Each eye was then surgically trimmed of all extraneous tissue such as ocular muscle and optic nerve before being placed in 200 µL of ELISA reagent diluent (1xPBS + 1%BSA) and homogenised (2.4.7). All samples were then diluted 1 in 10 in reagent diluent and run in triplicate. ELISA plate loading volume was 100µL / well.

Figure 27 shows the ELISA data. The results for the intrastromally injected muIL10 encoding virus are both well within the range of the standard curve and relatively consistent giving an average 0.14 ± 0.05ng/mL for the sample.

Two of the three data points (including the one highlighted by the red circle in Figure 27) for the subretinally injected muIL10 encoding virus were well beyond the range of the standard curve and are therefore unreliable. It is clear however that subretinal injection results in 10-100 fold more transgene product than intrastromal injection.

All of the data points for the control eGFP encoding virus were below the range of detection and can be considered negative for muIL10 by ELISA.

A

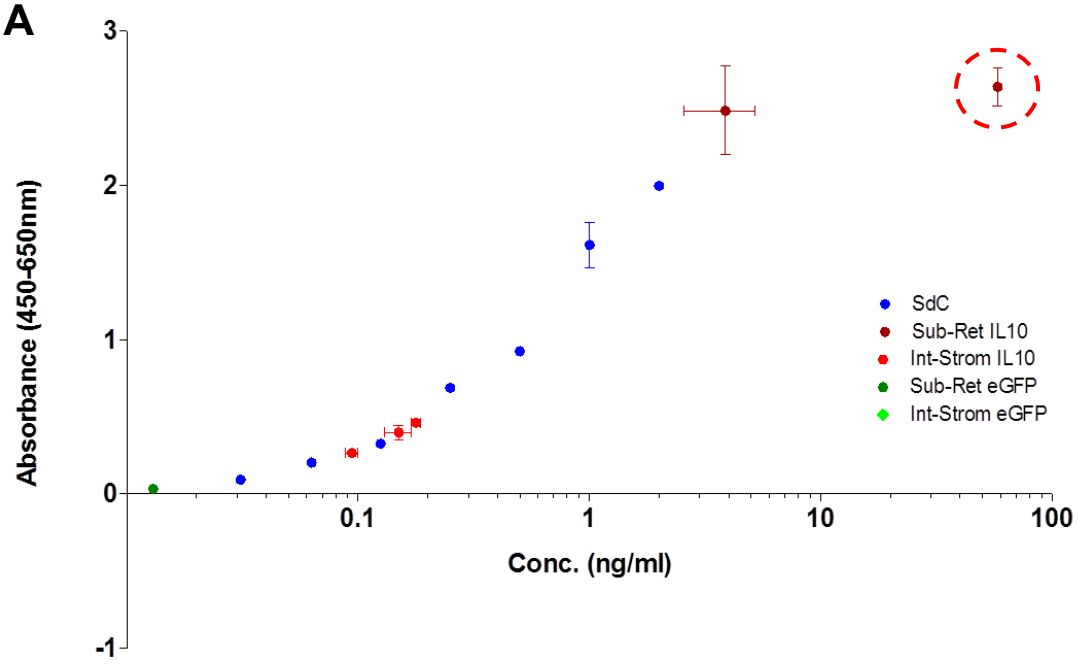

B

Subretinal / IL10 vector	Intrastromal / IL10 vector	Subretinal / eGFP vector	Intrastromal / eGFP vector
31.1 ng / mL (Out of Range - High)	0.14 ng /mL	0.0085 ng/mL (Out of Range – Low)	0 .004 ng/mL (Out of Range – Low)

Figure 27. Levels of vector mediated muIL10 detected in the murine eye 7 days post either intrastromal or subretinal injection of 2 µL of either AAV8(Y733F)-CMV-muIL10-IRES-eGFP or AAV8(Y733F)-CMV-eGFP . Assessed by ELISA of whole eye homogenates

A: ELISA data plot showing absolute concentration of muIL10 against absorbance at 450nm-650nm for the standard curve (blue points) and concentration of muIL10 calculated from standards against absorbance at 450nm-650nm for samples (red and green points)

B: Average concentration of muIL10 detected in the different samples.

4.2.10 Histological assessment of AAV2/8(Y733F)-mediated expression in human cornea 7 days post intrastromal injection *ex vivo*

Having established the transgene expression profile mediated by AAV2/8(Y733F) transduction in the murine cornea following intrastromal injection, this experiment was undertaken to ensure similar results are obtainable in human tissue.

A pair of human corneas were obtained from the eyebank, at the point they were obtained they had been in organ bank culture for only 48 hours making them extremely fresh for this kind of sample.

As a human cornea is so much larger than a murine cornea a larger volume of virus will be required to mediate a similar area of transduction, based on some approximate calculations (below) a volume of 50µL was selected as roughly equivalent. The human corneas were mounted on an artificial anterior chamber and injected intrastromally with 50µL of diluted AAV2/8(Y733F)-CMV-eGFP, total dose $4.38x10^{10}$ vgs.

Corneas were incubated at 37°C / 5% CO_2 in Culture Medium I (BiochromAG) for 7 days before being fixed in 4% PFA. One cornea was prepared for cryosectioning and the other flat mounted.

The approximate calculations below illustrate the difference in volume between human murine corneas in relationship to injection volume and virus titre. Data on dimensions of murine cornea taken from reference [294].

Murine cornea

Surface area of ~21mm^2 and an average thickness of ~0.15mm, resulting in a volume of ~3.15mm^3. Injected: 2µL of vector of titre of $3.5x10^{12}$ vg/mL, total virus dose $7x10^9$ vgs

Injection volume: Cornea volume = 1 : 1.575

Vector / unit volume: $2.22x10^9$ / mm^3

Human cornea

Surface area of ~135mm^2 and an average thickness of ~0.5mm, resulting in a volume of ~67mm^3. Injected 12.5µL of vector of titre of $3.5x10^{12}$ vg/mL diluted up to 50µL in PBS-MK, total virus dose: $4.38x10^{10}$ vgs

Injection volume : Cornea volume = 1 : 1.34

Vector / unit volume: $6.54x10^8$ / mm^3

Figure 28A & A' show orthographic projections of z-stacks taken through the endothelium and posterior stroma of the flat mounted cornea. The entire thickness could not be imaged as the sample was too thick. Transgene (eGFP) expression is widespread throughout the stroma in the area imaged which was representative of the majority of the tissue. Note that in Figure 28A the endothelium is patchy.

Figure 28B shows a representative cryosection. Transgene (eGFP) expression is again widespread although appears brighter in the posterior stroma closest to Descemet's membrane (most of the endothelium has been lost from the area imaged). The red bar shows the approximate thickness of a human cornea *in vivo*, thus the cultured tissue has swollen considerably to almost 4x this thickness

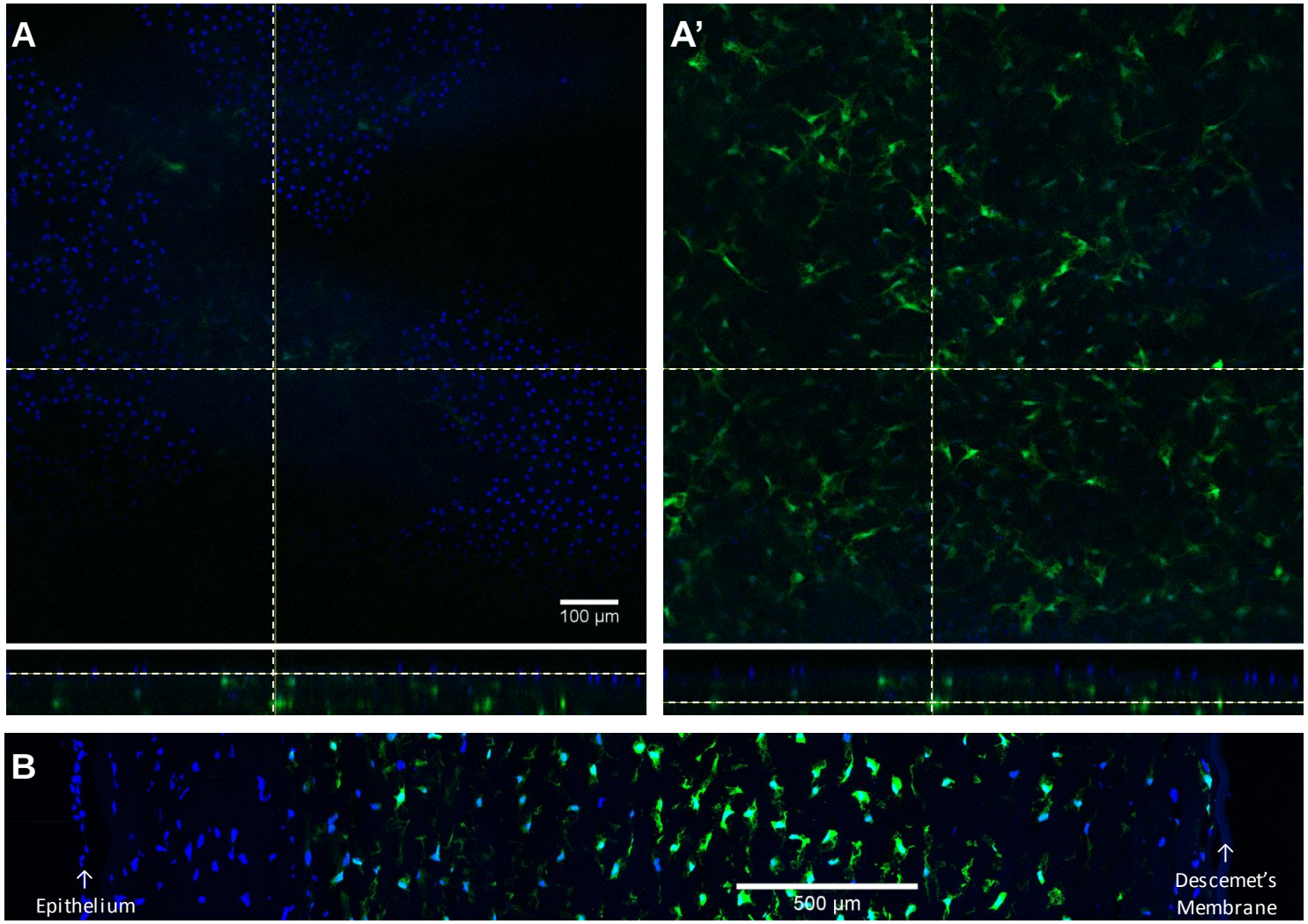

Figure 28. ***Images showing vector mediated eGFP expression in human cornea 7 days after ex vivo intrastromal injection of 50 µL of AAV2/8(Y733F)-CMV-eGFP. Total virus dose: 4.23x10^{10} vgs***

A & A': Orthographic projections of confocal z-stack taken through flat-mounted cornea at 10x magnification. Only XY (single plane) and XZ shown.
B: Transverse section (18µm) through injected human cornea. In **All**: Blue = DAPI, Green = Vector mediated eGFP

4.2.11 Short term assessment by ELISA of the amount of soluble transgene product within the human cornea (*ex vivo*) post intrastromal injection of AAV2/8(Y733F)

In translation from the murine *in vivo* to the human *ex vivo* conditions it is not feasible to sample corneal tissue itself for transgene expression over time due to the extremely limited supply of human samples. An alternative approach would be to sample the conditioned tissue culture medium for secreted transgene product in order to assess vector mediated expression over time.

This experiment was designed as a short term pilot to establish if such an approach was feasible, i.e. if transgene product was indeed secreted from the tissue ex vivo, and if the resulting levels in the conditioned media would be detectable by ELISA.

The transgene used in this experiment (as in 4.2.9) was *muIL10* as it was both convenient and a potentially useful transgene product.

A pair of fresh (~48 hours in culture) human corneas were obtained from the eyebank. One was injected intrastromally with 50 µL of diluted AAV2/8(Y733F)-CMV-muIL10-IRES-eGFP, total dose 1 x 10^{11} vgs. The other was injected with PBS-MK to act as a control

Both corneas were incubated at 37°C / 5% CO_2 in Culture Medium I (BiochromAG) and the concentration of muIL10 in the conditioned medium assessed by ELISA at various time points shortly post injection. The culture media was replaced after each time point.

Below are the time points at which conditioned media was taken and the total volume of media for each point. As it was unknown what muIL10 concentration might be expected the sample volume and incubation time was varied in an attempt to ensure that at least one point fell within the range of ELISA standard curve.

Time sample taken post injection	**Total conditioned media / sample volume.**
55 hours (55 hour incubation)	20 mL
96 hours (41 hour incubation)	20 mL
120 hours (24 hour incubation)	3 mL

After 120 hours the corneas were placed in 10 mL of fresh medium and incubated for a further 24 hours. At this 144 hour time point they were removed from culture and rinsed briefly with 1xPBS. They were then blotted as dry as possible using tissue paper and

weighed using an analytical balance. A 4mm biopsy punch (Stiefel) was then used to remove a disk from the central cornea, this too was then weighed. These corneal disks were then homogenised in 400 µL of ELISA reagent diluent and assayed for muIL10 concentration by ELISA

All samples (both conditioned media and tissue homogenate) were assayed at the same time, earlier samples had been stored at -20°C between collection and ELISA. All samples were run in triplicate both neat and diluted 1:10 in reagent diluent. ELISA plate loading volume was 100 µL / well.

Figure 29 shows the ELISA data. Only results for the neat samples are presented as they were all well within the range of the standard curve rendering the dilutions irrelevant. Figure 29A shows the raw concentration data obtained whereas in Figure 29B the same data is presented as total amount of muIL10 in the entire volume of conditioned media, thus adjusting for the variable total volume of conditioned media at different time points. The total amount of muIL10 released into the culture medium from the transduced tissue appears relatively consistent over the period measured at between 6 and 8 ng. The final 96-120 hour period appears reduced compared to the two previous time points in Figure 29B however it should be noted that the incubation time for this point is roughly half that of those previous. Data corrected for incubation time is not shown as there is the additional factor of IL10 half-life within the medium to consider.

Figure 29C shows the concentration of muIL10 detected within the tissue homogenates 144hours post injection. Figure 29D shows the recorded masses of both the whole corneas and the excised 4mm discs. It also shows the amount of muIL10 calculated to be present in both based by extrapolating the amount detected in the assayed sample to the total volume / mass.

The amount of muIL10 that remains in the tissue at this one time point appears be roughly one order of magnitude lower than that assayed in the conditioned media at any time point (0.47ng vs 2.7 – 8.1ng) This perhaps indicates that the majority of soluble protein produced does not remain within the tissue under these circumstances

All of the PBS-MK injected control samples were below the range of detection and can be considered negative for muIL10 by ELISA.

Based upon these results it is clear that following intrastromal injection of AAV in the context of human tissue *ex vivo* transgene product is released from the tissue into the conditioned media in easily detectable amounts. A more long term experiment is therefore feasible.

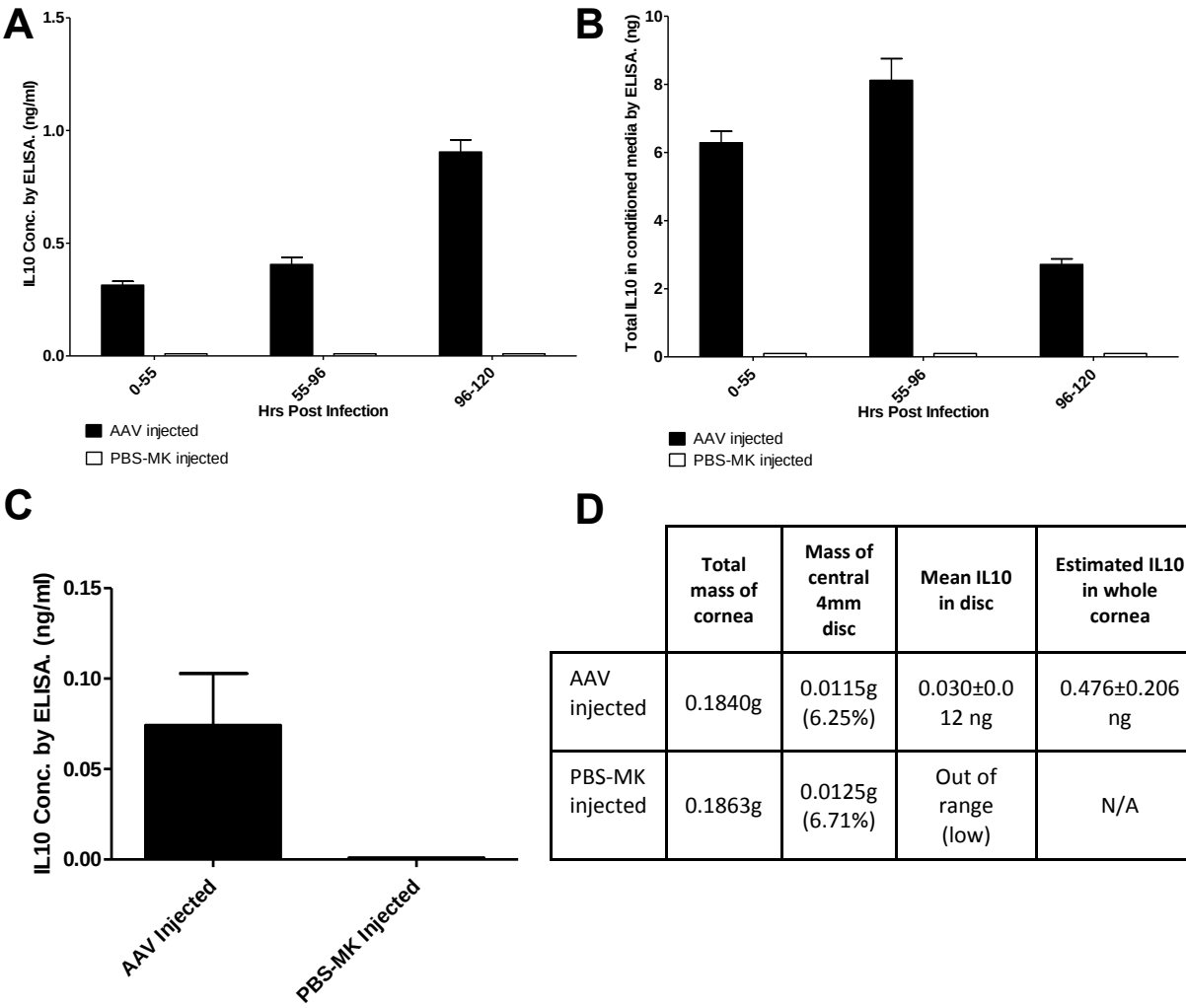

	Total mass of cornea	Mass of central 4mm disc	Mean IL10 in disc	Estimated IL10 in whole cornea
AAV injected	0.1840g	0.0115g (6.25%)	0.030±0.012 ng	0.476±0.206 ng
PBS-MK injected	0.1863g	0.0125g (6.71%)	Out of range (low)	N/A

Figure 29. Levels of vector mediated muIL10 released into culture medium and retained within the tissue over 144 hour period following intrastromal injection of 50 µL of either AAV8(Y733F)-CMV-muIL10-IRES-eGFP or PBS-MK. Human corneas ex vivo assessed by ELISA

A: Concentration of muIL10 in conditioned culture medium at three time periods; 0-55hrs, 55-96hrs, 96-120hr. Media changed between time points.

B: Data in A corrected for different culture medium volumes at different time points which were as follows; 0-55hrs = 20mLs, 55-96hrs = 20mLs, 96-120hrs = 3mLs

C: Concentration of muIL10 in homogenised, centrally positioned, 4mm diameter tissue disk excised at 144hrs post injection, 400µL volume.

D: Table presenting the masses of the whole corneas and excised buttons and calculated amount of muIL10 present in both.

4.2.12 Very long term assessment by ELISA of the amount of soluble transgene product within the human cornea (*ex vivo*) post intrastromal injection of AAV2/8(Y733F)

Following on from the experiment in 4.2.11 the amount of transgene product (muIL10) produced in the human cornea was assessed over a much long time period. Initially a period of 4 months (120 days) was selected but based upon initial results this was extended to 1 year.

A human cornea (~1 week in organ bank culture) was obtained from the eye bank and injected intrastromally with 50µL of diluted AAV2/8(Y733F)-CMV-muIL10-IRES-eGFP, total dose 1 x 10^{11} vgs. The corneas were incubated at 37°C / 5% CO2 in 25mL of Culture Medium I (BiochromAG). Approximately every 6-9 days following procedure was performed:

- The conditioned media (25mLs) was removed and replaced with a fresh 25mLs (preheated to 37°C). Cornea was returned to the incubator in this fresh media.
- The conditioned media was passed through a 0.22µm filter to remove any cellular contaminants.
- From the 25mL filtrate 1.4mL samples were taken in triplicate the rest was discarded.
- Samples were stored at -80°C until assayed.
- For one time point (192 days post injection) the remainder of the conditioned media was returned to the incubator for a further 7 days in the absence of the corneal tissue. This was to gain some insight into how much muIL10 might be degraded over this time.

Periodically the container (100mL sterile plastic bottle) in which the injected cornea was stored was changed. All samples were assayed for muIL10 concentration by ELISA at the same time at the end of the experiment. All samples were run neat in quadruplicate. ELISA plate loading volume was 100µL / well.

Figure 30A shows the ELISA data. Between 0 and 70 days post injection the muIL10 concentration assayed is consistently high between 1 and 2 ng / mL. Between 70 and 180 days post injection this level has decreased and remains consistent between 0.5 and 1 ng / mL. After 180 days post injection the level increases dramatically to a level beyond the upper limit of the ELISA standard curve reaching a peak at around 200 days post injection before dropping off to nothing by 270 days post injection. No muIL10 was then detected in any sample between 270 days and the end of the experiment at 367 days post injection.

Red bars represent samples taken from incubation periods >9 days and thus are likely incomparable.

Figure 30B shows that the concentration of muIL10 detected in one sample (192 days) decreased by approximately 6 fold when the conditioned media was incubated for a further 7 days in the absence of the corneal tissue.

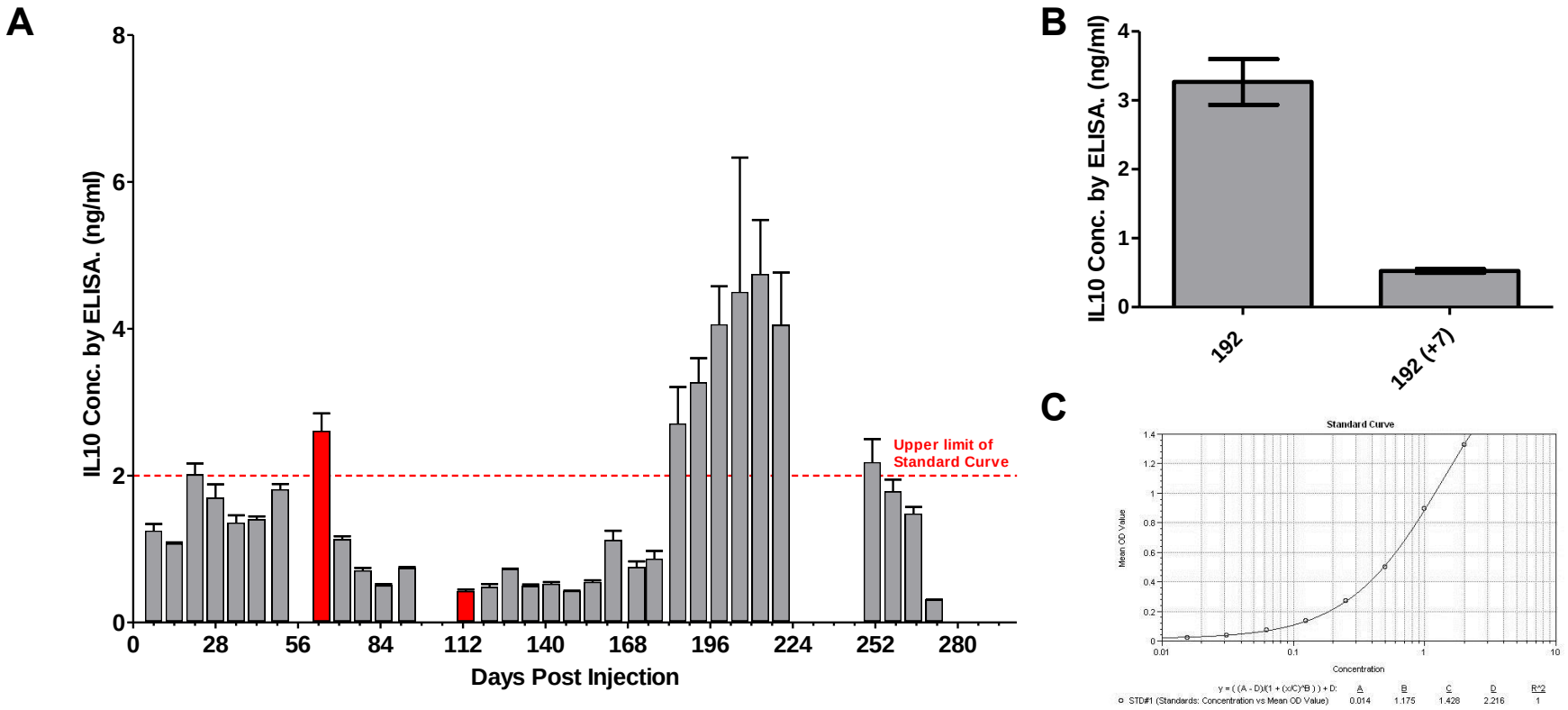

Figure 30. ***Levels of vector mediated muIL10 released into culture medium over 52 week period following intrastromal injection of 50 µL of AAV8(Y733F)-CMV-muIL10-IRES-eGFP. Human cornea ex vivo, assessed by ELISA***

A: Concentration of muIL10 in conditioned culture medium over time, each grey bar represents a 7±2 day culture period. Media was changed between time points. Red bars represent time points with a > 9 day culture period.

B: Concentration of muIL10 in conditioned media the 192 day post injection time point compared with itself after a further 7 days incubation at 37°C in the absence of the corneal tissue.

C: ELISA assay standard curve.

4.3 Discussion

The work in this chapter focused upon characterising AAV based transduction of the corneal stroma to establish the feasibility of utilising stromal cells as production sites for a therapeutic transgene product to be secreted into the cornea. The keratocytes of the stroma are traditionally considered to be quiescent undergoing no cell division, cell death or any significant change under normal circumstances. The primary role of stromal keratocytes under normal circumstances being the synthesis and maintenance of the stromal extra cellular matrix (ECM).They are therefore an attractive target cell population to be co-opted into an additional role in the production and secretion of transgenic product.

Initial experiments were indicative of the serotype AAV2/8(Y733F) mediating a higher level of transgene expression in the stroma than either of the other two serotypes chosen for comparison, particularly AAV2/9 which mediated a markedly lower level of transgene product at the time point assessed. This finding was in line with expectation, and the tyrosine mutant AAV vectors are described to mediate a higher level of transgene efficiency due to their more efficient escape from the endosome [187], a process that should be relatively cell type independent. Additionally an increased level of transgene expression in other ocular tissues such as the retina has been observed by both ourselves and others [295].

However the number of animals / eyes used in this initial trial was small and perhaps the observed difference between AAV2/8 and AAV2/8(Y733F) was not especially significant. Nonetheless both serotypes mediated a high level of expression and thus the selection of AAV2/8(Y733F) as the candidate for further development remains valid.

The time course of transgene expression following intrastromal injection with AAV2/8(Y733F) was well characterised in two separate experiments using different doses of vector delivering eGFP. The onset of transgene expression is rapid, being easily detectable by slit lamp imaging only 2 days post injection. Expression reaches its peak around 7 days post injection; however, this level is not maintained and falls off rapidly, with the majority having been lost by 12 days post injection. After this a basal level of expression is maintained for at least 148 days (~5 months) post injection.

This exact pattern of transduction has not to our knowledge been replicated in the literature. Sharma et al. [251] showed that expression from various AAV serotypes (applied topically following epithelial removal *in vivo*) continued to increase over time up to 30 days post transduction beyond which they did not follow up. Work by Hippert et al. in which vector was injected intrastromally [253] is in broad agreement with this pattern as they too observed a

slow increase of transgene expression over time up to 4 weeks post injection which then persisted up to 17 months post injection. The different pattern of transgene expression observed here is likely the result of a combination of factors.

Firstly it is clear that this combination of vector and injection methodology has resulted in transgene expression not only in the stroma but also off-target within corneal epithelial cells. A very high level of transgene expression is seen within the epithelium at 7 days post injection (Figure 19) and the patterns of transgene expression observed by fundoscopy at the 7 day time point in both 4.2.2 and 4.2.3 are reminiscent of epithelial cells labelled by transgenic means [90]. This epithelial transduction is however lost relatively rapidly due to the normal turnover processes of the epithelium as shown by the relative lack of epithelial transduction at 14 days post injection (Figure 18) or at any later time point. This process likely accounts for the majority of the loss of transgene expression observed by fundoscopy between days 7 and 14 post injection.

This off-target transduction of the epithelium was not the focus of this study and was a highly unexpected result. Intrastromal injection would be expected to only result in a very limited exposure of the epithelium to vector so the means by which such a large proportion of the epithelium became transduced is unknown. Additionally AAV vectors have not previously been shown to mediate anything more than a very limited transduction of the epithelium as discussed in 1.7.4. Such widespread off-target transduction of the epithelium has also not been reported in any other study targeting the stroma for transduction by AAV. In the case of Sharma et al. [250] this is perhaps unsurprising as in their studies the epithelium was removed prior to application of vector, however Hippert et al. [253] injected vector intrastromally by an almost identical method to ourselves and observed only extremely limited epithelial transduction at 3 days post injection. This study by Hippert et al. used a different vector serotype (AAV2/8) and whilst this serotype was assessed in our initial pilot experiments we did not at that time focus upon or compare epithelial transduction. Some transduction of the epithelium is seen with both AAV2/8 and AAV2/8(Y733F) at 14 days post injection (Figure 12) however by this time point most transduced cells may have already been lost. It remains possible therefore that AAV2/8(Y733F) displays a greatly increased epithelial tropism compared to AAV2/8 or any other serotype tested to date although further work is required to confirm this.

For the intended purpose of expressing a soluble transgene for augmentation gene therapy this reproducible off-target expression in the epithelium is likely beneficial as it will initially increase the amount of soluble transgene produced, boosting the therapeutic effect albeit transiently. If however application required that transduction be limited to the stroma then a tissue specific promoter could be utilised to eliminate this off-target transgene expression.

The pattern of transgene expression observed here within the stroma is also at odds with that widely reported within the literature. The study by Hippert et al. is the most directly comparable to that presented here as they used a near identical vector titre, injection volume and vector delivery method in combination with a very similar AAV serotype. At seven days post injection however Hippert et al. did not achieve the a high level of stromal transgene expression shown here, and whilst they report transgene expression increasing over time, even by 1 month post injection expression was still far lower than that seen here at early time points. This disparity cannot be explained by the serotype difference between the two studies. Whilst the majority of this study utilised AAV2/8(Y733F), exactly the same serotype used by Hippert et al. (AAV2/8) was tested in initial experiments and was also found to mediate a high level of stromal transgene expression at 14 days post injection (Figure 12).

Hippert et al. did achieve a high level of stromal expression comparable to that shown here via a subsequent intrastromal injection of PBS in procedure they termed “hyper-activation” and they hypothesised that this induced increase in AAV mediated expression proceeded from inflammatory processes. As a concept this has merit as AAV has previously been shown to increase its transgene expression within inflammatory environments in the cornea [226].

The very high level stromal transgene expression observed here could therefore be a result of a similar hyper-activation but mediated by the initial injection without the requirement for any subsequent boosting by PBS injection. This discrepancy might result from a difference in vector purity as our vectors may contain a greater number of inflammatory impurities than those used by Hippert et al. Their paper does not describe their AAV production and purification protocol in full detail but does mention final concentration by iodixanol gradient. This method would be expected to result in virus of a high purity, whilst we are aware that our ion exchange based method, whilst producing higher titres, may not be as pure. Our initial injection may therefore have constituted a sufficiently inflammatory event for transgene production by AAV to be essentially hyper-activated as described by Hippert et al. almost immediately upon injection. Thus the dampening down or resolution of this event may also have contributed to the observed reduction in transgene expression over time.

Due to the fact that they observed no difference in the capacity of PBS and LPS to stimulate hyper-activation Hippert et al. concluded that “It is the lesion rather than the substance that causes the inflammation”. The results presented here would tend to partially contradict that statement. If indeed we are observing hyper-activation after the initial injection it cannot be solely a result of the injection itself as in that regard our procedure was essentially identical to that performed by Hippert et al. who observed no immediate hyper-activation. Hippert et al’s results show that whilst the injection itself is certainly effective in promoting hyper-

activation of an established rAAV transduction the results presented here indicate that some additional factor must be required to produce such the effect from an initial injection. Further experiments are required to confirm this hypothesis. Our vector purification methodology has recently been improved / modified to utilise an affinity based FLPC column specifically designed for AAV purification which has resulted in a marked improvement in vector purity. An experiment could therefore now be undertaken where by a highly purified vector is co-injected with either LPS or vehicle to confirm whether hyper-activation is indeed occurring and dissect the factors influencing the initial inflammatory response.

Following our injections we observed no obvious macroscopic evidence of inflammation, such as clouding / haze of the cornea, redness or neovascularisation at any early time point. All corneas initially appeared healthy and fully transparent. At later time points some but not all eyes developed fibrotic corneal scarring as shown in Figure 18; however this is a commonly observed event within the lab primarily associated with repeated general anaesthetic and ocular imaging with bright light sources rather than any other intervention.

At the cellular level we did observe an increase in F4/80 positive cells (activated macrophages) in the corneal stroma in the case of AAV injected eyes at 10 days post injection which was not observed in the control. Hippert et al. did not observe any increase in F4/80 positive cells in the stroma following either their initial injection or subsequent hyper-activation by PBS injection, providing further evidence that our initial injection provided a stronger inflammatory drive than either injection by Hippert et al. and is thus producing a hyper-activated response. It should be established however whether these cells remain present once transgene expression has plateaued to the lower level sustained over the long term.

Another factor that is likely involved in the observed changes in transgene expression in the stroma over time is the wound healing response of the stroma to the insult of the injection. The normal response of corneal keratocytes to injury has been well characterised, although has only been extensively studied in two distinct injury types due to their clinical relevance; epithelial injuries of various severity and direct incisions into the stroma itself of a type associated with refractive surgery. Most stromal wound healing responses have been characterised as occurring very rapidly after injury; keratocyte apoptosis occurs with hours [38,39], repair responses begin shortly afterwards [32] and the majority of healing process being well established or essentially over by 1 week post injury [41].

This timescale does not fit with the observed changes in this study, which did not become apparent until 7 to 12 days post injection at the earliest. By this time the main events of a typical corneal wound healing response would be expected to be complete. Surprisingly

however the pattern of results that emerged around this time point and later was in many respects extremely similar to what has been observed to be associated with a typical stromal wound healing response to an epithelial injury, although much delayed.

Assessment of transgene (eGFP) expression in two separate experiments (flat mount imaging at 28 days post injection - Figure 23, and cryosectioning at 148 days post injection - Figure 18) showed that expression becomes largely restricted to the posterior stroma. This is in contrast to images taken earlier at 7 and 14 days post injection where full thickness stromal transduction is visible. There are two possible explanations for this finding; anterior cells are either being lost or are down regulating transgene expression. The former of these two possibilities is perhaps the most likely.

Following an intrastromal injection two distinct insults to the cornea have been made that might trigger anterior keratocyte apoptosis and a wound healing response, firstly the acute process of injection and secondly a potential low level inflammation to the vector itself developing over time. During the process of intrastromal injection the needle causes a penetrating injury to both the epithelium and stroma, although epithelial involvement is localised to a single point. The injection then causes a widespread separation of the stromal matrix and opacification of the cornea, although this rapidly resolves appearing macroscopically normal within 24 hours.

It is conceivable that the damage to the stromal matrix resulting from intrastromal injection is somewhat focused upon the anterior stroma. During injection the needle tip was not guided to any specific position within the Anterior - Posterior axis of the cornea, although care was taken to avoid penetration of the anterior chamber which may have favoured anterior positioning of the needle tract. Additionally for reasons of ease of corneal penetration the needle was positioned bevel upward during injection and therefore expulsion of liquid from the needle will have been initially directed anteriorly. Anterior keratocyte apoptosis is regularly observed as the initial event in normal stromal wound healing in the case of anterior (epithelial) injuries and it is extremely likely that intrastromal injection would trigger some apoptosis given that even relatively minor corneal wounds such as epithelial scrapes do so [40,296].

However, given that anterior stroma transgene expression is widespread at 7 days post injection, and that apoptosis to the acute injury of injection should have occurred within hours, it is unlikely that the injection itself has resulted in apoptosis unless the process is greatly delayed in the case of this specific insult.

At 10 days post injection TUNEL staining revealed a relatively widespread apoptosis occurring within the stroma. This staining whilst of sufficient quality to be convincing of

increased apoptosis overall could not be said to be sufficiently clear to establish whether apoptosing cells were anteriorly restricted. The TUNEL assay proved to be highly unreliable so attempts were made to use immunohistological staining for the apoptosis marker activated caspase 3 in order to confirm the TUNEL result and better reveal any anterior localisation of the apoptosis. Unfortunately despite multiple attempts under different conditions no positive cells for activated caspase 3 were ever observed in the positive control region (the apical epithelium) or elsewhere in the cornea using this antibody, suggesting it is ineffective in this tissue. This is in line with the experience within the lab which suggests that whilst this antibody works well for staining of cells grown *in vitro,* its application to cryosectioned ocular tissue is limited. The apoptosis observed at 10 days post injection likely is too late to be injection related and may well be induced by the same inflammatory response within the cornea that may be driving a hyper-activation of transgene expression from AAV.

At the later time point of 18-21 days post injection of vector, a wave of EdU uptake indicative of cell proliferation was observed to occur within the stroma. This proliferative wave is localised to the posterior stroma across the entire corneal diameter. This is again extremely similar to what is observed following an epithelial injury to the cornea [41] but much delayed. Such proliferation is indicative of the keratocytes transitioning to an activated wound healing state to repopulate and repair the stroma. In the context of stromal wound healing this is a process that initiated by the apoptosis of adjacent keratocytes [38,41] and thus the pattern of proliferation observed is strongly indicative of extensive anterior keratocyte apoptosis having taken place.

Additionally this posterior proliferation was only observed in the AAV injected cornea and not in the vehicle injected control. This was also the case with the increase in F4/80 staining (indicative of an inflammatory event) that was discussed earlier. This response is therefore specific to the vector solution and unrelated to the trauma of intrastromal injection, adding more weight to the hypothesis of vector induced inflammation being primarily responsible for driving all of the effects observed.

It is difficult to explain in this context why a widely distributed vector induced inflammation is driving a response typical in many respects of a wound to the anterior cornea such as an epithelial debridement. It has been hypothesised that stromal keratocytes directly underlying the epithelium undergo apoptosis readily in response to even minor epithelial wounds or infections to act as a “firebreak” against spread of infection [297] and do so in response to cytokine factors released by the epithelium such as soluble Fas ligand and IL1 in particular [298]. Any kind of inflammation we have induced is likely to result in the production of IL1 possibly mediated by the activated macrophages we have observed within the stroma post

injection [299]. This could potentially mimic the epithelial derived signal to induce anterior keratocyte apoptosis and it is also possible that due to their “firebreak” role anterior keratocytes are perhaps more sensitive to undergoing apoptosis in response to such signals than those more posteriorly.

This hypothesis could be tested in a number of ways. Firstly experiments aimed at delivery of recombinant IL1 or Fas ligand to the stroma in various doses to determine if anterior keratocytes preferentially apoptose in response could be undertaken, although it is difficult to conceive of a method by which the cytokines might be delivered to this location whilst avoiding the complicating factors of epithelial or injection damage. Secondly the properties of the anterior and posterior keratocytes could be assessed for any differences that might indicate a variable response to cytokine signals, such as differential expression of cell surface receptors to cytokines.

In conclusion the effects of the low level inflammation in the stroma induced by AAV injection are twofold: On the one hand the effect may be beneficial, leading to hyper-activation of AAV transgene expression and an increased production of transgene product. By contrast the process may also be mildly deleterious as this inflammation eventually results in the activation of a stromal wound healing response and the loss of transduced keratocytes from the anterior stroma. With regard to the expression sustained over the long term (up to ~5 months) by which time any inflammation related processes should have resolved it has not been established here whether the level of transgene expression remaining at this time would have been comparable had there been no inflammation that may have triggered hyper-activation. Data from Hippert et al. [253] suggests levels pre and post hyper-activation would be comparable as this is what was observed in their study.

Given that no macroscopic evidence of damage was ever observed in response to the vector induced inflammation then perhaps the initial increase in stromal expression that results could be utilised therapeutically. However if a technique known to induce a limited stromal inflammation is to be of utility then it is important that the process be very tightly controlled due to its inherent pathogenic nature.

Despite this extensive discussion regarding the possible effects of an AAV2/8(Y733F)-CMV-eGFP mediated stromal inflammation upon transgene expression there can be no doubt that a widespread transgene expression profile remained evident up to 148 days (~5 months) post injection *in vivo* localised to the posterior stroma (Figure 18B). Whilst not truly quantitative the eGFP signal observed was not obviously weaker on a cell by cell basis than comparable imaging at earlier time points. This remaining expression also appears to be of a

higher level than the most extensive non-hyperactivated expression reported in the literature [253] and is thus likely still of use for application to production of a therapeutic protein for secretion over the long term.

The most convincing evidence for this comes from the data on human tissue *ex vivo* (4.2.12). After intrastromal injection of a comparable AAV dose (scaled up by volume from mouse tissue) a large amount of transgene product (muIL10) was detected by ELISA in the conditioned media for the first 50 days post injection. During this initial period concentrations of muIL10 close to the upper detection limit of the assay (1-2 ng / mL) were detected. The cornea was cultured in 25 mLs of medium that was replaced weekly meaning that at the point of assay a total of 25-50 ng of muIL10 was present in the total volume. This level represents an underestimate of the amount produced over the whole week in culture due to degradation of secreted muIL10 over time. To illustrate this the concentration of muIL10 present in conditioned media was shown to be reduced 6-fold after 1 week of incubation at 37°C in the absence of transduced tissue. Assuming one-phase decay kinetics this would give muIL10 a half-life of approximately 65 hours under tissue culture conditions.

These initial results exceeded expectations both in terms of level and duration of transgene expression produced. Duration in particular was surprising. Corneas are rejected for transplantation as a matter of course after only 2-4 weeks in organ culture for reasons of insufficient quality. This is usually due to decreasing endothelial cell density over time in culture. Initially therefore this experiment was planned to last for 2 months, as we expected corneal viability to have decreased too much to be of further use by this time. This period elapsed however with no real change or drop off in transgene expression being noted so these results would suggest that the cells of the stroma must be substantially more robust than those of the endothelium under these conditions. The experiment was thus extended until such a time as expression could no longer be detected up to a maximum of 1 year post injection.

Between 50 and 85 days post injection the concentrations of muIL10 detected steady dropped to around half the previous level to 0.5 and 1 ng / mL which then maintained until 180 days. This somewhat mimics the decrease observed *in vivo* although much delayed. Any extrapolation of mechanisms between the murine *in vivo* and human *ex vivo* condition is however likely to be invalid due to the dramatic differences between these two conditions. Nonetheless there is some indication that the posterior restriction of stromal transgene expression also occurs in the human tissue provided by the cryosectioning of human tissue 7 days post injection (Figure 28B) although it is possible this is merely an artefact of the high level of tissue oedema that occurs in culture.

After 180 days a dramatic increase in muIL10 level was observed, to concentrations beyond the range of the assay standard curve. This could perhaps be attributed to the cells dying and tissue integrity failing both of which might result in release of any muIL10 retained within the tissue. This hypothesis would be supported by the fact that after this pulse of high muIL10 levels dropped to zero with no further muIL10 detected between 279 days and the end of the experiment at 367 days. However, the fact that the high level pulse lasted for over 2 months is perhaps an unfeasibly long period to be attributed to the process of tissue death / failure. The event of the high level pulse is therefore difficult to explain and it would be important to establish whether it is reproducible, or a one off event observed in this experiment only.

Conclusions

- Intrastromal injection *in vivo* of the vector AAV2/8(Y733F)-CMV-eGFP results initially in a high level transduction of corneal keratocytes over the entire thickness and diameter of the cornea. In addition widespread off-target transduction of the corneal epithelium also occurs.
- Transgene expression peaks at 7 days post injection before dropping off to a basal level which is maintained *in vivo* for at least 148 days post injection.
- The drop off in transgene expression is largely the result of the loss of transduced epithelium to turnover, however the resolution of an inflammatory induced hyper-activation of AAV expression and the apoptosis of some transduced keratocytes may also contribute.
- In multiple respects the response of the stromal cells to the inflammation induced by the vector injection mimics that typical of a wound to the anterior cornea such as an epithelial scrape, although much delayed.
- Transgene expression in the stroma after drop off is still spread across the entire diameter of the cornea but has become restricted to the posterior stroma.
- Data obtained in both murine tissue *in vivo* and human tissue *ex vivo* indicated that intrastromal injection is capable of mediating a long lasting transgene expression in the stroma at moderate to high levels. The approach is therefore likely to be applicable in an augmentation gene therapy approach to corneal disease acting through a secreted product.

5. Intrastromal injection of AAV2/8(Y733F) delivering sFlt1 to treat corneal neovascularisation

5.1 Introduction

Work in this chapter will develop the AAV2/8(Y733F) mediated transduction of the cornea by intrastromal injection (Chapter 4) for application in prevention of corneal neovascularisation, a pathology of high clinical relevance as discussed in the introduction (1.5).

A gene augmentation approach will be applied in which gene transfer via AAV2/8(Y733F) will result in the production of a soluble anti-angiogenic factor within the stroma over the long term. The soluble molecule chosen for expression is soluble fms-like tyrosine kinase-1 (sFlt1) also known as soluble vascular endothelial growth factor receptor 1 (sVEGFR1). This molecule was selected as it is a potent anti-angiogenic factor which has seen widespread use in the suppression of angiogenic responses in the eye, additionally it has been shown that the expression of sFlt1 within the cornea is critical to the tissue's naturally avascular state [110]. This molecule therefore seems an ideal candidate for corneal overexpression in order to ameliorate pathological corneal neovascularisation. In order to minimise any potential complications arising from species differences it was decided that the murine sFlt1 protein (musFlt1) would be used. The human protein whilst sharing 77% identity with the murine is still dissimilar enough to potentially result in sub-optimal efficacy.

To assess the effectiveness of the approach it will be tested within a commonly used murine (C57Bl/6J) model system in which corneal neovascularisation is induced by the placement of multiple sutures penetrating the full thickness of the cornea. Whilst obviously artificial, this model has the benefit of inducing neovascularisation via stimulation of the same physiological processes that generate a corneal neovascular response in many clinical cases, i.e. via trauma and inflammation.

5.1.1 Aims

The aim of the work presented in this chapter is to determine whether the corneal neovascularisation induced by the corneal suture model can be reduced or prevented via augmentation gene therapy in which intrastromal injection of AAV2/8(Y733F) mediates the production of murine sFlt1 within the cornea.

5.2 Methods and results

5.2.1 Confirmation of murine *sFlt1* transgene expression *in vitro* from AAV2/8(Y733F)-CMV-musFlt1 vector

Before use *in vivo* the vector AAV2/8(Y733F)-CMV-musFlt1 was tested and validated *in vitro*.

293T cells were seeded into a 6-well plate and grown until approximately 80% confluent. At this point 2 of the wells were infected with 5 µL of AAV2/8(Y733F)-CMV-musFlt1 vector total dose (6×10^9 vgs). The remaining 4 wells were left uninfected as controls.

After 48 hours both cells and the conditioned media were harvested from all wells. Cells were scraped off the bottom of the wells with a cell scraper and collected in the conditioned media (5 mL per well). The conditioned media + cells underwent 2 rapid freeze / thaw cycles (Dry ice + isopropanol bath at -77°C, followed by water bath at 37°C) to lyse the cells. Cellular debris was pelleted by centrifugation at 1000g and discarded. The supernatant from virus infected wells was diluted 2 x 10-fold in ELISA reagent diluent (1x PBS+1% BSA). For infected wells both diluted and neat supernatant was used as sample in an ELISA for murine sFlt1 (2.4.8). Supernatant from uninfected wells was only used neat.

All samples were run in quadruplicate and ELISA plate loading volume was 100µL / well.

Figure 31 shows the results of the ELISA, only the undiluted samples from vector infected wells gave any detectable level of murine sFlt1. Both infected wells were assayed to contain ~1.3 ng of musFlt1 / mL of sample. The 1 in 10, 1 in 100 dilutions of sample and all of the uninfected controls did not give readings above the lower limit of detection.

The vector has been demonstrated to mediate transgene expression and translation *in vitro*, with resulting transgene product being detectable by ELISA. The vector has therefore been validated for use *in vivo.*

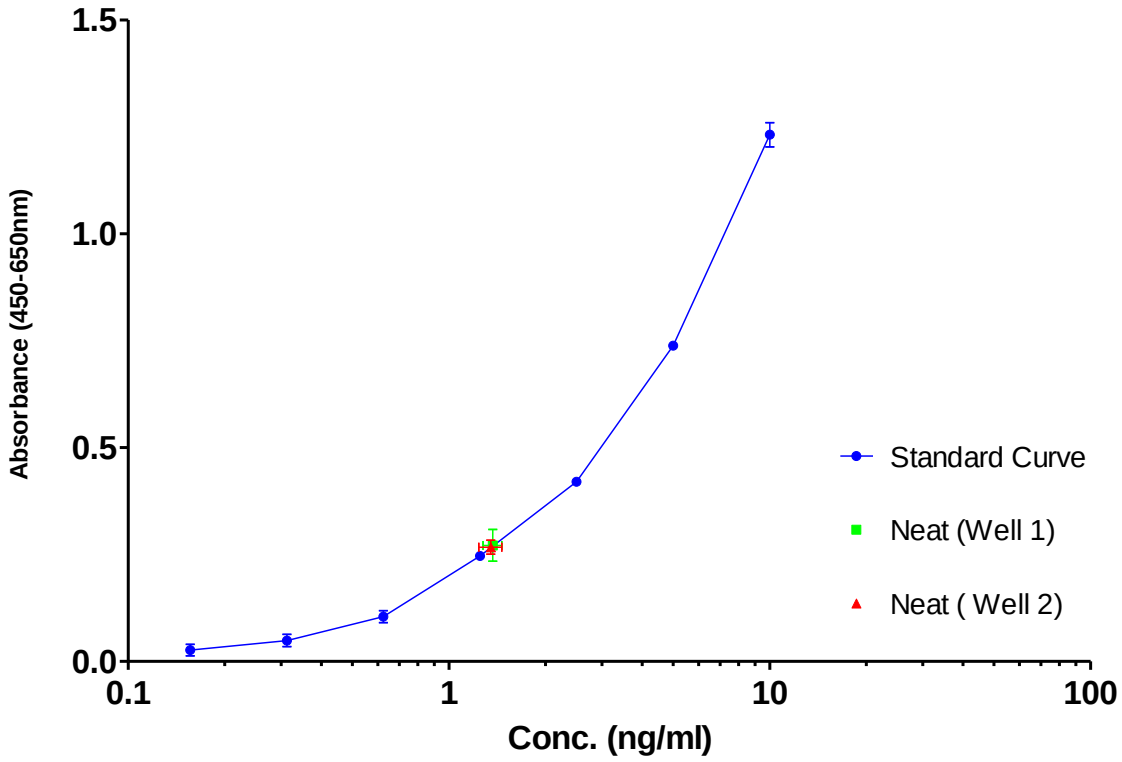

Figure 31. ***Levels of musFlt1 detectable by ELISA after*** **in vitro** ***infection of 293T cells with AAV2/8(Y733F)-CMV-muSFlt1***

5.2.2 Reduction of neovascular area in a murine model of induced corneal neovascularisation by intrastromal injection of AAV2/8(Y733F) encoding sFlt1

Having established that intrastromal injection of AAV2/8(Y733F) is able to mediate sustained expression of transgene within the stroma and produce nanogram scale quantities of soluble protein product the technique was applied to the treatment of corneal neovascularisation in the suture induced mouse model (2.3.9) which in the course of this work had been optimised to reliably induce consistent neovascularisation.

For use in this experiment two AAV2/8(Y733F) based vectors were prepared. The therapeutic vector encoding murine *sFlt1* under the control of the CMV promoter and a control NULL vector developed within the lab. The *sFlt1* encoding vector was validated to produce transgene product *in vitro* in 5.2.1. The NULL vector consisted of a construct originally designed to express the gene retinitis pigmentosa GTPase regulator (RPGR) which has been modified so that both the start codon of the gene and the promoter region are removed. It has been shown *in vitro* to mediate no gene expression as assessed by qPCR.

The titres of the two vectors assessed by Dotblot (2.2.3):

AAV2/8(Y733F)-CMV-musFlt - $1.2x10^{12}$ vgs / mL

AAV2/8(Y733F)-NULL - $3.5x10^{13}$ vgs / mL

Before injection therefore the NULL vector was diluted 1 in 20 in PBS-MK to approximately titre match. Before injection the vectors were randomised by a 3rd party so that those undertaking the experiment and analysis did not know which vector was which, knowing them only as A and B. They were only unmasked once all analysis was complete.

A total of 10 animals received bilateral intrastromal injections of 2 µL vector. Each animal received murine *sFlt1* encoding virus in one eye and NULL in the other. Which vector (A or B) was received in which eye was randomised. Three days later all corneas were sutured to induce corneal neovascularisation. In the previous chapter it was shown that transgene expression mediated by AAV2/8(Y733F) peaks at around 7 days post intrastromal injection before falling off. To maximise chances of success the timing of vector injection and induction of vascularisation was designed so that the period of peak transgene expression should coincide with the strongest neovascular drive. A full schematic of the experimental time line is shown in Figure 32

At 14 days post suture (17 days post injection) all animals were bilaterally assessed for neovascular development by scanning laser ophthalmoscope fluorescein angiography (SLO-FA) before being culled. Due to the extremely rapid spread of fluorescein through the tissue

it was inevitable that within each animal the eye imaged first would produce a clearer image with less leakage of fluorescein than the second. For every animal the right eye was imaged first and the left second. As vector administration was randomised between the eyes this should ensure this factor does not significantly affect the result.

Indocyanine green (ICG) angiography which does not suffer so much from dye leakage was trialled however it was found to be both far weaker than fluorescein and in addition ICG visualised the iris vasculature, which were hard to distinguish from corneal neovascular vessels.

Each eye was examined immediately post mortem for the presence of the sutures. In the majority of cases all 3 sutures were still in place at this time. In the small number of cases where 1 or more sutures had been lost the eye was excluded from further analysis. Angiography images from the SLO were compiled (2.5.3) and the neovascular area quantified (2.5.4).

The experiment was repeated, being undertaken in 2 cohorts of 10 mice each.

Figure 33 shows the results of the fluorescein angiography for both cohorts. In both cohorts 9 mice (18 eyes) were analysed at the end of the experiment, 1 animal from each cohort either having died before analysis or was deemed unsuitable for analysis.

Figure 33A & A' show the compiled SLO-FA images for the eyes injected with the NULL vector for both cohorts. In most cases extensive neovascularisation is visible, and at least some has occurred in every eye.

Figure 33B & B' show the compiled SLO-FA images for the eyes injected with the *musFlt1* encoding vector for both cohorts. For cohort 1 (Figure 33B) almost no neovascularisation is visible in any of the eyes, for cohort 2 (Figure 33B') the result is less striking however 6 out of the 9 eyes display little or no neovascularisation.

Figure 33C & C' shows quantification (as described in 2.5.4) of the neovascular area comparing the NULL injected with the musFlt1 injected for both cohorts. In both cases the observed reduction in neovascular area between the NULL and the musFlt1 groups is very significant ($p < 0.0001$ and $p = 0.014$ respectively).

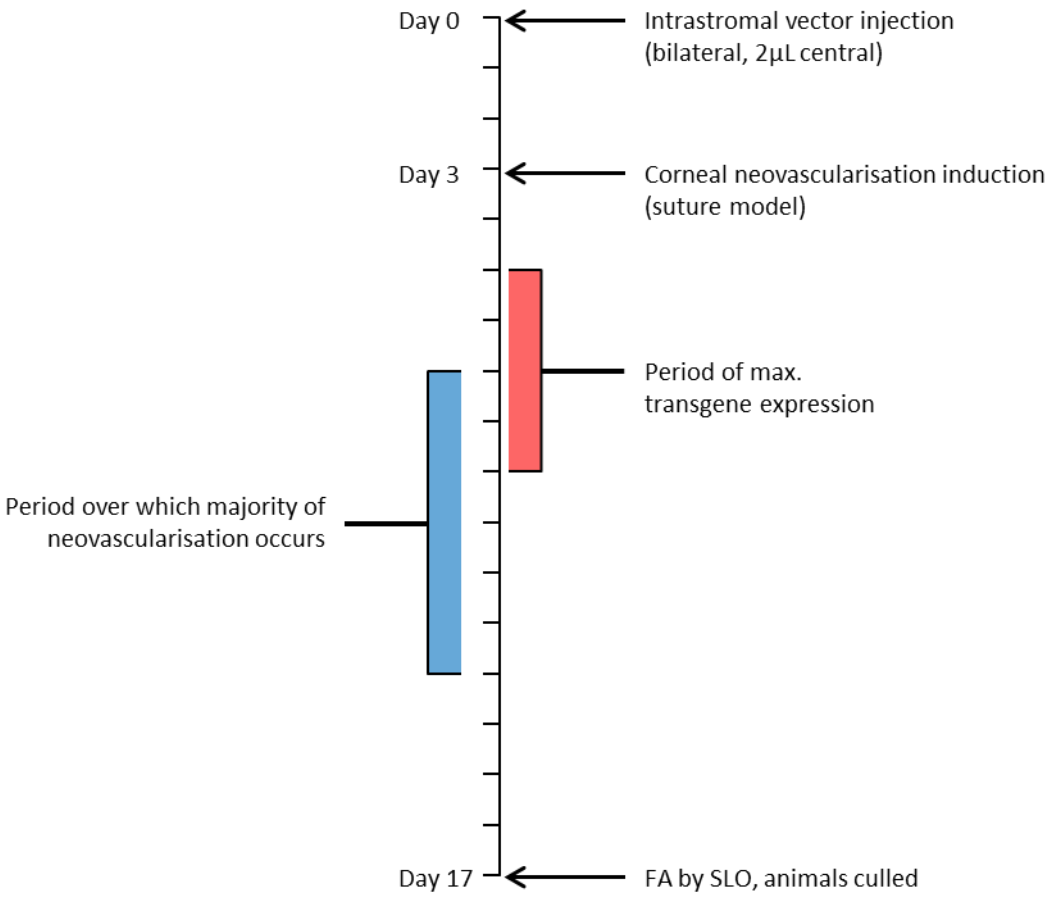

Figure 32. Schematic representation of timing of procedures in experiment to assess the capacity of intrastromal injection of AAV2/8(Y733F)-CMV-musFlt1 vector to ameliorate suture induced corneal neovascularisation, Cohorts 1 and 2 (SLO-FA)

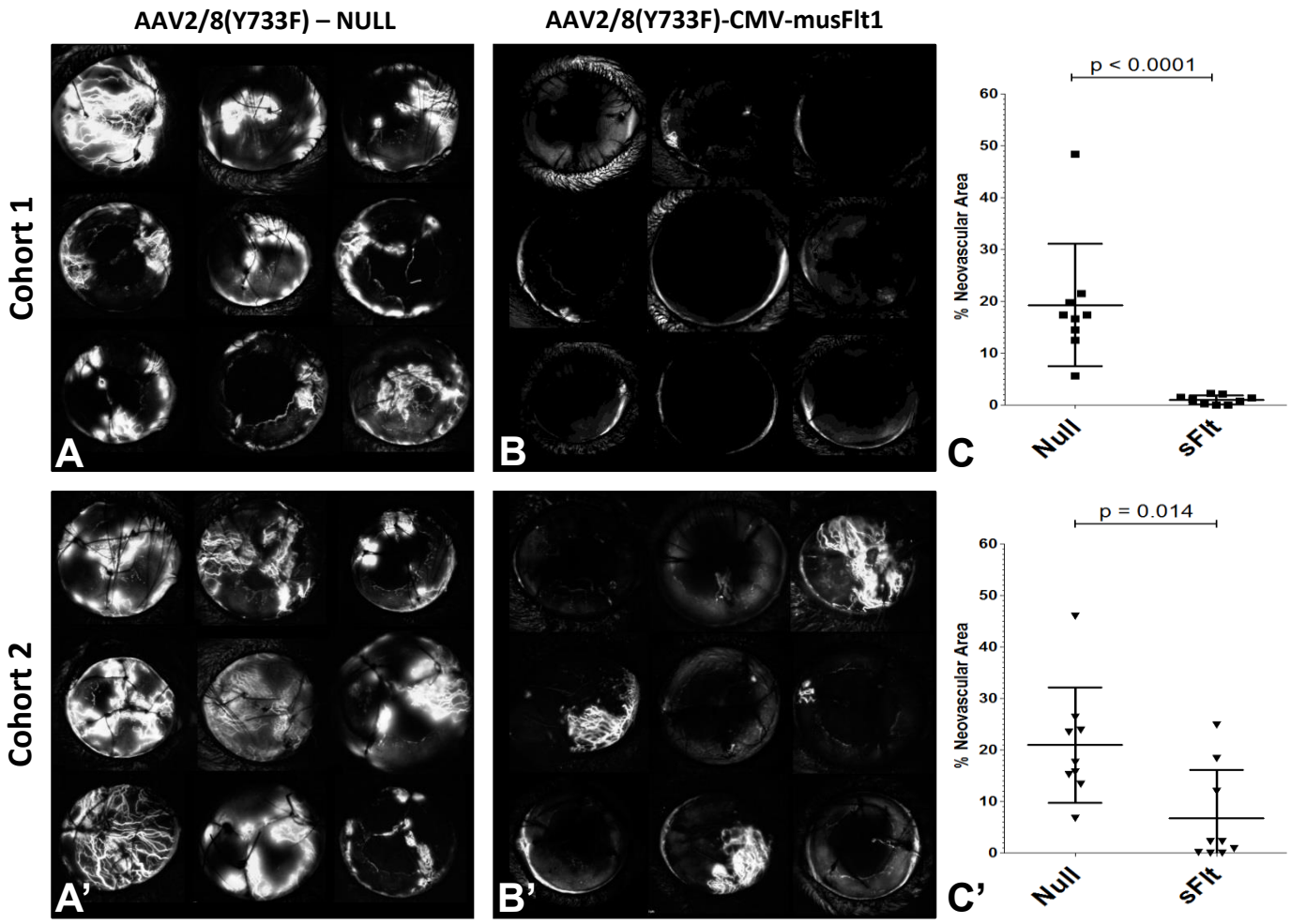

Figure 33. ***Effect upon suture-induced corneal neovascularisation of 2µL intrastromal injection of AAV2/8(Y733F)-CMV-musFlt1 compared to control vector. Assessed by fluorescein angiography (in vivo, SLO) at 17 days post injection / 14 day post induction (Cohort 1 and 2)***

A – A': Fluorescein angiography of eyes treated with AAV2/8(Y733F)-NULL (Control), in two cohorts of 9 mice.

B – B': Fluorescein angiography of eyes treated with AAV2/8(Y733F)-CMV-musFlt1 (Treatment), in two cohorts of 9 mice.

C – C': Quantification and comparison of neovascular area between AAV2/8(Y733F)-NULL (Control) and AAV2/8(Y733F)-CMV-musFlt1 (Treatment), in two cohorts of 9 mice.

5.2.3 Histological assessment of reduced neovascular area following treatment of corneal neovascularisation by intrastromal injection of AAV2/8(Y733F) encoding murine *sFlt1*

Following the promising results obtained in 5.2.2 it was decided to induce and treat a third cohort and in addition to assessment by SLO-FA collect tissue for histology after angiography.

The initial phase of this experiment was essentially a third cohort of the experiment performed in 5.2.2. Vectors were again masked before injection and a total of 10 animals received bilateral intrastromal injections of 2 µL vector. Each animal received musFlt1 encoding virus in one eye and NULL in the other. Three days later all corneas were sutured to induce corneal neovascularisation. At 14 days post suture (17 days post injection) all animals were bilaterally assessed for neovascular development by SLO fluorescein angiography (SLO-FA). Immediately after angiography the sutures were removed. This was done as carefully as possibly but if neovascular vessels were well established some bleeding was inevitable. After removal, 1 % chloramphenicol ointment (FDC International) was carefully applied topically on the cornea and anaesthesia reversed. The animals were then allowed to recover for 2 days to allow both the flushing of the fluorescein from the body and the healing of any damage caused by suture removal. On the third day the animals were culled, and the vasculature stained by DiI perfusion (2.4.5). After perfusion each eye was prepared for further staining (2.4.3). The corneas were post fixed in 4% PFA and additionally stained for LYVE1 (a marker of lymphatic vessels) and DAPI. Once tissue had been fully processed corneal flat mounts were imaged by confocal microscopy.

A full schematic of the experimental time line is shown in Figure 34.

Figure 35 shows the results of the fluorescein angiography for cohort 3. In this cohort a total of 4 eyes were excluded or lost from the analysis, 1 from the NULL group and 3 from the musFlt1 group.

Figure 35A shows the compiled SLO-FA images for the eyes injected with the NULL vector. In 6 out of 9 eyes extensive neovascularisation is visible; only one eye appears relatively free of neovascularisation.

Figure 35B shows the compiled SLO-FA images for the eyes injected with the musFlt1 encoding vector. Very little neovascularisation is visible with only 3 out of 7 eyes displaying relatively minor symptoms.

Figure 35C shows quantification (as described in 2.5.4) of the neovascular area comparing the NULL injected with the musFlt1 injected eyes. The observed reduction in neovascular area between the NULL and the musFlt1 groups is very significant ($p = 0.0115$).

Figure 36 shows representative DiI staining of blood vasculature (Figure 36A) and LYVE1 staining of lymph vasculature (Figure 36B) in an unprocedured murine cornea. Note the complete avascularity (blood and lymph) of the central cornea. All visible staining is restricted to the region of the limbal vascular arcades.

Figure 37 shows the DiI and LYVE1 staining obtained in the animals of cohort 3 when culled 20 days post intrastromal injection (17 days post induction of neovascularisation). All images have been thresholded (as described in 2.5.4) to best distinguish signal from background. Blood neovasculature (DiI, red) within the central cornea appears far more pronounced in the NULL treated group (Figure 37A) than in the murine sFlt1 treated group (Figure 37A'). There is no obvious difference in the extent of lymph neovasculature (LYVE1, green) within the central cornea between the NULL and murine sFlt treated groups (Figure 37B vs B').

Figure 38 shows quantification (as described in 2.5.4) of the neovascular area in the images presented in Figure 37 comparing the NULL injected with the musFlt1 injected eyes for both blood and lymph vasculature. Figure 38A & B shows quantification of blood and lymph neovascular area respectively. This quantification was done upon the basis of the number of stained pixels for each as a proportion of the total central area in the image. For blood vessels (DiI) there is a highly significant ($p=0.0079$) reduction in stained area in the musFlt1 treated group when compared to the NULL treated group. For Lymph vessels there is no significant difference between the groups. Figure 38C & D present the same quantification as in Figure 38A & B but calculated differently. The DiI stain gave an extremely high fluorescent signal and therefore had a tendency to bleed into the other channel, for this reason each stained pixel count had subtracted from it the number of pixels that stained positive in both the DiI and LYVE1 channels. This should ensure any effects of channel bleed through are excluded from the analysis. Figure 38E – E'' shows an example of the two channels (DiI and LYVE1) and the bleed through between them.

This more stringent method of analysis had no effect on the result, there remains a highly significant ($p=0.0079$) reduction in stained area for blood vessels (DiI) when the murine sFlt1 treated group is compared to the NULL treated group, and no significant difference in the degree of lymph neovascularisation between the groups.

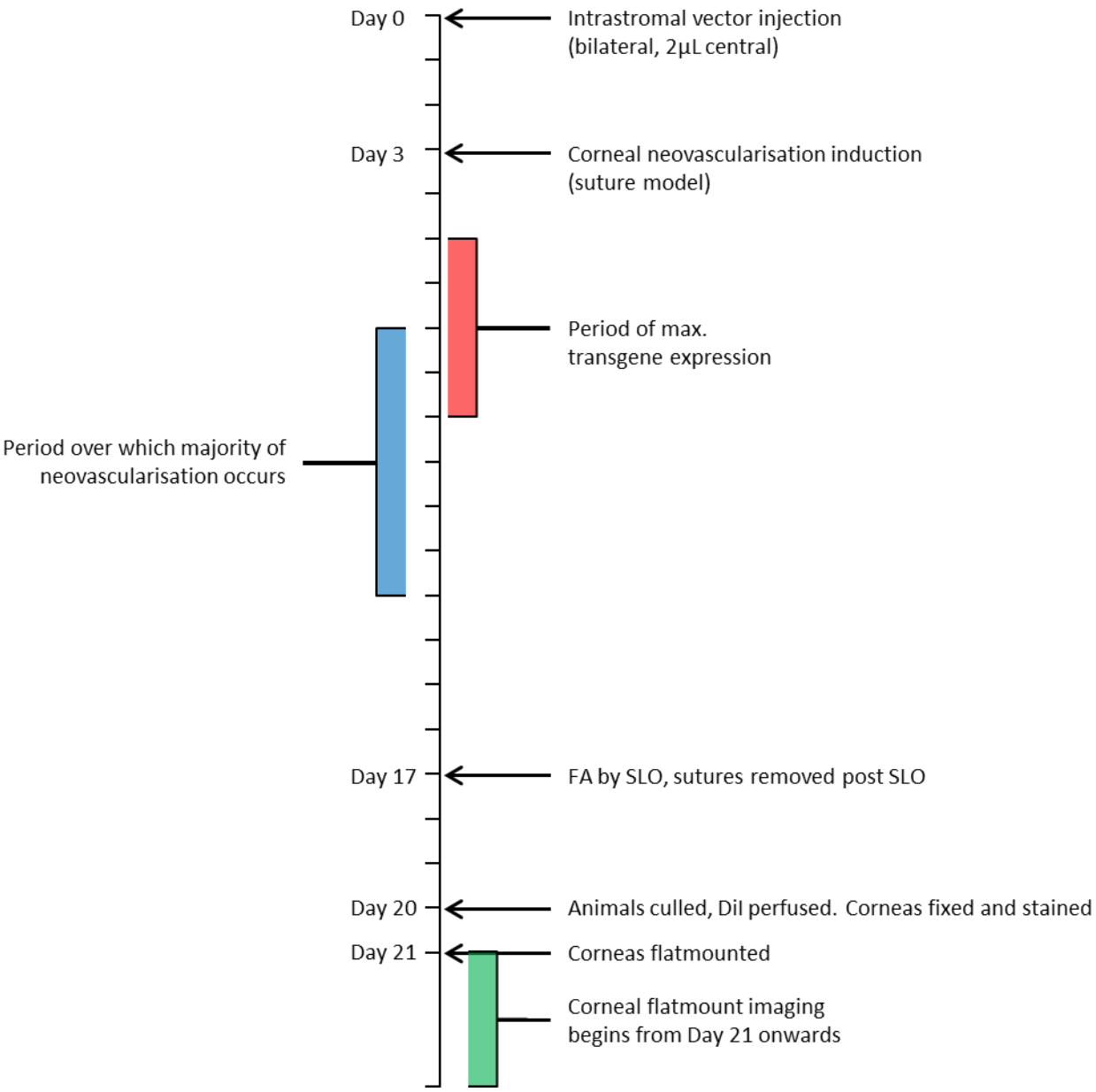

Figure 34. Schematic representation of timing of procedures in experiment to assess the capacity of intrastromal injection of AAV2/8(Y733F)-CMV-musFlt1 vector to ameliorate suture induced corneal neovascularisation. Cohort 3 (SLO-FA and histology)

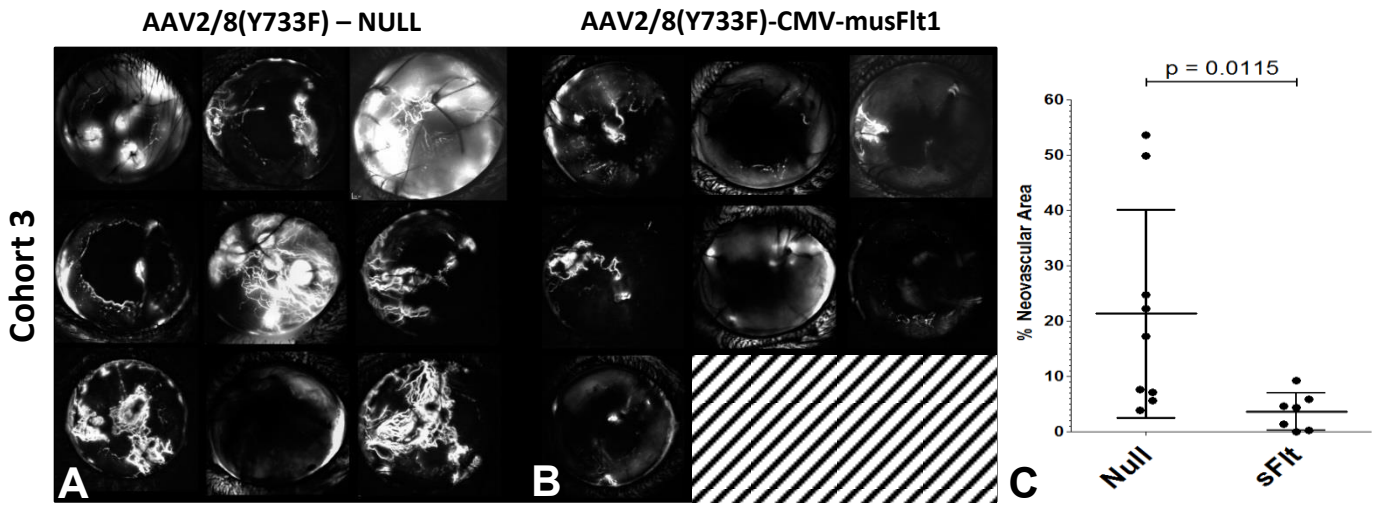

Figure 35. ***Effect upon suture-induced corneal neovascularisation of 2µL intrastromal injection of AAV2/8(Y733F)-CMV-musFlt1 compared to control vector. Assessed by fluorescein angiography (in vivo, SLO) at 17 days post injection / 14 day post induction (Cohort 3)***

A: Fluorescein angiography of eyes treated with AAV2/8(Y733F)-NULL (Control), in a 3rd cohort of 9 mice.

B: Fluorescein angiography of eyes treated with AAV2/8(Y733F)-CMV-musFlt1 (Treatment), in a 3rd cohort of 9 mice.

C: Quantification and comparison of neovascular area between AAV2/8(Y733F)-NULL (Control) and AAV2/8(Y733F)-CMV-musFlt1 (Treatment), in a 3rd cohort of 9 mice.

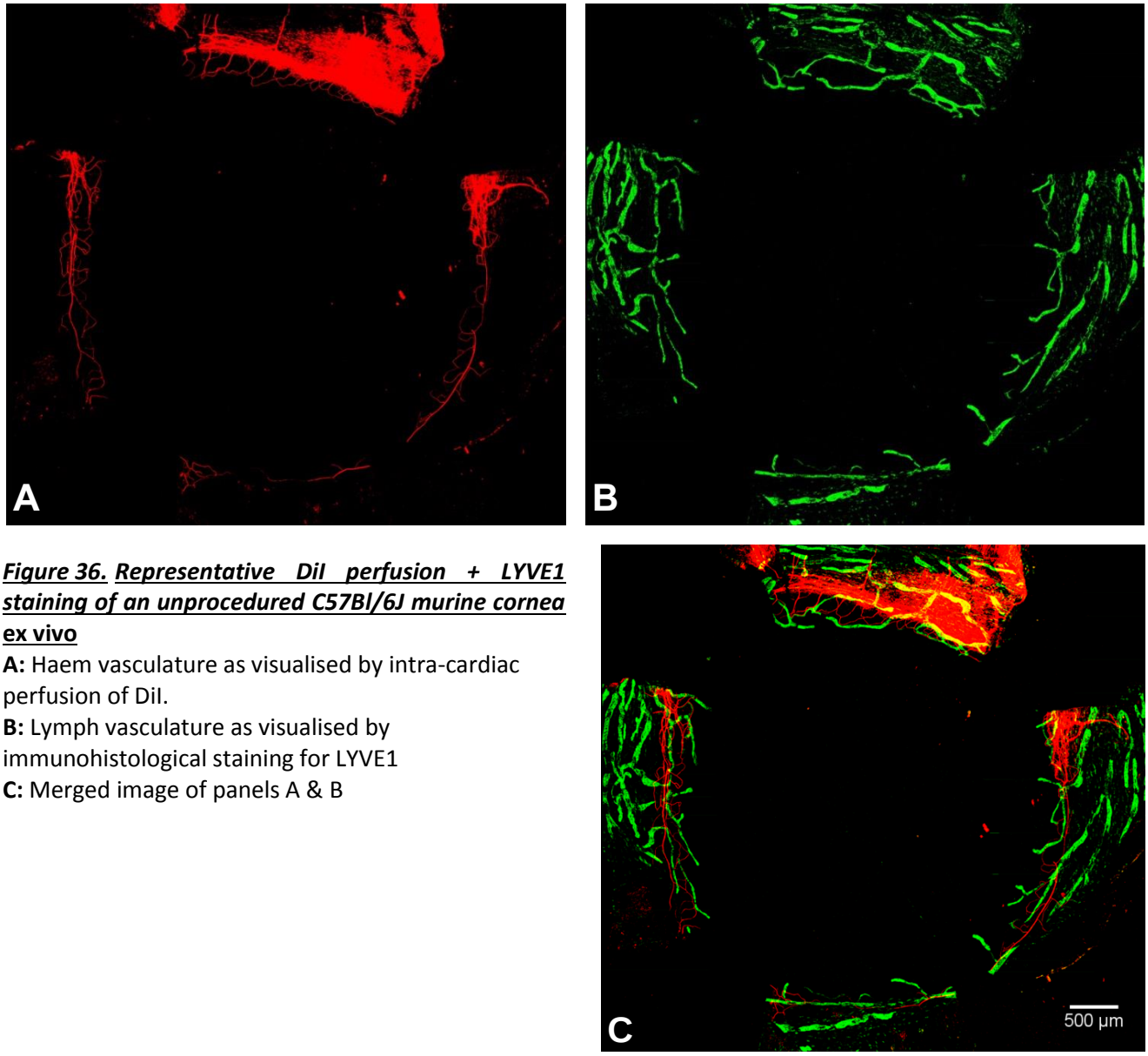

Figure 36. ***Representative DiI perfusion + LYVE1 staining of an unprocedured C57Bl/6J murine cornea ex vivo***

A: Haem vasculature as visualised by intra-cardiac perfusion of DiI.

B: Lymph vasculature as visualised by immunohistological staining for LYVE1

C: Merged image of panels A & B

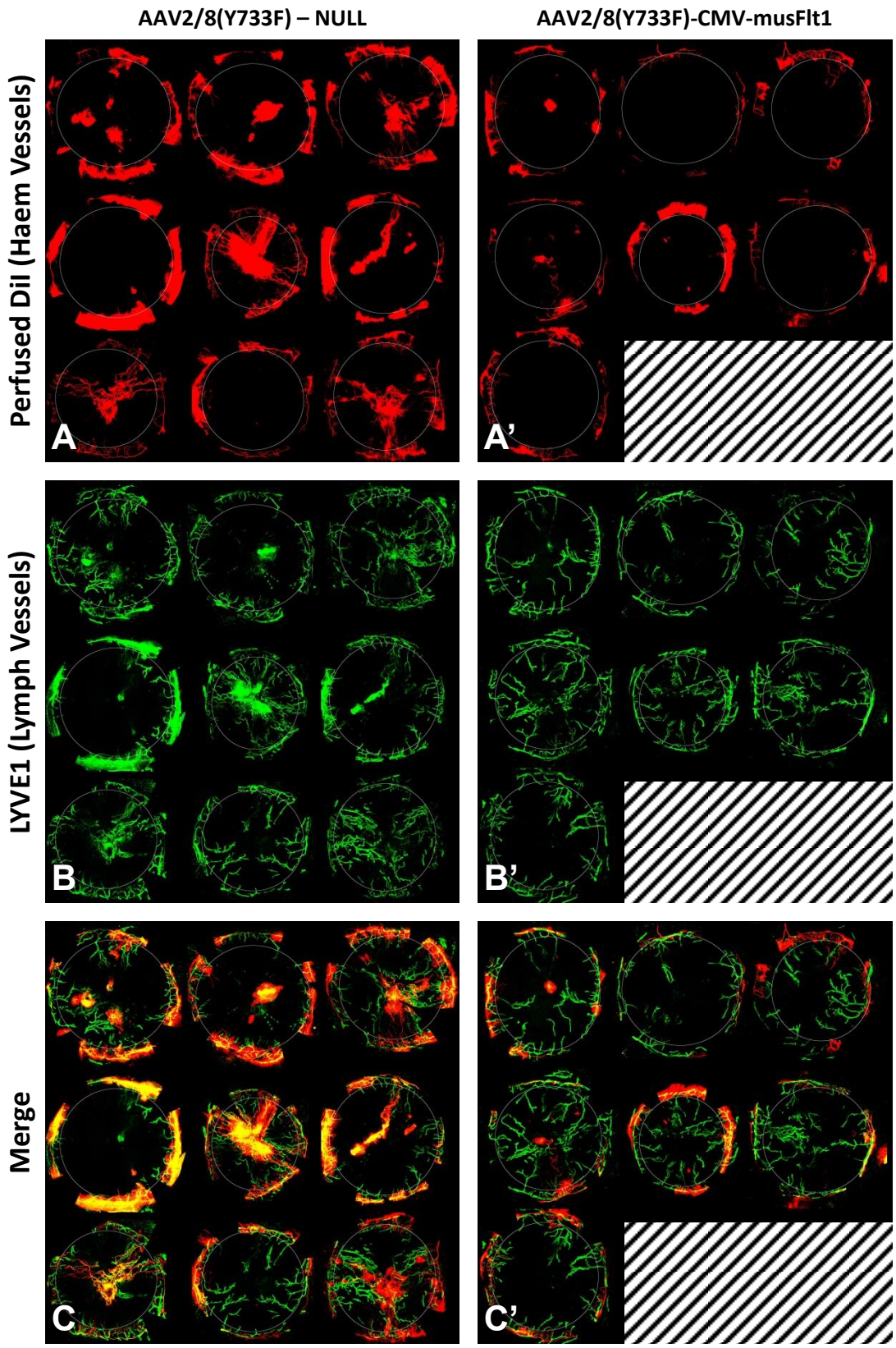

Figure 37. Haem and Lymph vessels visualised in corneal flatmounts post suture-induced neovascularisation and intrastromal injection of AAV2/8(Y733F)-NULL and AAV2/8(Y733F)-CMV-musFlt1. 19 days post injection / 17 day post induction

A & A': Blood vasculature (red) visualised by intra-cardiac perfusion of DiI. NULL and musFlt1 vector injected corneas respectively. **B & B':** Lymph vasculature (green) visualised by LYVE1 immunohistological staining. NULL and musFlt1 vector respectively. **C & C':** Merged images of A+B and A'+B' respectively.

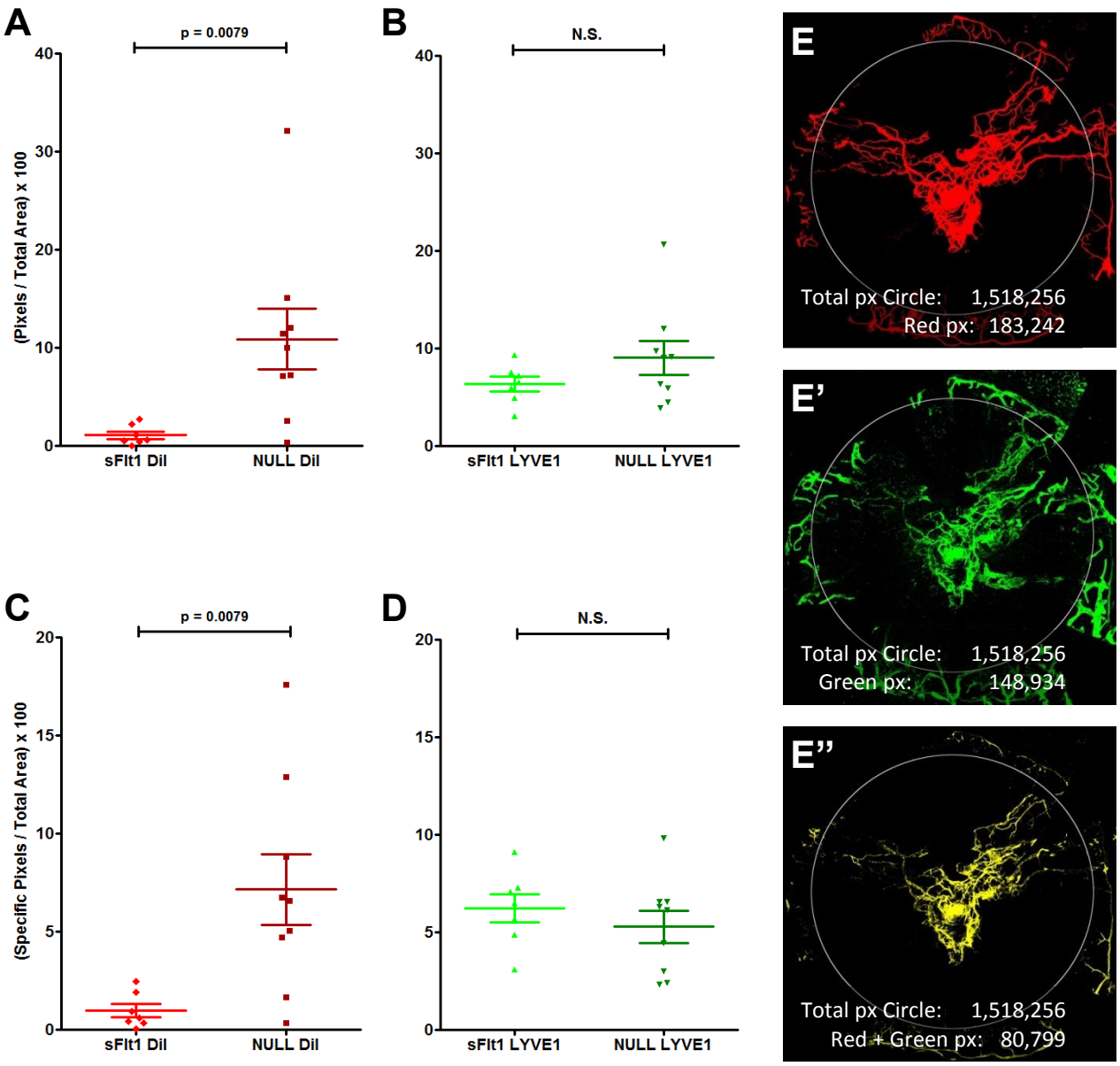

Figure 38. Quantification of Haem and Lymph neovascularisation in corneal flatmounts post suture-induced neovascularisation and intrastromal injection of AAV2/8(Y733F)-NULL and AAV2/8(Y733F)-CMV-musFlt1. 19 days post injection / 17 day post induction. Based upon images presented in Figure 37

A: Comparison of Blood neovascular area between NULL and musFlt treated eyes, calculated as follows: No. DiI (Red) pixels / Total pixels in central cornea x 100

B: Comparison of Lymph neovascular area between NULL and musFlt treated eyes, calculated as follows: No. LYVE1 (Green) pixels / Total pixels in central cornea x 100

C: Comparison of Blood neovascular area between NULL and musFlt treated eyes, calculated as follows: (No. DiI (Red) pixels – No. Yellow pixels) / Total pixels in central cornea x 100

D: Comparison of Lymph neovascular area between NULL and musFlt treated eyes, calculated as follows: (No. LYVE1 (Green) pixels – No. Yellow pixels) / Total pixels in central cornea x 100

E – E'': Single eye as example of analysis showing the area defined as central cornea (circle), DiI Staining (E), LYVE1 Staining (E') and possible bleed through between the two signals (E'')

5.3 Discussion

Work in this chapter aimed to apply the initially high level, long lasting gene transfer to the corneal epithelium / stroma via AAV2/8(Y733F) demonstrated in the previous chapter to an augmentation gene therapy based approach to ameliorate or prevent corneal neovascularisation in the suture-induced model via the production and secretion of sFlt from transduced cells.

The results achieved convincingly demonstrate that overexpression of sFlt1 mediated by intrastromal injection of AAV2/8(Y733F)-CMV-musFlt1 vector is able to significantly reduce the amount of haemangiogenesis induced by the suture model. The result proved to be highly reproducible, being observed in three independent experiments in which the identity of the vector being injected was masked on both injection and analysis. The effect was especially marked however in cohort 1 where haemangiogenesis was essentially completely eliminated in all eyes injected with the *sFlt1* encoding vector. The reason for the especially high efficacy in cohort 1 remains unknown and is perhaps best explained as simply falling within experimental variation.

Previous studies within the literature have attempted to treat corneal neovascularisation by a number of approaches, many involving the blockade of VEGF-A signalling in a similar manner to that performed here.

The most directly comparable work to that presented here has been performed by the group of Lai et al. This group initially aimed to treat angiogenesis induced by silver / potassium nitrate cauterisation in rats via anterior chamber injections delivering *sFlt1* encoded by either adenovirus [300] or AAV2/2 [152]. Some inhibition of neovascularisation was achieved however the transgene expression profile from both viruses was extremely limited, AAV in terms of extent and adenovirus in terms of duration.

Lai et al. did not therefore further pursue these approaches and switched to a different strategy involving a subconjuntival route of vector administration and an alternative transgene. The transgene selected was endostatin, a factor based upon the C-terminal fragment of collagen XVIII well characterised to inhibit angiogenesis via disruption of endothelial cell migration and proliferation [301]. An AAV2/2 vector encoding endostatin under the control of a CMV promoter was injected subconjuntivally in CD1 mice to treat angiogenesis induced by the same cauterisation model [260]. In contrast to the previous work it was shown that transgene expression was sustained over the long term (8 months) and was partially effective in inhibiting induced angiogenesis when induction took place two

weeks post injection, significantly reducing the severity of induced neovascularisation observed as assessed by *in vivo* microscopy.

The approach we have selected has the advantage of utilising a serotype of AAV generally regarded to be more effective [187] and mediating production of transgene within the cornea itself, rather than in an adjacent tissue. Nonetheless the subconjunctival route represents a valid mode of administration and presents the potential advantage of being less invasive. It is inapplicable however to use in the context of pre-treatment of corneal grafts to improve their survival as during corneal engraftment in clinic no conjunctival tissue is transplanted

Another study utilising AAV as the gene delivery method was performed by Mohan et al. [264]. In this case decorin was the transgene selected as this proteoglycan is both endogenous to the corneal stroma and has been shown to be involved in the regulation of angiogenesis in other tissues [302]. AAV5 encoding decorin was applied topically to the stroma following epithelial debridement, angiogenesis having been induced 1 day earlier by the implantation of a device releasing VEGF-A.

A reduction in induced neovascularisation of around 50% was demonstrated although the area analysed appears to be extremely small localised to the extreme limbus. Untreated vascularised area covered only around $12mm^2$ per cornea, a comparatively small proportion of an entire rabbit cornea. This was possibly due to the highly localised induction produced by the implant. Whilst useful in assessing a molecule's antiangiogenic potential (as was done for decorin in this case) the implant induction methodology is of limited relevance as it is not associated with any of the factors that cause neovascularisation clinically, such as trauma, injury or infection. The authors themselves acknowledge this limitation.

A more popular approach to gene therapy based treatment of corneal neovascularisation seems to be in the use of various non-viral gene delivery methods ranging from injection of naked DNA / RNA species via various routes [265,303–306], the use of lipid based transfection reagents [261,307] or more complex nanoparticles [266,308]. Whilst these approaches have proved effective, in many of cases (especially those involving naked DNA / RNA species) repeated administration of the therapeutic agent at high doses over the course of the experiments (usually lasting around 1-2 weeks) was required to produce a therapeutic effect. This is the key disadvantage of many non-viral methods; the therapeutic gene constructs can be relatively unstable and penetration of target cells is often limited [309].

One of the chief advantages therefore of the AAV methodology presented here is that the duration and level of expression mediated is superior to that of any current non-viral method and should thus provide an enhanced therapeutic effect.

In the previous chapter it was shown that expression of transgene product from intrastromally injected vector rises rapidly, achieving its maximal level seven days post injection before declining. This initial high level expression is likely the result of dual transduction of both the epithelium and the stroma and possibly an inflammatory mediated hyper-activation of the transgene delivered by AAV. The AAV2/8(Y733F)-CMV-musFlt1 vector injected in this study was proven to express the correct transgene product in easily detectable quantities *in vitro* (5.2.1) and the strong, reproducible inhibitory effect on the induction of neovascularisation leaves little doubt that the transgene is being expressed at a physiologically useful level *in vivo*. However we did not directly determine the expression levels of sFlt1 we were achieving *in vivo* or any variation in this level over time, and thus cannot say with certainty that the temporal expression pattern observed in the previous chapter was repeated here. Both the murine *sFlt1* expressing and control NULL vector were made following exactly the same production methodology as the eGFP expressing vector used in the previous chapter and delivered in exactly the same manner, therefore a similar pattern of transgene expression would be expected. This should be confirmed however by the assessment of pan-corneal sFlt1 levels by ELISA at various time points post vector injection.

The experiments presented here were designed to take best advantage of the initial high level expression expected to be mediated, with vector being injected pre-induction of neovascularisation timed in such a way as to ensure synchronicity of maximal transgene expression and neovascular drive. In addition this experimental timescale has the benefit of being clinically relevant. The most likely clinical context in which a gene therapy based approach to prevent pathogenic corneal neovascularisation would be of utility is in the prevention of corneal graft rejection in “high risk” engraftments into hosts with pre-existing neovascularisation [121]. Donor corneas are routinely stored in organ culture for up to four weeks pre-transplantation, providing an opportune window *ex vivo* for gene therapy to be applied and transgene expression to develop within the graft.

Whilst the period immediately post transplantation might be expected to represent a period of particular graft vulnerability due to the speed of innate responses it would also be desirable to determine whether the lower basal level of expression in the stroma alone shown in the previous chapter to be established ~12-14 days post injection and maintained over the longer term (likely indefinitely) is still able to mediate the strong antiangiogenic effect observed over the initial 2 week period, and thus in the clinical context continue to protect engrafted tissue from neovascularisation and the associated immunological rejection over the long term. This could easily be assessed in the murine suture model by increasing the interval between injection and induction of neovascularisation.

It has also not been determined if AAV mediated *sFlt1* overexpression in the cornea is capable of inducing the regression of an already established chronic corneal neovascularisation such as that present in hosts receiving high risk corneal transplants. The suture model used here however does not model such a situation and is unsuitable for this purpose as the angiogenesis induced is relatively acute and temporary. The peak of neovascularisation induced by the model occurs at around two weeks post induction (the point of analysis in this study) and by 5 weeks most of the sutures are no longer in place and the neovascularisation has largely regressed. This time frame is likely too short for any treatment induced regression to be distinguished from the normal healing process. If the potential of the treatment to induce regression of established vessels is to be assessed a more chronic model of corneal neovascularisation will be required. Some published work [266] in which a longer interval between induction and treatment (10 days) was left suggests that angiogenic induction by alkali burn might constitute such a model, and this methodology will be investigated.

As discussed one of the major clinical applications of this technique would be to improve corneal graft survival in high risk grafts and so we should also apply our AAV based technique to a murine allograft model to assess its ability to promote graft survival. We do not currently process sufficient surgical experience of corneal transplantation in mice to begin these experiments but this capacity is being developed.

Whilst the musFlt1 transgene expression mediated by AAV2/8(Y733F) post intrastromal injection proved highly effective in ameliorating corneal haemangiogenesis induced in the corneal suture model in repeated experiments, it appeared to have little to no effect in preventing lymphangiogenesis, as shown by immunohistological staining for the lymph vessel marker LYVE1 in cohort 3.

Whilst it has been well established that haemangiogenesis is associated with corneal graft failure [121], and there is no doubt that haemangiogenesis is deleterious to vision in of itself, there is an increasing weight of evidence to suggest that to focus solely upon haemangiogenesis may be somewhat misdirected. Haemangiogenesis is often very apparent, easily observable in clinic and causes obvious impairment of vision. By contrast lymphangiogenesis will generally pass unnoticed as lymph vessels are invisible to macroscopic examination. Indeed until relatively recently the lymph vasculature was also difficult to visualise histologically due a lack of immunohistological markers and this likely exacerbated the lack of attention they received. The advent of more definite and reliable markers for lymph vessels has made it clear however that lymphangiogenesis almost invariably accompanies the more obvious haemangiogenesis [126,310] and that in fact it is likely lymphangiogenesis is the primary driving force behind immune mediated graft failure

[127]. It would therefore be highly desirable to inhibit lymphangiogenesis in addition to haemangiogenesis and there are a number of gene products that might be delivered to achieve this.

The VEGF family of ligands and receptors is the primary regulatory pathway of both haemangiogenesis and lymphangiogenesis [311] and is summarised in simplified form in Figure 39 below. Broadly speaking haemangiogenesis is mediated through ligand binding to either VEGFR1 or VEGFR2 whilst lymphangiogenesis through binding to VEGFR3. As can be seen from Figure 39 however there are many points of cross over between these two basic pathways.

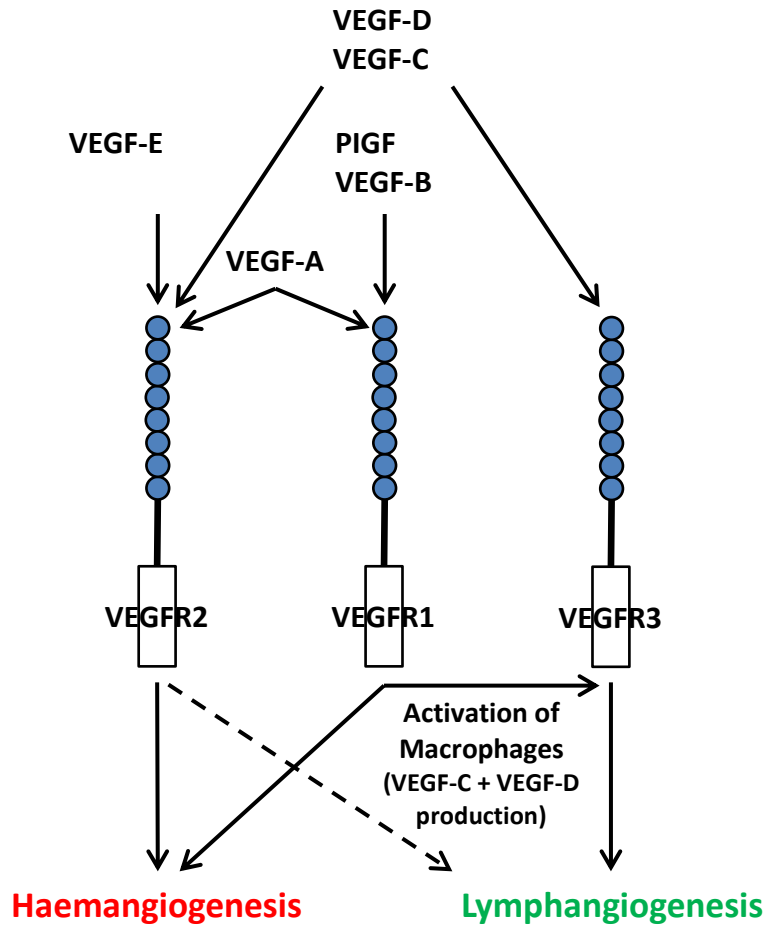

Figure 39. Simplified schematic of the VEGF pathway as it relates to Haem / Lymphangiogenesis

There is generally considered to not be any direct interaction between VEGF-A and the lymphangiogenesis pathway mediated through VEGFR3, however there are multiple lines of evidence suggesting that VEGF-A may affect lymphangiogenesis via an alternative mechanism either directly or indirectly. An overexpression of VEGF-A has been shown to stimulate lymphatic development in the absence of VEGF-C/D detection [312] although the

lymph vessels generated were abnormal, and possibly only of relevance to malignancy. The mechanism of action, if direct, is unknown although Nagy et al. [312] proposed that it may proceed via VEGFR2 binding due to high expression levels of this receptor on normal lymphatic endothelium. Further evidence supporting the effect being mediated via VEGFR2 mechanism has subsequently been found in the context of the skin [313]. Additionally, VEGF-A is involved in the recruitment of macrophages [314], which are able to directly stimulate lymphangiogenesis by production of VEGF-C/D and subsequent VEGFR3 pathway activation. This indirect action of VEGF-A has also been shown to be of relevance to the cornea [310,315].

Within the cornea it has been demonstrated by Bock et al. [316] that the VEGF-A binding antibody based therapeutic Bevacizumab (Avastin) is capable of dual inhibition of both haemangiogenesis and lymphangiogenesis in the suture model. As Bevacizumab does not bind either VEGF-C or VEGF-D, the two members of the VEGF family primarily responsible for driving lymphangiogenesis it cannot be mediating its effect by a direct blockade of VEGFR3 signalling. Bock et al. therefore hypothesize that the inhibitory effect they observed on lymphangiogenesis may have occurred either indirectly via the two mechanisms discussed previously, a reduction in macrophage recruitment (leading to diminished secretion of VEGF-C/D) or directly via an as yet unknown VEGFR3 independent action of VEGF-A, possibly via VEGFR2 as has been shown in other tissues.

Additionally it has been claimed that the drug VEGFTrap which comprises binding motifs from both VEGFR1 and VEGFR2 is able to inhibit lymphangiogenesis as well an haemangiogenesis [306]. Whilst the VEGFR2 motif might have been expected to bind VEGF-C and thus mediate inhibition of lymphangiogenesis via reduced VEGFR3 signalling, VEGFTrap was in fact shown not to bind either VEGF-C or D [310].

The results presented here partially dispute these findings, at least within the context of the animal model used. Bock et al. themselves demonstrated that Bevacizumab binds to murine VEGF-A at a far lower (10-1000x) affinity that it does to the human form [316]. The treatment we have applied with sFlt1 acts via an identical mechanism to that of Bevacizumab; the binding and sequestration of VEGF-A resulting in inhibition of its pro-angiogenic signal. Additionally as the native murine form of sFlt1 was used here it might be expected that the greater binding affinity would lead to VEGF-A sequestration being more efficient / complete and yet we observed no reduction in lymphangiogenesis. Additionally the widespread, florid lymphangiogenic induction we observed here in the controls is striking upon comparison with almost all published data in the field (including Bock et al's Bevacizumab study) in which the lymphangiogenesis induced appears far more modest.

These differences are likely due, at least in part, to strain specific difference between mouse models used. The work presented here was performed in C57Bl/6J animals which have been shown to exhibit both more extensive pre-existing lymphatics at the corneal limbus [317] and a more pronounced lymphangiogenesis upon stimulation [318] than the BALB/C animals that appear more commonly used within other studies.

We would therefore conclude that any action of VEGF-A directly or indirectly upon lymphangiogenesis is a relatively minor factor within the context of the strong lymphangiogenic drive present within this strain, or induced by our methodology. Any effect of sFlt1 mediated VEGF-A blockade is likely being overcome by stronger signalling mediated through VEGF-C / VEGFR3. The effects of VEGF-A blockade upon lymphangiogenesis observed by Bock / Bachmann et al. were perhaps only evident due to a combination of very high, repeated doses of therapeutic agent being applied and a relatively limited lymphangiogenic drive being in effect within the mouse model used.

This raises the question of which strain of animals is best suited for further experiments. A treatment effect would be easier to observe in BALB/C animals due to a reduced baseline response, although the albinism of this strain is a complicating factor. It would be best therefore to continue to work within C57's, at least initially. This strain lacks the obvious and far reaching genetic defect of albinism and due to its more robust lymphangiogenic response any treatment effect achieved is likely to be of high efficacy and thus of wider utility to more severe disease. If treatment of lymphangiogenesis within the C57Bl/6J strain proves unfeasible, BALB/C's could form a second line of investigation

There is a single example of an inhibitory effect upon lymphangiogenesis mediated via VEGF-A within the C57/Bl6J model found within the literature. Tarallo et al., (2012) demonstrated reduced lymphangiogenesis when VEGFR1 signalling was blockaded via a modified form of PIGF1, unable to bind VEGFR1 but still able to sequester VEGF-A by heterodimerisation. A result that was not replicated in the VEGF-A / PIGF1 blockade via sFlt1 presented here.

In conclusion any further attempts to inhibit lymphangiogenesis via the VEGF-A pathway alone represent a sub-optimal approach as any effects of this pathway upon lymphangiogenesis are either secondary to the pathways primary function or indirect. Direct modulation of other VEGF pathways is likely to be more effective.

Soluble VEGFR2 (sFlk1) is an alternative candidate for overexpression that should be able to bind and sequester factors that promote both haemangiogenesis and lymphangiogenesis such as VEGF-A, VEGF-C and VEGF-D, and thus may be effective in ameliorating both.

Indeed a soluble monomeric form of VEGFR2 that can function to inhibit corneal lymphangiogenesis has been found to be expressed endogenously [320]. It was found however that the endogenous form was not able to inhibit haemangiogenesis as it is monomeric and in this form is unable to bind VEGF-A.

In contradiction to this finding Yu et al. [267] had earlier shown that delivery of an artificial form of sVEGFR2 via adenovirus to the anterior chamber was able effectively inhibit haemangiogenesis in a alkali burn model of corneal neovascularisation in the rat. This disagreement perhaps indicates the sVEGFR2 form used by Yu et al. may have been dimeric. In Yu et al's study lymphangiogenesis was not assessed.

Work by Uehara et al. in 2013 [321] utilised a morpholino antisense oligomer delivered subconjunctivally to shift the endogenous splicing of VEGFR2 in favour of the soluble form, simultaneously increasing sVEGFR2 and decreasing VEGR2 to potentially inhibit both lymphangiogenesis and haemangiogenesis respectively. This elegant approach proved to be effective within the cornea, increasing the survival of corneal allografts and reducing both forms of angiogenesis induced in both the transplants and the suture model within BALB/C mice.

Whilst is has certainly proven to be effective increased expression of sVEGFR2 (monomeric or dimeric) is likely to constitute a suboptimal approach to the inhibition of both haemangiogenesis and lymphangiogenesis. This is due to the fact the ligands to which it binds and sequesters (VEGF-A, and VEGF-C/D) have endogenous receptors with much higher affinity (VEGFR1 and VEGFR3 respectively) which may outcompete sVEGFR2 if lymphangiogenic drive is sufficiently strong, such as that seen in C57Bl/6J mice. We believe a superior approach would be to deliver soluble forms of both VEGFR1 (sFlt1) and VEGFR3 (sFlt4) simultaneously in order to maximise sequestration of VEGF-A, C & D and thus inhibition of both forms of angiogenesis. Additionally delivery sVEGFR1 (sFlt1) has the advantage over sVEGFR2 of being able to bind and sequester other molecules that act to promote haemangiogenesis through VEGFR1, but which do not bind to VEGFR2, such as PIGF. In the context of AAV mediated delivery this could be achieved either by the simultaneous injection of two vectors each encoding one of the two factors, or a bicistronic construct encoding both. In this case the bicistronic approach would be feasible as the sequences for both sFlt1 and sFlt4, plus promoters and polyadenylation signals would fit within AAV's maximum packaging capacity of 4.7kb. This proposed strategy of sVEGFR3 + sVEGFR1 combination gene therapy was very recently shown to be of considerable merit. Whilst soluble forms of both VEGFR1 and VEGFR2 have been found to be expressed endogenously, until recently the soluble form of VEGFR3 was thought only to be found *in vivo* as a biomarker of malignancy [322]. We had thus begun the process of producing an

AAV genomic plasmid encoding an artificial soluble form of VEGFR3 based upon genetic manipulation to remove the transmembrane and intracellular domains.

This year however Singh et al. [323] demonstrated that a natural form of sVEGFR3 is expressed endogenously within the cornea and is essential for the maintenance of corneal alymphaticity. Additionally they showed using a non-viral gene therapy approach in BALB-C mice that over expression of sVEGFR3 was able to improve corneal allograft survival and reduce corneal lymphangiogenesis in the suture model. A reduction in haemangiogenesis was observed although this was less pronounced, and mediated through sequestration of VEGF-C, reducing its binding to VEGFR2. Despite these extremely promising results a substantial area of the cornea remained vascularised in the treatment group, which we are confident maybe improved by the application of a viral gene therapy method.

The proposed approach of dual viral mediated gene therapy to overexpress both sVEGFR1 (sFlt1) and sVEGFR3 (sFlt4) therefore shows great promise. If sVEGFR3 mediated inhibition of lymphangiogenesis via this route proves as effective as the sFlt1 mediated inhibition of haemangiogenesis already demonstrated, then near complete inhibition of both forms of neovascular response should be achievable. Additionally the long lasting expression mediated by AAV may lead to both effects being sustained over the long term. Work upon this approach is on-going.

Finally it is possible that a soluble factor expressed within the stroma may reach therapeutic levels within more posterior tissues of the eye. Such an approach has previously been demonstrated within a different context. Injection of a lentiviral vector into the anterior chamber encoding an IL10 (which is both anti-inflammatory and anti angiogenic) has been shown to effectively reduce the infiltration of inflammatory cells into the vitreous in murine model of uveitis via transgene product production in the corneal endothelium and iris [154]. Thus intrastromal injection of AAV may provide an additional minimally invasive method by which more posterior pathogenic conditions such as uveitis or choroidal neovascularisation might be treated. This possibility is being investigated although it must first be established whether a soluble protein produced in the stroma is able to exit the cornea via the endothelium and reach an appropriate therapeutic level in the posterior segment.

5.3.1 Conclusions

- Overexpression of musFlt1 mediated by AAV delivery by intrastromal injection is able to convincingly and reproducibly inhibit corneal haemangiogenesis in the corneal suture model. In many cases this inhibition is near complete.
- Such an overexpression of musFlt1 had no significant effect upon the induction of lymphangiogenesis indicating that in the context of C57/B6J animals at least the contribution of VEGF-A (and other sFlt1 binders) to lymphangiogenesis is minimal.
- The intrastromal delivery route of AAV is able to deliver physiologically relevant levels of soluble transgene product to the cornea and is validated for use with other potentially useful soluble factors such as sVEGFR3 to inhibit lymphangiogenesis.

6. Lentiviral gene transfer to limbal epithelial stem cells for permanent epithelial transgene expression

6.1 Introduction

Due to the highly dynamic nature of the corneal epithelium, achieving long lasting gene transfer to this layer is highly challenging as transduced cells will inevitably be lost over time during the normal turnover processes of the tissue. The only way a lasting transduction could be achieved is by gene transfer to the limbal epithelial stem cells (LESC) with an integrating vector. The epithelium is composed entirely of the daughter cell lineages of the LESCs and thus genomic integration of a transgenic construct within these cells should lead to a sustained pan-epithelial transduction.

The work presented in this chapter was therefore focused upon development of a technique by which the LESCs might be transduced *in vivo* with a gene therapy vector, something which as far as we are aware has never been convincingly demonstrated previously. Only one study to date has attempted such a transduction, Igarashi et al. [324] demonstrated epithelial cell transduction lasting up to 6 weeks post gene delivery via a lentiviral vector applied topically after limbal epithelial debridement. In the course of work preliminary to that presented here these results could not be replicated, and we do not believe that 6 weeks is a long enough period of follow-up to claim LESC transduction with certainty.

Limbal epithelial stem cells (LESC's) are known to reside in the far peripheral epithelium, at the corneoscleral junction between the cornea, trabecular meshwork and conjunctiva. In humans a specific limbal structure called the palisades of Vogt is associated with the LESC niche, however whilst these structures have been identified in some non-human corneas such as the pig, they do not appear to be present in the mouse [325].

Despite being located near the outer surface of the eye this compartment can be extremely difficult to access surgically. Firstly the target area is extremely small, the entire murine epithelial thickness at the limbus being only ~20µm, [294] with the stem cell niche being a smaller sub division within this thickness. Secondly all the structures proposed as the niche of LESC's in humans at least are highly convoluted structures, further complicating access for both surgical instruments and vector solutions. In point of fact it is likely that the LESC

niche is specifically structured to protect the stem cells from exactly the type of access this work aims to achieve.

The work in this chapter attempted to mediate lentiviral LESC transduction *in vivo* by direct injection of vector in or very close to the LESC niche using an ultrafine glass pipette and formed part of collaboration with Dr Satoshi Kawasaki of Kyoto Prefectural University of Medicine.

6.1.1 Aims

The primary aim of the work presented in this chapter was to achieve a permanent widespread gene transfer to the corneal epithelium, a tissue that undergoes continuous regeneration, via lentiviral gene transfer to the limbal epithelial stem cells (LESC's) *in vivo*.

6.2 Methods and results

6.2.1 Comparison of two different injection methodologies to target limbal epithelial stem cells for lentiviral transduction

To deliver vector as close as possible to the LESC niche it was decided to inject with an ultrafine glass needle produced with a micropipette puller, pulled from borosilicate glass capillaries of 1mm O.D. x 0.78mm I.D.(Harvard Apparatus) approximate dimensions of which are shown in Figure 40. This work was performed in collaboration with Dr Satoshi Kawasaki (Kyoto Prefectural University of Medicine) who prepared the needles and took the Scanning Electron Micrograph (SEM) of the tip shown in Figure 40.

The two target routes of injection to be compared in this experiment were:

- "Limbal-intrastromal" which aimed to inject vector into the anterior limbal stroma, to target the LESC niche located immediately anterior to this area.
- "Limbal-subepithelial" which aimed to essentially inject directly into the LESC niche itself.

Both are represented in Figure 41

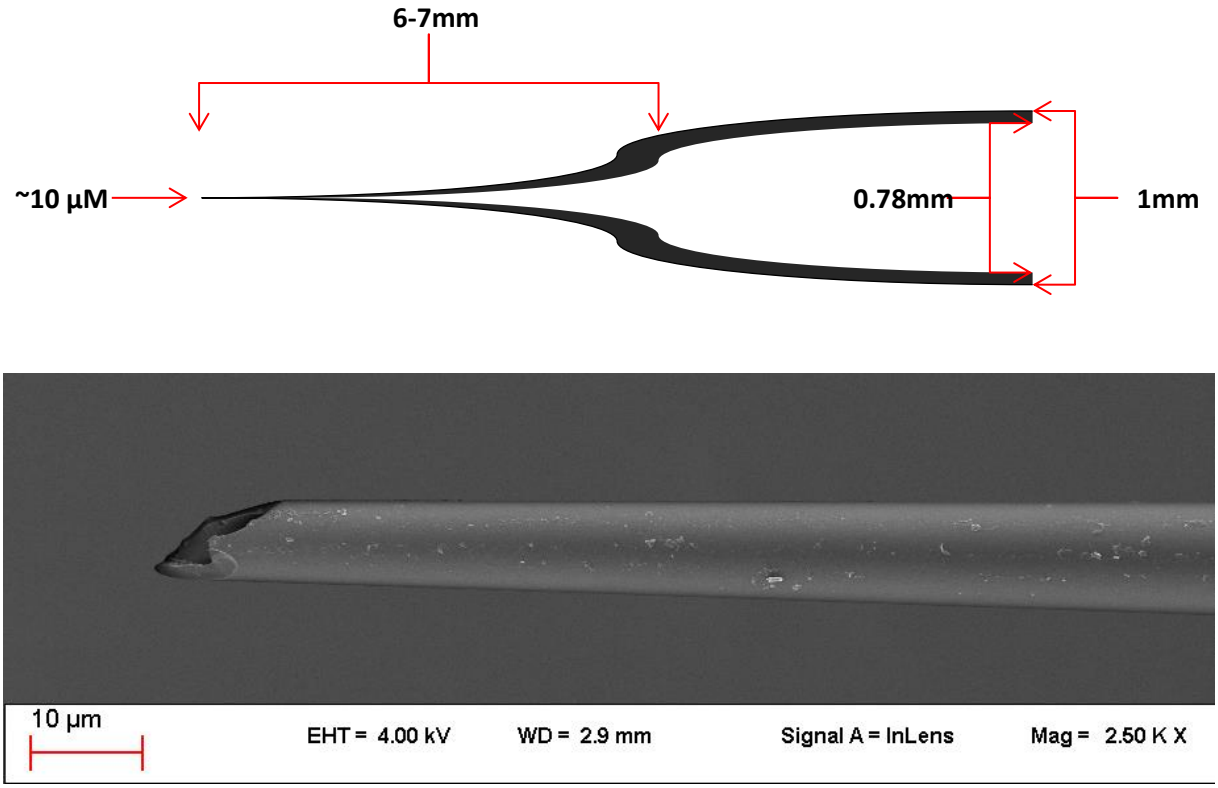

Figure 40. Schematic (not to scale) and SEM image of glass needle morphology used to deliver vector in 6.2.1

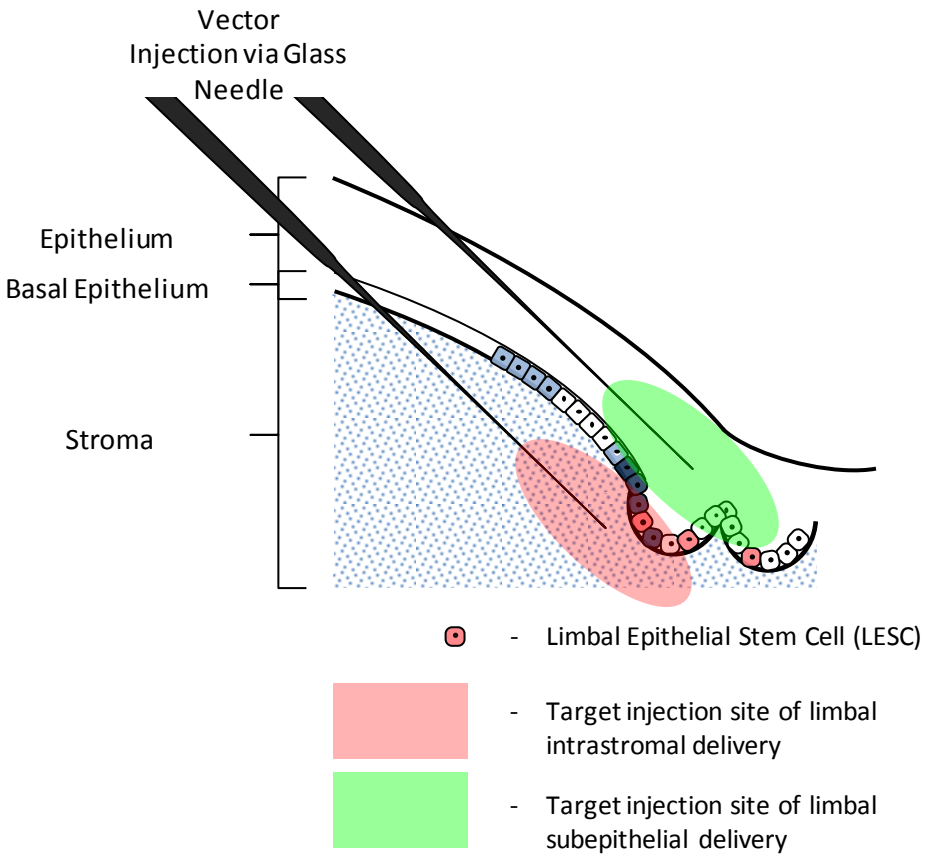

Figure 41. Schematic representation of the two routes of injection trialled in 6.2.1; Limbal-intrastromal and limbal-subepithelial

A total of 16 mice were injected bilaterally, 8 via the limbal-intrastromal route and 8 via the limbal-subepithelial route. Unfortunately one animal from each group did not recover from the procedure.

The vector injected was a lentivirus encoding eGFP under the control of the ubiquitous spleen focus forming virus (SFFV) promoter. The vector had a titre of $1x10^7$ vg / mL and was injected as described in 2.3.5.

Each needle had a capacity of ~50 µL and this volume of vector was preloaded immediately prior to injection. During injection the vector was continuously expressed from the tip by air pressure which was applied via a 50 mL volume syringe compressed to 5-10 mL. Due to this continuous flow no vector dose per eye can be accurately calculated. Repeated injections were preformed around the entire circumference of the limbus, approximately 30-50 injections were performed per eye.

The glass needles were extremely fragile and slender, because of this they had a strong tendency to break or become clogged during the procedure. If this occurred the needle was replaced and if clogging became frequent the vector solution was occasionally diluted up to 10 fold in OptiMEM (Gibco) to ameliorate the issue.

After injection the mice were initially assessed weekly for the eGFP expression in the cornea by Scanning Laser Ophthalmoscopy (SLO) (2.3.11).

Figure 42 shows SLO results from the first 4 weeks post injection from four representative eyes. For those injected limbal-intrastromally strong expression is seen around the limbus at week 1, however in all cases this expression is severely reduced or lost completely by week 2 onwards. For those injected limbal-subepithelially in some cases (7 / 14 eyes) the development of streak like expression patterns extending from the limbus to the central cornea were observed, such as those seen in Figure 42E & G.

At one week post injection a single animal (chosen upon the basis of an intermediate level of eGFP expression, i.e. neither the most nor the least promising) from each injection group was selected to be culled and assessed by histology, one eye was cryosectioned whilst the other was flatmounted.

Figure 43 show transverse cryosections imaged by confocal microscopy through both an intrastromally (Figure 43A) and subepithelially (Figure 43B, C & C') injected eye taken one week post injection. The intrastromally injected eye shows no evidence of epithelial transduction, however a large area of transduction around the posterior of the eye is apparent. Possible tissues transduced include conjunctiva, sclera and ocular muscle. The subepithelially injected eye shows several small patches of epithelial transduction in the cornea. These are located relatively centrally and all layers of the epithelium appear to have been transduced. No transduction of other layers of the cornea, or of other ocular tissues was noted.

Figure 44 & Figure 45 show corneal flat mounts taken at 1 week post injection and imaged by confocal microscopy for an intrastromally and a subepithelially injected eye respectively.

In Figure 44A & D a large area of non-epithelial limbal tissue appears to have been transduced. This appears to be mostly conjunctiva. A very small amount of epithelial transduction has also been achieved in highlighted area 1 of Figure 44A. This area is shown in greater detail in Figure 44C & C' revealing a small number of epithelial cells transduced in all layers of the epithelium.

In Figure 45 a larger (although still relatively small) area of epithelial transduction can be seen in highlighted area 1. This area is shown in greater detail in Figure 45C & C' revealing

a larger number of epithelial cells transduced in all layers of the epithelium. No significant expression was noted in any other layer of the cornea or more peripheral tissues.

Figure 46 shows a more limbal area (highlighted area 2) of the same eye presented in Figure 45. In this location too there is transduction evident in all epithelial layers. Of particular note are transduced cells shown in Figure 46E which appear to be located close to involuted structures in the limbus reminiscent of structures associated with the LESC niche in humans [64], although it is possible these folds are merely an artefact of the flat mounting procedure.

After 4 weeks of SLO follow up of the limbal intrastromal group with no expression being seen past week one. Observations were terminated and the animals culled.

Due to the promising results obtained from the subepithelial group, follow up was continued. This group will henceforth be referred to as “Subepithelial Cohort 1”.

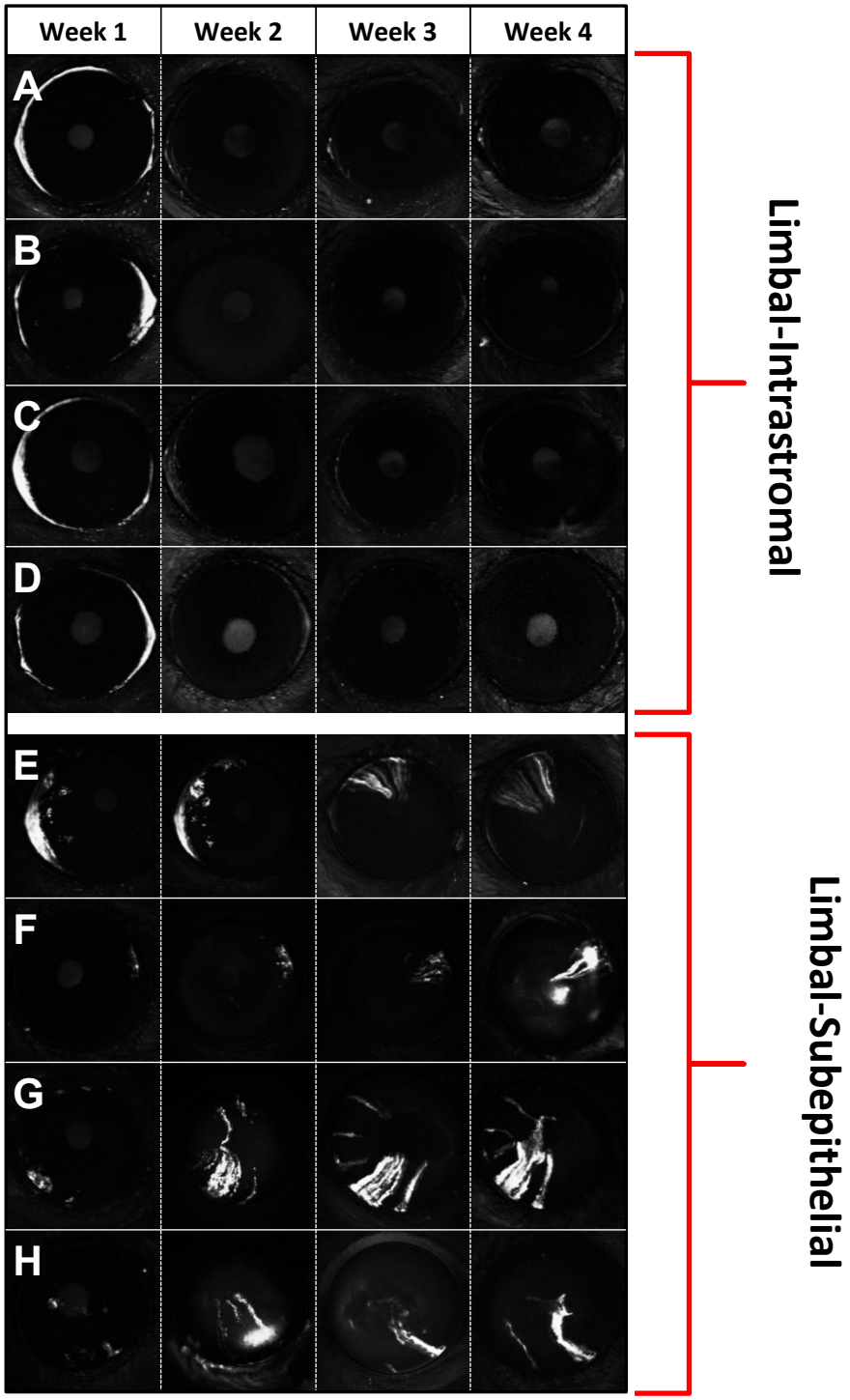

Figure 42. ***Representative images showing lentivirus mediated corneal eGFP expression assessed by SLO weekly after either limbal-intrastromal or limbal-subepithelial injection of vector***

A-D: Four representative eyes showing lenti-mediated eGFP expression over 4 weeks following limbal-intrastromal injection

E-F: Four representative eyes showing lenti-mediated eGFP expression over 4 weeks following limbal-subepithelial injection

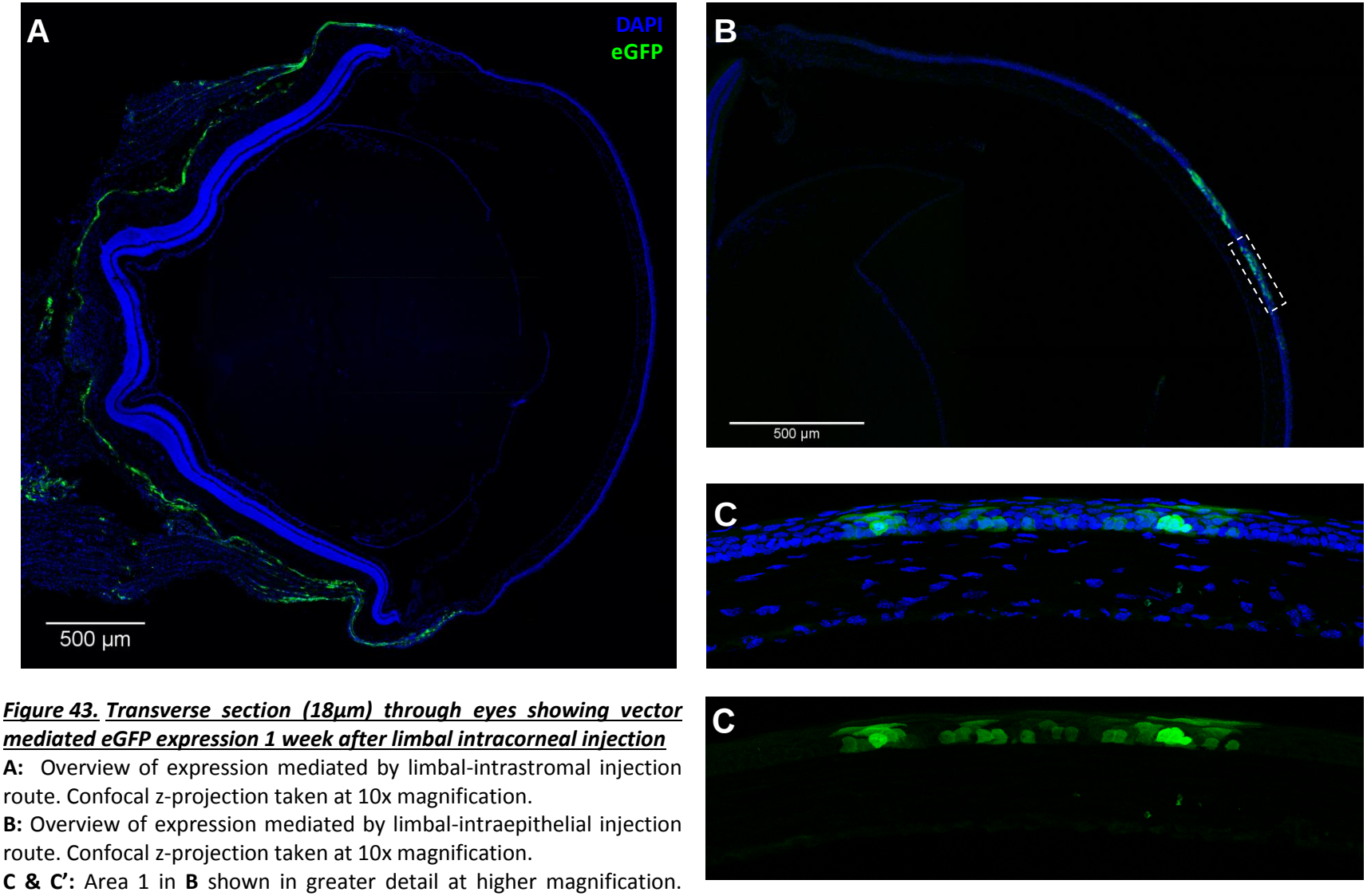

Figure 43. ***Transverse section (18µm) through eyes showing vector mediated eGFP expression 1 week after limbal intracorneal injection***

A: Overview of expression mediated by limbal-intrastromal injection route. Confocal z-projection taken at 10x magnification.

B: Overview of expression mediated by limbal-intraepithelial injection route. Confocal z-projection taken at 10x magnification.

C & C': Area 1 in **B** shown in greater detail at higher magnification. Confocal z-projection taken at 40x magnification.

In all images: Blue = DAPI, Green = vector mediated eGFP

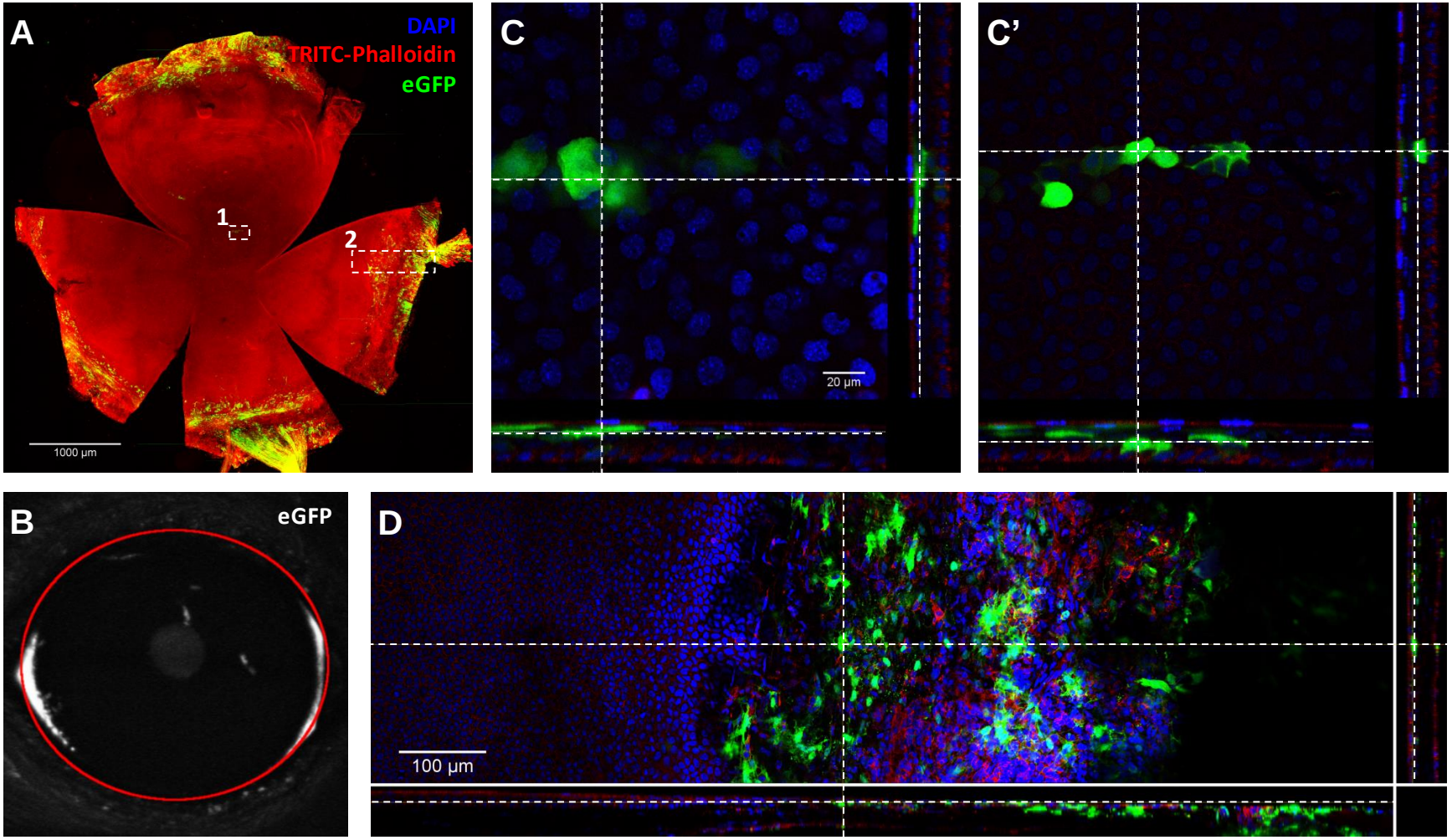

Figure 44. Corneal flatmount showing vector mediated eGFP expression 1 week after limbal-intrastromal injection of LNT-SFFV-eGFP

A: Overview of the whole flat mount with 2 areas highlighted. Confocal z-projection taken at 10x magnification.

B: Comparable SLO image of the same eye taken shortly before animal was culled and tissue fixed.

C & C': Orthographic projection of confocal z-stack taken at position 1 in A at 40x magnification, **C** = Superficial epithelium, **C'** = Basal epithelium.

D: Orthographic projection of confocal z- stack taken at position 2 in A at 40x magnification.

In **A, C, C' & D:** Blue = DAPI, Red = TRITC-Phalloidin, Green = vector mediated eGFP. In **B:** White = vector mediated eGFP

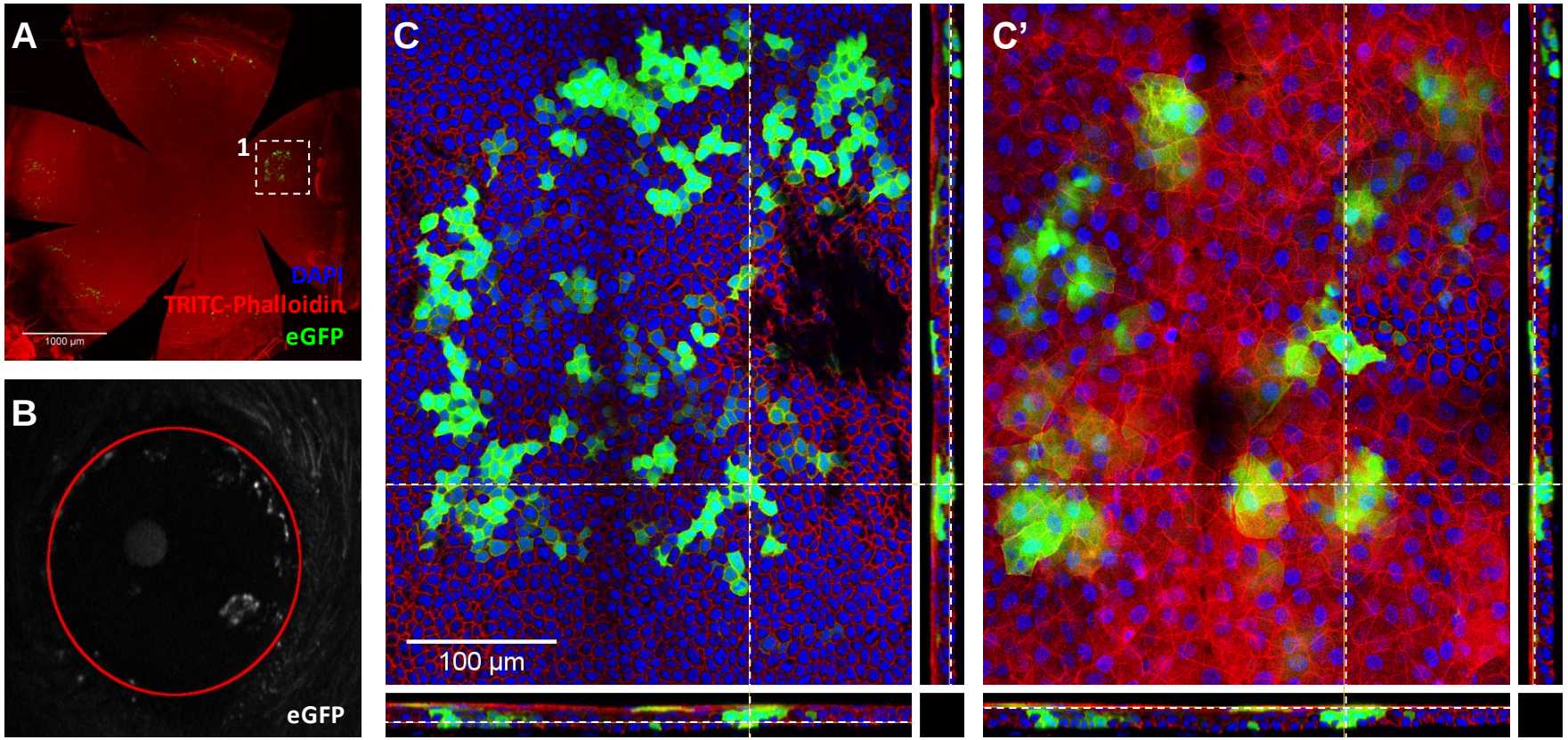

Figure 45. ***Corneal flatmount showing vector mediated eGFP expression 1 week after limbal-subepithelial injection of LNT-SFFV-eGFP***

A: Overview of the whole flatmount with a single area highlighted. Confocal z-projection taken at 10x magnification.

B: Comparable SLO image of the same eye taken shortly before animal was culled and tissue fixed.

C & C': Orthographic projections of confocal z-stack taken at position 1 in A at 40x magnification, **C** = Basal epithelium, **C'** = Superficial epithelium.

In **A, C & C'**: Blue = DAPI, Red = TRITC-Phalloidin, Green = vector mediated eGFP

In **B:** White = vector mediated eGFP

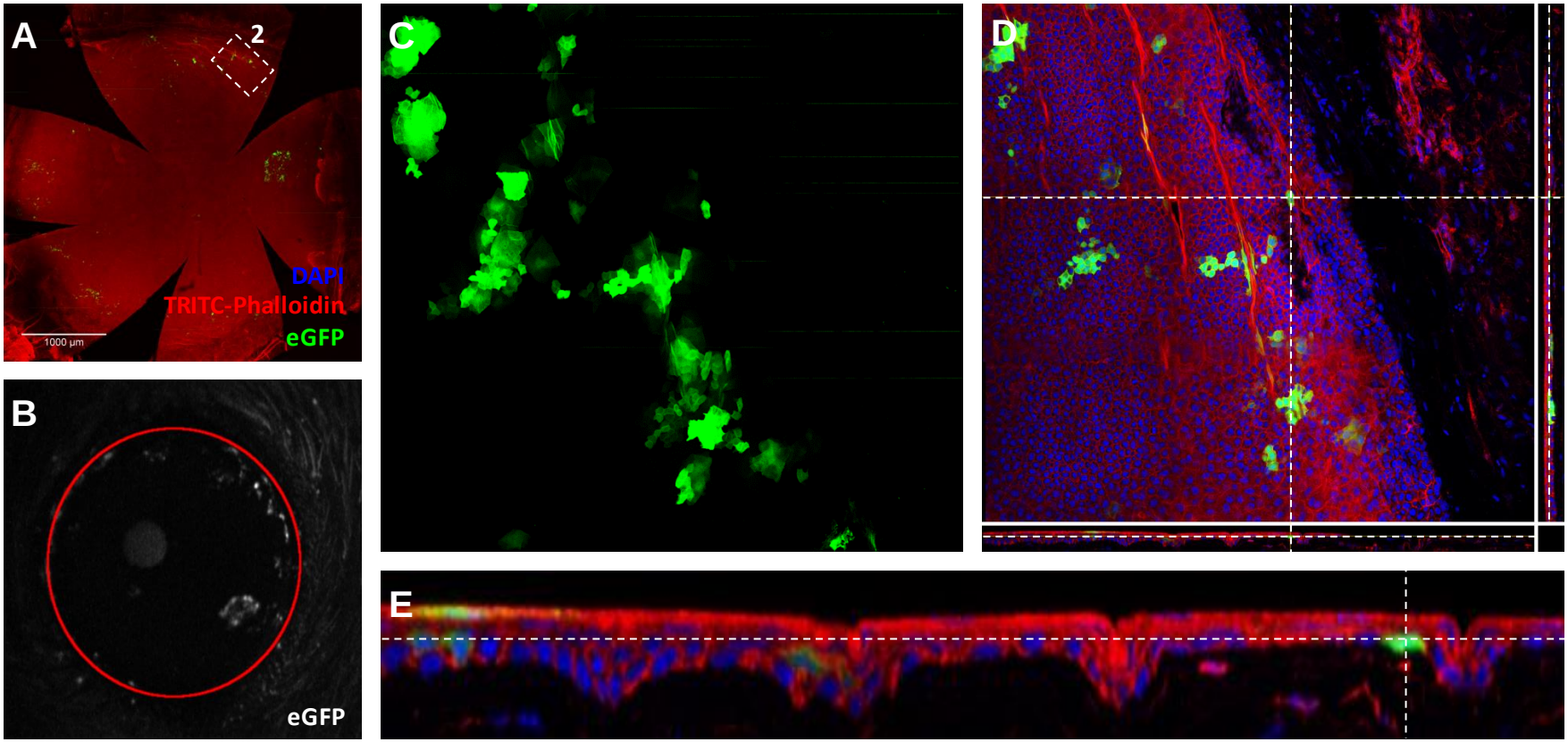

Figure 46. ***Corneal flatmount showing vector mediated eGFP expression 1 week after limbal subepithelial injection of LNT-SFFV-eGFP***

A: Overview of the whole flat mount with a single area highlighted. Confocal z-projection taken at 10x magnification.

B: Comparable SLO image of the same eye taken shortly before animal was culled and tissue fixed.

C: Confocal z-projection of area 2 in **A** of green channel only showing all eGFP transduced cells in the area. Taken at 40x magnification.

D: Orthographic projections of confocal z-stack taken at position 2 in A at 40x magnification.

E: XZ axis of D shown in more detail

In **A, C, D & E**: Blue = DAPI, Red = TRITC-Phalloidin, Green = vector mediated eGFP

In **B:** White = vector mediated eGFP

6.2.2 Subepithelial cohort 2; Refinement of needle morphology to maximise lentiviral transduction of epithelial cells / LESCs

Following on from the initial promising results obtained in 6.2.1 with the subepithelial injection route a second cohort of mice was injected via this route.

The long thin glass needle morphology used in 6.2.1 (termed “slow taper”) had proven to be prone to breakage and clogging during the injection procedure. The needle tip was also difficult to position, being more prone to amplify operator movements.

For these reasons a different shorter needle morphology was trialled, this was termed “fast taper”. The difference between slow and fast taper needles is illustrated in Figure 47

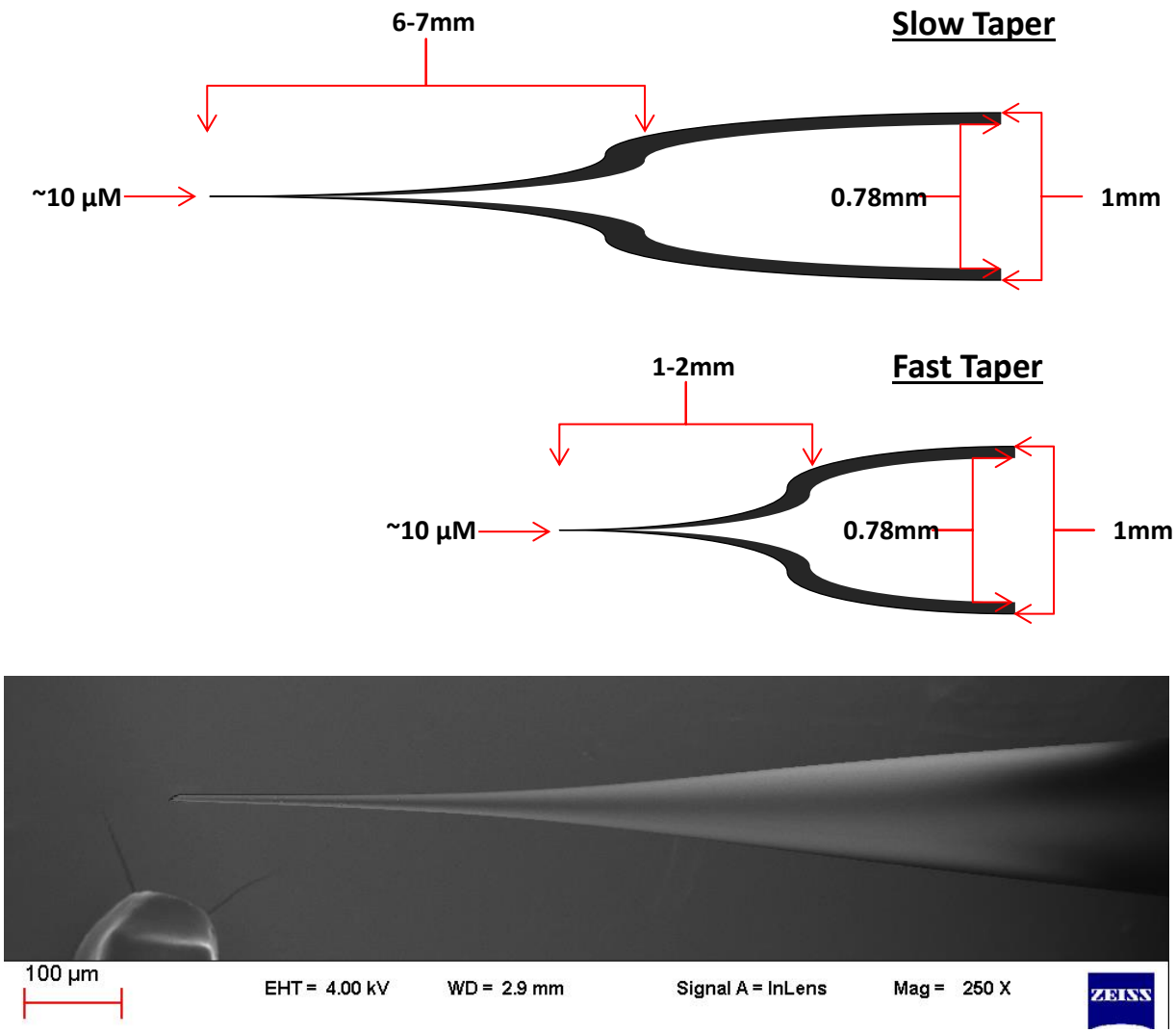

Figure 47. Schematic (Not to Scale) and SEM image illustrating “fast taper” glass needle morphology used to deliver vector in 6.2.2

A total of 21 mice were injected bilaterally, all via the limbal-subepithelial route. As in 6.2.1 the vector injected was lentivirus encoding eGFP under the control of the SFFV promoter. The vector had a titre of $1x10^7$ vg / mL and was injected as described in 2.3.5. After injection the mice were initially assessed at 1, 2, 4 and 7 weeks post injection for the eGFP expression in the cornea by SLO (2.3.11).

Figure 48 shows four representative eyes from cohort 2 for the first 4 time points imaged; 1, 2, 4 and 7 weeks post injection. Large areas of a static punctate transgene expression are visible, highlighted by red asterisks. These do not appear to be epithelial as the areas do not move or change in anyway over time. Some streak-like expression (red arrowhead) was also visible in some eyes (6 / 38 eyes at week 7).

Figure 49 shows a corneal flat mount from an animal in subepithelial cohort 2 taken at 4 weeks post injection and imaged by confocal microscopy. A large area of the punctate transgene expression pattern is apparent a small area of which is highlighted in Figure 49A area 1. Figure 49C shows this area in greater detail and reveals the eGFP expression to be localised to cells of the anterior stroma.

Figure 50 shows an epithelial streak (highlighted area 2) present in the same eye presented in Figure 49. Note that the streak appears discontinuous (area of discontinuity highlighted by red marker in Figure 50D). Please note that in these images the DAPI stain has not fully penetrated the whole tissue, likely due to incomplete permeabilisation.

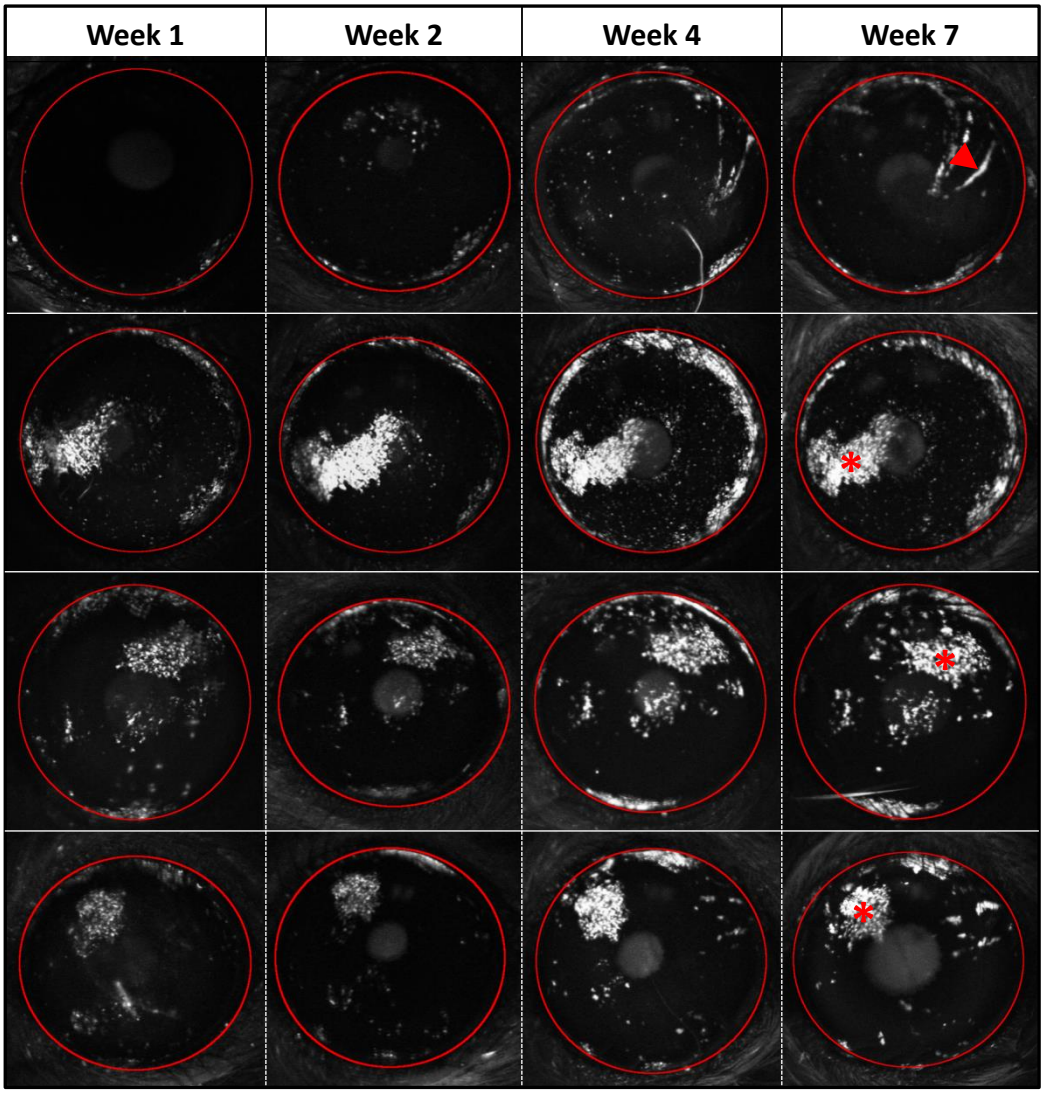

Figure 48. Representative images showing lentivirus mediated corneal eGFP expression assessed by SLO after limbal-subepithelial injection of vector (Cohort 2)

Red asterisks highlight areas of a static punctate transgene expression which are likely non-epithelial. Red arrowhead highlights streak-like transduction pattern that is likely epithelial.

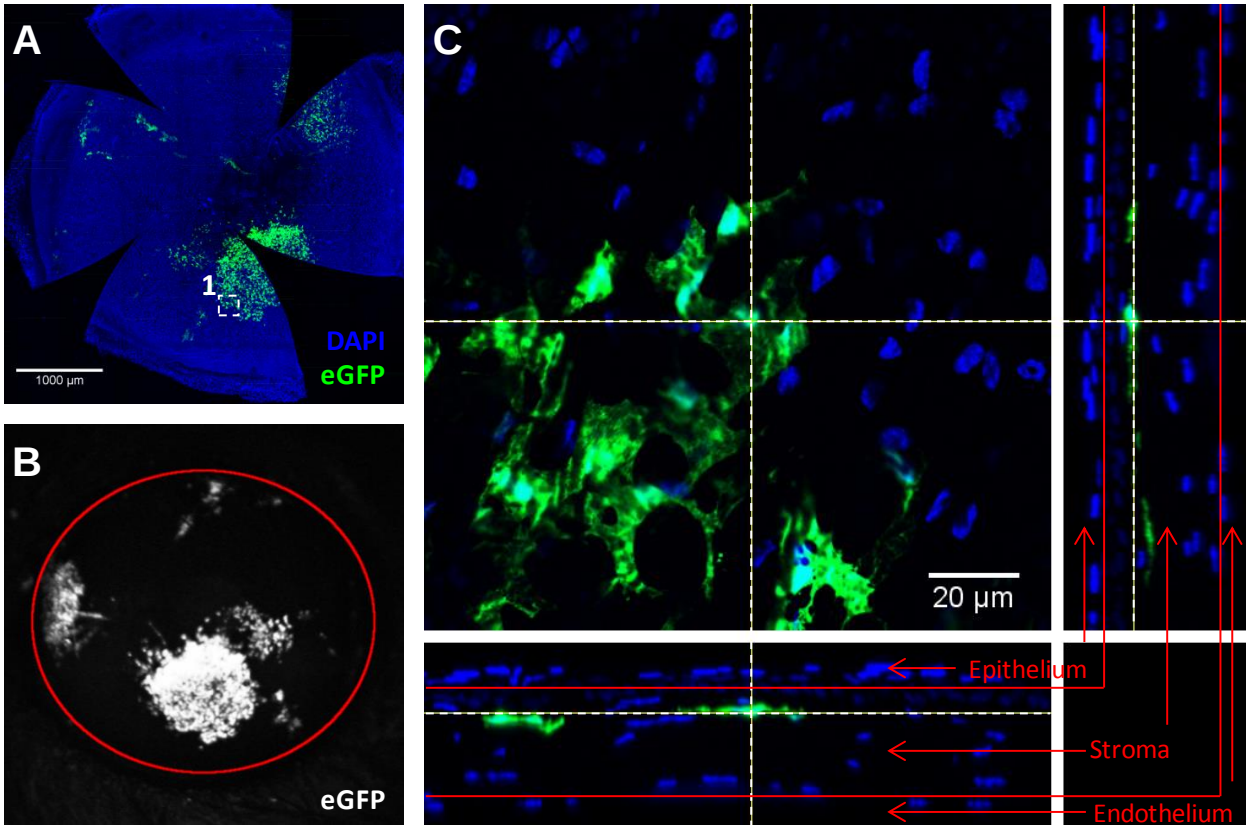

Figure 49. Corneal flatmount showing vector mediated eGFP expression 4 weeks after limbal-subepithelial injection of LNT-SFFV-eGFP (Cohort 2)

A: Overview of the whole flatmount with a single area highlighted. Confocal z-projection taken at 10x magnification.

B: Comparable SLO image of the same eye taken shortly before animal was culled and tissue fixed.

C: Orthographic projection of confocal z-stack taken at position 1 in **A** at 40x magnification.

In **A & C:** Blue = DAPI, Green = Vector mediated eGFP

In **B:** White = vector mediated eGFP

Figure 50. Corneal flatmount showing vector mediated eGFP expression 4 weeks after limbal-subepithelial injection of LNT-SFFV-eGFP (Cohort 2)

A: Overview of the whole flatmount with a single area highlighted. Confocal z-projection taken at 10x magnification.

B: Comparable SLO image of the same eye taken shortly before animal was culled and tissue fixed.

C: Confocal z-projection of area 2 in **A** of green channel only showing all eGFP transduced cells in the area. Taken at 40x magnification.

D: Orthographic projection of confocal z-stack taken at position 1 in **A** at 40x magnification. Only XY (single plane) and XZ shown.

In **A, C & D**: Blue = DAPI, Green = Vector mediated eGFP

In **B**: White = vector mediated eGFP

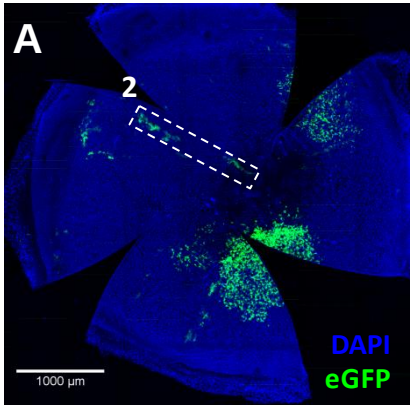

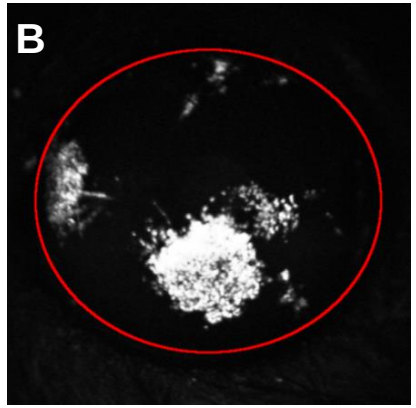

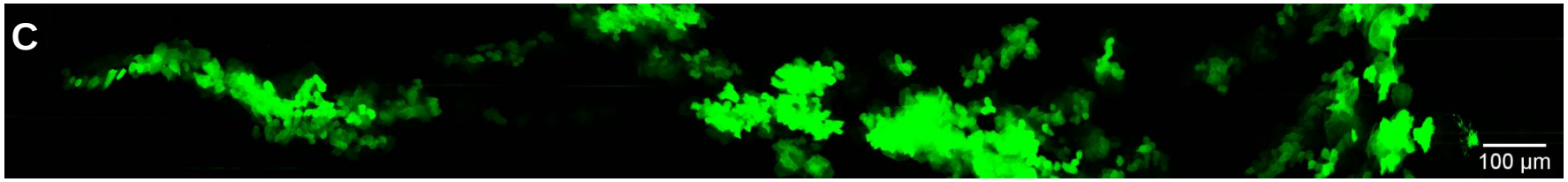

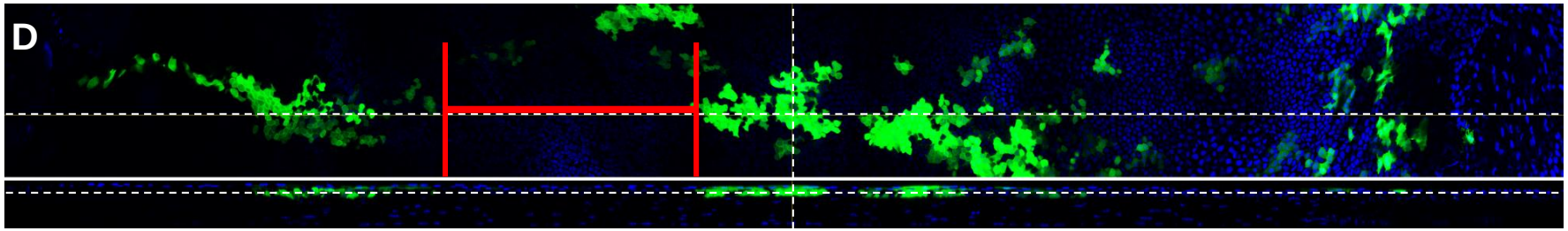

6.2.3 Injection of subepithelial cohort 3 and long term follow up by SLO of all 3 cohorts

Follow up of the 2 cohorts injected in 6.2.1 and 6.2.2 revealed that the number of eyes displaying the epithelial streaks of transgene expression (henceforth referred to a epithelial streaks) that might indicate LESC transduction was a relatively small proportion of the total injected. Therefore in order to both increase the numbers and make use of the expertise gained to date with this highly challenging procedure, a third cohort was injected via the subepithelial route.

The fast taper needle morphology trialled in 6.2.2 did not appear to result in any improvement in the amount of epithelial transduction achieved. In addition the use of fast taper needles resulted in large areas of stromal transduction, which obfuscate the desired result. Therefore it was decided that for the injection of a third cohort the original slow taper needle morphology would be used.

For cohort 3 a total of 19 mice were injected bilaterally, all via the limbal -subepithelial route. As in 6.2.1 and 6.2.2 the vector injected was lentivirus encoding eGFP under the control of the SFFV promoter. The vector had a titre of $1x10^7$ vg / mL and was injected as described in 2.3.5.

Due to the relative lack of epithelial streaks observed to develop in the earlier time points of the previous 2 cohorts it was decided that the first time point imaged by SLO for cohort 3 would be taken at 3 weeks post injection, followed by 7 and then 10 weeks post injection. After this assessments would be made monthly.

Those animals still alive from Cohorts 1 and 2 would also be assessed for eGFP transgene expression by SLO monthly. If any animal displayed no eGFP expression at all bilaterally for two consecutive time points then the animal was excluded from further follow up and culled.

The epithelial streaks thus far observed to develop in some eyes could be a result of either LESC transduction or early transient amplifying cell (eTAC) transduction. To distinguish between these two possibilities a long term follow-up was required. LESC transduction would be expected to result in an essentially permanent expression, whilst eTAC transduction would be expected to disappear with time. Exactly how long will be required to make this distinction is unclear. The longest recorded timeframe for complete corneal epithelial turnover under non-wounded conditions found in the literature is 12-13 weeks (Buck, 1985). This therefore represents a minimum timeframe, but a much longer follow-up would be preferable if permanent transduction is to be claimed. It was therefore decided that a 1 year follow-up period should be assessed

All the SLO data collected for all three cohorts is presented in Appendix 9.2

Figure 51 shows the long term follow-up of four eyes that displayed some of the most extensive epithelial streaks observed over all 3 cohorts injected. In these four examples the streaks persisted until the final 1 year time point.

Observations were also made that might provide some insight into the normal cellular dynamics of corneal epithelial homeostasis. Without continuous observation it is impossible to be certain that a streak observed at one time point is in fact temporally continuous with one observed at the next. However streaks that appeared consistent in terms of point of origin in the limbus and overall morphology between time points were assumed to be the same streak.

Figure 52 shows one eye in which the temporal continuity of streaks was particularly difficult to assess.

Upon detailed analysis streaks were subdivided into two subtypes.

Type 1: Were defined as highly consistent in appearance over time, being strong, continuous and always connected to the limbus. An example is presented in Figure 53.

Type 2: Were defined as appearing more variable in terms of length, continuity and attachment to the limbus. An example is presented in Figure 54.

In cohort 3 in particular, but also throughout the other 2 cohorts it was noted that epithelial expression patterns that were initially patchy and discontinuous appeared to “firm up” into distinct streak like patterns over time. Two of the clearest examples of this are shown in Figure 55. Failure of this process was also observed but only rarely; Figure 56 shows an example in which widespread patchy expression only results in very limited subsequent streak formation.

Figure 57 shows a single clear example in which the development of both a type 1 and a type 2 streak is delayed until 12 to 18 weeks post injection of vector, after which they persist.

Figure 58 shows a corneal flat mount from an animal in subepithelial cohort 3 which died at 10 weeks post injection imaged by confocal microscopy. Multiple epithelial streaks are visible the largest of which is shown in more detail in Figure 58C

Figure 59 and Figure 60 show corneal flat mounts of the eyes of a single animal from subepithelial cohort 3 which was culled at 52 weeks post injection. This animal was chosen for sacrifice due to an intermediate number of epithelial streaks being present. Those with more extensive streaking or single streaks were preserved for more extensive analysis at a later date.

Imaging of the eye shown in Figure 59 was attempted *in vivo* using a two-photon microscope immediately post SLO imaging whilst the animal was under terminal anaesthesia. Unfortunately, as the two photon microscope is a very new piece of equipment within the lab its use *in vivo* is still being optimised and thus during the procedure a large amount of damage was caused to the epithelial layer. This was likely due to the laser power being set too high or suboptimal imaging technique. Areas of damage are highlight by red arrow heads and delimited by red dotted lines in Figure 59B, and account for why only the limbal portion of the streaks could be imaged in Figure 59B, C & D. Please note that in Figure 59 the TRITC-Phalloidin stain has not fully penetrated the whole tissue, likely due to incomplete permeabilisation.

Figure 61 shows that the off-target stromal transduction produced can be highly variable in terms of longevity of expression. In some cases such as that shown in Figure 61A the stromal transduction lasted for the entire duration of the experiment, in other cases such as in Figure 61C it was lost after only a few weeks. Stromal loss of transgene expression when it occurred was always rapid, with complete loss usually occurring over the space between consecutive time points. Figure 61B shows the only example in which a possible intermediate phase of loss was observed.

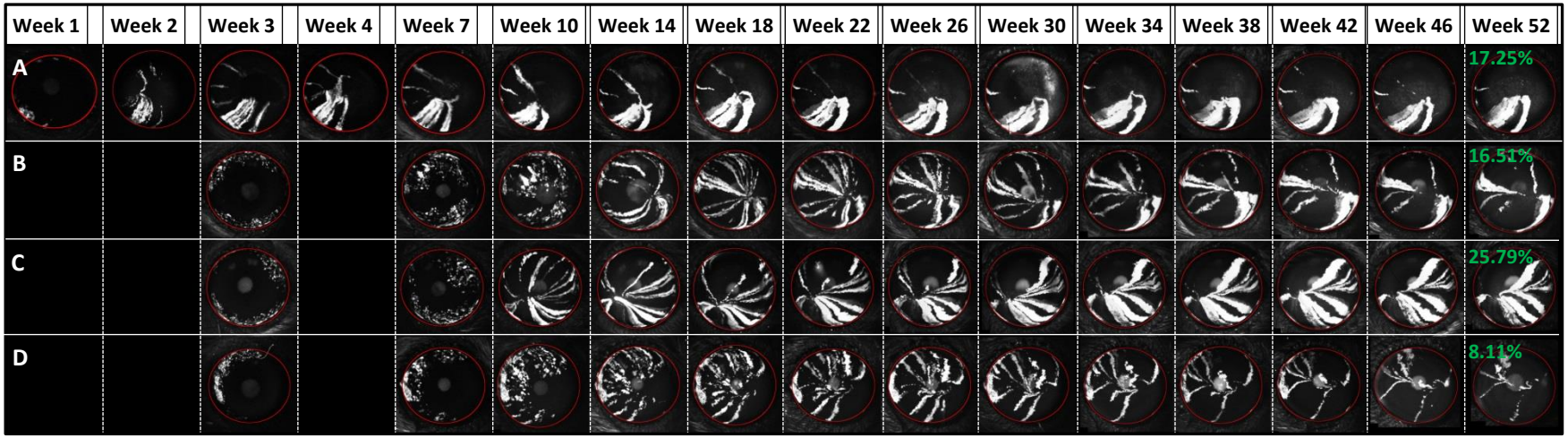

Figure 51. ***SLO images showing time course of vector mediated eGFP expression*** **in vivo** ***up to 52 weeks after limbal-subepithelial injection of LNT-SFFV-eGFP***

A-D: Four eyes representing some of the most extensive, long lasting transduction achieved. Green text inlayed into week 52 image indicates proportion of visible area transduced.

Time points showing no image (black) indicate that this animal / cohort was not imaged at that time point.

In All: White = vector mediated eGFP. Red ring delimits the globe of the eye.

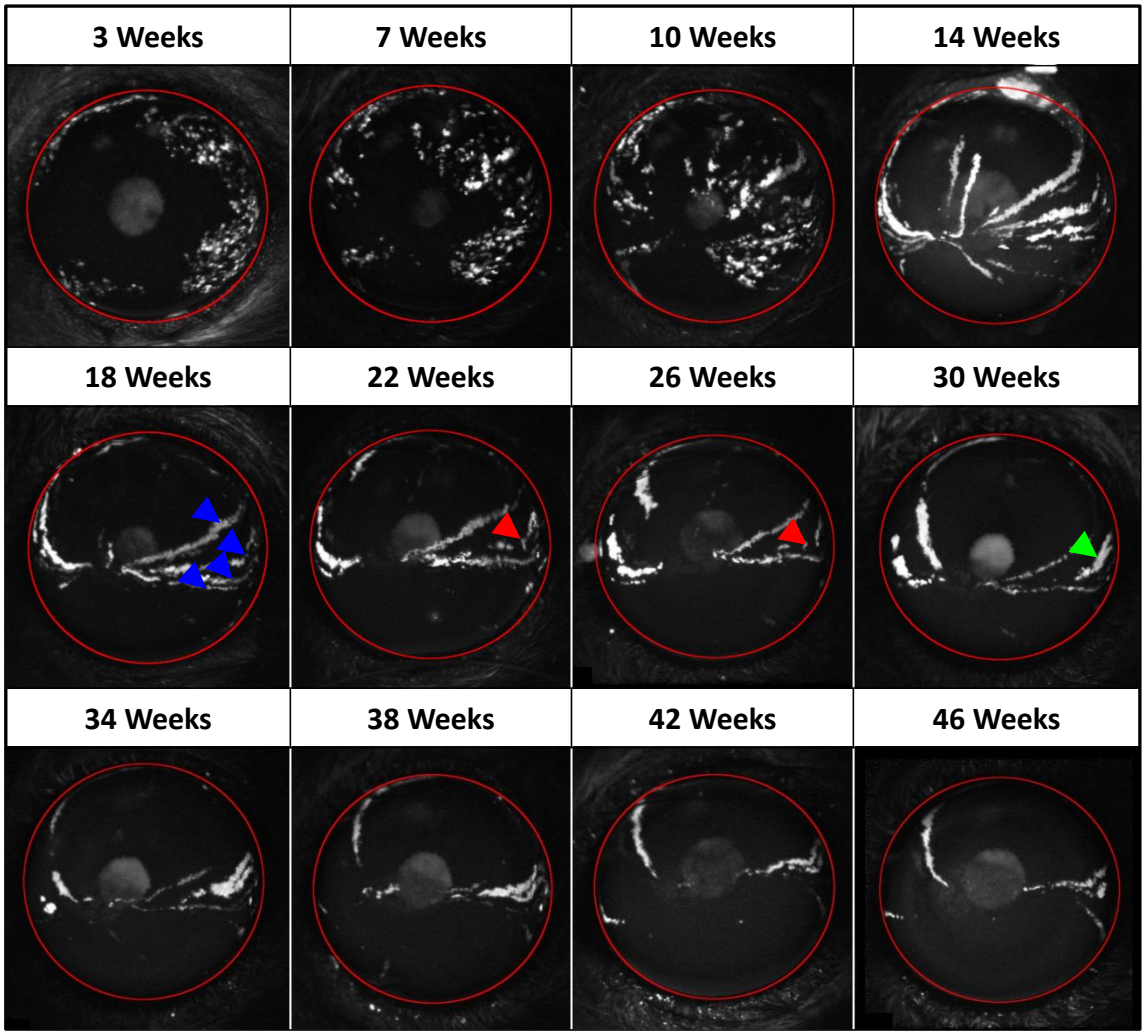

Figure 52. Example eye in which streak continuity over time was extremely difficult to assess due to close proximity of multiple streaks

Blue arrowheads at the 18 week time point highlight up to 4 distinct streaks in close proximity to each other.

The eGFP expression highlighted by the red arrowheads may indicated stages of loss of one or more of these streaks.

The streak highlighted by the green arrowhead maybe either a recurrence of the one or more of the streaks that appeared to be being lost, or an entirely new streak.

In All: White = vector mediated eGFP. Red ring delimits the globe of the eye.

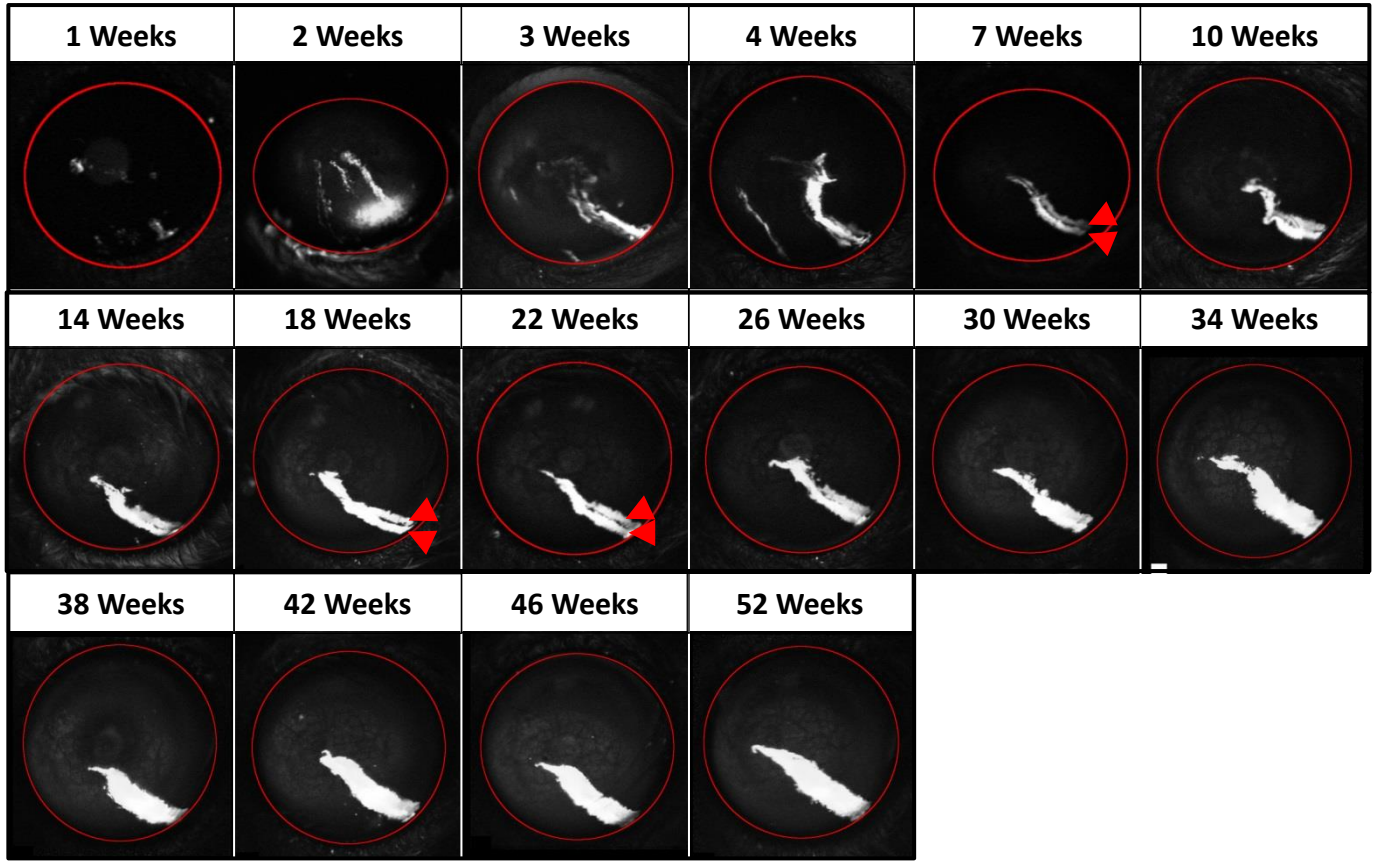

Figure 53. Example of a "Type 1" epithelial streak, characterised by always appearing strong, continuous and connected to the limbus

The example shown here is likely to be 2 such type 1 streaks which become increasingly merged over time.
Red arrowheads highlight some images in which two points of streak origin can be seen.
In All: White = vector mediated eGFP. Red ring delimits the globe of the eye.

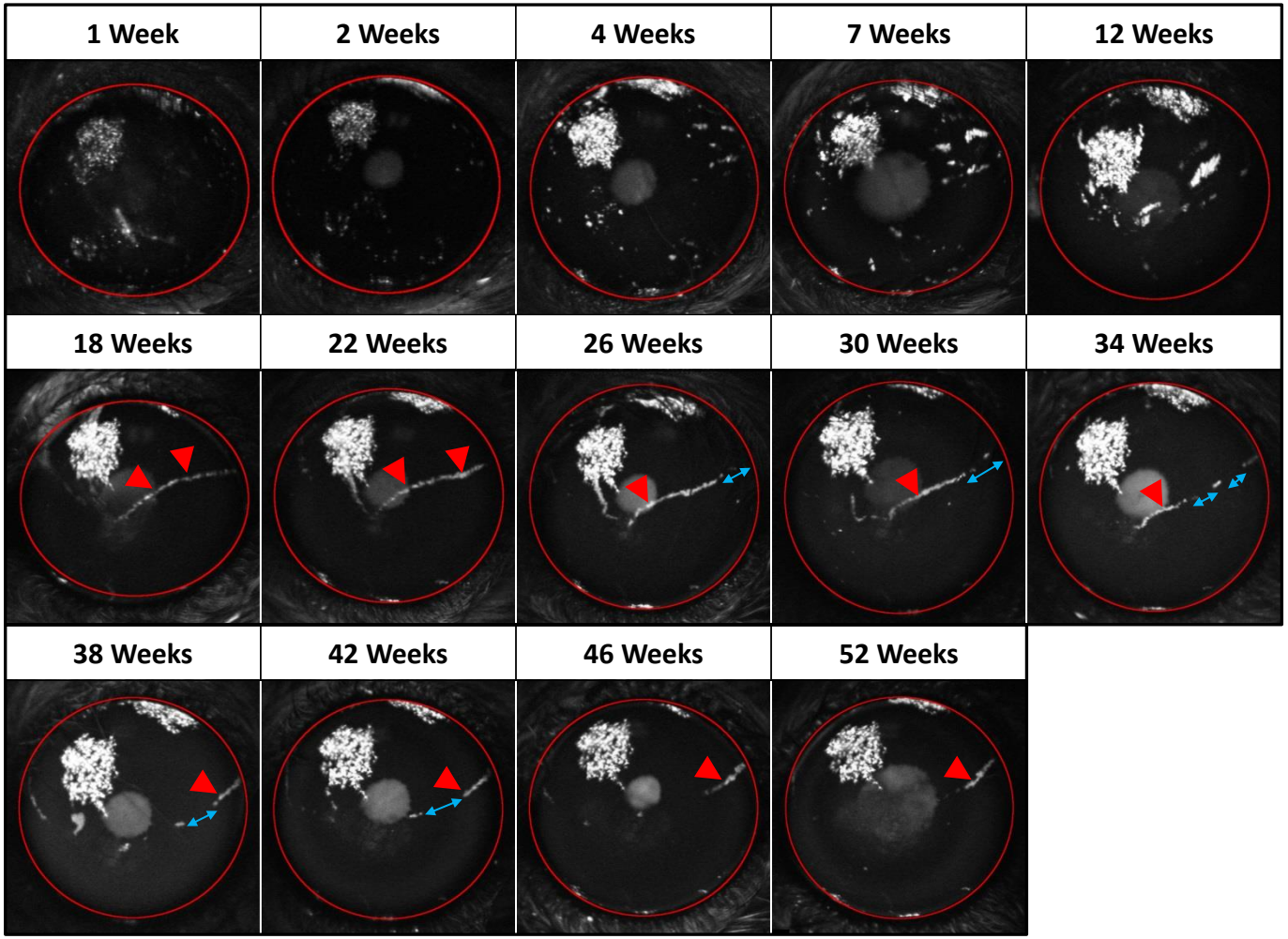

Figure 54. Example of a "Type 2" epithelial streak, characterised by being variable in appearance in regard to length, continuity and connection to the limbus

Red arrowheads highlight the streak in question. Blue double-ended arrows highlight areas of discontinuity.
In All: White = vector mediated eGFP. Red ring delimits the globe of the eye.

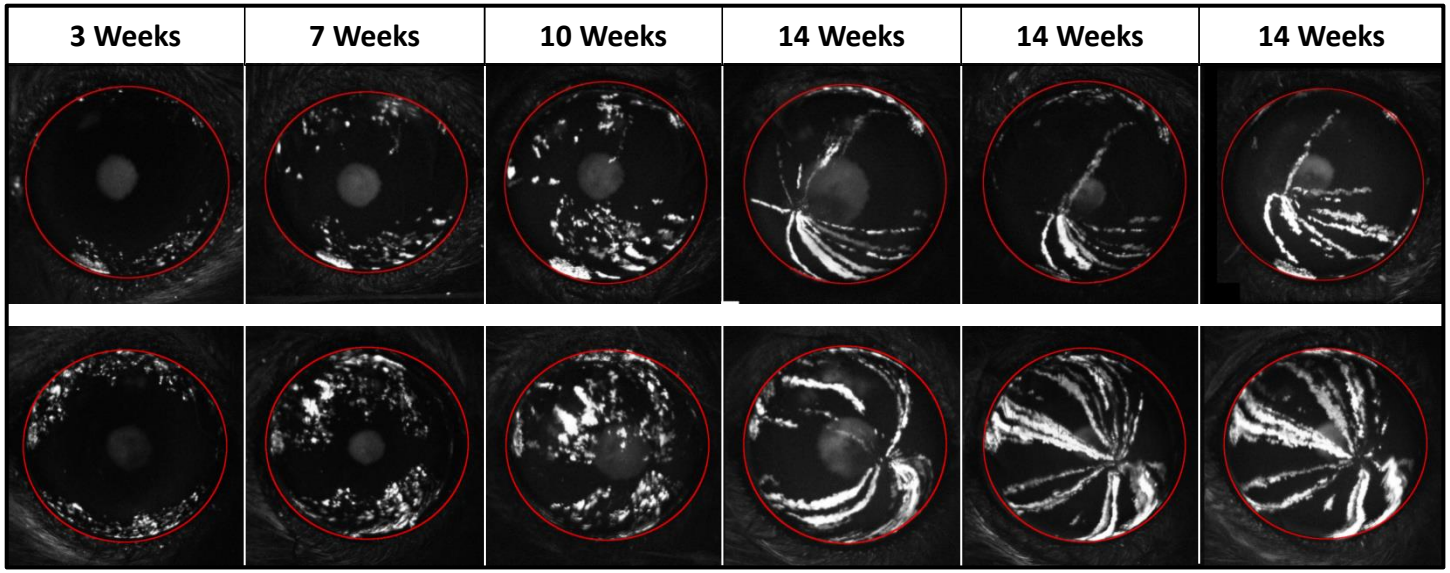

Figure 55. ***Two examples from Cohort 3 illustrating the "firming up" of initial patchy discontinuous epithelial transgene expression into distinct streaks over time***

In both examples the process of "firming up" appears to have taken place between 10 and 14 weeks post injection.
In All: White = vector mediated eGFP. Red ring delimits the globe of the eye.

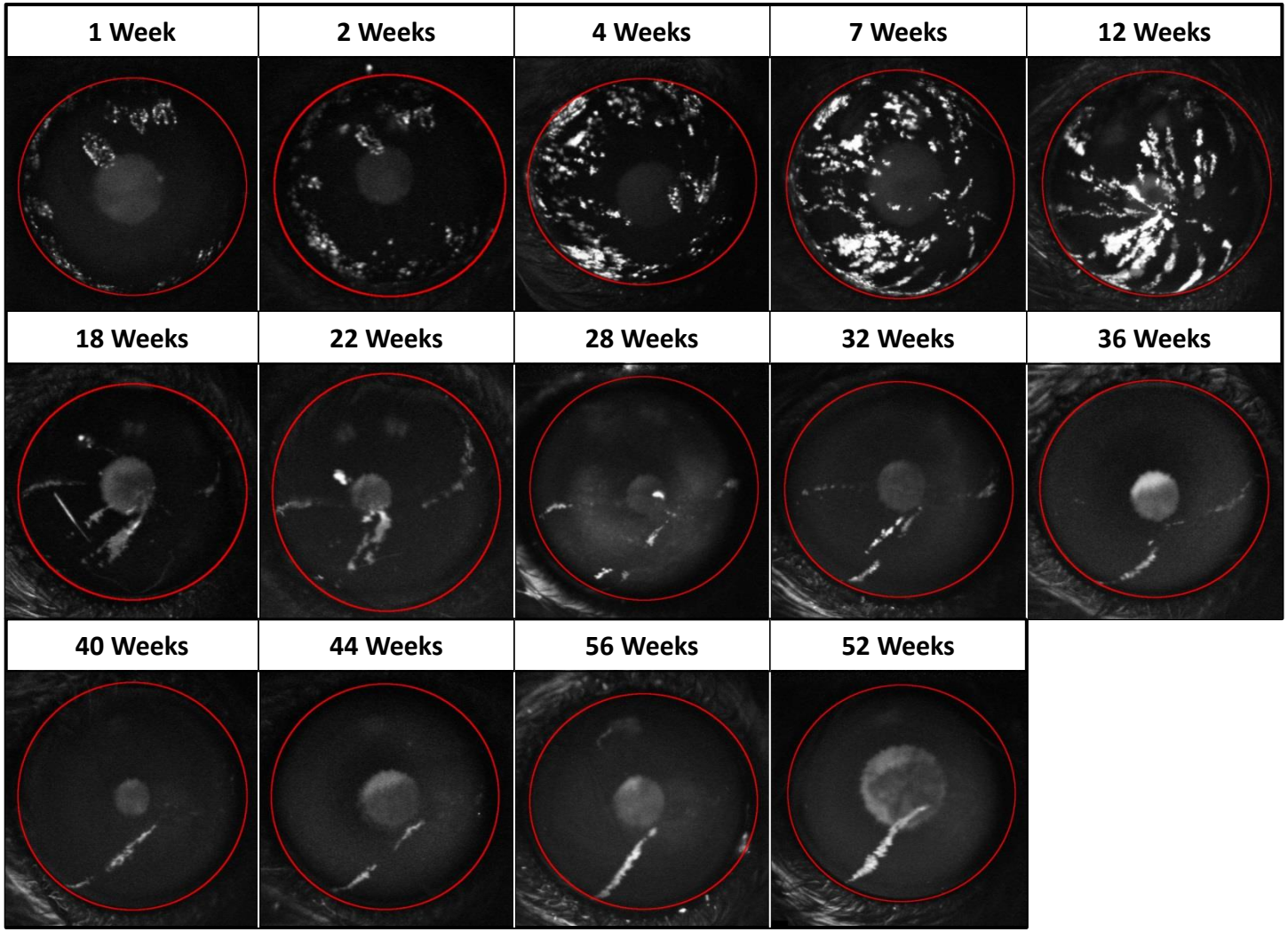

Figure 56. ***One example in which the process of "firming up" largely fails***

Widespread patchy epithelial transduction is seen at 4 weeks post injection. At 7 and 12 weeks post injection these patches become increasingly streak-like. After this however few firm streaks develop or persist. In All: White = vector mediated eGFP. Red ring delimits the globe of the eye.

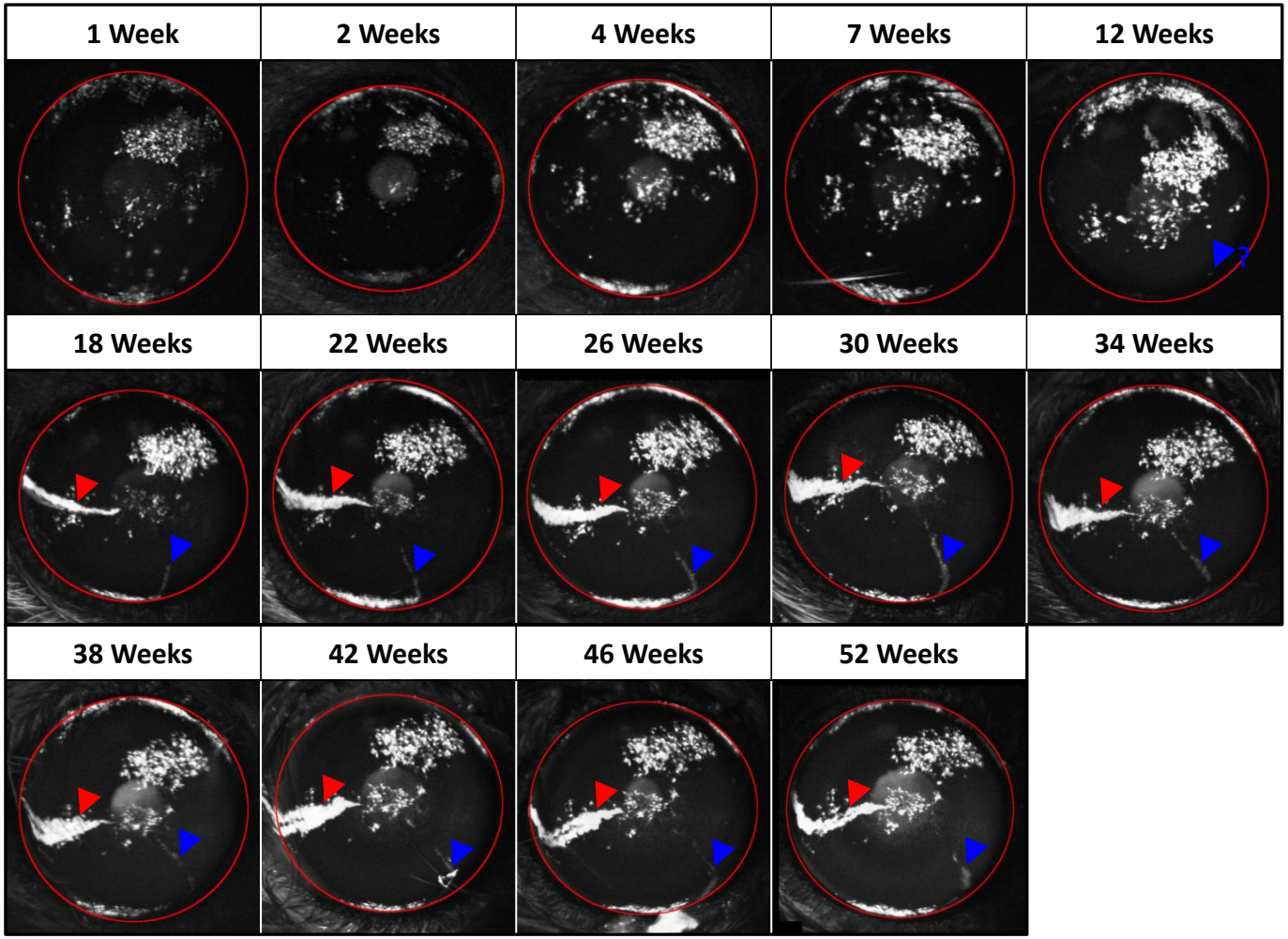

Figure 57. SLO images showing the late onset of an epithelial streak of LNT-SFFV-eGFP mediated eGFP expression
Red and Blue arrowheads highlight the progression of two streaks of cell growth beginning from 12(?) to 18 weeks after injection. In All: White = vector mediated eGFP. Red ring delimits the globe of the eye.

Figure 58. ***Corneal flatmount showing vector mediated eGFP expression 10 weeks after limbal-subepithelial injection of LNT-SFFV-eGFP***

A: Overview of the whole flat mount with a single area highlighted. Confocal z-projection taken at 10x magnification.
B: Comparable SLO image of the same eye taken shortly before animal was culled and tissue fixed.
C: Confocal z-projection of area 1 in **A** of green channel only showing all eGFP transduced cells in the area. Taken at 40x magnification.
In **A & C:** Red = TRITC-Phalloidin, Green = vector mediated eGFP. In **B**: White = vector mediated eGFP

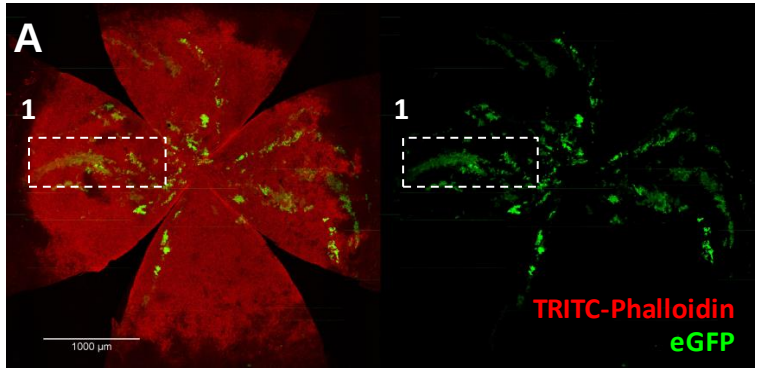

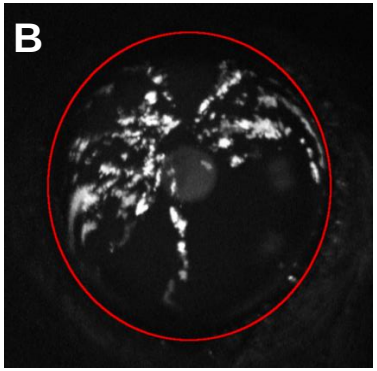

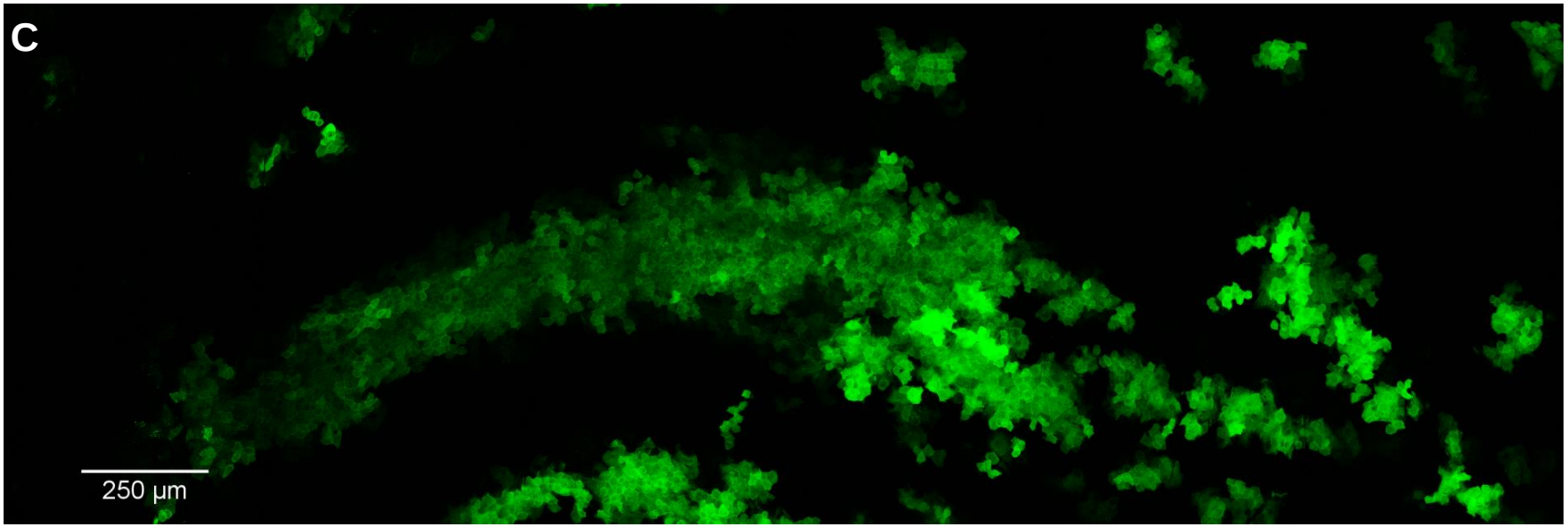

Figure 59. ***Corneal flatmount showing vector mediated eGFP expression 52 weeks after limbal subepithelial injection of LNT-SFFV-eGFP***

A: SLO image of the eye taken shortly before animal was culled and tissue fixed, streak shown in **B** and **C** is highlighted.
B: Confocal z-projection of area 1 in **A** of green channel only showing all eGFP transduced cells in the area. Taken at 40x magnification.
C: Orthographic projection of confocal z-stack taken at position 1 in A at 40x magnification. Two XZ planes are shown taken at different depths in z axis. The second one (orange gridlines) shows under lying stromal transduction.
In A: White = vector mediated eGFP
In C: Red = TRITC-Phalloidin, Blue = DAPI
In B & C: White arrow heads highlight transduced non-epithelial cells, Green = vector mediated eGFP

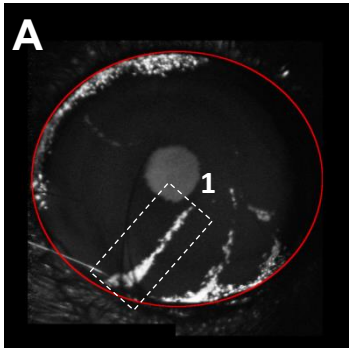

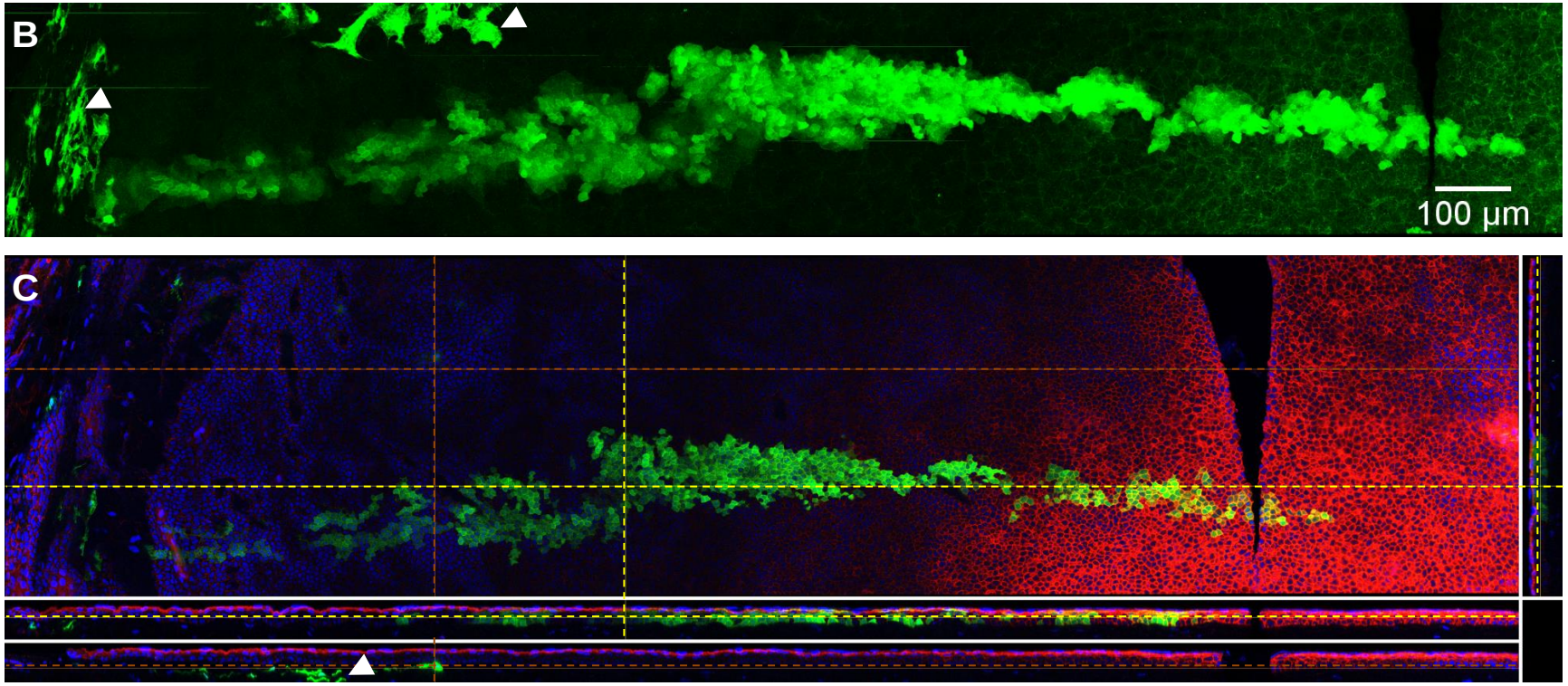

Figure 60. Corneal flatmount showing vector mediated eGFP expression 52 weeks after limbal subepithelial injection of LNT-SFFV-eGFP

A: SLO image of the same eye taken shortly before animal was culled and tissue fixed. Area shown in C and D is highlighted

B: Overview of the whole flat mount with a single area highlighted. Confocal z-projection taken at 10x magnification. Red arrowheads / dashed areas highlight areas of severe tissue damage due to attempts a 2 photon microscopy *in vivo.*

C: Confocal z-projection of area 1 in A & B of green channel only showing all eGFP transduced cells in the area. Taken at 40x magnification.

D: Orthographic projection of confocal z-stack taken at position 1 in **A** at 40x magnification.

In A: White = vector mediated eGFP
In B, C &D: Green = vector mediated eGFP
In C & D, White arrowheads highlight transduced non-epithelial cells.
In B & D: Red = TRITC-Phalloidin, Blue = DAPI

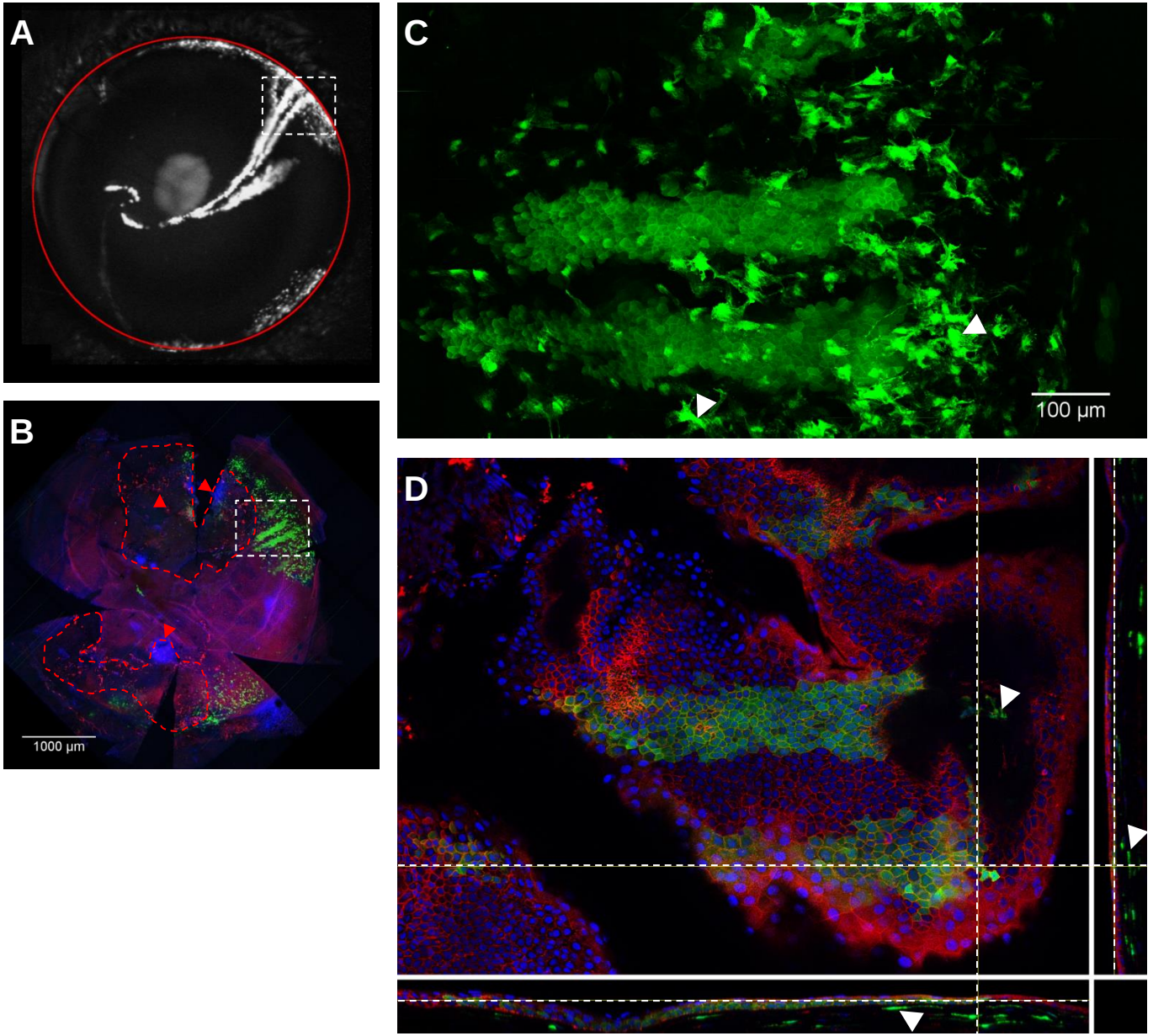

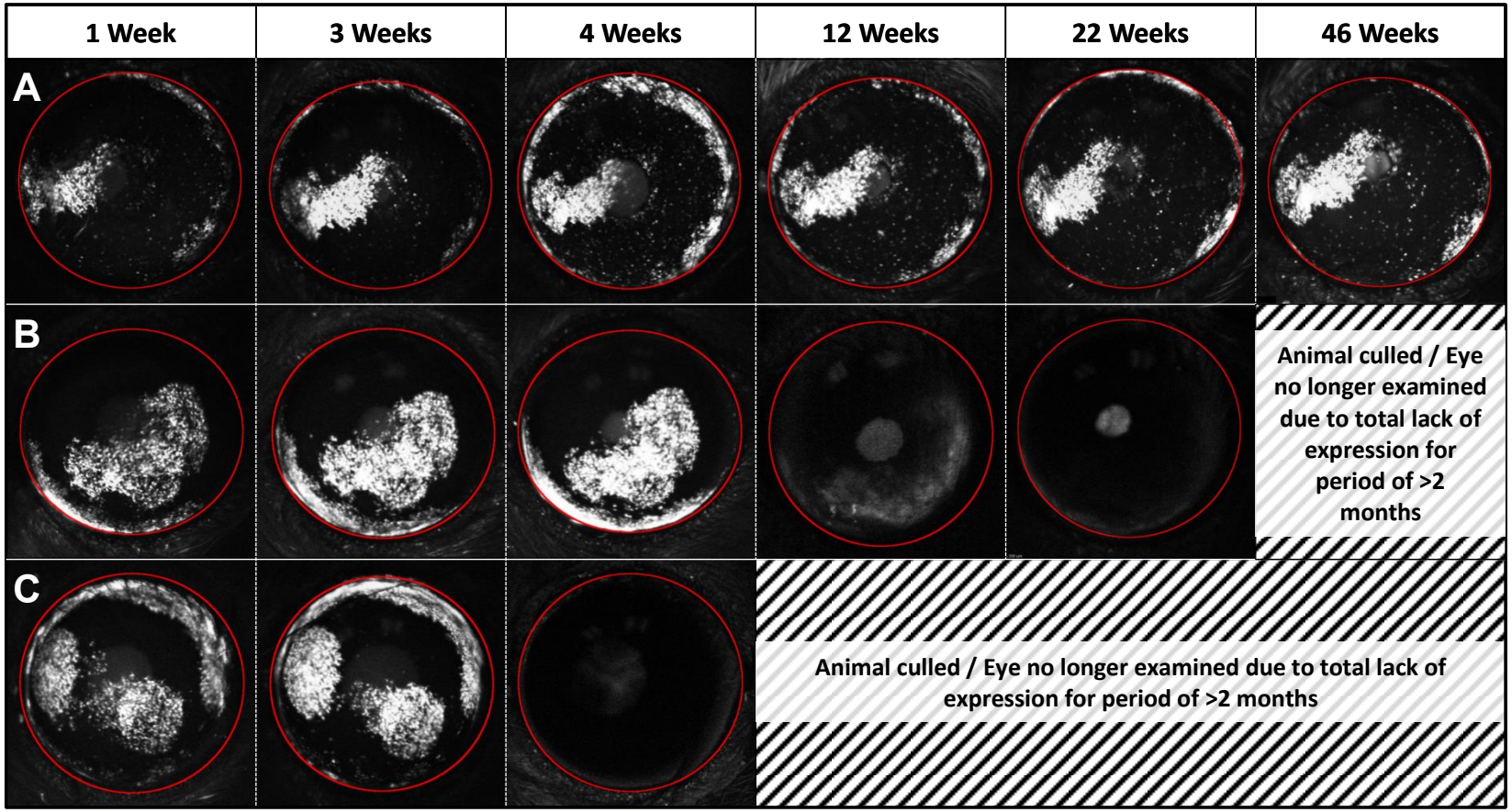

Figure 61. SLO images showing variability in longevity of expression of vector mediated eGFP in stromal cells transduced as a side effect of limbal-subepithelial injection of LNT-SFFV-eGFP

A-C: Three eyes showing variability in longevity of expression of vector mediated eGFP transduction of stromal cells
In All: White = Vector mediated eGFP. Red ring delimits the globe of the eye.

6.3 Discussion

6.3.1 Transduction of epithelial cells for application in gene therapy

The work presented in this chapter primarily aimed to provide proof of concept for pan epithelial gene delivery via transduction of the limbal epithelial stem cells (LESC) with an integrating lenti vector in the adult mouse.

The first and most substantial challenge to be overcome in the development of a technique to transduce limbal epithelial stem cells *in vivo* was the delivery of the lentiviral gene therapy vector to the putative site where the cells reside. This site whilst extending the whole circumference of the cornea at the corneal scleral junction is tightly localised in the anterior / posterior axis consisting of a small number of cells in the basal layer of the limbal epithelium.

It is also relatively well protected from external access from both anterior and posterior approaches being overlaid by multiple layers of epithelia and the anterior conjunctiva and underlaid by the rest of the corneal thickness. In particular the two acellular posterior layers of Bowman's layer and Decesmet's membrane are likely to act as significant barriers to surgical / needle access.

An anterior approach was therefore selected as being both technically less challenging and presenting fewer barriers to LESC niche access. Initial preparation work for these experiments mainly performed by our collaborator Dr Satoshi Kawasaki of the Kyoto prefectural university of medicine (and thus not presented here), attempted to gain vector access to the LESC niche via approaches such as epithelial debridement or direct incisions into the limbus followed by topical application of vector. All such approaches were unsuccessful resulting in, at best, a very limited, short-lived transduction of the epithelium.

Direct injection of vector into the LESC niche was therefore selected as the only viable approach. The usual device used within the lab for such delivery of vector to various ocular compartments (in particular the subretinal space) is a 10µL Hamilton syringe with attached 34G microneedle. This device is inappropriate for LESC niche injection as it is far too large. The needle has an outer diameter of approximately 200 µm whilst the entire murine epithelial thickness at the limbus is only around 25 µm (Henriksson et al., 2009), with the epithelial niche being only a small sub division of this,1-2 cells thick at most.

The only appropriate device for such injections was a glass micropipette of a type commonly used for electrophysiology or intracellular injections. Such pipettes can be produced with extremely fine tip diameters with submicron tips being achievable. However in order to inject fluid through such a small aperture very high application pressures are required. Additionally

lentiviral vectors are relative large at ~120nm diameter and our production method does not result in especially pure vector relying as it does on ultracentrifugation. A very small tip therefore whilst providing the potential benefit of highly specific injection site positioning would also be extremely prone to clogging. At the time these experiments were undertaken specialised stereotactic equipment was not available and thus the needle tip was to be guided manually. Specificity of injection site would therefore be chiefly dependent upon surgical skill of the operator with reproducible submicron accuracy likely being beyond what is achievable by this method.

For these reasons a tip diameter of 5-10 µm was selected as an appropriate compromise between size relative to target site, accuracy of tip positioning and free fluid flow for injection. Initially the needles pulled were relatively long (6-7 mm), with a relatively slow taper to the tip.

Two different target areas were selected, both to be approached from the anterior direction and are illustrated in Figure 41. Limbal-intraepithelial aimed to directly target the LESC niche itself. Limbal-intrastromal aimed to inject into the very anterior stroma just beneath Bowman's layer in the area of the LESC niche. This second approach was selected as it was slightly easier to assess needle depth during injection as penetration of Bowman's layer into the stroma results in a resistance that can be felt and assessed by the operator. It was hoped that both the needle tract and the relative thinness of Bowman's layer in the mouse would still allow vector access to the more anteriorly located LESC niche.

The results from the first cohort of mice injected via the limbal-intraepithelial route were promising. Assessment by SLO of transgene (eGFP) expression over the first 6 weeks post injection showed that in 5 of the 12 eyes (41.6%) injected convincing streak like patterns typical of LESC or early transient amplifying cell (eTAC) transduction were visible and a further 3 eyes (14.3%) displayed more limited streak like patterns. In one especially promising case several confluent streaks appear to cover roughly a 5^{th} of the entire corneal surface.

The limbal-intrastromal route was far less promising; SLO imaging showed that transgene expression was entirely limited to the extreme periphery of the cornea, possibly in more posterior, non-corneal tissues.

When histology was performed at 1 week post injection to supplement these observations *in vivo* it was demonstrated that limbal intraepithelial injection had indeed transduced epithelial cells in both the basal and superficial layers. The number of cells observed was relatively limited but this was as expected given that only the less promising examples were chosen

for histological analysis in order to preserve the more promising examples for further follow-up *in vivo*.

Histology also confirmed that limbal-intrastromal injection had resulting in a much more limited epithelial transduction, with only a very few cells being observed. It was also showed that the majority of transduction had occurred in tissues more posterior to the cornea such as the conjunctiva and trabecular meshwork, with transgene expression extending round tissues of the entire posterior globe. This possibly indicated that targeting the limbal intrastromal area had in fact directed vector into Tenon's capsule, or subconjunctivally.

Based on these initial results the limbal intrastromal route was abandoned and a second cohort was injected intraepithelially. The needle design was modified for this cohort; tip diameter was kept within the 5-10 µm range but the needle was made shorter with a faster taper to the tip. It was felt that this might result in more accurate tip positioning as the shorter length would reduce any amplification of operator movements.

This proved not to be the case; SLO results from cohort 2 were far less promising that those obtained in cohort 1. In the first 7 weeks post injection only 7 of the 42 (16.6%) of the eyes injected showed any evidence of streak formation. A large number of eyes (52.4%) however displayed a static punctate transgene expression pattern which histology at 4 weeks post injection showed was due to off-target transduction of stromal cells.

The stromal transduction pattern was often visible across an extremely wide area of the cornea, including in the central cornea where vector / injection was not intentionally directed. Whilst stromal cells do migrate in response to injury this movement is usually very limited and localised to the site of injury itself and thus it is unlikely that central stromal transgene expression can be explained in terms of migration of transduced cells. Such stromal transduction therefore indicates that Bowman’s layer has been frequently accidently penetrated and that this has either occurred unknowingly in the central cornea or that vector has been able to spread through the stroma itself from limbal to central cornea.

The frequent accidental penetration of Bowman’s layer is unlikely to be due to any increased penetrative pressure. Such an increase in pressure would have to result either from increased force originating from the operator or a decrease in tip diameter and both of these factors were kept as constant as possible between cohorts 1 and 2. Likewise it is unlikely that it is a result of any ballistic effect of vector expulsion from the needle as the two factors which might affect particle injection velocity; tip diameter and injection pressure were also kept constant.

The frequent penetration into the stroma observed in cohort 2 is potentially due to a difference in rigidity / flexibility between the two needle morphologies. The longer slow taper

needle used in cohort 1 was far more flexible than the shorter fast taper design used in cohort 2 and thus could be subjected to a certain amount of bending force without breaking. It is possible therefore that upon encountering Bowman's layer at the shallow angle of injection used the slow taper needles were able to bend in response to the increased resistance essentially being deflected by the stroma and ensuring the tip remained in the epithelium. By contrast the much more rigid fast taper needles could not be deflected and penetrated into the stroma.

The fast taper morphology was therefore abandoned and a third cohort was injected using the slow taper morphology by the intraepithelial route in duplication of the method used in cohort 1. This was to ascertain if LESC/eTAC transduction level could be improved upon and confirm that slow taper needle morphology reduced off-target stromal transduction.

Initial results indeed confirmed that much less of the stromal transduction pattern was visible; however in regards to assessment epithelial transduction results in cohort 3 were initially disappointing. Up until 10 weeks post injection only 10 out of 38 eyes (26.3%) showed any streak like morphology and the majority of these were not especially convincing. Figure 58 shows histological imaging of one of the more promising examples at 10 weeks post injection. The widespread transgene expression seen is localised entirely to the epithelia, however few of the streak like patterns observed are continuous and connect to the limbus, the only example to fulfil both criteria is shown in detail in Figure 58C. This is in contrast to the most convincing streaks observed by SLO in both cohorts 1 and 2 in which appear both continuous and continually connected to the limbus. Upon longer follow up however cohort 3 proved to be the most successful cohort injected; by 22 weeks post injection 20 of the 38 eyes injected (52.6%) displayed some evidence of streak-like morphology

The next question to be addressed was whether LESCs have truly been transduced. Both LESC and eTACs are resident at the target site of injection and if transduced both would be expected to produce a streak like transgene expression pattern as daughter cells migrate centripetally. It was expected that the only difference by which LESC and eTAC transduction might be distinguished is duration of expression. LESC's do not migrate centripetally and are capable of self-renewal, thus streaks derived from LESC transduction might be expected to be essentially permanent (there is some evidence that individual LESC lineages are lost with age, although this is a slow process [89]) and that the streaks would always remain connected to the limbus.

In contrast an eTAC transduction should result in a streak that becomes disconnected from the limbus as the originally transduced cells move centripetally. The entire eTAC derived

streak would also be expected to eventually extinguish as the whole lineage is lost to epithelial turn over.

The exact timeframe over which transgene expression patterns should be monitored in order to observe this difference was not entirely clear. Based upon direct measurements of rate of centripetal cell movement in the mouse [86,326] estimates of between ~8-13 weeks can be made for cells to traverse the distance from limbus to central cornea. Other studies based upon the observations of streak progression labelled from birth by transgenic means have given both comparable (~10 weeks from Hayashi et al. [90]) or much shorter (3-4 weeks from Collinson et al. [87]) estimates for this process to occur.

The process of loss is also likely to be stochastic. Whilst the majority of the epithelium may have turned over within a particular timeframe it would likely take longer for an entire eTAC lineage to become completely extinct. This was shown by Kinoshita et al. [328] who concluded that in the case of replacement of donor epithelium by that of the host in corneal transplants the loss of donor cells was “time-dependent, but not necessarily linear”.

It was decided therefore that firstly the follow-up period would have to be at least as long as the maximum estimate for epithelial turnover in the literature (13 weeks). This should be perhaps doubled (26 weeks) to allow for near complete eTAC lineage extinction and that a period of 1 year (52 weeks) post injection would be sufficient to prove beyond any reasonable doubt that any remaining streaks must be derived from LESC transduction.

The use of immunohistochemistry to show co-localisation of eGFP with stem cell markers was also considered. Given however that there is no one definitive marker of LESC’s that can distinguish between the LESC and an eTAC derived the asymmetric division of a LESC, and that even the validity of marker combinations is hotly debated, it was decided that duration of expression would form a far more definitive indicator of LESC transduction.

Of the 92 eyes injected in total over all three cohorts 38 (41.3%) were followed up for the full 52 week period. Most of those eyes not followed up for the whole period were discontinued when no streak-like patterns of any kind being observed at 2 consecutive time points (spanning a period of 8 weeks).

Of those 38, 25 displayed convincing streaks present at the final time point, the best examples of which are shown in Figure 51. In these examples between 8 and 25% of the corneal surface was covered by transduced epithelium as assessed by comparison of white pixels with black within the eye field of the images. This is likely an underestimate as flat / en face images do not account for the curvature of the cornea.

It can be concluded beyond reasonable doubt therefore that the transduction of a significant number of LESC's by a lentiviral vector in the adult mouse *in vivo* has been achieved, and that gene delivery by such a vector results in transgene expression within the whole clone / lineage of the LESC transduced. Additionally the data generated here is far more convincing than the only previous report within the literature [324] that has claimed such transduction, which only followed up for 6 weeks, did not make it clear where within the epithelium transduced cells were located and showed no evidence of centripetal migration. In this study we observed a large number of eyes in which epithelial transduction lasted for 6 weeks (or longer) but was not sustained beyond ~12-14 weeks indicating that that a 6 week follow up is too short a time period to prove LESC transduction.

The technique however still has substantial room for improvement. Even in the best example the ultimate goal of 100% epithelial coverage has not been achieved. The results are also highly variable, with some eyes displaying widespread LESC transduction patterns, others displaying none, and most displaying evidence of more limited LESC transduction.

Much of this improvement could potentially be made by standardisation of the injection technique itself, mainly to remove the current high level of variability due to operator dependence. Accurate positioning of needle depth in the anterior posterior axis formed the greatest challenge for the operator and this could be more finely controlled through the use of stereotactic equipment of a type commonly used for injection into precisely targeted areas of the brain. Unlike the brain however the eye cannot be secured firmly immobile by skull fixation as it is supported more loosely within the orbit by connective and muscular tissue. Nonetheless the more precise needle control enabled by stereotactic equipment would no doubt be advantageous to the procedure.

In these experiments injection was mediated by application of air pressure to the needle preloaded with vector solution. Pressure was produce by manual compression of a 50mL syringe to ~5 mL marker, resulting in approximately 10 Atm of pressure which resulted in a steady slow flow of vector solution. This variable too could be easily standardised by the use of a mechanical compressor with a more finely controllable output air pressure.

In order to maximise LESC transduction injections were placed around the entire circumference of the limbus. This was achieved by holding the injection device in a relatively fixed position and rotating the whole animal. This was for reasons of operator comfort and restricted space although as an approach it is likely sub optimal. A better methodology might be to fix the eye as immobile as possible and rotate the needle at a fixed angle around a pivot point located directly above the centre of the eye.

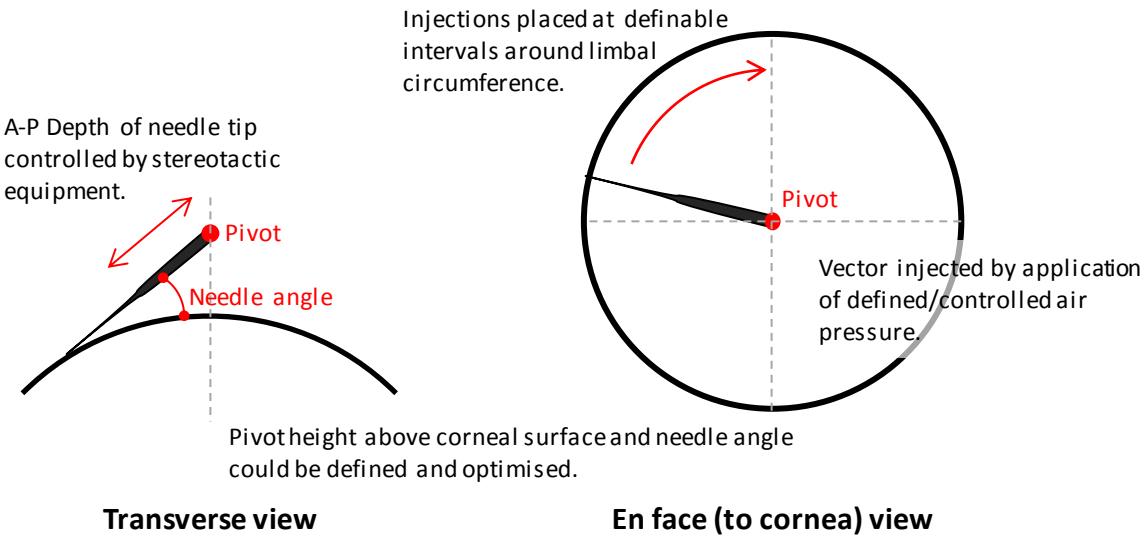

Figure 62. Schematic design of proposed device to standardise intra epithelial injections to target the LESC niche

This would allow for injection into a consistent location in the transverse axis of the cornea. An outline design of a specialised instrument to perform the injections is shown in Figure 62 above.

During the injection procedure it was also noted that the needle was prone to clogging. This is likely a function of both the application pressure and purity of the vector solution itself. As stated earlier our lenti vectors are concentrated from clarified tissue culture medium by ultracentrifugation and are therefore not likely to be of a high purity. It is likely that the use of a more highly purified vector would both ameliorate this issue and also result in greater standardisation of the procedure.

Finally the mouse eye is small and the LESC niche is not coincident with any macroscopically observable anatomical feature. The human eye by contrast is much larger, the epithelium is thicker at the limbus and the LESC niche has been associated with the Palisades of Vogt and other structures which are more easily observable [64,329]. It is likely therefore that direct injections into the LESC niche may prove less challenging in a human cornea. It is even conceivable as imaging technology improves techniques such as optical coherence topography (OCT) [330] or confocal microscopy [64] might be utilised in real time at the point of injection to guide the needle to the LESC niche.

6.3.2 Corneal epithelial cellular dynamics in normal homeostasis

Whilst it was not the primary aim of this work, the ability to transduce LESCs with a clonally inherited label, such as that demonstrated here using Lenti-eGFP also has the potential to provide insight into the cellular dynamics of corneal epithelial homeostasis. More specifically this technique is capable of selectively labelling a small subset of LESC's and their progeny allowing them to be studied in isolation from the rest of the tissue.

This is in contrast to almost all previously published studies involving the direct labelling of LESC and their progeny with detectable markers which have utilised either transgenic approaches [86,87,90], or more non-specific viral labelling during embryogenesis [331]. Both of these approaches result in the labelling of a large proportion of LESC's with the label being expressed from birth (or earlier) onwards. Whilst extremely useful in elucidating overall patterns within corneal epithelial homeostasis such techniques do not allow the processes involved to be easily followed on a cell by cell basis, and are unable to clearly distinguish between individual clonal lineages. Additionally these approaches are limited in their ability to assess any cell movement over time due to both very large numbers of adjacent cells being labelled and there being no point in the adult animal where expression of the marker can be "switched on" as such markers are expressed from birth.

The single comparable technique found within the literature is a study by Buck in 1983 [326] in which India ink was directly injected into epithelial cells in order to demonstrate and measure centripetal migration speed. This experiment however was very short term, did not label LESCs and the marker used would be diluted out by cell division.

The work presented here was not designed to take best advantage of the technique in this regard. The experiment was designed for long term follow-up rather than the high temporal resolution that might be required to accurately follow cell migration etc. over time. Despite this however some insights can nonetheless be drawn from the data.

Firstly it was noted that streaks fell broadly into two categories:

Type 1: Those that were highly consistent in appearance over time, being strong, continuous and always connected to the limbus. Example shown in Figure 53.

Type 2: Those that appeared more variable over time in terms of length, continuity and attachment to the limbus. Example shown in Figure 54.

These two different streak patterns could be explained in terms of number of LESCs transduced in a particular area at the point of injection.

In the case of type 1 streaks the vast majority of LESCs in that particular area may have been transduced and thus even if all the LESCs is the area are dividing asynchronously every daughter cell that is produced in that area will carry the eGFP label resulting a firm uninterrupted patch of transgene expression at the limbus. Subsequent centripetal migration is thought not to be the result of any active migratory process (in the non-wounded context) but rather a function of the increased proliferative capacity of more peripheral TACs, and cells being pushed more centrally over time as a result [52]. Thus in the situation described for type 1 streaks both all the new cells produced immediately peripheral to the initial TACs and all the daughter cells of the TACs themselves will be labelled. Thus over time a continuous unbroken streak from the limbus should be produced regardless of any asynchronicity or otherwise in cell division.

In contrast type 2 streaks might result from the transduction of a more limited number of LESCs in a particular area. Thus if all the LESCs in a particular area divide over time and only a smaller number are transduced, the area immediately peripheral to this section of the LESC niche would become populated by both transduced and untransduced TACs. As these themselves divide and are pushed inwards by a largely random process, discontinuity of labelled cells might easily result. Additionally there may be long periods were all the transduced LESCs are simultaneously non-dividing, in which case all the fresh TACs (and their daughter cells) produced in that area during this period will be unlabelled and a disconnection of the streak from the limbus would result.

Taking this idea further; if hypothetically a very small number, or single LESC in a particular area was transduced it might be expected that as LESC are by definition slow cycling that no distinct streak would ever be produced, only occasional disconnected patches of cells, surrounded by the progeny of the more numerous untransduced LESCs.

To confirm this hypothesis regarding the generation of type 1 or type 2 streaks being dependent upon initial number of LESC transduced the number itself would have to be directly assessed, work in the next chapter will focus upon possible methods by which this might be achieved. Alternatively a mathematical model of the process could be produced using LESC transduction efficiency as the primary input variable.

Another feature that was noted was that the majority of streaks became more distinct over time in a process that was termed “firming up”. This was especially notable in cohort 3, which was initially felt to have been poorly transduced due to the relative lack of streaks seen in the first 10 weeks post injection. Over time however the discontinuous patchy epithelial transduction that was initially evident was replaced with firm streaks located at

approximately the same locations around the limbal circumference. Examples are shown in Figure 55.

This observation could be explained in terms of the slow cycle time of LESCs. At the point of injection both the LESCs and TACs in a particular area of the limbal circumference may have been transduced. Over the first ten weeks the TACs would be expected to undergo multiple rounds of division separated by as much as 60 hours [81] whilst migrating centripetally, which might result in a patchy pattern moving centrally such as that observed. The LESCs however might undergo no division during this time. There are few precise estimates of *in vivo* LESC cycle time under unwounded conditions to be found in the literature, although they are commonly defined as being able to retain label for up to 6 weeks indicating minimal division over this timescale. It is conceivable therefore that firming up of a streak like pattern is only able to occur once the transduced LESCs have undergone division and produced the potential for an unbroken streak to be formed. This observation would indicate that the cycle time of LESC *in vivo* can be as long as 10-12 weeks.

There were also rare examples of the process of firming up largely failing with very few streaks resulting from a much more widespread patchy transduction (example shown in Figure 56). This could be a result of the majority of transduction being limited to TACs, with LESC transduction not being achieved as widely.

The initial patchy patterns observed before firming up are reminiscent of those observed in work involving transgenic models showing that it takes up to 12 weeks after birth for streak-like patterns to become fully established [87,90,331]. It is hypothesised for the first 2 weeks of life an alternative source of stems cells may be located throughout the basal layer of the epithelium rather than being confined only to the limbus and these are generate and regenerate the layer during late embryonic development and shortly after birth [90].

The patterns observed here are not be confused with this process. Whilst some animals in this study were younger than 12 weeks old upon injection all those in cohort 3 (in which the patterns were most widely seen) were older than this at the time of injection and all examples shown in the relevant figures are taken from animals older than 12 weeks at point of injection.

A particularly interesting example of streak formation is shown in Figure 57. For the first 12 weeks post injection there is no evidence at all of a streak in the 9 o'clock position of the eye. By 18 weeks post injection a relatively strong streak is present in that location (red arrowheads) extending from limbus to central cornea, which is then maintained for the remainder of full 52 week period. The LESCs responsible for generating this streak must

have been infected at or very shortly after the point of injection as lentiviral vectors are known to be highly labile at 25-37°C; losing all infectivity in less than 24 hours [332]. The transduced LESCs therefore must have remained entirely non-dividing for at least 12 weeks post injection, providing more evidence of a ~12 week cycle time for LESCs *in vivo*.

The streak that is formed between 12 and 18 weeks is a type 1 streak, appearing strong and consistent until the end of the experiment at 52 weeks. At several time points it also appears to have multiple points of origin in the limbus. Both of these factors argue for it being derived from a large group of LESCs. The fact that no streak at all is seen for 12 weeks and within 6 weeks a type 1 streak with multiple points of origin has fully developed would imply a degree of cell cycle synchronicity between the LESCs in this specific area of the LESC niche.

Additionally within the same eye there is also a type 2 streak (blue arrowheads) that develops in a parallel manner over the same timeframe, but which is located in a different area of the cornea its origin being localised in the ~5 o'clock position. This combined with the fact that the process of "firming up" discussed earlier also often appeared to occur in all streaks simultaneously might argue for synchronicity of cell division across the entire LESC niche.

All the discussion presented here has thus far been framed in the context of a non-wounded cornea, with observations assumed to be representative of normal homeostasis rather than the increased proliferative / migration rate shown to be typical of epithelial wound healing [47,81]. This assumption was made as no deliberate wound except the insult of injection was ever inflicted upon any of the corneas and injection damage should have been mild and resolved quickly. However it is possible that the process of imaging (generally conducted once a month) may have been damaging due to slight drying of the cornea and application of high intensity laser light. Additionally it is important to remember that the experiment involved living animals housed together and that occasional incidence of epithelial wounding might be expected under such conditions.

The distinctions between cell behaviour in the wounded and unwounded states is especially important to bear in mind when discussing the centripetal migration speed of epithelial cells as large variation could potentially result from relatively minor wounds.

In the case of the type 1 streak shown in Figure 57 the 42 day period between the 12 and 18 week observations was also sufficient for epithelial cells to migrate centripetally across the entire radius of the cornea, establishing a low resolution estimation of the time taken for this process which is roughly in the middle of range presented by the literature (3-13 weeks). Imaging over a higher temporal resolution would be required to provide more accurate and definitive data on centripetal migration speed.

Across the whole dataset it was also observed that not all of the individual streak-like patterns that developed remained visible for the full 52 week experimental period. Loss of a type 1 streak was rare although easier to define than the loss of type 2 streaks which are by definition variable in appearance over time. A weakening of streak intensity over time was also sometimes observed. This perhaps provides some confirmation of observations made by Mort et al. [89] in an X-inactivated LacZ expressing model which indicated reduction of LESC clone number with age. However in this study the possibility that transduced cells have lost transgene expression via epigenetic silencing of the integrated provirus SFFV promoter cannot be excluded. Such silencing has been shown to occur in stem cell lineages in particular [333].

Finally, and unrelated to the epithelium, a variability in the accidental off target transduction of stromal cells was also noted and is shown in Figure 61. In some cases the stromal transduction patterns appeared essentially permanent remaining unchanged over the entire 52 weeks of the experiment. In other cases the stromal expression was lost. Loss when observed did not occur at any fixed time point post injection and was always rapid. It is likely that loss is due to sudden triggering of the stromal wound healing response or possibly an immune mediate effect although the cause for either is unknown.

6.3.3 Conclusions

- Widespread / long duration expression of transgene in the corneal epithelium has been achieved via the transduction of limbal epithelial stem cells with lentivirus in the adult mouse *in vivo.*
- Transgene expression mediated in the LESCs is inherited by their centripetally migrating daughter cells resulting in transgene expression extending the whole corneal radius.
- A slow taper, flexible glass micropipette / needle morphology proved to be the most suitable to deliver vector directly to the LESC niche, with more rigid shorter needles resulting in off-target stromal transduction.
- This technique also shows significant promise as a tool for the study of the cellular dynamics of corneal epithelial homeostasis.
- LESCs appear to have a cell cycle time *in vivo* of around 10-12 weeks

- LESCs may synchronise their divisions *in vivo* either locally or possibly throughout the whole LESC niche.
- Centripetal migration of epithelial cells from limbal to central cornea can take a maximum of 6 weeks (42 days).

7. Techniques to develop lentivirus mediated LESC transduction for the study of epithelial cellular dynamics

7.1 Introduction

Work in the previous chapter was focused upon the development of a technique to mediate gene transfer to the entire corneal epithelium via *in vivo* transduction of the cells responsible for regenerating the layer, the limbal epithelial stem cells (LESC). The intended application of this methodology was in the gene therapy for genetic conditions of the epithelium, in particular gelatinous drop like dystrophy (GDLD) as discussed later in 8.1.3. It was also noted however that the technique could be of great utility in the study of the cellular dynamics of the homeostasis within the corneal epithelium.

Improved data regarding factors such as the centripetal migration speed of epithelial cells could be generated by simply applying the technique as already developed at a higher temporal resolution; however this would provide little insight into questions relating to interactions between distinct clonal lineages. The data presented in the previous chapter has raised a number of such questions such as:

- Do the various streak-like patterns observed correlate with the number of LESCs initially transduced? i.e. do stronger more consistent streaks result from the transduction of a larger number of LESCs?
- Is the division of LESCs synchronised either locally or across the entire niche?
- Are TACs really limited to a maximum of three divisions as has previously been proposed [81]?

The use of a single fluorescent label allows division of clonal lineages into two types; labelled and unlabelled, only one of which can be visualised and is thus of limited application to such questions. Work by Weber et al. [334,335] however describes a multi-colour technique by which a large number of LESC clones might be distinguished. The system is based upon co-infection of target cells with three different lentiviral vectors each encoding a different fluorescent protein. At an optimal multiplicity of infection each cell will receive by chance a different dosage of red, green and blue fluorescent transgenes which when expressed in combination will result in the generation of a large number of unique colours by

the additive colour model. Due to the integration of lentivirus within the genome the colour signature of an individual cell should be inherited in a clonal fashion.

Such a system could be easily adapted to the lentivirus mediated transduction of the limbal epithelial stem cells demonstrated in the previous chapter, labelling each LESC clone with a unique colour which could be tracked to provide detailed information regarding the composition of the streak-like patterns resulting from centripetal migration of epithelial cells.

Due to the semi-random integration of lentivirus each integration will occur at a near unique site within the host genome. Integration site analysis therefore provides another means by which LESC clones might be distinguished, however, can only be performed upon tissue extracts and thus cannot be directly correlated with transduction patterns observed *in vivo,* nonetheless such analysis would provide useful data and to be successfully applied a pure isolate of epithelial DNA is required.

7.1.1 Aims

Work in this chapter aims to develop techniques that might be applied to future work characterising the cellular dynamics of corneal epithelial homeostasis, in particular means to distinguish individual LESC clones from each other, *in vivo, ex vivo* or *in vitro* will be developed.

More specifically the Lenti Go (LeGO) vector system will be adapted for application to LESCs, and a means of isolating transduced epithelial tissue from the rest of the cornea to obtain a purely epithelial DNA sample for integration site analysis will be developed.

7.2 Methods and results

7.2.1 *In vitro* development of LeGO vectors for clonally specific cell labelling

The microscope filter setup suggested by Weber et al. in their paper [334] originally describing the RGB Lenti Go (LeGO) labelling technique is unfortunately incompatible with any fluorescent microscope available for this work. Therefore in order to ensure that the three fluorophores used by this technique are clearly distinguishable from one another when combined in our hands a modified setup was designed and evaluated using LeGO viruses *in vitro*.

Figure 63 shows the proposed filter set up for use on a Leica DM5500 confocal microscope, designed to follow as closely as possible the specifications suggested by Weber et al. [334].

The three lentiviral transgene constructs used by Weber et al. to produce LeGO viruses are commercially available (Addgene) and were used to make the three lentiviruses in our own production methodology (2.2.4) and were established to have the following infectious titres:

LeGO-Venus 4.95×10^8 vg / mL

LeGO-mCherry 2.0×10^8 vg / mL

LeGO-Cerulean 2.2×10^8 vg / mL

In order to approximately titre match the following dilutions were made in Opti-MEM

2 µL of LeGO-Venus in 500 µL Opti-MEM, = ~2.0×10^6 vg / mL

5 µL of LeGO-mCherry in 500 µL Opti-MEM, = ~2.0×10^6 vg / mL

5 µL of LeGO-Cerulean in 500 µL Opti-MEM, = ~2.0×10^6 vg / mL

To test the setup 293T cells were seeded at ~50% confluency on an 8 well chamber slide (PAA / GE Healthcare). Immediately after cells had been seeded, before they had fully attached to the growth surface the 3 wells were infected as follows:

Well 1 – 50 µL, LeGO-Venus virus dilution (~10^5 vgs)

Well 2 – 50 µL, LeGO-mCherry virus dilution (~10^5 vgs)

Well 3 – 50 µL, LeGO-Cerulean virus dilution (~10^5 vgs)

A mixture of the viruses was then made by combining 100 µL of each of the three virus dilutions and a 3 fold dilution series made of this mixture (diluent, OptiMEM, Gibco).

Three wells were then infected as follows:

Well 4 – 150 µL, Neat virus mixture (~10^5 vgs of each virus)

Well 5 – 150 µL, 1:3 dilution of virus mixture (~3.3 x 10^4 vgs of each virus)

Well 6 – 150 µL, 1:9 dilution of virus mixture (~1.1 x 10^4 vgs of each virus)

All wells were left for 24 hours for expression to develop before the cells were fixed in 4% PFA and imaged by confocal microscopy.

Figure 64A-D shows the wells 1-3 imaged using the microscope channels proposed in Figure 63. The Venus and Cerulean channels appear specific, only detecting the fluorophores they are designed to pick up. The mCherry channel however also seems to detect the emission of Venus as shown in Figure 64C. The mCherry channel's emission detection range was therefore modified from 580-640nm to 600-650nm and the 532 laser power was reduced from 20% to 15%. After this change had been made Venus bleed into the mCherry channel was much reduced and all the channels essentially specific only for the fluorophore they were designed to detect as shown in Figure 64E-H.

Figure 65A-D shows the wells 4-6 imaged the microscope channels proposed in Figure 63.

Figure 65E-H shows the wells 4-6 imaged using the modified mCherry channel discovered to lead to better fluorophore discrimination in Figure 64.

The greatest variety of distinct colours resulting from the co-infection appears to have occurred in the 1:3 dilution imaged using the channel set known to allow Venus emission to bleed into the mCherry channel, Figure 65C.

Henceforth this channel setting will be referred to as LeGO settings 1

The channel settings that minimises Venus bleed into the mCherry channel will be referred to as LeGO settings 2

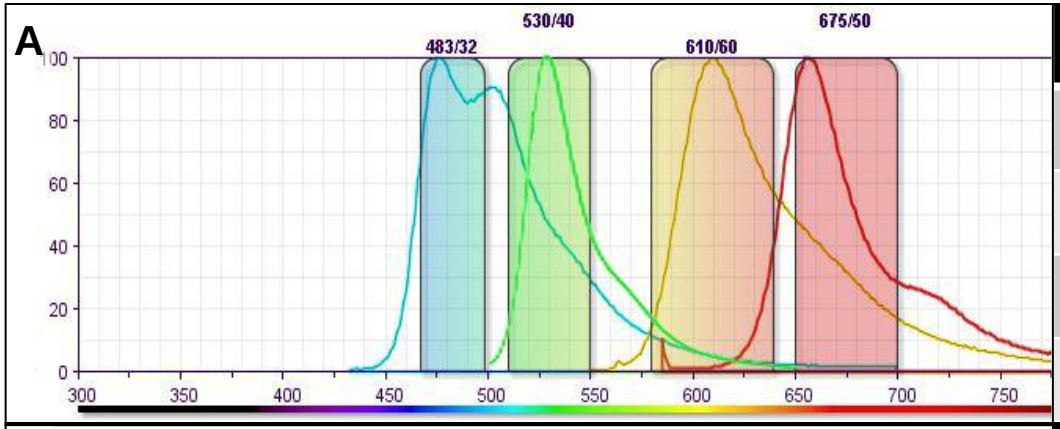

Fluorophore	Bandpass selected to detect Emission (nm)
Cerulean	483/32 (467-499)
Venus	530/40 (510-550)
mCherry	610/60 (580-640)
To-Pro-3	675/50 (650-700)

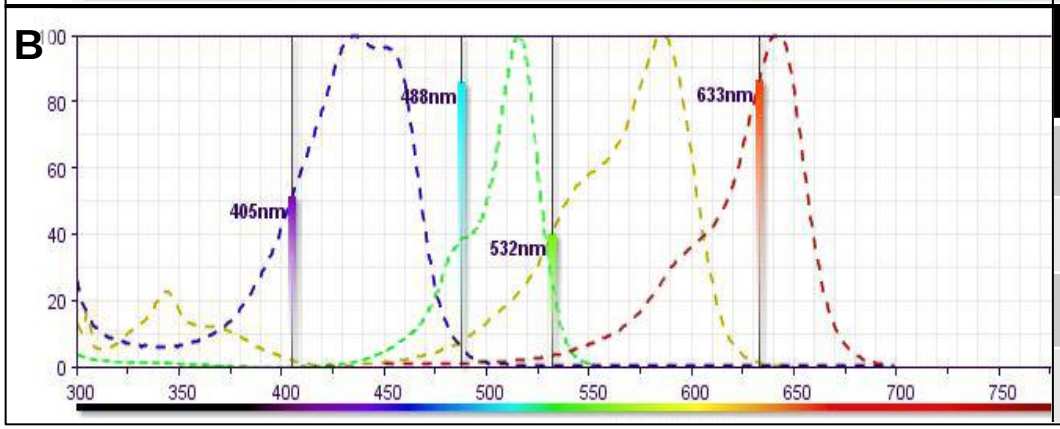

Fluorophore	Most appropriate Laser Available	Estimated Efficiency of Excitation
Cerulean	405 nm	51%
Venus	488 nm	40%
mCherry	532 nm	40%
To-Pro-3	633 nm	86%

Figure 63. ***Schematic of proposed set up for Leica DM5500 to image cells transduced with the 3 colour LeGO System***

A: Emission spectra of the three fluorophores used in the LeGO system and the nuclear stain To-Pro3. Filter settings proposed to optimally detect emission.

B: Excitation spectra of the three fluorophores used in the LeGO system and the nuclear stain To-Pro3. Most appropriate lasers to excite the dyes and estimates efficiency of excitation.

Spectra and images modified from BD Fluorescent Spectra Viewer. Found here:
http://www.bdbiosciences.com/research/multicolor/spectrum_viewer/index.jsp

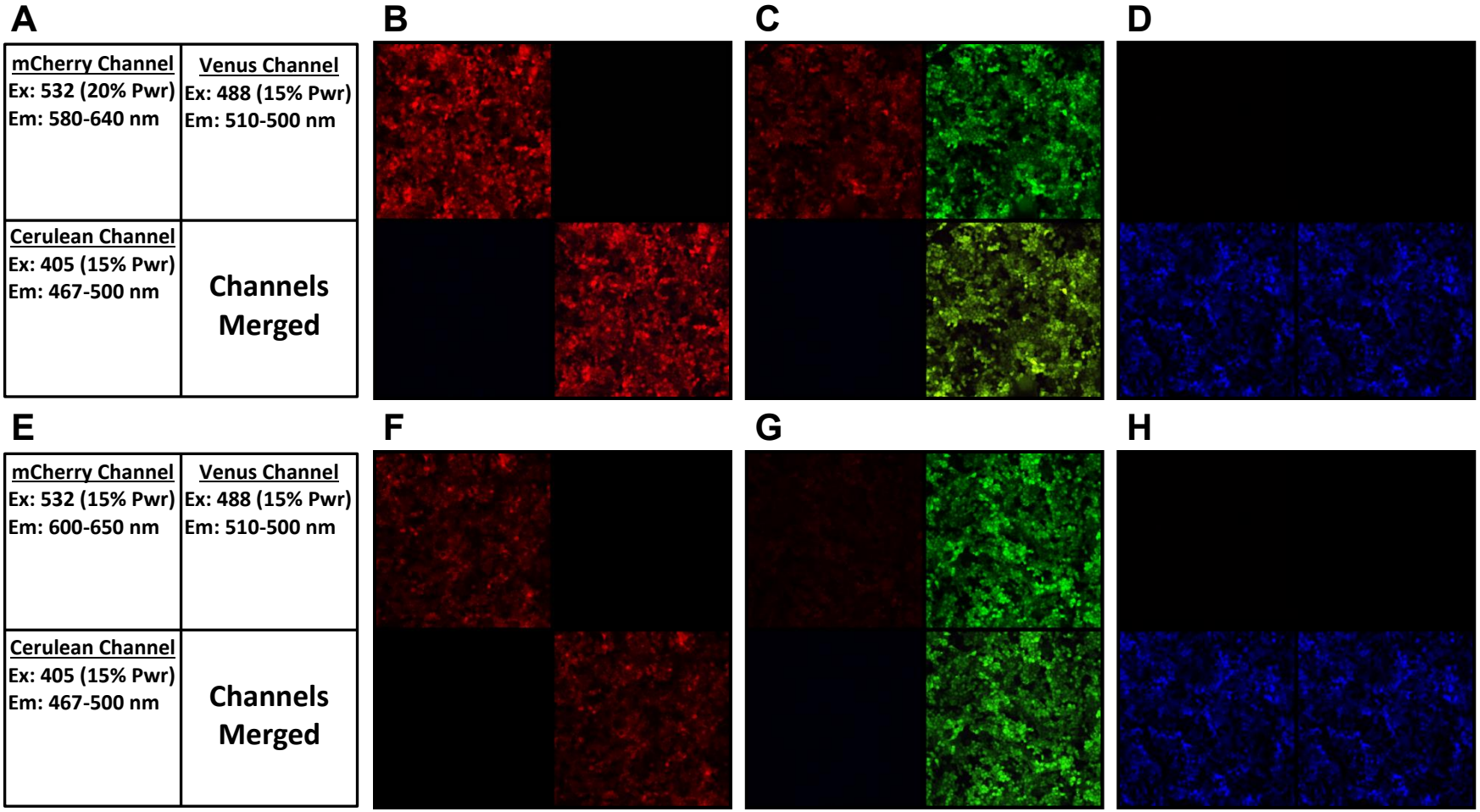

Figure 64. ***Channel specificity test of microscope setup in Figure 63 using LeGO viruses on 293T cells*** **in vitro**

A: Schematic showing the imaging settings used in each quadrant of panels **B-D**.

B-D: 293T cells infected with LeGO virus encoding mCherry (**B**), Venus (**C**) and Cerulean (**D**) respectively imaged using the 3 channel settings shown in **A**. Fixed and imaged 24 hrs post infection.

E: Schematic showing the imaging settings used in each quadrant of panels **F-H**, modified from A due to channel cross talk seen in **C**.

F-H: 293T cells infected with LeGO virus encoding mCherry (**F**), Venus (**G**) and Cerulean (**H**) respectively imaged using the 3 channel settings shown in **E.** Fixed and imaged 24 hrs post infection.

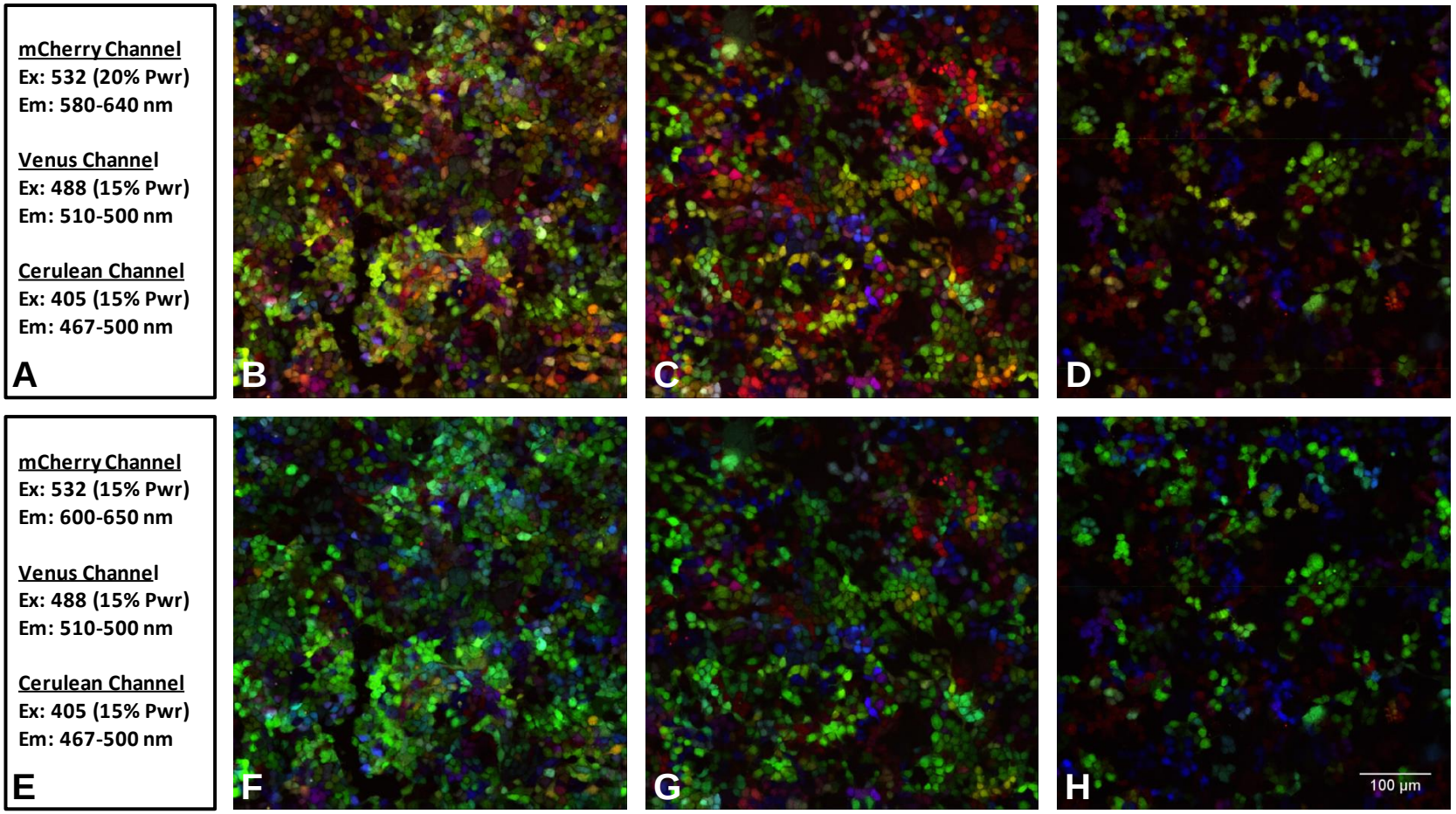

Figure 65. ***LeGO co-infection test on 293T cells*** **in vitro** ***using LeGO lentiviruses at various dilutions and two imaging settings (described in Figure 64)***

A: Imaging settings used in B-D, known to allow some Venus emission to bleed into mCherry Channel (Figure 64).

B-D: 293T cells co-infected with all 3 LeGO viruses at the following dilutions respectively Neat, 1:3 and 1:9. Fixed and imaged 24 hrs post co-infection.

E: Imaging settings used in **F-H.**

F-H: 293T cells co-infected with all 3 LeGO viruses at the following dilutions respectively Neat, 1:3 and 1:9. Fixed and imaged 24 hrs post co-infection.

7.2.2 Confirmation that labelling mediated by LeGO vectors is clonally specific *in vitro*

Having established that a large number of unique colours can be generated by the LeGO labelling system the next step was to confirm that these colours are indeed inherited by daughter cells upon cell division thus labelling all cells within a clone.

Observations in the previous experiment were indicative of clonal specificity, with adjacent cells often appearing the same colour. However the cells were relatively near confluency upon infection with only 1-2 cell divisions likely to have occurred over the time frame observed and thus any infected clones would be too small to draw any firm conclusions.

Cells were therefore seeded at a much lower density to allow more extensive clonal growth to be observed. Initial experiments were complicated by HEK293T cells decreased viability and growth at low densities, HeLa cells were therefore utilised instead which proved to be more tolerant of low density culture, although these too exhibited reduced viability.

HeLa cells were initially grown within a density range of 20 – 90% confluent, as is usual for standard culture of this cell type. During this period they were infected with the LeGO vectors. Infection was performed under standard culture conditions rather than after low density seeding to minimise any additional stress on cells during periods of low density.

Infection was carried out as follows:

A single well of a 6-well plate (9.5 cm^2) of 60-70% confluent HeLa cells were infected with:

10µL	LeGO-mCherry	- 3.96 x 10^5 vgs	~4.00 x 10^5 vgs
4µL	LeGO-Venus	- 4.00 x 10^5 vgs	
10µL	LeGO-Cerulean	- 3.40 x 10^5 vgs	

Post infection cells were left for ~16 hours, by which time they were near 100% confluency

Cells were then passaged as normal, and once trypsinised cells were counted using a haemocytometer and a proportion were reseeded at low density.

Two approaches to low density seeding were taken;

1) LeGO infected cells alone were seeded in 8 well chamber slides (surface area per well: 0.88 cm^2) at densities of
    a. ~1000 cells / well (1136 cells / cm^2)
    b. ~200 cells / well (227 cells / cm^2)
2) LeGO infected cells were seeded in combination with uninfected cells, in order to maintain a reasonable overall cell density to promote cell viability whilst infected cell

density remains low. Both infected and uninfected cells were seeded into 1 well chamber slides (surface area of well: 10.84cm^2). Seeding densities were:

a. Uninfected: ~100,000 cells / well (9225 cells / cm^2)
b. LeGO Infected: ~2500 cells /well (230 cells / cm^2)

Infected cells that were seeded alone were imaged using the an inverted microscope (Zeiss) at 10x magnification ~7 hours post seeding in order to observe initial seeding density directly. Cells were then left for 7 days to expand before being fixed in 4% PFA and imaged by confocal microscopy using LeGO settings 1.

Figure 66 shows the results of the imaging. At both seeding densities areas are visible in which a large number of adjacent cells all share the same colour label which is highly indicative of the label being clonally specific.

There are also areas in which cells containing two different colour labels appear to have become mixed, likely due to clones expanding into one another or two or more cells having been seeded in close proximity. As would be expected such areas of mixing are more evident in the denser seeding condition.

Infected and uninfected cells seeded together grew more rapidly and were fixed and imaged after 5 days, by which time they were approaching confluency. After fixation these cells were labelled with the nuclear marker To-Pro3. This allowed all cells (infected and uninfected) to be visualised. As To-Pro 3 fluoresces in the far red (Ex/Em: 642／661 nm) it can be used without bleed through into the LeGO channels (Figure 63).

Figure 67 shows the results of the imaging. The presence of multiple patches of infected cells in which all adjacent cells share the same colour label is highly indicative of the label being clonally specific. In Figure 67C at least 7 distinct colours can be easily distinguished by eye. The white asterisk indicates a cell cluster in which the green channel is over exposed masking colour differentiation, although perhaps two colours can be distinguished within this cluster. The Pink asterisk in Figure 67C & D indicated a labelled cluster in which the cells appear to be either dying or hyperproliferating as shown by high density To-Pro3 staining

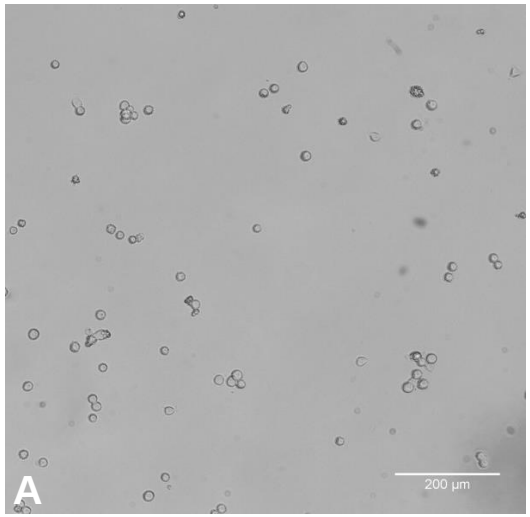

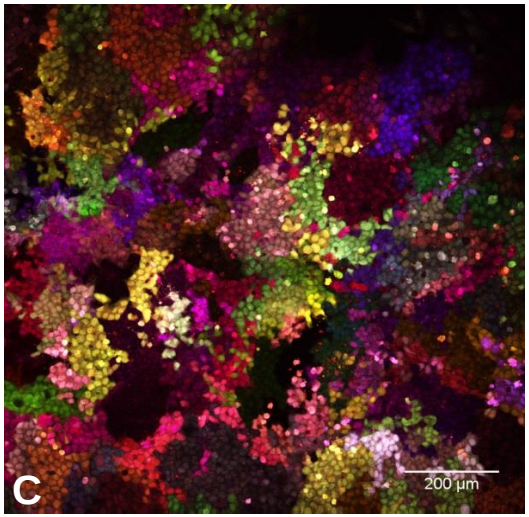

Figure 66. ***LeGO infected HeLa cells seeded alone at two low densities to demonstrate clonal specificity of labelling***

A: Cells imaged ~7 hours post seeding at 1000 cells /well, 10x magnification to illustrate seeding density.

B: Cells imaged ~7 hours post seeding at 200 cells /well, 10x magnification to illustrate seeding density.

C: Cells fixed and imaged by confocal microscopy 7 days after seeding at 1000 cells / well. Imaged using LeGO settings 1

D: Cells fixed and imaged by confocal microscopy 7 days after seeding at 200 cells / well. Imaged using LeGO settings 1

D': Digitally modified version of image shown in D in which levels have been modified as follows to enhance brightness:

Red: 0-255 → 0-100

Green: 0-255 → 0-150

Blue: 0-255 → 0-100

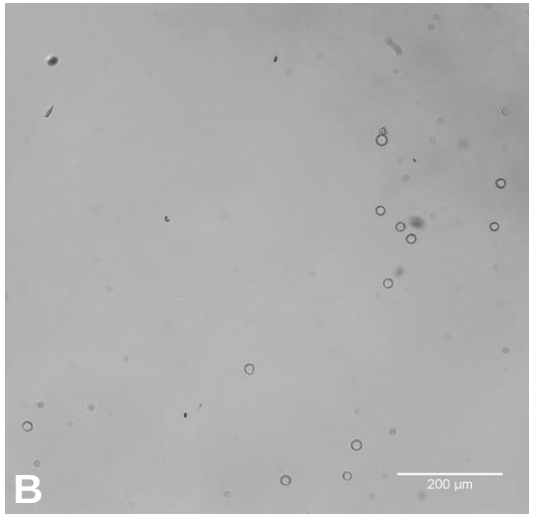

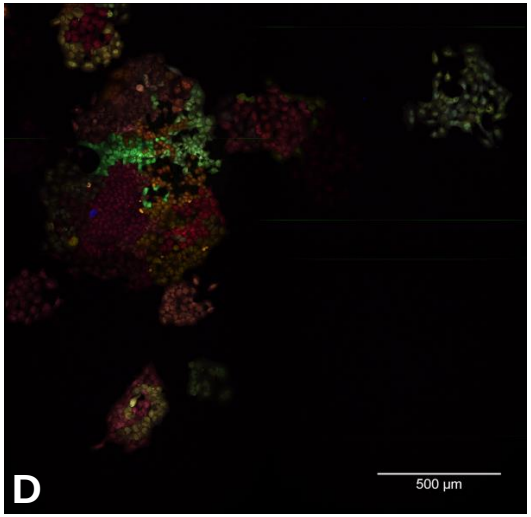

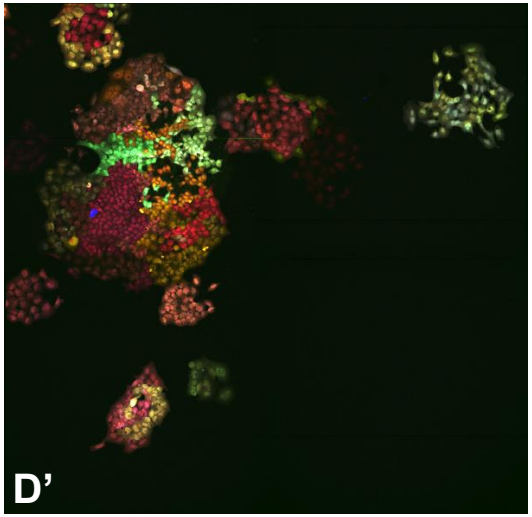

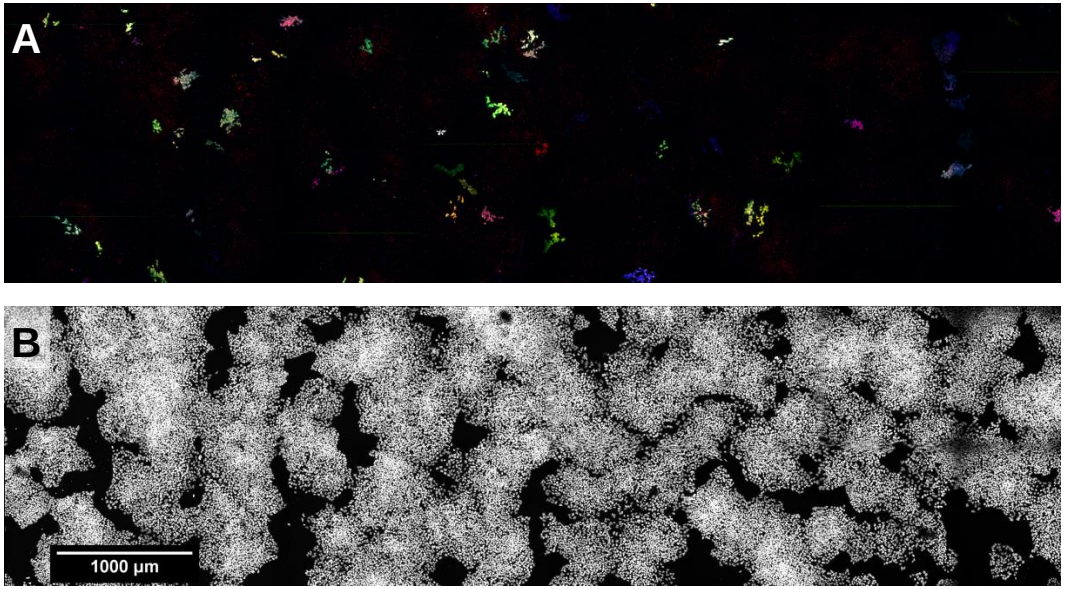

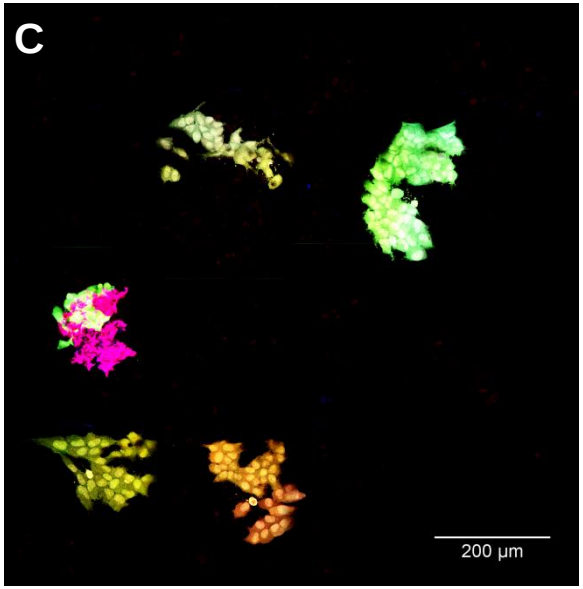

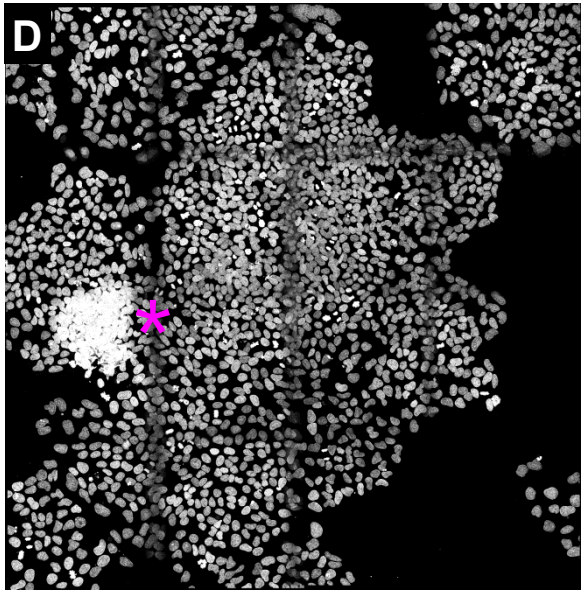

Figure 67. ***LeGO infected HeLa cells seeded at low density in combination with uninfected cells to demonstrate clonal specificity of labelling***

A: LeGO vector mediated expression in infected cells. Cells fixed and imaged by confocal microscopy 5 days after seeding at 2,500 infected + 100,000 uninfected cells / well. Imaged using LeGO settings 1 at 10x magnification, confocal z-projection.

B: To-Pro3 nuclear staining of all cells present in **A**. Imaged at 10x magnification, confocal z-projection.

C: Higher magnification image of the condition shown in **A.** Exact area imaged in **C** is not visible in **A**. Imaged using LeGO settings 1 at 40x magnification, confocal z-projection. White asterisk highlights cells in which the green channel is over exposed.

D: Higher magnification image of the condition shown in **B.** Exact area imaged in **D** is not visible in **B**. Imaged using LeGO settings 1 at 40x magnification, confocal z-projection. **C&D:** Pink asterisk highlights cells in which may be dying or hyperproliferative.

7.2.3 Development and validation of protocol to isolate murine epithelial sheet for the purposes of further molecular analysis

In order to undertake molecular analysis of lentivirus transduced epithelium it would be advantageous to isolate only the tissue of interest (corneal epithelium) from all surrounding tissues to minimise the chances of any factors derived from other tissues contaminating the sample.

The protocol developed here was based upon various published protocols [336–340] all based upon incubation with Dispase II.

The majority of such work has been done in either human or rabbit tissue with only Kobayashi et al. [340] having described the technique in mice. Mice have a relatively thin Bowman's layer compared to other mammals (including rabbits) [341] and therefore it was not known whether the murine epithelium would display sufficient structural integrity for intact isolation.

The technique developed is described below:

Mice were terminated and the eyes enucleated. The eye was then placed in a small dish containing Keratinocyte-SFM supplemented with 1x Antibiotic / Antimycotic, 30ug/mL Bovine Pituitary Extract (BPE) and 0.2ng/mL Epithelial Growth factor (EGF) (All Gibco). Dissection was performed with the eye submerged in this media using corneal notched forceps (Acrofine) and Vannas Capsulotomy Scissors (Albert Waeschle).

The cornea was dissected away from the rest of the globe with an orbital cut just posterior to the limbus. Any non-corneal tissue that came away attached to the cornea was carefully removed. Once isolated the cornea was placed in a single well of a 48 well plate containing 400µL dispase solution formulated as follows:

100µL - Stock dispase solution: Powder (Sigma) dissolved in supplemented K-SFM to a final concentration of 13.3 Units / mL

296uL - Supplemented Keratinocyte-SFM

4µL - 30mM $CaCl_2$ in dH_2O.

Cornea was then incubated in the dispase solution at 4°C overnight. Following dispase incubation the cornea was returned to a small dish containing supplemented Keratinocyte-SFM for further dissection. Using two pairs of Dumont #5 forceps it proved possible to grasp and peel a sheet of epithelium away from the remainder of the cornea. Non-epithelial tissue was then usually discarded.

Figure 68 shows a series of images illustrating this dissection.

The isolated epithelial sheet can then be further dissected, fixed and stained or stored for short periods of time in supplemented K-SFM for further processing.

Figure 69 shows an isolated sheet of murine epithelium flatmounted Bowman's layer down. The sheet is remarkably intact. Viewed under the microscope it is almost indistinguishable from corneal epithelium seen upon a whole cornea flat mount. Both basal and more superficial cells can be seen Figure 69B & B'. No cells of the stroma were observed at all indicating the isolation from more posterior tissues of the cornea was complete.

Further dissociation was attempted with the aim of obtaining a single cell suspension of the epithelium. The isolated epithelial sheets proved **highly** resistant any form of further dissociation, reagents tried included:

Trypsin-EDTA (0.05%) up to 2 hours at 37°C

TrypLE Express (1x) up to 2 hours at 37°C

Papain (20 units / mL) up to 1 hour at 37°C

Collagenase D (0.1 mg / mL) up to 1 hour at 37°C

Even when combined with mechanical sheer forces (repeated aspiration with a P200 pipette) none of the above resulted in a homogeneous single cell suspension. All suspensions that resulted contained large clumps of non-dissociated cells and also often displayed a high level of cell death.

It was therefore decided that any analysis should be performed upon the intact sheets.

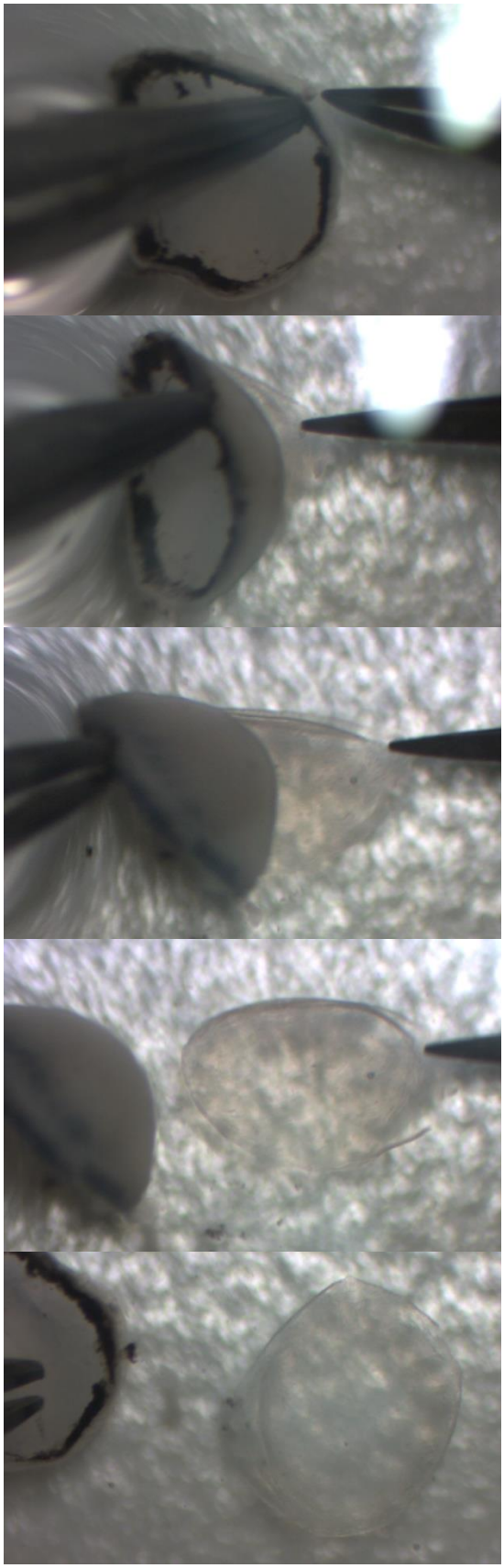

Figure 68. ***Image sequence showing surgical removal of the epithelial layer from an isolated murine cornea*** **ex vivo** ***post overnight incubation in Dispase II***

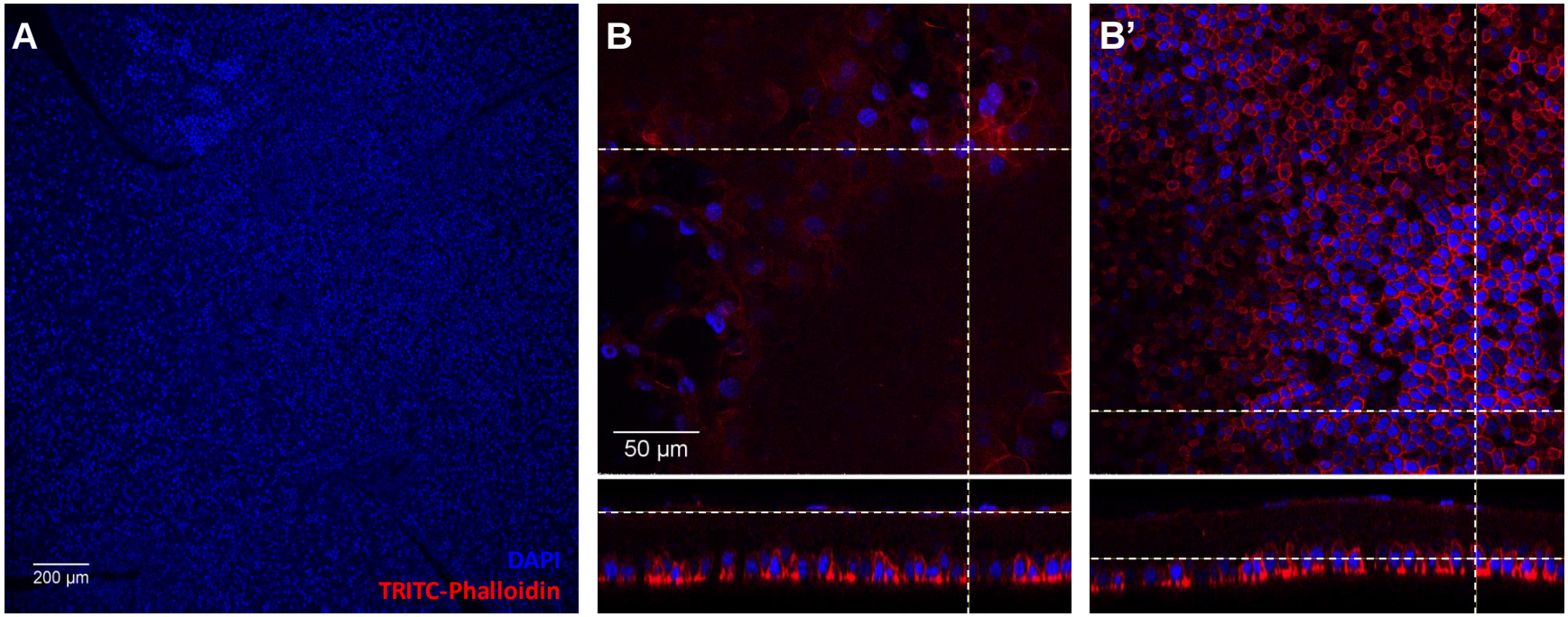

Figure 69. ***Flatmount of isolated sheet of murine corneal epithelium obtained from incubation of whole cornea* ex vivo *in dispase II, mounted Bowman's layer down***

A: Image taken at 10x magnification showing DAPI staining of ~60% of the entire sheet

B & B': Orthographic projections of confocal z-stack taken at 40x magnification. Only XY (single plane) and XZ shown.

In All: Blue = DAPI, Red = TRITC-Phalloidin

7.3 Discussion

This chapter describes some initial pilot experiments focused upon development of techniques by which transduced limbal epithelial stem cell (LESC) clones might be distinguished from one another following labelling by intraepithelial injection of lenti vector encoding a fluorescent transgene product.

An extremely promising and elegant method by which this might be achieved is the RGB Lenti-go (LeGO) system described by Weber et al. [334]. This system is claimed to enable the lentiviral labelling virus of cells with a unique, clonally inherited colour signature. In theory such a system should be readily adaptable to our purpose of *in vivo* labelling of LESCs and their clones.

The first question to be addressed in translating this system to the lab was to determine whether the commercially available LeGO lentiviral constructs would be efficiently packaged to produce vector of acceptable titre within our lenti production methodology. These constructs themselves are very similar in genomic structure to those used as a matter of routine within the lab however the 3rd generation production system used by Weber et al. is slightly different; providing the HIV1 genes required for vector production *in trans* via two plasmids rather than one. Fortunately this difference proved inconsequential and vectors of high titre (10^8 vg / mL range) were produced.

The exact microscopy / filter block set up recommended by Weber et al. for the imaging of labelled cells was unfortunately incompatible with the capabilities of any instrument within the lab and could not be implemented without incurring substantial expense. However the confocal instrument (Leica DM5500) available is highly adaptable / tuneable in terms of the emission spectra that it can detect and is equipped with laser excitation sources suitable to excite each of the 3 fluorophores used with in the LeGO system. In addition a 4th excitation wavelength in the far red (633nm) is available that could be used to combine a nuclear marker with the technique. A channel setup for LeGO imaging was therefore designed for this instrument intended to be as comparable as possible to that described by Weber et al. and include the possibility to add in a 4th far red channel for the nuclear stain To-Pro-3. The channel setup is shown in Figure 63

Upon initial testing of this setup to detect expression from individual LeGO vectors *in vitro* it was found that fluorescent signal from the fluorophore Venus was detectable in the mCherry channel in addition to its own. This was initially deemed to be sub optimal and was corrected by red shifting the mCherry detection range by 20nm and narrowing it slightly. The laser

power used to excite this channel was also reduced by 5%. The resulting modified set up reduced the bleed through signal from Venus into the mCherry channel although at the cost of reducing the detected expression from mCherry itself. To a degree this could be compensated for by increasing the electronic gain but this often comes with the disadvantage of decreasing the signal to noise ratio.

When tested in the context of HEK293T cells infected *in vitro* with the LeGO viruses in combination it was initially disappointing that the channels optimised for minimal signal bleed through resulted in images in which only a limited range of colours was apparent. Green was by far the strongest hue, dominating all the others (Figure 65F-H). By contrast the channel setup that allowed Venus→mCherry bleed through resulted in an image in which far more distinct colours can be seen (Figure 65B-D). The green dominance of the images produced by the more discriminating settings is a function of the reduced red signal intensity produced as an unavoidable side effect of reducing channel bleed through. This can be proven by digital manipulation of the images produced. By stretching the range of red pixel intensity so that 130 is taken as the maximum rather than 255 (using the levels function of GIMP) the image taken with the settings that minimise bleed through can be made apparently identical to the image taken with the settings that allowed the Venus→mCherry bleed through as seen in Figure 70 below (A vs C).

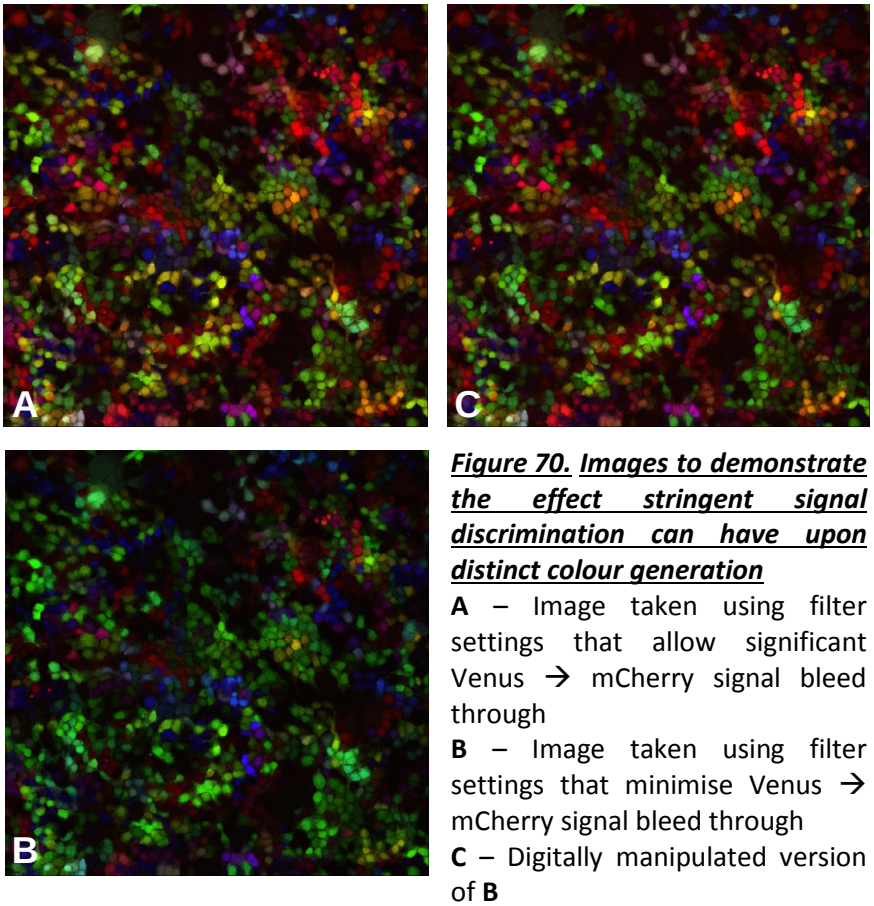

Figure 70. ***Images to demonstrate the effect stringent signal discrimination can have upon distinct colour generation***

A – Image taken using filter settings that allow significant Venus → mCherry signal bleed through

B – Image taken using filter settings that minimise Venus → mCherry signal bleed through

C – Digitally manipulated version of **B**

The images however are not equivalent. The digitally manipulated image (Figure 70C) is less data dense than the one resulting from channel bleed through (Figure 70A), this is due to the fact that the red correction process applied essentially discards almost half of the data that could potentially have been collected for this channel; stretching the other half over the whole intensity range. For further application therefore it would be preferable to use the channel setup that allows bleed through as this allows the full range of intensity data from all three channels to be used to generate the image and the distinct colours.

Whilst 100% channel separation is vital for many applications (for example studies of co-localisation) it is not of particular importance to this technique. For clonal tracking to be effective the generation of a large number of clearly distinct colours is preferable to complete channel separation. Limited spill over of signal between the channels whilst incongruous should be completely consistent as it is a function of the emission spectra of the dyes themselves which are invariable. Limited spill over is therefore irrelevant to primary goal in this case and in fact may actually act to enhance the generation of clearly distinct colours.

The molecular biology of the RGB LeGO system should ensure that that the specific colour signature a cell gains upon infection should be inherited by all daughter cells upon division and thus will be present in all cells of the resulting clone. However as this is the most critical point relevant to useful application of the technique it was decided that clonal specificity of labelling should be confirmed experimentally.

The pattern of colours produced from the infection of 293T cells in the initial experiments presented here (Figure 65) provide some evidence of this; with similarly coloured cells often being observed in close proximity to one another. However the context in which these *in vitro* experiments were conducted only allowed the cells in question to undergo a maximum of ~3 divisions before the experiment was ended or confluency was reached; insufficient to conclude clonal specificity with any certainty. Ideally an experiment should be undertaken where by the expansion of a number of clones is directly observed and all cells and cell divisions that formed each clone visually tracked. These observations could then be correlated to cell colour once the clones had been fixed and imaged.

This experiment proved to be more challenging than initially anticipated due to a number of complicating factors. Firstly HEK293T cells were found to be unsuitable for use in any such an experiment. When plated at sufficiently low density for clonal colony formation these cells displayed an extremely low viability; even when plated at higher density that allowed some cell-cell contact HEK293Ts still exhibited a much reduced rate of cell division producing inconclusive data. HeLa cells were therefore used instead which proved more tolerant of low density growth conditions.

Time lapse microscopy to directly monitor the expansion of clones and track all cells / cell divisions by direct observation was attempted however the instrument used (JuLi microscope, Bulldog Bio) proved unable to perform the task. The images produced were of insufficient resolution or phase contrast to accurately track cell divisions and the instrument had difficulty maintaining fine focus over the entire time-lapse period.

Two surrogate approaches were therefore adopted in which LeGO infected HeLa cells were plated at low plating densities to allow isolated colony formation and expansion in the absence of time-lapse imaging. The cells were either plated alone (2 different densities) or co-plated with a higher density of uninfected cells in order to improve cell viability / growth characteristics whilst maintaining a low effective density of infected cells.

The infected cell densities upon seeding in these experiments where selected to ensure cells were spaced out sufficiently for mixing of clones to be limited. The cells were assessed by microscopy post seeding to confirm such adequate spacing. In the images produced by these experiments (Figure 66 & Figure 67) it can be clearly seen that there are large areas of adjacent cells sharing the same colour label which is highly indicative of the label being clonally specific as claimed. The proposed experiments upon LESCs *in vivo* however will likely be conducted over the far longer term, it should therefore be determined if colours remain constant and colony specific over a timescale of months. This could be attempted by multiple follow ups over time of a single labelled clone *in vitro*. Such a culture could be established by seeding <96 infected cells across 96 well plate.

The LeGO system provides a potentially elegant means by which the LESC clones and streak composition might be tracked although its application *in vivo* will require a fresh round of epithelial injections using all three the LeGO vectors in combination, and MOI will have to be reoptimised to the *in vivo* condition; these injections are planned to be carried out in the near future. Unfortunately the SLO instrument used to follow eGFP transgene expression *in vivo* in Chapter 6 is only able to visualise fluorescence in the green and infrared wavelengths. An alternative instrument would therefore be required to follow all three LeGO fluorophores *in vivo* and the lab has recently acquired a two photon microscope that might be suitable although this instrument is not yet fully optimised for use *in vivo*.

The LeGO system also cannot be applied retrospectively to animals that have already been injected with lenti-eGFP and for which long term follow up of streak formation has already be assessed (Chapter 6). For these animals an alternative means must be found to determine the number of LESC transduced and provide insight into the composition of the epithelial streaks observed.

One potential methodology that might be applied to these animals would be determination of the location and pattern of the sites at which the lenti genome has integrated within the host's. Integration of the lenti provirus into the genome is semi random. In actively dividing cells types (such as the corneal epithelium) integration shows preference towards genomic areas that are transcriptionally active [202], whereas in non-dividing cells the process appears more truly random [342]. The preference for transcriptionally active sites is likely due to the chromatin rearrangements associated with active transcription rendering these areas more accessible to the provirus.

Despite this preference however it remains highly unlikely that any two individual integration events will result in provirus integrating into precisely the same location within the host genome. Each cell infected with a lentivirus should therefore carry a unique signature of integration sites within its genome, which as they essentially form part of the host genome itself, will be inherited by all daughter cells.

These integration site signatures can be determined using the technique of linear amplification mediated PCR (LAM-PCR) as described by Schmidt et al. [343].

This technique involves the following steps:

Genomic DNA is extracted from the tissue of interest and linear amplification is performed using a biotinylated probe complimentary to the LTR sequence of the lentivirus. This results in the production of a single stranded DNA species for each integration site present labelled with the biotinylated probe on the 5' end and spanning the integration site from the LTR into the host genome. These DNA fragments are then extracted and purified by means of streptavidin coated magnetic beads.

Second strand synthesis is then performed upon the ssDNA fragments before they are digested with a frequently cutting restriction enzyme. The length of each individual fragment is essentially randomised by this process as it is unpredictable exactly where in the unknown host sequence the enzyme will cut. For each integration site a DNA species has now been generated that is of random length and bounded by the LTR primer sequence on one end and a known restriction enzyme cut on the other.

A DNA linker is then ligated to the cut end of these species which contains a known sequence to which a primer has been designed. PCR can then be performed to exponentially amplify every fragment, using primers binding the LTR and the linker, the two known sequences that now bound every fragment.

The resulting PCR products can either be sequenced to determine the exact sites of genomic integration present within the sample or analysed by gel electrophoresis to give a

fingerprint of all the integration sites combined. Generally speaking the number of bands / integration sites that make up this fingerprint should approximately correlate to the initial number of cells transduced. Cells containing multiple integration sites are of course a possibility and the frequency of this occurrence will scale with initial MOI. Such multiple integration events can be detected and controlled for to a degree by analysing relative band intensity. For example, a clone of a particular size containing 3 integration sites would result in three bands of equal intensity once intensity differences related to size have been corrected for. The technique has its limits however. Too many clones / integrations will result in too high a density of data to analyse and an increased probability of two distinct integration sites producing fragments of indistinguishable length.

As a first step in the application of LAM-PCR integration site analysis to our labelled tissue, the epithelium must be isolated from any other tissue which may have been transduced and would thus contaminate the analysis. The stroma is of particular concern as occasional off-target stromal transduction was not uncommon, especially in injected cohort 2. (Chapter 6)

There are multiple published techniques where by such epithelial isolation is achieved via incubation of corneal tissue with Dispase II, followed by a mechanical peel of Bowman's layer + epithelium away from the rest of the tissue. [336–340]

The published protocols however refer in the majority to rabbit tissue rather than mouse and aim to isolate dissociated cells for the establishment of a primary cell culture. For this endpoint the maintenance of cell viability across the entire tissue is desirable although not critical as such a culture can be established from a relatively small number of cells if need be. It was uncertain therefore if these protocols could be successfully adapted to our purpose. Mice have a thinner Bowman's layer than rabbit [341] possibly making mechanical isolation more challenging and additionally the maintenance of high overall tissue viability post digestion is critical or the loss of LESC clones from the analysis might occur.

The dissociation protocol was successfully adapted in such a way as to be suitable for our purpose. Dispase digestion was performed overnight at 4°C in an effort to slow and reduce the potential impact of the digestion on cell viability. Mechanical isolation proved to be relatively straight forward with Bowman's + epithelium always peeling away as a single intact sheet.

This sheet could then be further dissected if need be for example to isolate specific streaks, but this could be challenging due to the sheets extreme thinness and resulting difficulty in mechanical manipulation. Further development of dissection technique is required in this area. The integrity of the sheet immediately post isolation was remarkable. Upon fixation and

flat mounting the sheet (and the basal TAC layer in particular) was almost indistinguishable by microscopy from an epithelium still *in situ* upon a freshly isolated intact cornea. The cells showed no particular signs of ill health and the basal layer remained almost 100% intact. There may have been some loss of more superficial epithelial cells although confocal microscopy at 40x magnification showed that at least some are still present. This potential loss of superficial cells should not prove detrimental to our intended application as all LESC clones should be represented in the intact basal layer.

The isolated epithelial sheet did not however maintain viability in the longer term. Extended culture at 37°C / 5% CO_2 in the same base medium used for dissection and dispase incubation (supplemented K-SFM) for 24 hours resulted in near complete loss of viability. The medium in question is serum free perhaps indicating that serum might be required for more long term culture. Long term viability is not however required for the primary application as genomic extraction could be performed immediately post isolation.

Initially it was planned to further dissociate the isolated epithelial sheet into a single cell suspension that could potentially be processed through a fluorescent automated cell sorter (FACS) to further isolate and purify the labelled population. However this proved unfeasible. The isolated sheet was highly resistant to any further dissociation, enzymatic or mechanical and any degree of success in further dissociation was accompanied by widespread cell death as shown by trypan blue uptake. This further dissociation and purification however is not strictly necessary as genomic DNA extraction could easily be performed on the entire isolated tissue sheet, which has already been shown to be free of contaminating non-epithelial cells. Attempts at further dissociation were thus abandoned.

Taking this technique forward, enough experience has now been gained to begin application of the technique to the transduced samples for which 1 year follow up *in vivo* is available, and a collaboration is being discussed with Dr Manfred Schmidt whose group at the National Centre for Tumour Diseases (NCT) in Heidelberg have pioneered the technique of LAM-PCR for integration site analysis.

7.3.1 Conclusions

- The RGB Lenti-Go (LeGO) system described by Weber et al. [334] has been successfully developed within the lab *in vitro* and has been verified to mediate clonally specific labelling as claimed.
- A technique has been developed that allows isolation of corneal epithelial sheets from murine corneas whilst maintaining the integrity of the tissue and cell viability

8. Discussion

The work presented within this thesis has developed multiple viral gene therapy based approaches effectively targeting transgene delivery to each of the three cellular layers of the cornea resulting in high level and long lasting transgene expression via application of novel vector species and optimisation of vector administration. The target cells within these three layers are heterogeneous in nature and thus each presented a different set of challenges to be overcome in order to mediate an effective gene delivery.

Key findings are summarised below:

- The new AAV serotype AAV2/6(ShH10) was shown to be able to transduce both murine and human corneal endothelial cells with high efficiency. No other AAV serotype is known to mediate any substantial gene delivery to this cell type.
- The transduction profile of AAV2/8(Y733F) following intrastromal injection has been characterised and shown to initially mediate high level of transgene expression in both the epithelium and stoma. Epithelial transduction is short lived but a substantial stromal transgene expression is sustained for at least 5 months in both mouse and human tissue.
- Corneal transduction by intrastromal injection of AAV2/8(Y733F) was shown to be effective in an augmentation gene therapy approach to inhibit corneal haemangiogenesis *in vivo* via expression of *musFlt1*.
- A methodology was developed that is able to mediate substantial sustained gene transfer to the epithelium via limbal epithelial stem cell (LESC) transduction *in vivo*. Expression was maintained within this replicative tissue for at least 1 year.

The potential applications for these techniques are wide ranging:

8.1 Applications in gene therapy for correction of genetic disorders

The first and most obvious potential application of any gene therapy based approach is to the correction of genetically inherited disorders. The disorders to which gene therapy has been most widely applied to date are monogenic disorders with an autosomal recessive inheritance pattern. This is largely due to the fact that such disorders are technically the least

difficult to correct, usually requiring simple gene supplementation, i.e. the expression of a wildtype functional gene product that is either entirely absent or non-functional in the disease state.

With the exception of those resulting from haploinsufficiency dominantly inherited disorders generally cannot be treated by gene supplementation alone and are thus more challenging to treat via gene therapy. Dominant disorders resulting from a gain of function or dominant negative mutations will require the translation of the mutated gene product to be reduced or eliminated. However this alone may be insufficient to restore normal function and merely convert the dominant form into a haploinsufficient form, in which case additional gene supplementation may also be required. There are a number of genetic disorders of the cornea to which the techniques developed here might be applied to mediate an effective treatment.

8.1.1 Endothelium directed gene transfer

The most common inherited disorder of the cornea primarily affects the endothelium, Fuchs endothelial dystrophy which is an autosomal dominant disorder, the late onset form of which occurs in around 4% of the population over 40 years of age. It is characterised by a thickening of Descemet's membrane, the formation of excrescences within Descemet's termed guttae and the progressive loss of endothelial cells leading to corneal oedema and clouding. Despite its relatively high frequency the molecular genetics and pathogenic mechanisms of late onset Fuchs are not fully understood. The disorder is certainly genetically heterogeneous, with mutations in many different genes having been associated with an increased risk of Fuchs [344]. Due to this lack of knowledge relating to causative genes / mechanisms no gene therapy based approach to correct the disorder can currently be attempted.

The much rarer early onset form of Fuchs is somewhat better characterised having been shown to be relatively strongly associated with dominant mutations within a single gene encoding alpha 2 collagen VIII (Col8a2) [344,345], and two knock-in mouse models have thus recently been generated based upon known disease associated point mutants of Col8a2 [346,347]. These models appear to mimic the human disorder in that they display an increased rate of progressive endothelial cell loss with age and the formation of guttae, cells of the endothelium in both models were also shown to display activation of the unfolded protein response and increased autophagy. Such models therefore have begun to provide some insight into the mechanisms by which early onset Fuchs might proceed (although these investigations are currently relatively preliminary) and could also be used to test the

efficacy of a gene therapy based treatment upon the phenotypes observed. The authors do not however describe any visual impairment due to corneal oedema for either model and this apparent lack of the primary sight threatening clinical phenotype within the model is a concern. Additionally, whilst the normal mouse endothelium has been shown to undergo age related decline in a similar manner to humans [348] it has also been shown that endothelial cell proliferative capacity varies between species [8]. Care must therefore be taken in extrapolation of results between species in light of such known species differences.

Although the animal models are imperfect and the disease mechanisms only have only begun to be elucidated a gene therapy approach to early onset Fuchs could perhaps be considered based upon an RNAi mediated knockdown of the specific mutant alleles present in these models. If such allele specific RNAi construct can be designed and validated then then gene delivery to the endothelium must then be achieved.

All endothelium direct gene therapy to date (discussed later in 8.2) has been carried out using either adeno or lentiviral mediated gene delivery as these are the only two vectors that have thus far been shown to effectively transduce the endothelium. Both these vectors carry substantial disadvantages however. The use of adenovirus within non-cancer gene therapy has declined in recent years as it became apparent that the immunogenicity of this virus would impose substantial limits upon its utility [163]. Lentiviruses remain widely used as they are far less immunogenic and their ability to integrate into the host genome is of great benefit for any application requiring gene delivery to replicative cell types. However the disruption to the host genome caused by integration combined with an apparent preference of the process for regions of high transcriptional activity [202] carries an ever present risk of insertional mutagenesis and oncogenic transformation [211,349].

AAV vectors display both a low immunogenicity and carry no significant risk of insertional mutagenesis and thus have become a widely used vector of choice, especially within the context of non-replicative cell types. However AAV mediated gene transfer approaches to the endothelium have thus not far been possible due to its extremely limited transduction of this cell type [223]. The novel finding presented here that AAV2/6(ShH10) serotype is able to mediate a widespread and substantial transduction of the endothelium in both mice and man has therefore enabled genetic manipulation of endothelial cells via AAV which could be of potential use in the development and application of a gene therapy based treatment for early onset Fuchs or any other genetic disorder of the endothelium.

8.1.2 Stroma directed gene transfer

The high level and long lasting stromal transduction shown here to be mediated by AAV2/8(Y733F) is of potential utility in gene therapy to treat the corneal phenotypes of two systemic genetic diseases: Mucopolysaccharidosis and Cystinosis.

The mucopolysaccharidoses (MPS) are a group of liposomal storage disorders, caused by recessive mutations in lysomal enzymes resulting in accumulation of glycosaminoglycans both intra and extracellularly throughout many tissues of the body. Disease phenotypes are therefore extensive and include skeletal abnormalities, defects in pulmonary and cardiac function, cognitive impairment, loss of both hearing and vision and reduced lifespan. Presentation is variable with 9 different subtypes associated with different genes having been characterised, each of which displaying variability in severity. More often than not however the condition is severe leading to premature death. [350]

MPS can lead to the manifestation of multiple pathologies within the eye including corneal opacification, retinopathy, optic nerve atrophy / swelling, ocular hypertension, and glaucoma. The corneal opacification in particular is present within all forms of the disease. [351] and has been shown to be due to abnormal arrangements of collagen fibrils within the corneal stroma [352,353].

Effective systemic treatment of some forms of the condition has been achieved by either bone marrow transplantation (BMT) [354,355] or MPS I enzyme replacement therapy [356]. These systemic therapies however are only partially effective, with skeletal and ocular abnormalities in particular often proving resistant to correction [356,357].

Pre-clinical gene therapy based approaches to MPS have largely been focused upon MPS VII due to the availability of both murine and canine models of this subtype [358]. Within these models efficacy of gene replacement has been demonstrated via AAV or lenti mediated transduction via various systemic or CNS directed routes of vector administration [359–362]. In common with the clinically applied therapeutic approaches of BMT or enzyme replacement, gene therapy has not proven effective in correction of corneal opacification even when directed towards more posterior segments of the eye. [363,364].

The corneal phenotype within the mouse model of MPS VII has been specifically targeted in a study by Kamata et al. [365] who attempted corneal gene replacement via intracameral injection of an adenoviral vector. Whilst this study demonstrated transgene expression within the cornea and showed evidence of structural improvement within the stroma it also showed the gene delivery mediated to be extremely limited and short lived.

The extensive, long lasting transduction of the corneal stroma shown here to be mediated by AAV2/8(Y733F) might therefore be of improved efficacy in the treatment of corneal abnormalities associated with MPS; a phenotype that seems unresponsive to systemic approaches.

Cystinosis is another recessively inherited syndromic condition for which gene delivery to the corneal stroma may be of significant benefit. Cystinosis has many points of similarity with MPS, namely that the condition is also a lysomal storage disease that leads to the pathogenic deposition of material throughout many tissues of the body leading to systemic dysfunctions [366]. Cystinosis is divided into three main subtypes all of which share the pathology of photophobia due to cystine crystal formation in the cornea; in the least severe from, ocular cystinosis, this is the primary disease phenotype [367].

Treatment of cystinosis is primarily mediated via cystine depleting drugs, although the dosing regime is oppressive with drugs having to be taken orally every 6 hours and hourly via eye drops [368]. In the more severe forms of the disease this treatment also does little to prevent the primary life threatening phenotype of renal failure, for which allogenic transplantation is required.

Gene therapy approaches to cystinosis have been relatively limited to date. Work on gene replacement in a murine knockout model [369] has shown that systemic delivery of adenovirus mediated transduction of hepatocytes and showed a short term, age dependent reduction in cystine levels. Efficacy in this case was likely limited by the short comings inherent of the adenoviral vector.

Unlike MPS treatment of cystinosis via secretion of wildtype protein from a systemic allograft such as BMT was not thought likely to be effective. This is due to the fact that the defective protein in cystinosis (CTNS) is a membrane transporter rather than an enzyme and thus cannot be secreted and requires a specific subcellular localisation in order to be functional.

Nonetheless Syres et al. [370] undertook allotransplantation of several different adult stem cell types into the CTNS knockout mouse hypothesising that healthy cells derived from the transplant would be able to integrate into multiple organs and the healthy function of these integrated cells would be sufficient to decrease tissue cystine levels. This hypothesis proved to be valid as it was shown that allografted haematopoietic stem cells (HSCs) were indeed able to integrate into variety of host organs (usually in the form of tissue resident macrophages) and mediate a reduction in tissue cystine levels. This technique was then further developed in order to avoid the potential risks involved with host vs graft disease by transplantation of autologous HSCs that had under gone lenti mediated gene replacement

with similar results [371]. These treatments appeared to be effective in the cornea although the results suggest that cystine crystal formation may have been delayed rather than prevented.

If only a relatively few integrated donor cells within the cornea are able to produce a beneficial reduction in tissue cystine levels then it is likely that CNTS gene replacement within corneal keratocytes themselves is likely to be of equal or greater efficacy. Additionally in cases of the mildest form of the condition, ocular cystinosis, treatment by BMT which is both highly invasive and carries a substantial risk is unlikely to be warranted. A gene therapy approach specifically targeted to the affected tissue (the cornea) would be far more clinically attractive.

Long term AAV2/8(Y733F) mediated transduction of the corneal stromal could therefore represent an attractive, minimally invasive therapeutic methodology by which the corneal phenotypes of cystinosis might be corrected. In the less severe forms of the cystinosis this approach could potentially largely cure the condition whilst in the more severe forms the need for cysteine depleting eyedrops could at least be eliminated.

8.1.3 Epithelium directed gene transfer

A gene therapy approach in which an integrating virus (such as lentivirus) is utilised to correct a genetic disorder via transduction of a stem cell and results in therapeutic gene expression throughout the entire resulting lineage is a well-established approach. Indeed some of the very first successful clinical applications of gene therapy utilised this methodology transducing hematopoietic stem cells *ex vivo* for the treatment of severe combined immune deficiency [372]. Such treatments however have always required the extraction of stem cells prior to gene transfer being carried out *ex vivo* followed by re-engraftment of the cells. We believe however that the work presented here in Chapter 6 may represent the first time such a gene transfer has been achieved by the direct transduction of the stem cell in its niche*, in vivo*. This constitutes a potentially significant milestone.

This work (Chapter 6) on gene transfer to the corneal epithelium via transduction of the limbal epithelial stem cells (LESCs) was performed as part of a collaboration with Dr Satoshi Kawasaki (Kyoto Prefectural University of Medicine) and was directed towards the development a potential treatment methodology for gelatinous drop-like corneal dystrophy (GDLD), a recessively inherited disorder of the epithelium with an estimated prevalence of between 1 in 30,000 [94] and 1 in 300,000 [95] in Japan and rarely reported elsewhere.

GDLD is caused by loss of function mutations in the TACSTD2 (aka M1S1, Trop2) gene and Dr Kawasaki's previously published work has both confirmed TACSTD2's involvement [373] and begun to elucidate the mechanism by which loss of function leads to pathogenesis [105]. It has been shown that TACSTD2 is able to bind and interact with various tight junction-related proteins and that loss of TACSTD2 function is associated with decreased expression or altered subcellular localization of these proteins and impaired epithelial barrier function. The primary phenotype of amyloid deposition then likely proceeds by fluid infiltration into the cornea from the tear film [374].

GDLD is therefore well suited to treatment by a supplementation gene therapy approach, as it is caused by a recessively inherited loss of function mutation. However the proposed pathogenic mechanism of epithelial barrier function impairment makes it likely that a widespread or near complete gene transfer to the epithelium will be required to ameliorate pathology. A more partial transduction will result in a mixed population of corrected and diseased epithelial cells and restoration of barrier function would therefore only be partial and significant fluid infiltration could still occur.

Currently the only available treatment for GDLD is a corneal transplant, however prognosis of transplantation is always poor as the procedure does not correct the underlying cause of the condition, the genetic defect of the host epithelium. Only the central portion of the cornea is transplanted and the host's defective LESCs remain in place. Over time therefore the donor's healthy epithelium is slowly replaced with the host's defective cells via epithelial turnover and the disease recurs [374], usually within a timeframe of around 1-2 years. Repeated engraftment is therefore required to maintain a treatment effect and each subsequent transplant carries with it an increased risk of failure [108]. The case for gene therapy to correct the underlying genetic defect is therefore compelling.

Treatment of GDLD via LESC transplantation has also been attempted, applied in combination with a central corneal graft [375,376]. As the host's LESCs are defective an allogenic source of donor LESCs was required. Results from this approach have been encouraging but not definitive. Only two studies have been undertaken to date; the first [376] treated nine eyes in seven patients and within a mean follow up period ~4 years eight of nine eyes were free of recurrence. The second study [375] only treated 3 eyes in 4 patients and reported no recurrence within a mean follow up time of ~2 years. However, whilst the engrafted corneas in this study were described as "clear" at the final point of follow up, measurements of visual acuity remained very low. Both studies employed post-operative immune suppression consisting short term topical steroids combined with longer term systemic administration of agents such as cyclosporine A and / or mycophenolate mofetil.

The apparent lack of recurrence in these studies is somewhat surprising. As the hosts LESCs were not destroyed or removed as part of the procedure, both healthy engrafted cells and defective host cells would be expected to be present within the treated eye, leading to competition between them for colonisation of the niche and regeneration of the cornea. LESC transplantation is more commonly used in cases of host LESC loss or deficiency, in which such competition would be absent or reduced and it has been shown that even in these cases the restored epithelium often contains both host and donor cells [77]. The only way to avoid this would be to destroy the hosts LESCs pre-transplantation, a procedure highly unlikely to be clinically acceptable. If successful therefore the epithelium resulting from transplantation in this case would be composed of a mosaic of both healthy and defective cells and, as discussed earlier, this is unlikely to fully restore epithelial barrier function which depends on correct tight junction formation between all or most cells.

It is possible however that a partial restoration of barrier function may have been effective in substantially delaying recurrence and whilst not curative this effect would still be of useful clinical application in prolonging graft survival. Further follow up of these grafts to assess the extent of their efficacy is required and the results to date are perhaps encouraging as they may indicate that even an incomplete gene transfer to the epithelium and partial restoration of barrier function might be a clinically effective treatment for GDLD.

The allografting procedure described also carries a risk of immune mediated rejection and indeed all patients in the study were subjected to immunosuppression to reduce this risk for up to 18 months. As far as we are aware the approach of gene therapy and expansion of autologous LESCs *ex vivo* followed by re-engraftment as not been attempted although such an approach would present the obvious benefit of a greatly reduced risk of immune mediate graft failure. This approach may be of merit, however both harvesting of LESCs and the re-engraftment are non-trivial surgical procedures that carry a risk of complications [73,377] and there is evidence that this form of LESC transplantation may not actually result in the permanent engraftment of the cells transplanted [78,79]. The long term epithelial restoration observed to result from such LESC transplants may be the result of the transplanted cells stimulating an enhanced activity of the remaining host cells which is sustained even once the transplanted cells are lost [378]. This would be of no beneficial effect in the case of GDLD in which the host cells are defective.

Therefore the *in situ* gene transfer to LESCs such as that demonstrated here potentially offers both the least invasive and potentially most effective means by which the gene defect causative of GDLD might be permanently corrected and if performed early in course of disease before symptoms first appear (within the first decade of life) may eliminate the requirement for corneal transplantation all together.

Whilst GDLD was very much the focus of this work the technique of epithelial gene delivery via lentiviral LESC transduction would be equally applicable to gene therapy of any other inherited disorders of the epithelium although such conditions are extremely rare. One disorder in which gene therapy may be of benefit is Meesman's epithelial corneal dystrophy (MECD), a disease characterised by the presence of microcysts within the anterior epithelium, foreign body sensation and photophobia. Often the condition is mild but more severe forms exist in which corneal erosion and scarring leads to significant loss of vision and the requirement for treatment by corneal transplantation. Meesman's is caused by dominant mutations in either keratins K3 or K12 which act antagonistically to the product of the wild type allele leading cytoskeletal dysfunction and mechanical fragility of epithelial cells [379].

Multiple gene therapy approaches might be applicable to a dominant negative mutation such as those causative of Meesman's. Gene supplementation could potentially prove effective as overexpression of the wildtype allele might result in sufficient production of normal gene product to both saturate the pathogenic mechanism and provide sufficient protein for normal function. A better strategy however would likely be an RNAi based gene knockdown approach to the mutated allele to directly address the pathogenic process itself. As it has been shown that there is no evidence of haploinsufficiency in a murine model of K12 deficiency [380] this approach should be effective without the need for any additional supplementation of the wildtype allele.

An RNAi based strategy has in fact already been developed by Liao et al. [381] who have designed and validated an siRNA construct able to mediate effective allelic discrimination and knockdown of a point mutant known to be associated with an especially severe form of MECD. Liao et al. convincingly demonstrate the efficacy of their construct *in vitro* but have not yet applied this strategy in either an animal model or clinically because as Liao et al. state in their paper "The biggest hurdle to clinical application of these siRNAs is that of finding an efficacious and non-invasive delivery system".

Lentiviruses have been well established as being able to deliver siRNA constructs for the purposes of gene knockdown [382] and thus the methodology developed here could therefore provide a minimally invasive method by which this hurdle to delivery could be overcome and mediate long lasting gene knockdown in the epithelium.

8.2 Applications in augmentation gene therapy

Augmentation gene therapy is an approach whereby the gene transfer does not aim to directly correct a specific mutation by either restoring the wildtype gene or down regulation of the mutant gene. Instead this approach aims to mediate a beneficial effect upon a specific pathological process (whose cause may or may not be genetic). The gene transfer itself can either deliver a factor that acts intracellularly in which case only the transduced cells themselves will be affected, or can induce the production of a secreted factor that can act more widely throughout an entire tissue or system. In the latter case the target cells themselves may not even be those affected by the pathology.

As discussed earlier (8.1.1) gene therapy to correct directly the defects of late onset Fuchs endothelial dystrophy is not currently possible due to a lack of knowledge of the molecular disease mechanisms. However it is well known that both the late and the early onset forms of Fuchs mediate their primary sight threatening phenotype via the progressive loss of endothelial cells (decompensation), a mechanism that may be amenable to modulation by a gene augmentation based approach. Endothelial decompensation is also of much wider significance beyond the context of Fuchs as it is also both a leading cause of corneal graft failure [26,119] and the primary reason corneal tissue is rejected for transplantation [383]. For this reason gene therapy of the endothelium has primarily been directed towards modulation of endothelial cell biology in order to maintain or increase their density. Approaches have included preservation of endothelial cells by lenti mediated overexpression of anti-apoptotic factors [238,239] or induction of endothelial cell replication via cell cycle modulation to increase density [151,241].

As mentioned in 8.1.1 all such work to date has been carried out using either adeno or lentiviral mediated gene delivery, with adenovirus proving too immunogenic for many therapeutic applications and use of lentivirus presenting the risk of oncogenic transformation via insertional mutagenesis. This feature of lentiviral transduction is of particular concern when the transgene in question is intended to promote cell proliferation or survival and is thus itself a potentially oncogenic factor. AAV mediated transduction is therefore an especially attractive option within the context of gene transfer for the modulation of endothelial cell survival or proliferation as due to its inability to integrate any potentially oncogenic transduction will become self-limiting over time due to episomal transgene expression in transduced cells being diluted or lost upon cell division. This loss of transgene however should not act to inhibit any therapeutic increase in endothelial cell number as in most cases a single division of each remaining endothelial cell would be more than sufficient

to restore a healthy endothelial cell density. An AAV2/6(ShH10) mediated transduction of the endothelium for this purpose therefore represents a potentially effective methodology with a much improved safety profile over all those used to date.

One gene augmentation approach arising from this work, the inhibition of corneal haem and lymphangiogenesis via sFlt1 gene delivery has already been discussed in detail in 5.3. However pathological haemangiogenesis within the eye is not limited to the cornea and is of considerable relevance to the posterior segment of the eye. Abnormal neovascular growth constitutes a blinding pathology within both age-related macular degeneration (AMD) and diabetic retinopathy, conditions that represent two of most frequent causes of retinal blindness within the western world [384]. Both conditions can currently be treated with antibody-based VEGF binding biologics; these are effective but are also extremely expensive and require repeat administration by intraocular injection to maintain efficacy, compounding costs and placing considerable burden upon both the patient and the healthcare system.

A gene therapy approach mediating the secretion of a VEGF binder (such as sFlt1) would potentially eliminate these issues, providing the treatment effect via a similar mechanism whilst only requiring a single treatment if sufficient expression can be mediated over the long term. Indeed such gene therapy approaches to both conditions have been proposed and employed.

Work in a murine model of AMD pathogenesis (laser induced CNV) has shown subretinal delivery of AAV encoding the anti angiogenic factors such as endostatin / angiostatin [385] or sFlt1 [386] can be effective in reducing CNV lesion size. Additionally a clinical trial [387] involving AAV2/2 mediated expression of sFlt1 following subretinal injection is also under way for wet AMD, based upon pre-clinical work with in a primate model [388].

Almost all such approaches to date have utilised subretinal injections for vector delivery aiming to mediate transduction of and secretion from photoreceptors. Such a route is appealing due to the very large number photoreceptors present within the eye likely resulting in a comparably large amount of transgene product being produced and secreted. Additionally subretinal injection of AAV has already proven to be relatively safe in trials to treat retinal dystrophies [218].

However, unless aiming to treat the photoreceptors themselves it is arguable that photoreceptor transduction and subretinal injection are best avoided. The subversion of any cell to a secretory role that does not form part of its endogenous function has the potential to disregulate endogenous processes within the cell. Although such complications have not

thus far been reported, the consequences of such disruption in a highly specialised cell type as critical to vision as photoreceptors could be severe. Additionally subretinal injection in animal models is often associated with a reduction in ERG amplitude indicating the procedure causes a degree of retinal damage. There is also mounting clinical evidence [181] to suggest that the macula in particular may be especially sensitive to subretinal injection related damage, with alternative injection routes receiving increasing attention.

Indeed multiple studies have demonstrated that an anti-angiogenic gene therapy approach to the prevention of retinal neovascular pathology via a non-subretinal vector delivery route can be effective. The ability of AAV2/2 to transduce retinal ganglion cells following intravitreal administration has been utilised by a number of studies aiming to treat diabetic retinopathy [389,390] or retinopathy of prematurity [391]. One study directed at AMD has employed the non-viral gene delivery method of electroporation to mediate sFlt1 secretion from the cillary muscle [392].

We believe that some of the gene delivery methods developed here may constitute superior, non-subretinal approaches to ocular augmentation gene therapy acting via a secreted factor. This is due to these methods potentially transducing a larger number of more widely distributed target cells and thus likely mediating an increased production of therapeutic protein.

Whilst we have demonstrated the efficacy of intrastromal gene delivery via AAV2/8(Y733F) in such approach directed towards the cornea itself (Chapter 5) we have not established whether this approach leads to secreted transgene products reaching more posterior tissues of the eye *in vivo*. In human tissue *ex vivo*, substantial amounts of transgene product were secreted from the tissue and detected within the conditioned medium, although it is questionable how comparable this highly artificial situation is to normal function *in vivo*. Further work is therefore required to determine the potential applicability of this technique to the posterior segment.

The transduction mediated by AAV2/6(ShH10) is potentially of the most promise in this regard. In addition to transduction of the corneal endothelium we also noted that this serotype mediated extensive transduction of the cillary body as seen in Figure 71 below. Additionally the ShH10 serotype was initially produced as the result of work aiming to develop AAV species able to transduce the Müller glia of the retina from an intravitreal injection [197] and has already been applied in an augmentation gene therapy context directed at promoting photoreceptor survival by glial production and secretion of the neurotropic factor GNDF [153], although in this study the authors did not examine expression in the anterior segment.

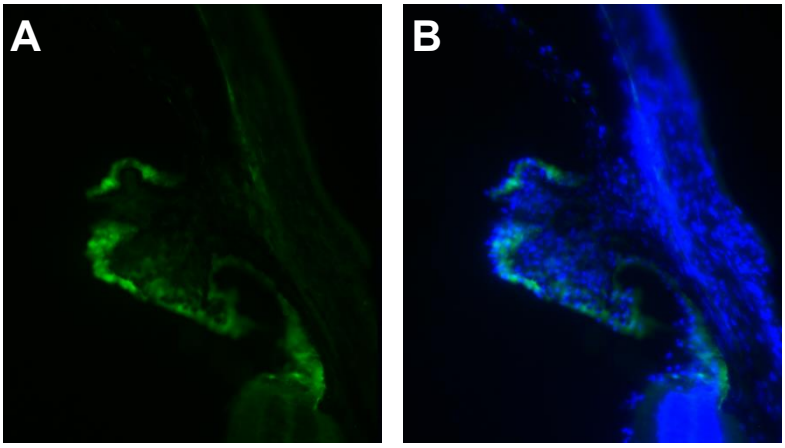

Figure 71. Transgene (eGFP) expression in the cillary body mediated by intravitreal injection of AAV2/6(ShH10)-CMV-eGFP

A: eGFP (Green) channel only
B: Merged image in which DAPI staining (blue) is also visible

AAV2/6(ShH10) therefore is able to transduce three different ocular tissues located in: the anterior segment, the posterior segment and around the limbal circumference from a single intravitreal injection. This serotype is therefore potentially the ideal vector for use in mediating a high level production and secretion of transgene products panocularly whilst minimising the involvement of cells critical to light perception such as retinal neurons.

AAV based augmentation gene therapy approaches have also been applied within the eye for the treatment of uveitis by secretion of various immune modulatory molecules [393–395]. For this application in particular route of administration may be critical [396]. In the context of an already inflamed environment the side-effects of a subretinal injection (such as retinal damage or further inflammation) may be aggravated, and work within the lab by Dr Colin Chu (unpublished) has provided some data to this effect. By contrast the intravitreal route of administration may lead to greater presentation of both vector capsid and transgene product to the immune system resulting in the development of vector or transgene directed adaptive immunity, potentially negating or severely limiting any possibility of repeat administration [397].

Route of vector administration for the gene therapy of uveitis therefore remains somewhat controversial, with each route presenting pros and cons to be balanced. Despite the possible disadvantages however the therapeutic potential of intravitreal AAV2/6(ShH10) for uveitis merits investigation.

8.3 Non-therapeutic gene transfer applications

Whilst the primary focus of this work and the gene therapy field more generally is usually upon clinical application, the gene delivery methods developed can also be of great utility in the study of cell biology. In combination with cell-type specific promoters vector mediated gene transfer can provide a relatively quick and easy method by which a cell type of interest might be labelled or have its gene expression modulated, both *in vitro* and *in vivo.*

As previously discussed in 6.3.2 the lentivirus mediated labelling of LESCs *in vivo* demonstrated here in Chapter 6 provides a potentially powerful tool for the study of epithelial cell behaviour both in homeostasis and pathogenesis. It enables the selective labelling of a small subset of LESCs with clonal inheritance of the label allowing high temporal resolution tracking of cell movement and turnover in a way not possible with the more extensive labelling resulting from transgenic manipulation. In addition, combination of LESC transduction with the LeGO method developed in Chapter 7 would allow the study of interactions between the different clonal populations of cells that make up the epithelium, providing an insight into the cellular dynamics of epithelial maintenance at a level of extreme detail not previously demonstrated.

The same techniques could also be applied to studies attempting to determine the fate of LESC cultured *ex vivo* upon cell transplantation. It has been shown that whilst such transplants do result in a long term beneficial effect, the transplanted cells themselves to do not survive, the mechanism by which they are lost and the means by which the epithelium is maintained after their loss are both unknown. Most investigations of this phenomenon have used DNA based techniques such as PCR to assess the survival of donor cells on the basis of their containing DNA sequences not present in the host, often resulting from a sex mismatch between host and donor [78,79]. Whilst this is the only viable technique for use in the clinical setting similar work in animal models could utilise a fluorescent marker to directly identify and track transplanted cells over time providing a much more detailed insight into the processes and timescale of loss.

One study by Yin et al. attempted such tracking by transplantation of a stably transfected LESC line expressing the fluorescent protein venus into a caprine model of LESC deficiency [398]. The follow up in this experiment was relatively short (3 months post-transplant), did not involve *in vivo* monitoring of fluorescence and the histological results obtained from the fluorescent label were poor and in our opinion inconclusive. More convincing data came from PCR which showed a greater proportion of donor cells remaining in the central epithelium than in the limbus, perhaps indicating loss proceeding via normal epithelial turn over.

The work presented here has shown that within the murine context at least a lentivirus is able to transduce LESCs and maintain the expression of fluorescent transgenic label over the long term although we have not established if the same is true in the larger animal models that are more commonly used in studies of cultivated LESC engraftment such as rabbits. If lentiviral transduction of cultivated LESCs in such a model proves possible then the fate of LESCs fluorescently labelled by this method could be tracked at the cellular level at a high temporal resolution; in combination with the LeGO system the fate or expansion of individual clones could also be monitored.

8.4 Conclusion

In comparison to other ocular tissues such as the retina the cornea has been somewhat neglected as a target for gene therapy despite its easy accessibility and immune privileged status. This relative lack of attention is likely due to both the rarity of congenital conditions affecting the cornea and the high success rate enjoyed by the well-established procedure of keratoplasty for the treatment of many corneal conditions. Transplantation however does not represent a corneal panacea; it is often ineffective for the treatment of genetic dystrophies (of the corneal epithelium in particular) and inflammation or vascularisation increases the risk of the procedure dramatically.

The application of corneal gene therapy has the potential to both correct genetic defects and act via augmentation gene therapy to improve the prognosis of corneal transplantation in high risk cases. The work presented in this thesis has demonstrated that gene delivery to all three cellular layers of the cornea can be achieved efficiently and safely, often with transgene expression being sustained over the long term. However this study has only begun to explore the potential applications for the gene therapy techniques it has developed. As discussed in this section such applications are incredibly wide ranging and effective corneal gene therapy could therefore potentially be of benefit to a substantial number of patients worldwide, ranging from those relatively small number of families suffering from an orphan congenital condition, to the millions of patients who receive corneal transplants each and every year.

8.5 Future Directions

Work to further develop some of the key findings of this thesis (summarised at the beginning of this chapter) is planned and this program of further work will be briefly outlined below.

Chapter 5 has convincingly demonstrated that intrastromal injection of an AAV2/8(Y733F) delivering sFlt1 is highly effective in prevention of induced corneal haem neovascularisation. However, the ingrowth of Lymph vessels into the cornea was not impeded by delivery of this transgene and thus the vascular privilege of the cornea was only partially protected. This approach alone is therefore likely to be suboptimal in regard to minimising the pathological consequences of corneal neovascularisation.

In order to more fully protect corneal vascular privilege and thus improve any potential therapeutic application it is planned to combine the current sFlt1 based approach with delivery of the recently discovered sFlt4 (sVEGFR3) that has been shown to inhibit lymph neovascularisation [323]. Initially this combination approach will proceed via the co-injection of two vectors although a bicistronic construct encoding both sFlt isoforms should also be possible.

Whilst the corneal suture model used in this study to date represents a robust model of short term, trauma induced neovascularisation it is perhaps not the most relevant model system in regard to clinical application. The intended application for this technique would be to improve the prognosis of high risk corneal transplants chiefly via the prevention of immunological rejection. Allogeneic murine corneal transplantation therefore represents the ideal model upon which to test the optimised therapeutic strategy, and the expertise to perform corneal grafts within mice is currently being developed within the lab.

The work presented in Chapter 6 has shown that long term transgene expression within the corneal epithelium is achievable via transduction of the LESCs with an integrating lentiviral vector. However, in the most extensive transduction shown only around 30% of the corneal surface became covered with transduced cells. In order to maximise the beneficial effect of gene therapy based upon this transduction it would be desirable to transduce the largest possible number of LESCs. This goal should be achievable via improvement in the precision and reproducibility of both needle morphology and vector injections techniques and these are the areas that will form the initial focus of further work.

The capacity to mediate a long term gene delivery to the epithelium was initially developed with a view to application in gene therapy for inherited corneal dystrophies, specifically GDLD. In order to progress towards this application it would be desirable to test gene supplementation within an animal model known to closely recapitulate the human disease. Unfortunately such models are currently lacking, a knockout mouse model for TACSTD2 (the gene implicated as causative of GDLD) is available but all work upon this model to date has focused upon the genes oncogenic potential [399,400] and a corneal phenotype has not been described, but may have been overlooked. Alternatively, work by Liao et al. [381] has demonstrated a promising gene therapy construct for the correction of the disease mechanism underlying Meesmann Epithelial Corneal Dystrophy (MECD) for which they lack an effective gene delivery mechanism. However, this condition also currently lacks an animal model and whilst Liao et al. have expressed and intention to develop a murine model of MECD no progress towards this goal has yet been published. The relevance / availability of animal models of inherited epithelial dystrophies will be further investigated however it is perhaps likely that work to develop epithelial transduction towards application in gene therapy may be currently restricted to *in vitro* work upon cultured patient cells.

Finally the patterns of transgene expression resulting from Lentiviral LESC transduction seen in Chapter 6 have raised a number of questions regarding the exact cellular dynamics by which the epithelium is maintained. More specifically the number of LESC lineages contributing to the various patterns observed is unknown. Chapter 7 therefore presented *in vitro* work to develop techniques by which the individual LESC lineages could be identified and tracked over time. This *in vitro* optimisation phase is now complete and these techniques are ready to be transferred *in vivo*.

Reference List

1. **Marfurt CF, Cox J, Deek S, Dvorscak L**. - Anatomy of the human corneal innervation. Exp Eye Res. 2010 Apr;90(4):478–92.

2. **Rózsa AJ, Beuerman RW**. - Density and organization of free nerve endings in the corneal epithelium of the rabbit. Pain. 1982 Oct;14(2):105–20.

3. **Pavelka M, Roth J**. - Descemet's Membrane. Functional Ultrastructure. 2010. p. 184–5.

4. **Waring 3rd GO, Bourne WM, Edelhauser HF, Kenyon KR**. - The corneal endothelium. Normal and pathologic structure and function. Ophthalmology. 1982/06/01 ed. 1982;89(6):531–90.

5. **Schütte E, Schulz I, Reim M**. - Cornea nutrition by intravenous glucose infusion. Albr von Graefes Arch f�r Klin und Exp Ophthalmol. 1972;185(2):161–9.

6. **Kumagai AK, Glasgow BJ, Pardridge WM**. - GLUT1 glucose transporter expression in the diabetic and nondiabetic human eye. Invest Ophthalmol Vis Sci. 1994 May;35(6):2887–94.

7. **Dartt DA, Bonanno JA**. - Molecular mechanisms underlying the corneal endothelial pump. Exp Eye Res. 2012;95(1):2–7.

8. **Joyce NC**. - Proliferative capacity of the corneal endothelium. Prog Retin Eye Res. 2003/07/11 ed. 2003;22(3):359–89.

9. **Joyce NC, Navon SE, Roy S, Zieske JD**. - Expression of cell cycle-associated proteins in human and rabbit corneal endothelium in situ. Invest Ophthalmol Vis Sci. 1996 Jul;37(8):1566–75.

10. **Hitani K, Yokoo S, Honda N, Usui T, Yamagami S, Amano S**. - Transplantation of a sheet of human corneal endothelial cell in a rabbit model. Mol Vis. 2008 Jan;14:1–9.

11. **Konomi K, Zhu C, Harris D, Joyce NC**. - Comparison of the proliferative capacity of human corneal endothelial cells from the central and peripheral areas. Invest Ophthalmol Vis Sci. 2005 Nov;46(11):4086–91.

12. **Welge-Lüssen U, May CA, Neubauer AS, Priglinger S**. - Role of tissue growth factors in aqueous humor homeostasis. Curr Opin Ophthalmol. 2001 Apr;12(2):94–9.

13. **Joyce NC, Harris DL, Mello DM**. - Mechanisms of mitotic inhibition in corneal endothelium: contact inhibition and TGF-beta2. Invest Ophthalmol Vis Sci. 2002 Jul;43(7):2152–9.

14. **Senoo T, Obara Y, Joyce NC**. - EDTA: a promoter of proliferation in human corneal endothelium. Invest Ophthalmol Vis Sci. 2000 Sep;41(10):2930–5.

15. **Okumura N, Koizumi N, Kay EP, Ueno M, Sakamoto Y, Nakamura S, et al.** - The ROCK inhibitor eye drop accelerates corneal endothelium wound healing. Invest Ophthalmol Vis Sci. 2013 Apr 3;54(4):2493–502.

16. **Walsh S V, Hopkins AM, Chen J, Narumiya S, Parkos CA, Nusrat A**. - Rho kinase regulates tight junction function and is necessary for tight junction assembly in polarized intestinal epithelia. Gastroenterology. 2001 Sep;121(3):566–79.

17. **Bourne WM, Nelson LR, Hodge DO**. - Central corneal endothelial cell changes over a ten-year period. Invest Ophthalmol Vis Sci. 1997/03/01 ed. 1997;38(3):779–82.

18. **Hollingsworth J, Perez-Gomez I, Mutalib HA, Efron N**. - A population study of the normal cornea using an in vivo, slit-scanning confocal microscope. Optom Vis Sci. 2001/11/10 ed. 2001;78(10):706–11.

19. **Edelhauser HF**. - The resiliency of the corneal endothelium to refractive and intraocular surgery. Cornea. 2000/06/01 ed. 2000;19(3):263–73.

20. **Joyce NC**. - Cell cycle status in human corneal endothelium. Exp Eye Res. 2005/08/02 ed. 2005;81(6):629–38.

21. **Bourne WM**. - Clinical estimation of corneal endothelial pump function. Trans Am Ophthalmol Soc. 1999/06/09 ed. 1998;96:229–42.

22. **Bourne WM**. - Cellular changes in transplanted human corneas. Cornea. 2001/07/27 ed. 2001;20(6):560–9.

23. **Fuchs E**. - Dystrophia epithelialis corneae. Albr von Graefes Arch für Ophthalmol. 1910;76:478–508.

24. **Waring 3rd GO, Rodrigues MM, Laibson PR**. - Corneal dystrophies. II. Endothelial dystrophies. Surv Ophthalmol. 1978/11/01 ed. 1978;23(3):147–68.

25. **Bourne WM, Hodge DO, Nelson LR**. - Corneal endothelium five years after transplantation. Am J Ophthalmol. 1994/08/15 ed. 1994;118(2):185–96.

26. **Ing JJ, Ing HH, Nelson LR, Hodge DO, Bourne WM**. - Ten-year postoperative results of penetrating keratoplasty. Ophthalmology. 1998/10/27 ed. 1998;105(10):1855–65.

27. **Birk DE, Fitch JM, Babiarz JP, Doane KJ, Linsenmayer TF**. - Collagen fibrillogenesis in vitro: interaction of types I and V collagen regulates fibril diameter. J Cell Sci. 1990 Apr;95 (Pt 4):649–57.

28. **Wenstrup RJ, Florer JB, Davidson JM, Phillips CL, Pfeiffer BJ, Menezes DW, et al.** - Murine model of the Ehlers-Danlos syndrome. col5a1 haploinsufficiency disrupts collagen fibril assembly at multiple stages. J Biol Chem. 2006 May 5;281(18):12888–95.

29. **Dunlevy JR**. - Identification of the N-Linked Oligosaccharide Sites in Chick Corneal Lumican and Keratocan That Receive Keratan Sulfate. J Biol Chem. 1998 Apr 17;273(16):9615–21.

30. **Hassell JR, Birk DE**. - The molecular basis of corneal transparency. Exp Eye Res. 2010;91(3):326–35.

31. **Funderburgh JL**. - Mini Reveiw: Keratan sulfate: structure, biosynthesis, and function. Glycobiology. 2000 Oct 1;10(10):951–8.

32. **Fini ME**. - Keratocyte and fibroblast phenotypes in the repairing cornea. Prog Retin Eye Res. 1999;18(4):529–51.

33. **Hahnel C, Somodi S, Weiss DG, Guthoff RF**. - The keratocyte network of human cornea: a three-dimensional study using confocal laser scanning fluorescence microscopy. Cornea. 2000 Mar;19(2):185–93.

34. **Piatigorsky J, Carson DD, Jester J V.** - Corneal crystallins and the development of cellular transparency. Semin Cell Dev Biol. 2008;19(2):82–93.

35. **Brissette-Storkus CS, Reynolds SM, Lepisto AJ, Hendricks RL**. - Identification of a novel macrophage population in the normal mouse corneal stroma. Invest Ophthalmol Vis Sci. 2002 Jul;43(7):2264–71.

36. **Pinnamaneni N, Funderburgh JL**. - Concise review: Stem cells in the corneal stroma. Stem Cells. 2012/04/11 ed. 2012;30(6):1059–63.

37. **West-Mays JA, Dwivedi DJ**. - The keratocyte: corneal stromal cell with variable repair phenotypes. Int J Biochem Cell Biol. 2006 Jan;38(10):1625–31.

38. **Wilson SE**. - Role of apoptosis in wound healing in the cornea. Cornea. 2000 May;19(3 Suppl):S7–12.

39. **Wilson SE, He Y-G, Weng J, Li Q, McDowall AW, Vital M, et al.** - Epithelial Injury Induces Keratocyte Apoptosis: Hypothesized Role for the Interleukin-1 System in the Modulation of Corneal Tissue Organization and Wound Healing. Exp Eye Res. 1996;62(4):325–38.

40. **Kallinikos P, Efron N**. - On the etiology of keratocyte loss during contact lens wear. Invest Ophthalmol Vis Sci. 2004 Sep;45(9):3011–20.

41. **Zieske JD, Guimarães SR, Hutcheon AE**. - Kinetics of keratocyte proliferation in response to epithelial debridement. Exp Eye Res. 2001 Jan;72(1):33–9.

42. **Wilson SE**. - Corneal myofibroblast biology and pathobiology: generation, persistence, and transparency. Exp Eye Res. 2012 Jun;99:78–88.

43. **Garana RM, Petroll WM, Chen WT, Herman IM, Barry P, Andrews P, et al.** - Radial keratotomy. II. Role of the myofibroblast in corneal wound contraction. Invest Ophthalmol Vis Sci. 1992 Nov;33(12):3271–82.

44. **Mohan RR, Hutcheon AE., Choi R, Hong J, Lee J, Mohan RR, et al.** - Apoptosis, necrosis, proliferation, and myofibroblast generation in the stroma following LASIK and PRK. Exp Eye Res. 2003;76(1):71–87.

45. **Barbosa FL, Chaurasia SS, Cutler A, Asosingh K, Kaur H, de Medeiros FW, et al.** - Corneal myofibroblast generation from bone marrow-derived cells. Exp Eye Res. 2010;91(1):92–6.

46. **Kinoshita S, Adachi W, Sotozono C, Nishida K, Yokoi N, Quantock AJ, et al.** - Characteristics of the human ocular surface epithelium. Prog Retin Eye Res. 2001 Sep;20(5):639–73.

47. **Lu L, Reinach PS, Kao WW**. - Corneal epithelial wound healing. Exp Biol Med (Maywood). Royal Society of Medicine; 2001 Jul 1;226(7):653–64.

48. **Dohlman CH**. - The function of the corneal epithelium in health and disease. The Jonas S. Friedenwald Memorial Lecture. Invest Ophthalmol. 1971 Jun;10(6):383–407.

49. **Zucker BB**. - Hydration and Transparency of Corneal Stroma. Arch Ophthalmol. American Medical Association; 1966 Feb 1;75(2):228–31.

50. **Secker GA, Daniels JT**. - Limbal epithelial stem cells of the cornea [Internet]. Stem Book.org. 2009.

51. **DelMonte DW, Kim T**. - Anatomy and physiology of the cornea. J Cataract Refract Surg. 2011;37(3):588–98.

52. **Sharma A, Coles WH**. - Kinetics of corneal epithelial maintenance and graft loss. A population balance model. Invest Ophthalmol Vis Sci. 1989 Sep;30(9):1962–71.

53. **Friedenwald JS**. - Growth pressure and metaplasia of conjunctival and corneal epithelium. Doc Ophthalmol. 1951 Jan;5-6:184–92.

54. **Kinoshita S, Friend J, Thoft RA**. - Biphasic cell proliferation in transdifferentiation of conjunctival to corneal epithelium in rabbits. Invest Ophthalmol Vis Sci. 1983 Aug;24(8):1008–14.

55. **Hanna C, O'Brien JE**. - Cell production and migration in the epithelial layer of the cornea. Arch Ophthalmol. 1960 Oct;64:536–9.

56. **Davanger M, Evensen A**. - Role of the pericorneal papillary structure in renewal of corneal epithelium. Nature. 1971 Feb 19;229(5286):560–1.

57. **Schermer A, Galvin S, Sun TT**. - Differentiation-related expression of a major 64K corneal keratin in vivo and in culture suggests limbal location of corneal epithelial stem cells. J Cell Biol. 1986 Jul;103(1):49–62.

58. **Cotsarelis G, Cheng SZ, Dong G, Sun TT, Lavker RM**. - Existence of slow-cycling limbal epithelial basal cells that can be preferentially stimulated to proliferate: implications on epithelial stem cells. Cell. 1989 Apr 21;57(2):201–9.

59. **Pellegrini G, Golisano O, Paterna P, Lambiase A, Bonini S, Rama P, et al.** - Location and clonal analysis of stem cells and their differentiated progeny in the human ocular surface. J Cell Biol. 1999 May 17;145(4):769–82.

60. **Kruse FE, Tseng SC**. - Serum differentially modulates the clonal growth and differentiation of cultured limbal and corneal epithelium. Invest Ophthalmol Vis Sci. 1993 Sep;34(10):2976–89.

61. **De Paiva CS, Chen Z, Corrales RM, Pflugfelder SC, Li D-Q**. - ABCG2 transporter identifies a population of clonogenic human limbal epithelial cells. Stem Cells. 2005 Jan;23(1):63–73.

62. **Bunting KD**. - ABC transporters as phenotypic markers and functional regulators of stem cells. Stem Cells. 2002 Jan;20(1):11–20.

63. **Dua HS, Shanmuganathan VA, Powell-Richards AO, Tighe PJ, Joseph A**. - Limbal epithelial crypts: a novel anatomical structure and a putative limbal stem cell niche. Br J Ophthalmol. 2005 May;89(5):529–32.

64. **Shortt AJ, Secker GA, Munro PM, Khaw PT, Tuft SJ, Daniels JT**. - Characterization of the limbal epithelial stem cell niche: novel imaging techniques permit in vivo observation and targeted biopsy of limbal epithelial stem cells. Stem Cells. 2007 Jun;25(6):1402–9.

65. **Majo F, Rochat A, Nicolas M, Jaoudé GA, Barrandon Y**. - Oligopotent stem cells are distributed throughout the mammalian ocular surface. Nature. 2008 Nov 13;456(7219):250–4.

66. **Sun T-T, Tseng SC, Lavker RM**. - Location of corneal epithelial stem cells. Nature. 2010 Feb 25;463(7284):E10–1; discussion E11.

67. **Schlötzer-Schrehardt U, Dietrich T, Saito K, Sorokin L, Sasaki T, Paulsson M, et al.** - Characterization of extracellular matrix components in the limbal epithelial stem cell compartment. Exp Eye Res. 2007 Dec;85(6):845–60.

68. **Chee KYH, Kicic A, Wiffen SJ**. - Limbal stem cells: the search for a marker. Clin Experiment Ophthalmol. 34(1):64–73.

69. **Schlötzer-Schrehardt U, Kruse FE**. - Identification and characterization of limbal stem cells. Exp Eye Res. 2005;81(3):247–64.

70. **Kenyon KR, Tseng SC**. - Limbal autograft transplantation for ocular surface disorders. Ophthalmology. 1989 May;96(5):709–22; discussion 722–3.

71. **Tseng SC**. - Concept and application of limbal stem cells. Eye (Lond). College of Ophthalmologists; 1989 Jan;3 (Pt 2)(2):141–57.

72. **Tsai RJ, Tseng SC**. - Human allograft limbal transplantation for corneal surface reconstruction. Cornea. 1994 Sep;13(5):389–400.

73. **Dua HS, Miri A, Said DG**. - Contemporary limbal stem cell transplantation - a review. Clin Experiment Ophthalmol. 2010 Mar;38(2):104–17.

74. **Pellegrini G, Traverso CE, Franzi AT, Zingirian M, Cancedda R, De Luca M**. - Long-term restoration of damaged corneal surfaces with autologous cultivated corneal epithelium. Lancet. 1997 Apr 5;349(9057):990–3.

75. **Shortt AJ, Secker GA, Notara MD, Limb GA, Khaw PT, Tuft SJ, et al.** - Transplantation of Ex Vivo Cultured Limbal Epithelial Stem Cells: A Review of Techniques and Clinical Results. Surv Ophthalmol. 2007;52(5):483–502.

76. **Levis HJ, Massie I, Dziasko MA, Kaasi A, Daniels JT**. - Rapid tissue engineering of biomimetic human corneal limbal crypts with 3D niche architecture. Biomaterials. 2013;34(35):8860–8.

77. **Djalilian AR, Mahesh SP, Koch CA, Nussenblatt RB, Shen D, Zhuang Z, et al.** - Survival of donor epithelial cells after limbal stem cell transplantation. Invest Ophthalmol Vis Sci. 2005 Mar 1;46(3):803–7.

78. **Daya SM, Watson A, Sharpe JR, Giledi O, Rowe A, Martin R, et al.** - Outcomes and DNA analysis of ex vivo expanded stem cell allograft for ocular surface reconstruction. Ophthalmology. 2005 Mar;112(3):470–7.

79. **Sharpe JR, Daya SM, Dimitriadi M, Martin R, James SE**. - Survival of cultured allogeneic limbal epithelial cells following corneal repair. Tissue Eng. 2007 Jan;13(1):123–32.

80. **Thoft RA, Friend J**. - The X, Y, Z hypothesis of corneal epithelial maintenance. Invest Ophthalmol Vis Sci. 1983/10/01 ed. 1983;24(10):1442–3.

81. **Lehrer MS, Sun TT, Lavker RM**. - Strategies of epithelial repair: modulation of stem cell and transit amplifying cell proliferation. J Cell Sci. 1998 Oct;111 (Pt 1:2867–75.

82. **Beebe DC, Masters BR**. - Cell lineage and the differentiation of corneal epithelial cells. Invest Ophthalmol Vis Sci. 1996 Aug;37(9):1815–25.

83. **Mann I**. - A study of epithelial Regeneration in the living eye. Br J Ophthalmol. 1944 Jan;28(1):26–40.

84. **Buck RC**. - Measurement of centripetal migration of normal corneal epithelial cells in the mouse. Invest Ophthalmol Vis Sci. 1985/09/01 ed. 1985;26(9):1296–9.

85. **Lemp MA, Mathers WD**. - Corneal epithelial cell movement in humans. Eye (Lond). 1989 Jan;3 (Pt 4):438–45.

86. **Nagasaki T, Zhao J**. - Centripetal movement of corneal epithelial cells in the normal adult mouse. Invest Ophthalmol Vis Sci. 2003/01/31 ed. 2003;44(2):558–66.

87. **Collinson JM, Morris L, Reid AI, Ramaesh T, Keighren MA, Flockhart JH, et al.** - Clonal analysis of patterns of growth, stem cell activity, and cell movement during the development and maintenance of the murine corneal epithelium. Dev Dyn. 2002/08/31 ed. 2002;224(4):432–40.

88. **Dua HS, Watson NJ, Mathur RM, Forrester J V**. - Corneal epithelial cell migration in humans: “hurricane and blizzard keratopathy”. Eye (Lond). College of Ophthalmologists; 1993 Jan;7 (Pt 1)(1):53–8.

89. **Mort RL, Ramaesh T, Kleinjan DA, Morley SD, West JD**. - Mosaic analysis of stem cell function and wound healing in the mouse corneal epithelium. BMC Dev Biol. 2009 Jan;9(1):4.

90. **Hayashi Y, Watanabe N, Ohashi Y**. - The “replacement hypothesis”: corneal stem cell origin epithelia are replaced by limbal stem cell origin epithelia in mouse cornea during maturation. Cornea. 2012/10/17 ed. 2012;31 Suppl 1:S68–73.

91. **Tanifuji-Terai N, Terai K, Hayashi Y, Chikama T, Kao WW-Y**. - Expression of keratin 12 and maturation of corneal epithelium during development and postnatal growth. Invest Ophthalmol Vis Sci. 2006 Feb 1;47(2):545–51.

92. **Ren H, Wilson G**. - The effect of a shear force on the cell shedding rate of the corneal epithelium. Acta Ophthalmol Scand. 1997 Aug;75(4):383–7.

93. **Ren H, Wilson G**. - The cell shedding rate of the corneal epithelium--a comparison of collection methods. Curr Eye Res. 1996 Oct;15(10):1054–9.

94. **OMIM**. - OMIM Entry - # 204870 - Corneal Dystrophy, Gelatinous Drop-Like; GDLD [Internet]. 2010.

95. **Orphanet**. - Gelatinous drop-like corneal dystrophy [Internet]. 2012.

96. **Ide T, Nishida K, Maeda N, Tsujikawa M, Yamamoto S, Watanabe H, et al.** - A spectrum of clinical manifestations of gelatinous drop-like corneal dystrophy in japan. Am J Ophthalmol. 2004;137(6):1081–4.

97. **Tsujikawa M, Kurahashi H, Tanaka T, Okada M, Yamamoto S, Maeda N, et al.** - Homozygosity mapping of a gene responsible for gelatinous drop-like corneal dystrophy to chromosome 1p. Am J Hum Genet. 1998 Oct;63(4):1073–7.

98. **Tsujikawa M, Kurahashi H, Tanaka T, Nishida K, Shimomura Y, Tano Y, et al.** - Identification of the gene responsible for gelatinous drop-like corneal dystrophy. Nat Genet. 1999 Apr;21(4):420–3.

99. **Ide T, Nishida K, Maeda N, Tsujikawa M, Yamamoto S, Watanabe H, et al.** - A spectrum of clinical manifestations of gelatinous drop-like corneal dystrophy in japan. Am J Ophthalmol. 2004 Jun;137(6):1081–4.

100. **Tsujikawa M**. - Gelatinous drop-like corneal dystrophy. Cornea. 2012 Nov;31 Suppl 1:S37–40.

101. **Klintworth GK**. - Corneal dystrophies. Orphanet J Rare Dis. 2009 Jan;4(1):7.

102. **Kinoshita S, Nishida K, Dota A, Inatomi T, Koizumi N, Elliott A, et al.** - Epithelial barrier function and ultrastructure of gelatinous drop-like corneal dystrophy. Cornea. 2000 Jul;19(4):551–5.

103. **Quantock AJ, Nishida K, Kinoshita S**. - Histopathology of recurrent gelatinous drop-like corneal dystrophy. Cornea. 1998 Mar;17(2):215–21.

104. **Takaoka M, Nakamura T, Ban Y, Kinoshita S**. - Phenotypic investigation of cell junction-related proteins in gelatinous drop-like corneal dystrophy. Invest Ophthalmol Vis Sci. 2007 Mar;48(3):1095–101.

105. **Nakatsukasa M, Kawasaki S, Yamasaki K, Fukuoka H, Matsuda A, Tsujikawa M, et al.** - Tumor-associated calcium signal transducer 2 is required for the proper subcellular localization of claudin 1 and 7: implications in the pathogenesis of gelatinous drop-like corneal dystrophy. Am J Pathol. 2010 Sep;177(3):1344–55.

106. **Klintworth GK, Valnickova Z, Kielar RA, Baratz KH, Campbell RJ, Enghild JJ**. - Familial subepithelial corneal amyloidosis--a lactoferrin-related amyloidosis. Invest Ophthalmol Vis Sci. 1997 Dec;38(13):2756–63.

107. **Nishida K, Quantock AJ, Dota A, Choi-Miura NH, Kinoshita S**. - Apolipoproteins J and E co-localise with amyloid in gelatinous drop-like and lattice type I corneal dystrophies. Br J Ophthalmol. 1999 Oct;83(10):1178–82.

108. **Bersudsky V, Blum-Hareuveni T, Rehany U, Rumelt S**. - The profile of repeated corneal transplantation. Ophthalmology. 2001 Mar;108(3):461–9.

109. **Menzel-Severing J**. - Emerging techniques to treat corneal neovascularisation. Eye (Lond). Royal College of Ophthalmologists; 2012 Jan;26(1):2–12.

110. **Ambati BK, Nozaki M, Singh N, Takeda A, Jani PD, Suthar T, et al.** - Corneal avascularity is due to soluble VEGF receptor-1. Nature. 2006 Oct 26;443(7114):993–7.

111. **Van Buskirk EM**. - The anatomy of the limbus. Eye (Lond). College of Ophthalmologists; 1989 Jan;3 (Pt 2)(2):101–8.

112. **Gupta D, Illingworth C**. - Treatments for Corneal Neovascularization: A Review. Cornea. 2011 Mar 11;

113. **Kaye S, Choudhary A**. - Herpes simplex keratitis. Prog Retin Eye Res. 2006;25(4):355–80.

114. **Ma DH-K, Chen J-K, Zhang F, Lin K-Y, Yao J-Y, Yu J-S**. - Regulation of corneal angiogenesis in limbal stem cell deficiency. Prog Retin Eye Res. 2006;25(6):563–90.

115. **Nakao S, Kuwano T, Tsutsumi-Miyahara C, Ueda S, Kimura YN, Hamano S, et al.** - Infiltration of COX-2-expressing macrophages is a prerequisite for IL-1 beta-induced neovascularization and tumor growth. J Clin Invest. American Society for Clinical Investigation; 2005 Nov 1;115(11):2979–91.

116. **Philipp W, Speicher L, Humpel C**. - Expression of vascular endothelial growth factor and its receptors in inflamed and vascularized human corneas. Invest Ophthalmol Vis Sci. 2000 Aug;41(9):2514–22.

117. **Borderie VM, Boëlle P-Y, Touzeau O, Allouch C, Boutboul S, Laroche L**. - Predicted Long-term Outcome of Corneal Transplantation. Ophthalmology. 2009;116(12):2354–60.

118. **Maguire MG, Stark WJ, Gottsch JD, Stulting RD, Sugar A, Fink NE, et al.** - Risk factors for corneal graft failure and rejection in the collaborative corneal transplantation studies. Collaborative Corneal Transplantation Studies Research Group. Ophthalmology. 1994 Sep;101(9):1536–47.

119. **Williams KA, Lowe M, Bartlett C, Kelly T-L, Coster DJ**. - Risk factors for human corneal graft failure within the Australian corneal graft registry. Transplantation. 2008 Dec 27;86(12):1720–4.

120. **Rahman I, Carley F, Hillarby C, Brahma A, Tullo AB**. - Penetrating keratoplasty: indications, outcomes, and complications. Eye (Lond). 2009 Jun;23(6):1288–94.

121. **Bachmann B, Taylor RS, Cursiefen C**. - Corneal neovascularization as a risk factor for graft failure and rejection after keratoplasty: an evidence-based meta-analysis. Ophthalmology. 2010/07/08 ed. 2010;117(7):1300–5 e7.

122. **Cursiefen C**. - Immune privilege and angiogenic privilege of the cornea. Chem Immunol Allergy. 2007 Jan;92:50–7.

123. **Niederkorn JY**. - Corneal transplantation and immune privilege. Int Rev Immunol. Informa Healthcare New York; 2013 Feb 29;32(1):57–67.

124. **Dana M, Streilein J**. - Loss and restoration of immune privilege in eyes with corneal neovascularization. Invest Ophthalmol Vis Sci. 1996 Nov 1;37(12):2485–94.

125. **Niederkorn JY**. - High-risk corneal allografts and why they lose their immune privilege. Curr Opin Allergy Clin Immunol. 2010 Oct;10(5):493–7.

126. **Regina M, Zimmerman R, Malik G, Gausas R**. - Lymphangiogenesis concurrent with haemangiogenesis in the human cornea. Clin Experiment Ophthalmol. 2007 Aug;35(6):541–4.

127. **Dietrich T, Bock F, Yuen D, Hos D, Bachmann BO, Zahn G, et al.** - Cutting edge: lymphatic vessels, not blood vessels, primarily mediate immune rejections after transplantation. J Immunol. 2010 Jan 15;184(2):535–9.

128. **Albuquerque RJC, Hayashi T, Cho WG, Kleinman ME, Dridi S, Takeda A, et al.** - Alternatively spliced vascular endothelial growth factor receptor-2 is an essential endogenous inhibitor of lymphatic vessel growth. Nat Med. 2009 Sep;15(9):1023–30.

129. **Zheng Y, Lin H, Ling S**. - Clinicopathological correlation analysis of (lymph) angiogenesis and corneal graft rejection. Mol Vis. 2011 Jan;17:1694–700.

130. **Pillai CT, Dua HS, Hossain P**. - Fine Needle Diathermy Occlusion of Corneal Vessels. Invest Ophthalmol Vis Sci. 2000 Jul 1;41(8):2148–53.

131. **Brooks BJ, Ambati BK, Marcus DM, Ratanasit A**. - Photodynamic therapy for corneal neovascularisation and lipid degeneration. Br J Ophthalmol. 2004 Jun;88(6):840.

132. **Chang JH, Garg NK, Lunde E, Han KY, Jain S, Azar DT**. - Corneal neovascularization: an anti-VEGF therapy review. Surv Ophthalmol. 2012/08/18 ed. 2012;57(5):415–29.

133. **Ibraheem D, Elaissari A, Fessi H**. - Gene therapy and DNA delivery systems. Int J Pharm. 2013 Nov 25;

134. **Glover DJ, Lipps HJ, Jans DA**. - Towards safe, non-viral therapeutic gene expression in humans. Nat Rev Genet. 2005 Apr;6(4):299–310.

135. **Xu J, Amiji M**. - Therapeutic gene delivery and transfection in human pancreatic cancer cells using epidermal growth factor receptor-targeted gelatin nanoparticles. J Vis Exp. 2012 Jan;(59):e3612.

136. **Koirala A, Conley SM, Makkia R, Liu Z, Cooper MJ, Sparrow JR, et al.** - Persistence of non-viral vector mediated RPE65 expression: Case for viability as a gene transfer therapy for RPE-based diseases. J Control Release. 2013 Dec 28;172(3):745–52.

137. **McCarthy HO, Wang Y, Mangipudi SS, Hatefi A**. - Advances with the use of bio-inspired vectors towards creation of artificial viruses. Expert Opin Drug Deliv. Informa UK Ltd London, UK; 2010 Apr 23;7(4):497–512.

138. **Raper SE, Chirmule N, Lee FS, Wivel NA, Bagg A, Gao G, et al.** - Fatal systemic inflammatory response syndrome in a ornithine transcarbamylase deficient patient following adenoviral gene transfer. Mol Genet Metab. 80(1-2):148–58.

139. **Sun JY, Anand-Jawa V, Chatterjee S, Wong KK**. - Immune responses to adeno-associated virus and its recombinant vectors. Gene Ther. 2003 Jun;10(11):964–76.

140. **Tan MH, Smith AJ, Pawlyk B, Xu X, Liu X, Bainbridge JB, et al.** - Gene therapy for retinitis pigmentosa and Leber congenital amaurosis caused by defects in AIPL1: effective rescue of mouse models of partial and complete Aipl1 deficiency using AAV2/2 and AAV2/8 vectors. Hum Mol Genet. 2009 Jun 15;18(12):2099–114.

141. **Maguire AM, Simonelli F, Pierce EA, Pugh EN, Mingozzi F, Bennicelli J, et al.** - Safety and efficacy of gene transfer for Leber's congenital amaurosis. N Engl J Med. 2008 May 22;358(21):2240–8.

142. **Seo S, Mullins RF, Dumitrescu A V, Bhattarai S, Gratie D, Wang K, et al.** - Subretinal gene therapy of mice with Bardet-Biedl syndrome type 1. Invest Ophthalmol Vis Sci. 2013 Jan 11;54(9):6118–32.

143. **Bainbridge JWB, Smith AJ, Barker SS, Robbie S, Henderson R, Balaggan K, et al.** - Effect of gene therapy on visual function in Leber's congenital amaurosis. N Engl J Med. 2008 May 22;358(21):2231–9.

144. **Wang Y, Zheng C-G, Jiang Y, Zhang J, Chen J, Yao C, et al.** - Genetic correction of β-thalassemia patient-specific iPS cells and its use in improving hemoglobin production in irradiated SCID mice. Cell Res. 2012 Apr;22(4):637–48.

145. **Cullen BR**. - Is RNA interference involved in intrinsic antiviral immunity in mammals? Nat Immunol. 2006 Jun;7(6):563–7.

146. **Castanotto D, Sakurai K, Lingeman R, Li H, Shively L, Aagaard L, et al.** - Combinatorial delivery of small interfering RNAs reduces RNAi efficacy by selective incorporation into RISC. Nucleic Acids Res. 2007 Jan;35(15):5154–64.

147. **Grimm D, Streetz KL, Jopling CL, Storm TA, Pandey K, Davis CR, et al.** - Fatality in mice due to oversaturation of cellular microRNA/short hairpin RNA pathways. Nature. 2006 May 25;441(7092):537–41.

148. **Boudreau RL, Monteys AM, Davidson BL**. - Minimizing variables among hairpin-based RNAi vectors reveals the potency of shRNAs. RNA. 2008 Sep;14(9):1834–44.

149. **Fuchsluger TA, Jurkunas U, Kazlauskas A, Dana R**. - Corneal endothelial cells are protected from apoptosis by gene therapy. Hum Gene Ther. 2011 May;22(5):549–58.

150. **Zarogoulidis P, Darwiche K, Sakkas A, Yarmus L, Huang H, Li Q, et al.** - Suicide Gene Therapy for Cancer - Current Strategies. J Genet Syndr Gene Ther. 2013 Aug 9;4.

151. **McAlister JC, Joyce NC, Harris DL, Ali RR, Larkin DF**. - Induction of replication in human corneal endothelial cells by E2F2 transcription factor cDNA transfer. Invest Ophthalmol Vis Sci. 2005/09/28 ed. 2005;46(10):3597–603.

152. **Lai YK, Shen WY, Brankov M, Lai CM, Constable IJ, Rakoczy PE**. - Potential long-term inhibition of ocular neovascularisation by recombinant adeno-associated virus-mediated secretion gene therapy. Gene Ther. 2002/06/01 ed. 2002;9(12):804–13.

153. **Dalkara D, Kolstad KD, Guerin KI, Hoffmann N V, Visel M, Klimczak RR, et al.** - AAV mediated GDNF secretion from retinal glia slows down retinal degeneration in a rat model of retinitis pigmentosa. Mol Ther. 2011 Sep;19(9):1602–8.

154. **Trittibach P, Barker SE, Broderick CA, Natkunarajah M, Duran Y, Robbie SJ, et al.** - Lentiviral-vector-mediated expression of murine IL-1 receptor antagonist or IL-10 reduces the severity of endotoxin-induced uveitis. Gene Ther. 2008 Nov;15(22):1478–88.

155. **Kershaw MH, Westwood JA, Darcy PK**. - Gene-engineered T cells for cancer therapy. Nat Rev Cancer. 2013 Aug;13(8):525–41.

156. **Murphy SR, Chang CC, Dogbevia G, Bryleva EY, Bowen Z, Hasan MT, et al.** - Acat1 knockdown gene therapy decreases amyloid-β in a mouse model of Alzheimer's disease. Mol Ther. 2013 Aug;21(8):1497–506.

157. **Chtarto A, Bockstael O, Gebara E, Vermoesen K, Melas C, Pythoud C, et al.** - An adeno-associated virus-based intracellular sensor of pathological nuclear factor-κB activation for disease-inducible gene transfer. PLoS One. 2013 Jan;8(1):e53156.

158. **Jakobsson J, Georgievska B, Ericson C, Lundberg C**. - Lesion-dependent regulation of transgene expression in the rat brain using a human glial fibrillary acidic protein-lentiviral vector. Eur J Neurosci. 2004 Feb;19(3):761–5.

159. **Finn JD, Nichols TC, Svoronos N, Merricks EP, Bellenger DA, Zhou S, et al.** - The efficacy and the risk of immunogenicity of FIX Padua (R338L) in hemophilia B dogs treated by AAV muscle gene therapy. Blood. 2012 Nov 29;120(23):4521–3.

160. **Law LK, Davidson BL**. - What does it take to bind CAR? Mol Ther. 2005 Oct;12(4):599–609.

161. **Wickham TJ, Filardo EJ, Cheresh DA, Nemerow GR**. - Integrin alpha v beta 5 selectively promotes adenovirus mediated cell membrane permeabilization. J Cell Biol. 1994 Oct;127(1):257–64.

162. **Ugai H, Watanabe S, Suzuki E, Tsutsui-Nakata H, Yokoyama KK, Murata T**. - Stability of a Recombinant Adenoviral Vector: Optimization of Conditions for Storage, Transport and Delivery. Cancer Sci. 2002 May;93(5):598–603.

163. **Hartman ZC, Appledorn DM, Amalfitano A**. - Adenovirus vector induced innate immune responses: impact upon efficacy and toxicity in gene therapy and vaccine applications. Virus Res. 2007/11/27 ed. 2008;132(1-2):1–14.

164. **Kafri T, Morgan D, Krahl T, Sarvetnick N, Sherman L, Verma I**. - Cellular immune response to adenoviral vector infected cells does not require de novo viral gene expression: implications for gene therapy. Proc Natl Acad Sci U S A. 1998 Sep 15;95(19):11377–82.

165. **Tripathy SK, Black HB, Goldwasser E, Leiden JM**. - Immune responses to transgene–encoded proteins limit the stability of gene expression after injection of replication–defective adenovirus vectors. Nat Med. 1996 May;2(5):545–50.

166. **Alba R, Bosch A, Chillon M**. - Gutless adenovirus: last-generation adenovirus for gene therapy. Gene Ther. 2005 Oct;12 Suppl 1:S18–27.

167. **McCaffrey AP, Fawcett P, Nakai H, McCaffrey RL, Ehrhardt A, Pham T-TT, et al.** - The host response to adenovirus, helper-dependent adenovirus, and adeno-associated virus in mouse liver. Mol Ther. 2008 May;16(5):931–41.

168. **Ali RR, Reichel MB, Byrnes AP, Stephens CJ, Thrasher AJ, Baker D, et al.** - Co-injection of adenovirus expressing CTLA4-Ig prolongs adenovirally mediated lacZ reporter gene expression in the mouse retina. Gene Ther. 1998 Nov;5(11):1561–5.

169. **Sweigard JH, Cashman SM, Kumar-Singh R**. - Adenovirus vectors targeting distinct cell types in the retina. Invest Ophthalmol Vis Sci. 2010 Apr;51(4):2219–28.

170. **Xie Q, Bu W, Bhatia S, Hare J, Somasundaram T, Azzi A, et al.** - The atomic structure of adeno-associated virus (AAV-2), a vector for human gene therapy. Proc Natl Acad Sci U S A. 2002 Aug 6;99(16):10405–10.

171. **Gonçalves MAF V**. - Adeno-associated virus: from defective virus to effective vector. Virol J. 2005 Jan;2(1):43.

172. **Asokan A, Schaffer D V, Samulski RJ**. - The AAV vector toolkit: poised at the clinical crossroads. Mol Ther. The American Society of Gene & Cell Therapy; 2012 Apr;20(4):699–708.

173. **Rahim AA, Wong AMS, Hoefer K, Buckley SMK, Mattar CN, Cheng SH, et al.** - Intravenous administration of AAV2/9 to the fetal and neonatal mouse leads to differential targeting of CNS cell types and extensive transduction of the nervous system. FASEB J. 2011 Oct;25(10):3505–18.

174. **Bemelmans A-P, Duqué S, Rivière C, Astord S, Desrosiers M, Marais T, et al.** - A single intravenous AAV9 injection mediates bilateral gene transfer to the adult mouse retina. PLoS One. Public Library of Science; 2013 Jan 15;8(4):e61618.

175. **Allocca M, Doria M, Petrillo M, Colella P, Garcia-Hoyos M, Gibbs D, et al.** - Serotype-dependent packaging of large genes in adeno-associated viral vectors results in effective gene delivery in mice. J Clin Invest. 2008 May;118(5):1955–64.

176. **Lai Y, Yue Y, Duan D**. - Evidence for the failure of adeno-associated virus serotype 5 to package a viral genome > or = 8.2 kb. Mol Ther. 2010 Jan;18(1):75–9.

177. **Daya S, Berns KI**. - Gene therapy using adeno-associated virus vectors. Clin Microbiol Rev. 2008 Oct 1;21(4):583–93.

178. **Ylä-Herttuala S**. - Endgame: Glybera Finally Recommended for Approval as the First Gene Therapy Drug in the European Union. Mol Ther. The American Society of Gene & Cell Therapy; 2012 Oct;20(10):1831–2.

179. **Allocca M, Tessitore A, Cotugno G, Auricchio A**. - AAV-mediated gene transfer for retinal diseases. Expert Opin Biol Ther. Informa UK Ltd London, UK; 2006 Dec 22;6(12):1279–94.

180. **Buch PK, Bainbridge JW, Ali RR**. - AAV-mediated gene therapy for retinal disorders: from mouse to man. Gene Ther. 2008 Apr 17;15(11):849–57.

181. **Hauswirth WW, Aleman TS, Kaushal S, Cideciyan A V, Schwartz SB, Wang L, et al.** - Treatment of leber congenital amaurosis due to RPE65 mutations by ocular subretinal injection of adeno-associated virus gene vector: short-term results of a phase I trial. Hum Gene Ther. 2008 Oct;19(10):979–90.

182. **McCarty DM, Fu H, Monahan PE, Toulson CE, Naik P, Samulski RJ**. - Adeno-associated virus terminal repeat (TR) mutant generates self-complementary vectors to overcome the rate-limiting step to transduction in vivo. Gene Ther. 2003 Dec;10(26):2112–8.

183. **Natkunarajah M, Trittibach P, McIntosh J, Duran Y, Barker SE, Smith AJ, et al.** - Assessment of ocular transduction using single-stranded and self-complementary recombinant adeno-associated virus serotype 2/8. Gene Ther. 2008 Mar;15(6):463–7.

184. **Qing K, Hansen J, Weigel-Kelley KA, Tan M, Zhou S, Srivastava A**. - Adeno-associated virus type 2-mediated gene transfer: role of cellular FKBP52 protein in transgene expression. J Virol. 2001 Oct;75(19):8968–76.

185. **Ferrari FK, Samulski T, Shenk T, Samulski RJ**. - Second-strand synthesis is a rate-limiting step for efficient transduction by recombinant adeno-associated virus vectors. J Virol. 1996 May;70(5):3227–34.

186. **Zhong L, Zhao W, Wu J, Li B, Zolotukhin S, Govindasamy L, et al.** - A dual role of EGFR protein tyrosine kinase signaling in ubiquitination of AAV2 capsids and viral second-strand DNA synthesis. Mol Ther. 2007 Jul;15(7):1323–30.

187. **Zhong L, Li B, Mah CS, Govindasamy L, Agbandje-McKenna M, Cooper M, et al.** - Next generation of adeno-associated virus 2 vectors: point mutations in tyrosines lead to high-efficiency transduction at lower doses. Proc Natl Acad Sci U S A. 2008 Jun 3;105(22):7827–32.

188. **Markusic DM, Herzog RW, Aslanidi G V, Hoffman BE, Li B, Li M, et al.** - High-efficiency transduction and correction of murine hemophilia B using AAV2 vectors devoid of multiple surface-exposed tyrosines. Mol Ther. 2010 Dec;18(12):2048–56.

189. **Qiao C, Zhang W, Yuan Z, Shin J-H, Li J, Jayandharan GR, et al.** - Adeno-associated virus serotype 6 capsid tyrosine-to-phenylalanine mutations improve gene transfer to skeletal muscle. Hum Gene Ther. 2010 Oct;21(10):1343–8.

190. **Qiao C, Yuan Z, Li J, Tang R, Li J, Xiao X**. - Single tyrosine mutation in AAV8 and AAV9 capsids is insufficient to enhance gene delivery to skeletal muscle and heart. Hum Gene Ther Methods. 2012 Feb;23(1):29–37.

191. **Boye SE, Boye SL, Lewin AS, Hauswirth WW**. - A comprehensive review of retinal gene therapy. Mol Ther. 2013 Mar;21(3):509–19.

192. **Petrs-Silva H, Dinculescu A, Li Q, Min S-H, Chiodo V, Pang J-J, et al.** - High-efficiency transduction of the mouse retina by tyrosine-mutant AAV serotype vectors. Mol Ther. 2009 Mar;17(3):463–71.

193. **Kay CN, Ryals RC, Aslanidi G V, Min SH, Ruan Q, Sun J, et al.** - Targeting Photoreceptors via Intravitreal Delivery Using Novel, Capsid-Mutated AAV Vectors. PLoS One. 2013 Jan;8(4):e62097.

194. **Pang J, Dai X, Boye SE, Barone I, Boye SL, Mao S, et al.** - Long-term retinal function and structure rescue using capsid mutant AAV8 vector in the rd10 mouse, a model of recessive retinitis pigmentosa. Mol Ther. 2011 Feb;19(2):234–42.

195. **Boye SL, Peshenko I V, Huang WC, Min SH, McDoom I, Kay CN, et al.** - AAV-mediated gene therapy in the guanylate cyclase (RetGC1/RetGC2) double knockout mouse model of Leber congenital amaurosis. Hum Gene Ther. 2013 Feb;24(2):189–202.

196. **Mohan RR, Tovey JCK, Sharma A, Tandon A**. - Gene therapy in the cornea: 2005--present. Prog Retin Eye Res. 2012 Jan;31(1):43–64.

197. **Koerber JT, Klimczak R, Jang J-H, Dalkara D, Flannery JG, Schaffer D V**. - Molecular evolution of adeno-associated virus for enhanced glial gene delivery. Mol Ther. 2009 Dec;17(12):2088–95.

198. **Klimczak RR, Koerber JT, Dalkara D, Flannery JG, Schaffer D V**. - A novel adeno-associated viral variant for efficient and selective intravitreal transduction of rat Müller cells. Fugmann SD, editor. PLoS One. Public Library of Science; 2009 Jan;4(10):e7467.

199. **Byrne LC, Khalid F, Lee T, Zin EA, Greenberg KP, Visel M, et al.** - AAV-Mediated, Optogenetic Ablation of Müller Glia Leads to Structural and Functional Changes in the Mouse Retina. PLoS One. 2013 Jan;8(9):e76075.

200. **Wiznerowicz M, Trono D**. - Harnessing HIV for therapy, basic research and biotechnology. Trends Biotechnol. 2005 Jan;23(1):42–7.

201. **Segura MM, Mangion M, Gaillet B, Garnier A**. - New developments in lentiviral vector design, production and purification. Expert Opin Biol Ther. Informa UK, Ltd. London; 2013 Jul 7;13(7):987–1011.

202. **Scherdin U, Rhodes K, Breindl M**. - Transcriptionally active genome regions are preferred targets for retrovirus integration. J Virol. 1990 Feb;64(2):907–12.

203. **Holman AG, Coffin JM**. - Symmetrical base preferences surrounding HIV-1, avian sarcoma/leukosis virus, and murine leukemia virus integration sites. Proc Natl Acad Sci U S A. 2005 Apr 26;102(17):6103–7.

204. **Dull T, Zufferey R, Kelly M, Mandel RJ, Nguyen M, Trono D, et al.** - A third-generation lentivirus vector with a conditional packaging system. J Virol. 1998 Nov;72(11):8463–71.

205. **Zufferey R, Dull T, Mandel RJ, Bukovsky A, Quiroz D, Naldini L, et al.** - Self-inactivating lentivirus vector for safe and efficient in vivo gene delivery. J Virol. 1998/11/13 ed. 1998;72(12):9873–80.

206. **Akkina RK, Walton RM, Chen ML, Li QX, Planelles V, Chen IS**. - High-efficiency gene transfer into CD34+ cells with a human immunodeficiency virus type 1-based retroviral vector pseudotyped with vesicular stomatitis virus envelope glycoprotein G. J Virol. 1996 Apr;70(4):2581–5.

207. **Cartier N, Hacein-Bey-Abina S, Bartholomae CC, Bougnères P, Schmidt M, Kalle C Von, et al.** - Lentiviral hematopoietic cell gene therapy for X-linked adrenoleukodystrophy. Methods Enzymol. 2012 Jan;507:187–98.

208. **Cavazzana-Calvo M, Payen E, Negre O, Wang G, Hehir K, Fusil F, et al.** - Transfusion independence and HMGA2 activation after gene therapy of human β-thalassaemia. Nature. Nature Publishing Group, a division of Macmillan Publishers Limited. All Rights Reserved.; 2010 Sep 16;467(7313):318–22.

209. **Candotti F, Shaw KL, Muul L, Carbonaro D, Sokolic R, Choi C, et al.** - Gene therapy for adenosine deaminase-deficient severe combined immune deficiency: clinical comparison of retroviral vectors and treatment plans. Blood. 2012 Nov 1;120(18):3635–46.

210. **Boztug K, Schmidt M, Schwarzer A, Banerjee PP, Díez IA, Dewey RA, et al.** - Stem-cell gene therapy for the Wiskott-Aldrich syndrome. N Engl J Med. 2010 Nov 11;363(20):1918–27.

211. **Hacein-Bey-Abina S, Garrigue A, Wang GP, Soulier J, Lim A, Morillon E, et al.** - Insertional oncogenesis in 4 patients after retrovirus-mediated gene therapy of SCID-X1. J Clin Invest. 2008 Sep;118(9):3132–42.

212. **Cockrell AS, Kafri T**. - Gene delivery by lentivirus vectors. Mol Biotechnol. 2007 Jul;36(3):184–204.

213. **Romano G, Marino IR, Pentimalli F, Adamo V, Giordano A**. - Insertional mutagenesis and development of malignancies induced by integrating gene delivery systems: implications for the design of safer gene-based interventions in patients. Drug News Perspect. 2009 May;22(4):185–96.

214. **Yanez-Munoz RJ, Balaggan KS, MacNeil A, Howe SJ, Schmidt M, Smith AJ, et al.** - Effective gene therapy with nonintegrating lentiviral vectors. Nat Med. 2006/02/24 ed. 2006;12(3):348–53.

215. **Roorda A**. - Adaptive optics for studying visual function: a comprehensive review. J Vis. 2011 Jan;11(7).

216. **Niederkorn JY**. - Cornea: Window to Ocular Immunology. Curr Immunol Rev. 2011 Aug;7(3):328–35.

217. **Hori J, Vega JL, Masli S**. - Review of ocular immune privilege in the year 2010: modifying the immune privilege of the eye. Ocul Immunol Inflamm. 2010 Oct;18(5):325–33.

218. **Bainbridge JW, Ali RR**. - Success in sight: The eyes have it! Ocular gene therapy trials for LCA look promising. Gene Ther. 2008 Sep;15(17):1191–2.

219. **Oshima Y, Sakamoto T, Yamanaka I, Nishi T, Ishibashi T, Inomata H**. - Targeted gene transfer to corneal endothelium in vivo by electric pulse. Gene Ther. 1998 Oct;5(10):1347–54.

220. **Tan PH, Manunta M, Ardjomand N, Xue SA, Larkin DFP, Haskard DO, et al.** - Antibody targeted gene transfer to endothelium. J Gene Med. 2003 Apr;5(4):311–23.

221. **Hudde T, Rayner SA, Comer RM, Weber M, Isaacs JD, Waldmann H, et al.** - Activated polyamidoamine dendrimers, a non-viral vector for gene transfer to the corneal endothelium. Gene Ther. 1999 May;6(5):939–43.

222. **Collins L, Fabre JW**. - A synthetic peptide vector system for optimal gene delivery to corneal endothelium. J Gene Med. 2004 Feb;6(2):185–94.

223. **Hudde T, Rayner SA, De Alwis M, Thrasher AJ, Smith J, Coffin RS, et al.** - Adeno-associated and herpes simplex viruses as vectors for gene transfer to the corneal endothelium. Cornea. 2000 May;19(3):369–73.

224. **Liu J, Saghizadeh M, Tuli SS, Kramerov AA, Lewin AS, Bloom DC, et al.** - Different tropism of adenoviruses and adeno-associated viruses to corneal cells: implications for corneal gene therapy. Mol Vis. 2008 Jan;14:2087–96.

225. **Lai L, Lin K, Foulks G, Ma L, Xiao X, Chen K**. - Highly efficient ex vivo gene delivery into human corneal endothelial cells by recombinant adeno-associated virus. Curr Eye Res. 2005 Mar;30(3):213–9.

226. **Tsai M-L, Chen S-L, Chou P-I, Wen L-Y, Tsai RJ-F, Tsao Y-P**. - Inducible Adeno-Associated Virus Vector-Delivered Transgene Expression in Corneal Endothelium. Invest Ophthalmol Vis Sci. 2002 Mar 1;43(3):751–7.

227. **Larkin DF, Oral HB, Ring CJ, Lemoine NR, George AJ**. - Adenovirus-mediated gene delivery to the corneal endothelium. Transplantation. 1996/02/15 ed. 1996;61(3):363–70.

228. **Kampik D, Ali RR, Larkin DF**. - Experimental gene transfer to the corneal endothelium. Exp Eye Res. 2011/07/23 ed. 2012;95(1):54–9.

229. **Jessup CF, Brereton HM, Coster DJ, Williams KA**. - In vitro adenovirus mediated gene transfer to the human cornea. Br J Ophthalmol. 2005 Jun;89(6):658–61.

230. **Klebe S, Sykes PJ, Coster DJ, Krishnan R, Williams KA**. - Prolongation of sheep corneal allograft survival by ex vivo transfer of the gene encoding interleukin-10. Transplantation. 2001 May 15;71(9):1214–20.

231. **Bainbridge JW, Stephens C, Parsley K, Demaison C, Halfyard A, Thrasher AJ, et al.** - In vivo gene transfer to the mouse eye using an HIV-based lentiviral vector; efficient long-term transduction of corneal endothelium and retinal pigment epithelium. Gene Ther. 2001 Nov;8(21):1665–8.

232. **Parker DG, Kaufmann C, Brereton HM, Anson DS, Francis-Staite L, Jessup CF, et al.** - Lentivirus-mediated gene transfer to the rat, ovine and human cornea. Gene Ther. 2007/02/16 ed. 2007;14(9):760–7.

233. **Rayner SA, Larkin DF, George AJ**. - TNF receptor secretion after ex vivo adenoviral gene transfer to cornea and effect on in vivo graft survival. Invest Ophthalmol Vis Sci. 2001 Jun;42(7):1568–73.

234. **Gong N, Pleyer U, Vogt K, Anegon I, Flügel A, Volk H-D, et al.** - Local overexpression of nerve growth factor in rat corneal transplants improves allograft survival. Invest Ophthalmol Vis Sci. 2007 Mar;48(3):1043–52.

235. **Beutelspacher SC, Pillai R, Watson MP, Tan PH, Tsang J, McClure MO, et al.** - Function of indoleamine 2,3-dioxygenase in corneal allograft rejection and prolongation of allograft survival by over-expression. Eur J Immunol. 2006 Mar;36(3):690–700.

236. **Albon J, Tullo AB, Aktar S, Boulton ME**. - Apoptosis in the endothelium of human corneas for transplantation. Invest Ophthalmol Vis Sci. 2000 Sep;41(10):2887–93.

237. **Crewe JM, Armitage WJ**. - Integrity of epithelium and endothelium in organ-cultured human corneas. Invest Ophthalmol Vis Sci. 2001 Jul;42(8):1757–61.

238. **Barcia RN, Dana MR, Kazlauskas A**. - Corneal graft rejection is accompanied by apoptosis of the endothelium and is prevented by gene therapy with bcl-xL. Am J Transplant. 2007 Sep;7(9):2082–9.

239. **Fuchsluger TA, Jurkunas U, Kazlauskas A, Dana R**. - Corneal endothelial cells are protected from apoptosis by gene therapy. Hum Gene Ther. 2010/12/17 ed. 2011;22(5):549–58.

240. **Fuchsluger TA, Jurkunas U, Kazlauskas A, Dana R**. - Anti-apoptotic gene therapy prolongs survival of corneal endothelial cells during storage. Gene Ther. 2011 Aug;18(8):778–87.

241. **Joyce NC, Harris DL, Mc Alister JC, Ali RR, Larkin DFP**. - Effect of overexpressing the transcription factor E2F2 on cell cycle progression in rabbit corneal endothelial cells. Invest Ophthalmol Vis Sci. 2004 May;45(5):1340–8.

242. **Joyce NC, Harris DL**. - Decreasing expression of the G1-phase inhibitors, p21Cip1 and p16INK4a, promotes division of corneal endothelial cells from older donors. Mol Vis. 2010 Jan;16:897–906.

243. **Blair-Parks K, Weston BC, Dean DA**. - High-level gene transfer to the cornea using electroporation. J Gene Med. 4(1):92–100.

244. **Oshima Y, Sakamoto T, Hisatomi T, Tsutsumi C, Sassa Y, Ishibashi T, et al.** - Targeted Gene Transfer to Corneal Stroma in vivo by Electric Pulses. Exp Eye Res. 2002;74(2):191–8.

245. **Sonoda S, Tachibana K, Uchino E, Okubo A, Yamamoto M, Sakoda K, et al.** - Gene transfer to corneal epithelium and keratocytes mediated by ultrasound with microbubbles. Invest Ophthalmol Vis Sci. 2006 Feb 1;47(2):558–64.

246. **Singh N, Amin S, Richter E, Rashid S, Scoglietti V, Jani PD, et al.** - Flt-1 intraceptors inhibit hypoxia-induced VEGF expression in vitro and corneal neovascularization in vivo. Invest Ophthalmol Vis Sci. 2005 May;46(5):1647–52.

247. **De la Fuente M, Seijo B, Alonso MJ**. - Novel hyaluronic acid-chitosan nanoparticles for ocular gene therapy. Invest Ophthalmol Vis Sci. 2008 May;49(5):2016–24.

248. **Carlson EC**. - In Vivo Gene Delivery and Visualization of Corneal Stromal Cells Using an Adenoviral Vector and Keratocyte-Specific Promoter. Invest Ophthalmol Vis Sci. 2004 Jul 1;45(7):2194–200.

249. **Bemelmans A-P, Arsenijevic Y, Majo F**. - Efficient lentiviral gene transfer into corneal stroma cells using a femtosecond laser. Gene Ther. Nature Publishing Group; 2009 Jul 23;16(7):933–8.

250. **Sharma A, Tovey JCK, Ghosh A, Mohan RR**. - AAV serotype influences gene transfer in corneal stroma in vivo. Exp Eye Res. 2010;91(3):440–8.

251. **Sharma A, Tovey JC, Ghosh A, Mohan RR**. - AAV serotype influences gene transfer in corneal stroma in vivo. Exp Eye Res. 2010/07/06 ed. 2010;91(3):440–8.

252. **Mohan RR, Sharma A, Cebulko TC, Tandon A**. - Vector delivery technique affects gene transfer in the cornea in vivo. Mol Vis. 2010 Jan;16:2494–501.

253. **Hippert C, Ibanes S, Serratrice N, Court F, Malecaze F, Kremer EJ, et al.** - Corneal transduction by intra-stromal injection of AAV vectors in vivo in the mouse and ex vivo in human explants. PLoS One. 2012/04/24 ed. 2012;7(4):e35318.

254. **Seitz B, Moreira L, Baktanian E, Sanchez D, Gray B, Gordon EM, et al.** - Retroviral vector-mediated gene transfer into keratocytes in vitro and in vivo. Am J Ophthalmol. 1998;126(5):630–9.

255. **Behrens A, Gordon EM, Li L, Liu PX, Chen Z, Peng H, et al.** - Retroviral Gene Therapy Vectors for Prevention of Excimer Laser-Induced Corneal Haze. Invest Ophthalmol Vis Sci. 2002 Apr 1;43(4):968–77.

256. **Song JC, McDonnell PJ, Gordon EM, Hall FL, Anderson WF**. - Phase I/II evaluation of safety and efficacy of a matrix-targeted retroviral vector bearing a

dominant negative cyclin G1 construct (Md-dnG1) as adjunctive intervention for superficial corneal opacity/corneal scarring. Hum Gene Ther. 2003 Feb 10;14(3):306–9.

257. **Sakamoto T, Ueno H, Sonoda K, Hisatomi T, Shimizu K, Ohashi H, et al.** - Blockade of TGF-beta by in vivo gene transfer of a soluble TGF-beta type II receptor in the muscle inhibits corneal opacification, edema and angiogenesis. Gene Ther. 2000 Nov;7(22):1915–24.

258. **Mohan RR, Tandon A, Sharma A, Cowden JW, Tovey JCK**. - Significant inhibition of corneal scarring in vivo with tissue-selective, targeted AAV5 decorin gene therapy. Invest Ophthalmol Vis Sci. 2011 Jun 1;52(7):4833–41.

259. **Tandon A, Sharma A, Rodier JT, Klibanov AM, Rieger FG, Mohan RR**. - BMP7 gene transfer via gold nanoparticles into stroma inhibits corneal fibrosis in vivo. Connon CJ, editor. PLoS One. Public Library of Science; 2013 Jan;8(6):e66434.

260. **Lai L-J, Xiao X, Wu JH**. - Inhibition of corneal neovascularization with endostatin delivered by adeno-associated viral (AAV) vector in a mouse corneal injury model. J Biomed Sci. 2007 May;14(3):313–22.

261. **Yoon KC, Bae JA, Park HJ, Im SK, Oh HJ, Lin XH, et al.** - Subconjunctival gene delivery of the transcription factor GA-binding protein delays corneal neovascularization in a mouse model. Gene Ther. 2009 Aug;16(8):973–81.

262. **Cheng H-C, Yeh S-I, Tsao Y-P, Kuo P-C**. - Subconjunctival injection of recombinant AAV-angiostatin ameliorates alkali burn induced corneal angiogenesis. Mol Vis. 2007 Jan;13:2344–52.

263. **Yoon KC, Ahn KY, Lee JH, Chun BJ, Park SW, Seo MS, et al.** - Lipid-mediated delivery of brain-specific angiogenesis inhibitor 1 gene reduces corneal neovascularization in an in vivo rabbit model. Gene Ther. 2005 Apr;12(7):617–24.

264. **Mohan RR, Tovey JCK, Sharma A, Schultz GS, Cowden JW, Tandon A**. - Targeted decorin gene therapy delivered with adeno-associated virus effectively retards corneal neovascularization in vivo. PLoS One. 2011 Jan;6(10):e26432.

265. **Stechschulte SU, Joussen AM, von Recum HA, Poulaki V, Moromizato Y, Yuan J, et al.** - Rapid Ocular Angiogenic Control via Naked DNA Delivery to Cornea. Invest Ophthalmol Vis Sci. 2001 Aug 1;42(9):1975–9.

266. **Qazi Y, Stagg B, Singh N, Singh S, Zhang X, Luo L, et al.** - Nanoparticle-mediated delivery of shRNA.VEGF-a plasmids regresses corneal neovascularization. Invest Ophthalmol Vis Sci. 2012 May;53(6):2837–44.

267. **Yu H, Wu J, Li H, Wang Z, Chen X, Tian Y, et al.** - Inhibition of corneal neovascularization by recombinant adenovirus-mediated sFlk-1 expression. Biochem Biophys Res Commun. 2007 Oct 5;361(4):946–52.

268. **Zagon IS, Sassani JW, Verderame MF, McLaughlin PJ**. - Particle-mediated gene transfer of opioid growth factor receptor cDNA regulates cell proliferation of the corneal epithelium. Cornea. 2005 Jul;24(5):614–9.

269. **Ljubimov A V., Hao J, Li SK, Kao WWY, Liu C-Y**. - Gene delivery to cornea. Brain Res Bull. 2010;81(2):256–61.

270. **Rosenblatt MI, Azar DT**. - Gene therapy of the corneal epithelium. Int Ophthalmol Clin. 2004 Jan;44(3):81–90.

271. **Tanelian DL, Barry MA, Johnston SA, Le T, Smith G**. - Controlled gene gun delivery and expression of DNA within the cornea. Biotechniques. 1997 Sep;23(3):484–8.

272. **Johnson LN, Cashman SM, Kumar-Singh R**. - Cell-penetrating peptide for enhanced delivery of nucleic acids and drugs to ocular tissues including retina and cornea. Mol Ther. The American Society of Gene Therapy; 2008 Jan 9;16(1):107–14.

273. **Tong Y-C, Chang S-F, Liu C-Y, Kao WW-Y, Huang CH, Liaw J**. - Eye drop delivery of nano-polymeric micelle formulated genes with cornea-specific promoters. J Gene Med. 2007 Nov;9(11):956–66.

274. **Spencer B, Agarwala S, Miskulin M, Smith M, Brandt CR**. - Herpes simplex virus-mediated gene delivery to the rodent visual system. Invest Ophthalmol Vis Sci. 2000 May;41(6):1392–401.

275. **Tsubota K, Inoue H, Ando K, Ono M, Yoshino K, Saito I**. - Adenovirus-mediated gene transfer to the ocular surface epithelium. Exp Eye Res. 1998 Nov;67(5):531–8.

276. **Danjo Y, Gipson IK**. - Specific Transduction of the Leading Edge Cells of Migrating Epithelia Demonstrates That They are Replaced During Healing. Exp Eye Res. 2002;74(2):199–204.

277. **Wang X, Appukuttan B, Ott S, Patel R, Irvine J, Song J, et al.** - Efficient and sustained transgene expression in human corneal cells mediated by a lentiviral vector. Gene Ther. 2000/03/01 ed. 2000;7(3):196–200.

278. **Li Y, Song Y, Zhao L, Gaidosh G, Laties AM, Wen R**. - Direct labeling and visualization of blood vessels with lipophilic carbocyanine dye DiI. Nat Protoc. 2008/10/11 ed. 2008;3(11):1703–8.

279. **Pollard VW, Malim MH**. - The HIV-1 Rev protein. Annu Rev Microbiol. 1999/01/19 ed. 1998;52:491–532.

280. **Van Maele B, De Rijck J, De Clercq E, Debyser Z**. - Impact of the central polypurine tract on the kinetics of human immunodeficiency virus type 1 vector transduction. J Virol. 2003 Apr;77(8):4685–94.

281. **Wang X, Appukuttan B, Ott S, Patel R, Irvine J, Song J, et al.** - Efficient and sustained transgene expression in human corneal cells mediated by a lentiviral vector. Gene Ther. 2000 Mar;7(3):196–200.

282. **Haberichter T, Madge B, Christopher RA, Yoshioka N, Dhiman A, Miller R, et al.** - A systems biology dynamical model of mammalian G1 cell cycle progression. Mol Syst Biol. 2007/02/15 ed. 2007;3:84.

283. **Wang WK, Chen MY, Chuang CY, Jeang KT, Huang LM**. - Molecular biology of human immunodeficiency virus type 1. J Microbiol Immunol Infect. 2000/10/25 ed. 2000;33(3):131–40.

284. **Charneau P, Alizon M, Clavel F**. - A second origin of DNA plus-strand synthesis is required for optimal human immunodeficiency virus replication. J Virol. 1992 May;66(5):2814–20.

285. **Zennou V, Petit C, Guetard D, Nerhbass U, Montagnier L, Charneau P**. - HIV-1 genome nuclear import is mediated by a central DNA flap. Cell. 2000 Apr 14;101(2):173–85.

286. **Singer RH, Penman S**. - Messenger RNA in HeLa cells: kinetics of formation and decay. J Mol Biol. 1973 Aug 5;78(2):321–34.

287. **Ross J**. - mRNA stability in mammalian cells. Microbiol Rev. 1995 Oct;59(3):423–50.

288. **Galla M, Will E, Kraunus J, Chen L, Baum C**. - Retroviral pseudotransduction for targeted cell manipulation. Mol Cell. 2004/10/21 ed. 2004;16(2):309–15.

289. **Toti P, Tosi GM, Traversi C, Schürfeld K, Cardone C, Caporossi A**. - CD-34 stromal expression pattern in normal and altered human corneas. Ophthalmology. 2002 Jun;109(6):1167–71.

290. **Sosnová M, Bradl M, Forrester J V**. - CD34+ corneal stromal cells are bone marrow-derived and express hemopoietic stem cell markers. Stem Cells. 2005 Apr;23(4):507–15.

291. **Ren H, Wilson G**. - Apoptosis in the corneal epithelium. Invest Ophthalmol Vis Sci. 1996 May;37(6):1017–25.

292. **Morris L, Graham C, Gordon S**. - Macrophages in haemopoietic and other tissues of the developing mouse detected by the monoclonal antibody F4/80. Development. 1991 Jun 1;112(2):517–26.

293. **Keadle TL, Stuart PM**. - Interleukin-10 (IL-10) ameliorates corneal disease in a mouse model of recurrent herpetic keratitis. Microb Pathog. 2005 Jan;38(1):13–21.

294. **Henriksson JT, McDermott AM, Bergmanson JP**. - Dimensions and morphology of the cornea in three strains of mice. Invest Ophthalmol Vis Sci. 2009/03/07 ed. 2009;50(8):3648–54.

295. **Petrs-Silva H, Dinculescu A, Li Q, Min SH, Chiodo V, Pang JJ, et al.** - High-efficiency transduction of the mouse retina by tyrosine-mutant AAV serotype vectors. Mol Ther. 2008/12/11 ed. 2009;17(3):463–71.

296. **Helena MC, Baerveldt F, Kim WJ, Wilson SE**. - Keratocyte apoptosis after corneal surgery. Invest Ophthalmol Vis Sci. 1998 Feb;39(2):276–83.

297. **Wilson SE, Pedroza L, Beuerman R, Hill JM**. - Herpes simplex virus type-1 infection of corneal epithelial cells induces apoptosis of the underlying keratocytes. Exp Eye Res. 1997 May;64(5):775–9.

298. **Wilson SE, Liu JJ, Mohan RR**. - Stromal-epithelial interactions in the cornea. Prog Retin Eye Res. 1999 May;18(3):293–309.

299. **Stylianou E, Saklatvala J**. - Interleukin-1. Int J Biochem Cell Biol. 1998;30(10):1075–9.

300. **Lai CM, Brankov M, Zaknich T, Lai YK, Shen WY, Constable IJ, et al.** - Inhibition of angiogenesis by adenovirus-mediated sFlt-1 expression in a rat model of corneal neovascularization. Hum Gene Ther. 2001 Jul 1;12(10):1299–310.

301. **O'Reilly MS, Boehm T, Shing Y, Fukai N, Vasios G, Lane WS, et al.** - Endostatin: an endogenous inhibitor of angiogenesis and tumor growth. Cell. 1997 Jan 24;88(2):277–85.

302. **Sulochana KN, Fan H, Jois S, Subramanian V, Sun F, Kini RM, et al.** - Peptides derived from human decorin leucine-rich repeat 5 inhibit angiogenesis. J Biol Chem. 2005 Jul 29;280(30):27935–48.

303. **Singh N, Amin S, Richter E, Rashid S, Scoglietti V, Jani PD, et al.** - Flt-1 intraceptors inhibit hypoxia-induced VEGF expression in vitro and corneal neovascularization in vivo. Invest Ophthalmol Vis Sci. 2005 May 1;46(5):1647–52.

304. **Cho YK, Uehara H, Young JR, Archer B, Zhang X, Ambati BK**. - Vascular endothelial growth factor receptor 1 morpholino decreases angiogenesis in a murine corneal suture model. Invest Ophthalmol Vis Sci. 2012 Feb;53(2):685–92.

305. **Zuo L, Fan Y, Wang F, Gu Q, Xu X**. - A siRNA targeting vascular endothelial growth factor-A inhibiting experimental corneal neovascularization. Curr Eye Res. 2010 May;35(5):375–84.

306. **Bachmann BO, Bock F, Wiegand SJ, Maruyama K, Dana MR, Kruse FE, et al.** - Promotion of graft survival by vascular endothelial growth factor a neutralization after high-risk corneal transplantation. Arch Ophthalmol. American Medical Association; 2008 Jan 1;126(1):71–7.

307. **Niu X, Wang W, Shi W, Xie L**. - [Inhibition of corneal neovascularization by liposomes mediated plasmid encoding human endostatin]. Zhonghua Yan Ke Za Zhi. 2005 Mar;41(3):260–4.

308. **Iriyama A, Usui T, Yanagi Y, Amano S, Oba M, Miyata K, et al.** - Gene transfer using micellar nanovectors inhibits corneal neovascularization in vivo. Cornea. 2011 Dec;30(12):1423–7.

309. **Nishikawa M, Takakura Y, Hashida M**. - Pharmacokinetics of plasmid DNA-based non-viral gene medicine. Adv Genet. 2005 Jan;53:47–68.

310. **Cursiefen C, Chen L, Borges LP, Jackson D, Cao J, Radziejewski C, et al.** - VEGF-A stimulates lymphangiogenesis and hemangiogenesis in inflammatory neovascularization via macrophage recruitment. J Clin Invest. 2004 Apr;113(7):1040–50.

311. **Olsson A-K, Dimberg A, Kreuger J, Claesson-Welsh L**. - VEGF receptor signalling - in control of vascular function. Nat Rev Mol Cell Biol. 2006 May;7(5):359–71.

312. **Nagy JA, Vasile E, Feng D, Sundberg C, Brown LF, Detmar MJ, et al.** - Vascular permeability factor/vascular endothelial growth factor induces lymphangiogenesis as well as angiogenesis. J Exp Med. 2002 Dec 2;196(11):1497–506.

313. **Hong Y-K, Lange-Asschenfeldt B, Velasco P, Hirakawa S, Kunstfeld R, Brown LF, et al.** - VEGF-A promotes tissue repair-associated lymphatic vessel formation via VEGFR-2 and the alpha1beta1 and alpha2beta1 integrins. FASEB J. 2004 Jul;18(10):1111–3.

314. **Maruyama K, Asai J, Ii M, Thorne T, Losordo DW, D'Amore PA**. - Decreased Macrophage Number and Activation Lead to Reduced Lymphatic Vessel Formation and Contribute to Impaired Diabetic Wound Healing. Am J Pathol. 2007;170(4):1178–91.

315. **Maruyama K, Ii M, Cursiefen C, Jackson DG, Keino H, Tomita M, et al.** - Inflammation-induced lymphangiogenesis in the cornea arises from CD11b-positive macrophages. J Clin Invest. American Society for Clinical Investigation; 2005 Sep 1;115(9):2363–72.

316. **Bock F, Onderka J, Dietrich T, Bachmann B, Kruse FE, Paschke M, et al.** - Bevacizumab as a potent inhibitor of inflammatory corneal angiogenesis and lymphangiogenesis. Invest Ophthalmol Vis Sci. 2007 Jun 1;48(6):2545–52.

317. **Nakao S, Maruyama K, Zandi S, Melhorn MI, Taher M, Noda K, et al.** - Lymphangiogenesis and angiogenesis: concurrence and/or dependence? Studies in inbred mouse strains. FASEB J. 2010 Feb 1;24(2):504–13.

318. **Regenfuss B, Onderka J, Bock F, Hos D, Maruyama K, Cursiefen C**. - Genetic heterogeneity of lymphangiogenesis in different mouse strains. Am J Pathol. 2010 Jul;177(1):501–10.

319. **Tarallo V, Bogdanovich S, Hirano Y, Tudisco L, Zentilin L, Giacca M, et al.** - Inhibition of choroidal and corneal pathologic neovascularization by Plgf1-de gene transfer. Invest Ophthalmol Vis Sci. 2012 Dec 5;53(13):7989–96.

320. **Albuquerque RJC, Hayashi T, Cho WG, Kleinman ME, Dridi S, Takeda A, et al.** - Alternatively spliced vascular endothelial growth factor receptor-2 is an essential endogenous inhibitor of lymphatic vessel growth. Nat Med. Nature Publishing Group; 2009 Sep;15(9):1023–30.

321. **Uehara H, Cho Y, Simonis J, Cahoon J, Archer B, Luo L, et al.** - Dual suppression of hemangiogenesis and lymphangiogenesis by splice-shifting morpholinos targeting vascular endothelial growth factor receptor 2 (KDR). FASEB J. 2013 Jan;27(1):76–85.

322. **Mouawad R, Spano J-P, Comperat E, Capron F, Khayat D**. - Tumoural expression and circulating level of VEGFR-3 (Flt-4) in metastatic melanoma patients: Correlation with clinical parameters and outcome. Eur J Cancer. 2009;45(8):1407–14.

323. **Singh N, Tiem M, Watkins R, Cho YK, Wang Y, Olsen T, et al.** - Soluble vascular endothelial growth factor receptor 3 is essential for corneal alymphaticity. Blood. 2013 May 16;121(20):4242–9.

324. **Igarashi T, Miyake K, Suzuki N, Kato K, Takahashi H, Ohara K, et al.** - New strategy for in vivo transgene expression in corneal epithelial progenitor cells. Informa UK Ltd UK; 2009 Jul 2;

325. **Mort RL, Douvaras P, Morley SD, Dorà N, Hill RE, Collinson JM, et al.** - Stem cells and corneal epithelial maintenance: insights from the mouse and other animal models. Results Probl Cell Differ. 2012 Jan;55:357–94.

326. **Buck RC**. - Measurement of centripetal migration of normal corneal epithelial cells in the mouse. Invest Ophthalmol Vis Sci. 1985 Sep;26(9):1296–9.

327. **Henriksson JT, McDermott AM, Bergmanson JPG**. - Dimensions and morphology of the cornea in three strains of mice. Invest Ophthalmol Vis Sci. 2009 Aug;50(8):3648–54.

328. **Kinoshita S, Friend J, Thoft RA**. - Sex chromatin of donor corneal epithelium in rabbits. Invest Ophthalmol Vis Sci. 1981 Sep;21(3):434–41.

329. **Goldberg MF, Bron AJ**. - Limbal palisades of Vogt. Trans Am Ophthalmol Soc. 1982 Jan;80:155–71.

330. **Lathrop KL, Gupta D, Kagemann L, Schuman JS, Sundarraj N**. - Optical coherence tomography as a rapid, accurate, noncontact method of visualizing the palisades of Vogt. Invest Ophthalmol Vis Sci. 2012 Mar;53(3):1381–7.

331. **Endo M, Zoltick PW, Chung DC, Bennett J, Radu A, Muvarak N, et al.** - Gene transfer to ocular stem cells by early gestational intraamniotic injection of lentiviral vector. Mol Ther. 2007 Mar;15(3):579–87.

332. **Carmo M, Alves A, Rodrigues AF, Coroadinha AS, Carrondo MJT, Alves PM, et al.** - Stabilization of gammaretroviral and lentiviral vectors: from production to gene transfer. J Gene Med. 2009 Aug;11(8):670–8.

333. **Herbst F, Ball CR, Tuorto F, Nowrouzi A, Wang W, Zavidij O, et al.** - Extensive methylation of promoter sequences silences lentiviral transgene expression during stem cell differentiation in vivo. Mol Ther. 2012 May;20(5):1014–21.

334. **Weber K, Thomaschewski M, Benten D, Fehse B**. - RGB marking with lentiviral vectors for multicolor clonal cell tracking. Nat Protoc. 2012/04/07 ed. 2012;7(5):839–49.

335. **Weber K, Thomaschewski M, Warlich M, Volz T, Cornils K, Niebuhr B, et al.** - RGB marking facilitates multicolor clonal cell tracking. Nat Med. Nature Publishing Group, a division of Macmillan Publishers Limited. All Rights Reserved.; 2011 Apr;17(4):504–9.

336. **Gipson IK, Grill SM**. - A technique for obtaining sheets of intact rabbit corneal epithelium. Invest Ophthalmol Vis Sci. 1982 Aug;23(2):269–73.

337. **Spurr SJ, Gipson IK**. - Isolation of corneal epithelium with Dispase II or EDTA. Effects on the basement membrane zone. Invest Ophthalmol Vis Sci. 1985 Jun;26(6):818–27.

338. **Espana EM, Romano AC, Kawakita T, Di Pascuale M, Smiddy R, Tseng SCG**. - Novel enzymatic isolation of an entire viable human limbal epithelial sheet. Invest Ophthalmol Vis Sci. 2003 Oct;44(10):4275–81.

339. **Koizumi N, Rigby H, Fullwood NJ, Kawasaki S, Tanioka H, Koizumi K, et al.** - Comparison of intact and denuded amniotic membrane as a substrate for cell-suspension culture of human limbal epithelial cells. Graefes Arch Clin Exp Ophthalmol. 2007 Jan;245(1):123–34.

340. **Kobayashi T, Yoshioka R, Shiraishi A, Ohashi Y**. - New technique for culturing corneal epithelial cells of normal mice. Mol Vis. 2009 Jan;15:1589–93.

341. **Hayashi S, Osawa T, Tohyama K**. - Comparative observations on corneas, with special reference to Bowman's layer and Descemet's membrane in mammals and amphibians. J Morphol. 2002 Dec;254(3):247–58.

342. **Bartholomae CC, Arens A, Balaggan KS, Yáñez-Muñoz RJ, Montini E, Howe SJ, et al.** - Lentiviral vector integration profiles differ in rodent postmitotic tissues. Mol Ther. The American Society of Gene & Cell Therapy; 2011 Apr;19(4):703–10.

343. **Schmidt M, Schwarzwaelder K, Bartholomae C, Zaoui K, Ball C, Pilz I, et al.** - High-resolution insertion-site analysis by linear amplification-mediated PCR (LAM-PCR). Nat Methods. Nature Publishing Group; 2007 Dec;4(12):1051–7.

344. **Hamill CE, Schmedt T, Jurkunas U**. - Fuchs Endothelial Cornea Dystrophy: A Review of the Genetics Behind Disease Development. Informa Healthcare USA, Inc. New York; 2013 Oct 18;

345. **Aldave AJ, Han J, Frausto RF**. - Genetics of the corneal endothelial dystrophies: an evidence-based review. Clin Genet. 2013 Aug;84(2):109–19.

346. **Jun AS, Meng H, Ramanan N, Matthaei M, Chakravarti S, Bonshek R, et al.** - An alpha 2 collagen VIII transgenic knock-in mouse model of Fuchs endothelial corneal dystrophy shows early endothelial cell unfolded protein response and apoptosis. Hum Mol Genet. 2012 Jan 15;21(2):384–93.

347. **Meng H, Matthaei M, Ramanan N, Grebe R, Chakravarti S, Speck CL, et al.** - L450W and Q455K Col8a2 knock-in mouse models of Fuchs endothelial corneal dystrophy show distinct phenotypes and evidence for altered autophagy. Invest Ophthalmol Vis Sci. 2013 Mar 28;54(3):1887–97.

348. **Jun AS, Chakravarti S, Edelhauser HF, Kimos M**. - Aging changes of mouse corneal endothelium and Descemet's membrane. Exp Eye Res. 2006;83(4):890–6.

349. **Heckl D, Schwarzer A, Haemmerle R, Steinemann D, Rudolph C, Skawran B, et al.** - Lentiviral vector induced insertional haploinsufficiency of Ebf1 causes murine leukemia. Mol Ther. 2012 Jun;20(6):1187–95.

350. **Muenzer J**. - Overview of the mucopolysaccharidoses. Rheumatology (Oxford). 2011 Dec 1;50 Suppl 5(suppl_5):v4–12.

351. **Ashworth JL, Biswas S, Wraith E, Lloyd IC**. - Mucopolysaccharidoses and the Eye. Surv Ophthalmol. 2006;51(1):1–17.

352. **Alroy J, Haskins M, Birk DE**. - Altered corneal stromal matrix organization is associated with mucopolysaccharidosis I, III and VI. Exp Eye Res. 1999 May;68(5):523–30.

353. **Young RD, Liskova P, Pinali C, Palka BP, Palos M, Jirsova K, et al.** - Large proteoglycan complexes and disturbed collagen architecture in the corneal extracellular matrix of mucopolysaccharidosis type VII (Sly syndrome). Invest Ophthalmol Vis Sci. 2011 Aug;52(9):6720–8.

354. **Peters C, Shapiro EG, Anderson J, Henslee-Downey PJ, Klemperer MR, Cowan MJ, et al.** - Hurler syndrome: II. Outcome of HLA-genotypically identical sibling and HLA-haploidentical related donor bone marrow transplantation in fifty-four children. The Storage Disease Collaborative Study Group. Blood. 1998 Apr 1;91(7):2601–8.

355. **Vellodi A, Young E, Cooper A, Lidchi V, Winchester B, Wraith JE**. - Long-term follow-up following bone marrow transplantation for Hunter disease. J Inherit Metab Dis. 1999 Jun;22(5):638–48.

356. **Kakkis ED, Muenzer J, Tiller GE, Waber L, Belmont J, Passage M, et al.** - Enzyme-replacement therapy in mucopolysaccharidosis I. N Engl J Med. 2001 Jan 18;344(3):182–8.

357. **Gullingsrud EO, Krivit W, Summers CG**. - Ocular abnormalities in the mucopolysaccharidoses after bone marrow transplantation. Longer follow-up. Ophthalmology. 1998 Jun;105(6):1099–105.

358. **Ellinwood NM, Vite CH, Haskins ME**. - Gene therapy for lysosomal storage diseases: the lessons and promise of animal models. J Gene Med. 2004 May;6(5):481–506.

359. **Bielicki J, McIntyre C, Anson DS**. - Comparison of ventricular and intravenous lentiviral-mediated gene therapy for murine MPS VII. Mol Genet Metab. 2010 Dec;101(4):370–82.

360. **Sferra TJ, Backstrom K, Wang C, Rennard R, Miller M, Hu Y**. - Widespread correction of lysosomal storage following intrahepatic injection of a recombinant adeno-associated virus in the adult MPS VII mouse. Mol Ther. 2004 Sep;10(3):478–91.

361. **Liu G, Chen YH, He X, Martins I, Heth JA, Chiorini JA, et al.** - Adeno-associated virus type 5 reduces learning deficits and restores glutamate receptor subunit levels in MPS VII mice CNS. Mol Ther. 2007 Feb;15(2):242–7.

362. **Sleeper MM, Fornasari B, Ellinwood NM, Weil MA, Melniczek J, O'Malley TM, et al.** - Gene therapy ameliorates cardiovascular disease in dogs with mucopolysaccharidosis VII. Circulation. 2004 Aug 17;110(7):815–20.

363. **Hennig AK, Ogilvie JM, Ohlemiller KK, Timmers AM, Hauswirth WW, Sands MS**. - AAV-mediated intravitreal gene therapy reduces lysosomal storage in the retinal pigmented epithelium and improves retinal function in adult MPS VII mice. Mol Ther. 2004 Jul;10(1):106–16.

364. **Li T, Davidson BL**. - Phenotype correction in retinal pigment epithelium in murine mucopolysaccharidosis VII by adenovirus-mediated gene transfer. Proc Natl Acad Sci U S A. 1995 Aug 15;92(17):7700–4.

365. **Kamata Y, Okuyama T, Kosuga M, O'hira A, Kanaji A, Sasaki K, et al.** - Adenovirus-mediated gene therapy for corneal clouding in mice with mucopolysaccharidosis type VII. Mol Ther. 2001 Oct;4(4):307–12.

366. **Nesterova G, Gahl WA**. - Cystinosis: the evolution of a treatable disease. Pediatr Nephrol. 2013 Jan;28(1):51–9.

367. **Anikster Y, Lucero C, Guo J, Huizing M, Shotelersuk V, Bernardini I, et al.** - Ocular nonnephropathic cystinosis: clinical, biochemical, and molecular correlations. Pediatr Res. 2000 Jan;47(1):17–23.

368. **Cherqui S**. - Is genetic rescue of cystinosis an achievable treatment goal? Nephrol Dial Transplant. 2013 Jul 16;gft270–.

369. **Hippert C, Dubois G, Morin C, Disson O, Ibanes S, Jacquet C, et al.** - Gene transfer may be preventive but not curative for a lysosomal transport disorder. Mol Ther. The American Society of Gene Therapy; 2008 Aug 24;16(8):1372–81.

370. **Syres K, Harrison F, Tadlock M, Jester J V, Simpson J, Roy S, et al.** - Successful treatment of the murine model of cystinosis using bone marrow cell transplantation. Blood. 2009 Sep 17;114(12):2542–52.

371. **Harrison F, Yeagy BA, Rocca CJ, Kohn DB, Salomon DR, Cherqui S**. - Hematopoietic stem cell gene therapy for the multisystemic lysosomal storage disorder cystinosis. Mol Ther. 2013 Feb;21(2):433–44.

372. **Cavazzana-Calvo M, Hacein-Bey S, de Saint Basile G, Gross F, Yvon E, Nusbaum P, et al.** - Gene therapy of human severe combined immunodeficiency (SCID)-X1 disease. Science. 2000 Apr 28;288(5466):669–72.

373. **Nakatsukasa M, Kawasaki S, Yamasaki K, Fukuoka H, Matsuda A, Nishida K, et al.** - Two novel mutations of TACSTD2 found in three Japanese gelatinous drop-like corneal dystrophy families with their aberrant subcellular localization. Mol Vis. 2011 Jan;17:965–70.

374. **Kawasaki S, Kinoshita S**. - Clinical and basic aspects of gelatinous drop-like corneal dystrophy. Dev Ophthalmol. 2011 Jan;48:97–115.

375. **Movahedan H, Anvari-Ardekani HR, Nowroozzadeh MH**. - Limbal Stem Cell Transplantation for Gelatinous Drop-like Corneal Dystrophy. J Ophthalmic Vis Res. 2013 Apr;8(2):107–12.

376. **Shimazaki J, Shimmura S, Tsubota K**. - Limbal stem cell transplantation for the treatment of subepithelial amyloidosis of the cornea (gelatinous drop-like dystrophy). Cornea. 2002 Mar;21(2):177–80.

377. **O'Callaghan AR, Daniels JT**. - Concise review: limbal epithelial stem cell therapy: controversies and challenges. Stem Cells. 2011 Dec;29(12):1923–32.

378. **Shortt AJ, Secker GA, Notara MD, Limb GA, Khaw PT, Tuft SJ, et al.** - Transplantation of ex vivo cultured limbal epithelial stem cells: a review of techniques and clinical results. Surv Ophthalmol. 52(5):483–502.

379. **Irvine AD, Corden LD, Swensson O, Swensson B, Moore JE, Frazer DG, et al.** - Mutations in cornea-specific keratin K3 or K12 genes cause Meesmann's corneal dystrophy. Nat Genet. 1997 Jun;16(2):184–7.

380. **Kao WW, Liu CY, Converse RL, Shiraishi A, Kao CW, Ishizaki M, et al.** - Keratin 12-deficient mice have fragile corneal epithelia. Invest Ophthalmol Vis Sci. 1996 Dec;37(13):2572–84.

381. **Liao H, Irvine AD, Macewen CJ, Weed KH, Porter L, Corden LD, et al.** - Development of allele-specific therapeutic siRNA in Meesmann epithelial corneal dystrophy. PLoS One. 2011 Jan;6(12):e28582.

382. **Tiscornia G, Singer O, Ikawa M, Verma IM**. - A general method for gene knockdown in mice by using lentiviral vectors expressing small interfering RNA. Proc Natl Acad Sci U S A. 2003 Mar 18;100(4):1844–8.

383. **Means TL**. - Viability of Human Corneal Endothelium Following Optisol-GS Storage. Arch Ophthalmol. American Medical Association; 1995 Jun 1;113(6):805.

384. **Pascolini D, Mariotti SP**. - Global estimates of visual impairment: 2010. Br J Ophthalmol. 2012 May 1;96(5):614–8.

385. **Balaggan KS, Binley K, Esapa M, MacLaren RE, Iqball S, Duran Y, et al.** - EIAV vector-mediated delivery of endostatin or angiostatin inhibits angiogenesis and vascular hyperpermeability in experimental CNV. Gene Ther. 2006 Aug;13(15):1153–65.

386. **Igarashi T, Miyake K, Masuda I, Takahashi H, Shimada T**. - Adeno-associated vector (type 8)-mediated expression of soluble Flt-1 efficiently inhibits neovascularization in a murine choroidal neovascularization model. Hum Gene Ther. 2010 May;21(5):631–7.

387. **Rakoczy E**. - Safety and Efficacy Study of rAAV.sFlt-1 in Patients With Exudative Age-Related Macular Degeneration (AMD) [Internet]. clinicaltrials.gov. 2012.

388. **Lai C-M, Estcourt MJ, Himbeck RP, Lee S-Y, Yew-San Yeo I, Luu C, et al.** - Preclinical safety evaluation of subretinal AAV2.sFlt-1 in non-human primates. Gene Ther. 2012 Oct;19(10):999–1009.

389. **Haurigot V, Villacampa P, Ribera A, Bosch A, Ramos D, Ruberte J, et al.** - Long-term retinal PEDF overexpression prevents neovascularization in a murine adult model of retinopathy. PLoS One. 2012 Jan;7(7):e41511.

390. **Ramírez M, Wu Z, Moreno-Carranza B, Jeziorski MC, Arnold E, Díaz-Lezama N, et al.** - Vasoinhibin gene transfer by adenoassociated virus type 2 protects against VEGF- and diabetes-induced retinal vasopermeability. Invest Ophthalmol Vis Sci. 2011 Nov;52(12):8944–50.

391. **Pechan P, Rubin H, Lukason M, Ardinger J, DuFresne E, Hauswirth WW, et al.** - Novel anti-VEGF chimeric molecules delivered by AAV vectors for inhibition of retinal neovascularization. Gene Ther. 2009 Jan;16(1):10–6.

392. **El Sanharawi M, Touchard E, Benard R, Bigey P, Escriou V, Mehanna C, et al.** - Long-term efficacy of ciliary muscle gene transfer of three sFlt-1 variants in a rat model of laser-induced choroidal neovascularization. Gene Ther. 2013 Nov;20(11):1093–103.

393. **Tian L, Yang P, Lei B, Shao J, Wang C, Xiang Q, et al.** - AAV2-mediated subretinal gene transfer of hIFN-α attenuates experimental autoimmune uveoretinitis in mice. PLoS One. 2011 Jan;6(5):e19542.

394. **Tsai M-L, Horng C-T, Chen S-L, Xiao X, Wang C-H, Tsao Y-P**. - Suppression of experimental uveitis by a recombinant adeno-associated virus vector encoding interleukin-1 receptor antagonist. Molecular Vision; 2009 Aug 8;

395. **Broderick CA, Smith AJ, Balaggan KS, Georgiadis A, Georgarias A, Buch PK, et al.** - Local administration of an adeno-associated viral vector expressing IL-10 reduces monocyte infiltration and subsequent photoreceptor damage during experimental autoimmune uveitis. Mol Ther. 2005 Aug;12(2):369–73.

396. **Chu CJ, Barker SE, Dick AD, Ali RR**. - Gene therapy for noninfectious uveitis. Ocul Immunol Inflamm. Informa Healthcare New York; 2012 Dec 7;20(6):394–405.

397. **Li Q, Miller R, Han P-Y, Pang J, Dinculescu A, Chiodo V, et al.** - Intraocular route of AAV2 vector administration defines humoral immune response and therapeutic potential. Mol Vis. 2008 Jan;14:1760–9.

398. **Yin J-Q, Liu W-Q, Liu C, Zhang Y-H, Hua J-L, Liu W-S, et al.** - Reconstruction of damaged corneal epithelium using Venus-labeled limbal epithelial stem cells and tracking of surviving donor cells. Exp Eye Res. 2013;115:246–54.

399. **Wang J, Zhang K, Grabowska D, Li A, Dong Y, Day R, et al.** - Loss of Trop2 promotes carcinogenesis and features of epithelial to mesenchymal transition in squamous cell carcinoma. Mol Cancer Res. 2011 Dec;9(12):1686–95.

400. **Yang J, Zhu Z, Wang H, Li F, Du X, Ma RZ**. - Trop2 regulates the proliferation and differentiation of murine compact-bone derived MSCs. Int J Oncol. 2013 Sep;43(3):859–67.

Abbreviations

AAV	Adeno-associated virus
ABCG2	ATP-binding cassette, sub-family G, member 2
AMD	Age-related macular degeneration
AP	Anterior / posterior
ARVO	Association for research in vision and ophthalmology
ATP	Adenosine triphosphate
BM	Basement membrane
BMP	Bone morphogenetic protein
BMT	Bone marrow transplant
BrdU	Bromodeoxyuridine
BSA	Bovine serum albumin
CD4	Cluster of differentiation 4
CMV	Cytomegalovirus (Usually refers to promoter)
CNS	Central nervous system
CNV	Choroidal neovascularisation
cPPT	Central polypurine tract
CTNS	Cystinosin
DAPI	4',6-diamidino-2-phenylindole
dH_2O	Distilled water
DMEK	Descemet's membrane endothelial keratoplasty
DMEM	Dulbecco's modified eagle's medium
DNA	Deoxyribonucleic acid
dNTP	Deoxyribonucleotide triphosphate
dPBS	Dulbecco's phosphate buffered saline
ds	Double stranded (prefix)
DSEK	Descemet's stripping endothelial keratoplasty
E2F2	E2 factor, transcription factor 2
ECM	Extra cellular matrix
EDTA	Ethylenediaminetetraacetic acid
EdU	5-ethynyl-2´-deoxyuridin
eGFP	Enhanced green fluorescent protein
EGFR-PTK	Epidermal growth factor receptor - protein tyrosine kinase
ELISA	Enzyme-linked immunosorbent assay
ERG	Electroretinography
eTAC	Early transient amplifying cell
FCS	Foetal calf serum
FKBP52	Tacrolimus (FK-506) binding protein 4
FPLC	Fast protein liquid chromatography
GDLD	Gelatinous drop-like
GDNF	Glial cell line-derived neurotrophic factor
GFAP	Glial fibrillary acidic protein
GIMP	GNU image manipulation program
GLUT1	Glucose transporter 1
HEK293T	Human embryonic kidney 239T (cell line)
HIV1	Human immunodeficiency virus type 1
HRA2	Heidelberg retina angiograph II
HRP	Horseradish peroxidase
HSCs	Hematopoietic stem cells
HSV	Herpes simplex virus
I.D.	Internal diameter

IL	Interleukin (usually suffixed with a number)
ILM	Inner limiting membrane
IMS	Industrial methylated spirit
IRES	Internal ribosome entry site
ITR	Inverted terminal repeat
KO	Knockout (genetically modified mouse model)
K-SFM	Keratinocyte serum free medium
LAM-PCR	Linear amplification–mediated polymerase chain reaction
LB	Lysogeny broth
LCA	Leber's congenital amaurosis
LEF	Late endothelial failure
LeGO	Lenti Go
LESC	Limbal epithelial stem cell
LMO2	LIM domain only 2
LNT	Lenti (abbreviation used only for genomic backbone plasmids)
LPS	Lipopolysaccharide
LTR	Long terminal repeat
Luc2	Firefly luciferase (Promega terminology)
LYVE1	Lymphatic vessel endothelial hyaluronan receptor 1
MECD	Meesmann's epithelial corneal dystrophy
miRNA	Micro ribonucleic acid
MLV	Murine leukaemia virus
MOI	Multiplicity of infection
MPS	Mucopolysaccharidosis
mu	Murine / mouse (prefix)
MW	Molecular weight
NFκB	Nuclear factor kappa-light-chain-enhancer of activated B cells
NGF	Nerve growth factor
NIH	National institutes of health
N.S.	Not significant
NTC	No target control
O.D.	Outer diameter
OTC	Ornithine transcarbamoylase
PBS	Phosphate buffered saline
PBS-MK	Phosphate buffered saline (+1 mM $MgCl_2$ & 2.5 mM KCl)
PCR	Polymerase chain reaction
PEI	Poly(ethylenimine)
PFA	Paraformaldehyde
PIGF	Placental growth factor
PTK	Phototherapeutic keratectomy
qPCR	Quantitative polymerase chain reaction
rAAV	Recombinant adeno-associated virus
RGB	Red / green / blue
RISC	RNA-induced silencing complex
RNA	Ribonucleic acid
RNAi	Ribonucleic acid interference
ROCK	Rho-kinase
ROI	Region of interest
RP	Retinitis pigmentosa
RPE	Retinal pigment epithelium
RRE	Rev response element
rt	Room temperature
scAAV	Self-complimentary adeno-associated virus
SCID	Severe combined immunodeficiency
SEM	Scanning electron microscopy

SFFV	Spleen focus-forming virus (Usually refers to promoter)
sFlt1	Soluble fms-like tyrosine kinase-1
shRNA	Short hairpin ribonucleic acid
SIN	Self-inactivating (lentivirus modification)
siRNA	Short interfering ribonucleic acid
SLO	Scanning laser ophthalmoscope
SLO-FA	Scanning laser ophthalmoscope, fluorescein angiography
SOC	Super optimal broth with catabolic repressor
ss	Single stranded (prefix)
sVEGFR	Soluble vascular endothelial growth factor receptor
TAC	Transient amplifying cell
TACSTD2	Tumour-associated calcium signal transducer 2
TBE	Tris borate EDTA
TBS	Tris buffered saline
TGF	Transforming growth factor
TMB	3,3',5,5'-Tetramethylbenzidine
TNF	Tumour necrosis factor
TRITC	Tetramethylrhodamine
tRNAlys	Transfer ribonucleic acid for lysine
TUNEL	Terminal deoxynucleotidyl transferase dUTP nick end labelling
VEGF	Vascular endothelial growth factor
VEGFR	Vascular endothelial growth factor receptor
vg	Virus / vector genome
VP1,2 or 3	Viral protein 1, 2 or 3 (AAV capsid proteins)
VSV-G	Vesicular stomatitis virus glycoprotein
WPRE	Woodchuck Hepatitis Virus Posttranscriptional Regulatory Element
ZO-1	Zona occludens protein 1

9. Appendices

9.1 Appendix 1 – Plasmid maps

LNT-SFFV-MCS – Default 2nd generation genomic backbone for the production of Lentiviral vectors. Poly cloning site positioned behind the SFFV promoter, and before the WPRE. Used in 3.2.1 as base for modification to produce both LNT-SFFV-Luc2 and LNT-*d*PBS-Luc2

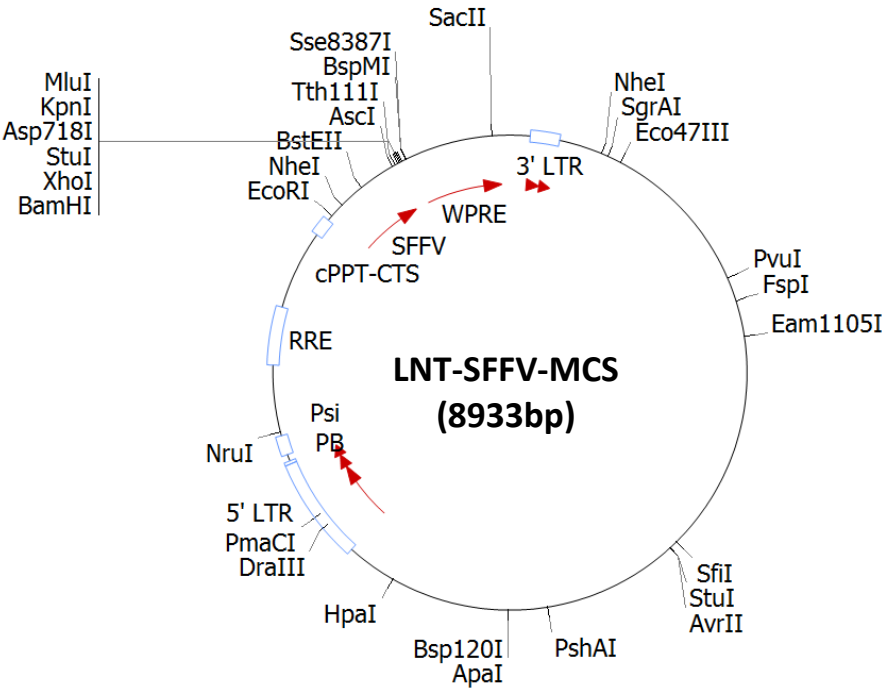

pGL4-10 – Luciferase (Luc2) expression plasmid from Promega. Used as source of Luc2 gene for cloning to produce LNT-SFFV-Luc2 and LNT-*d*PBS-Luc2 in 3.2.1

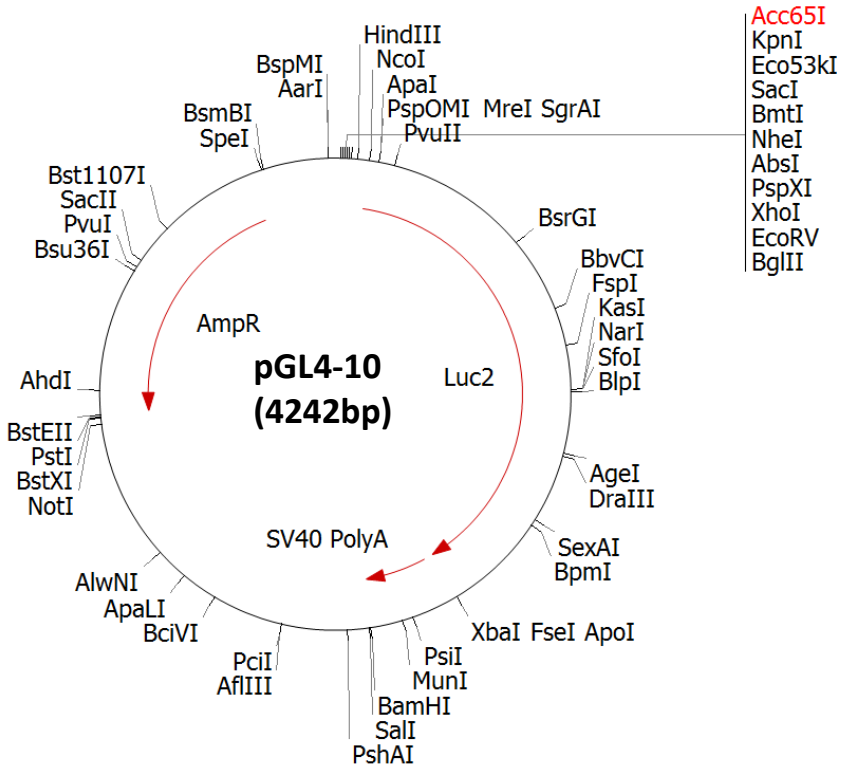

LNT-SFFV-Luc2 – Lentiviral genomic construct for luciferase expression from the SFFV promoter. Generated in 3.2.1

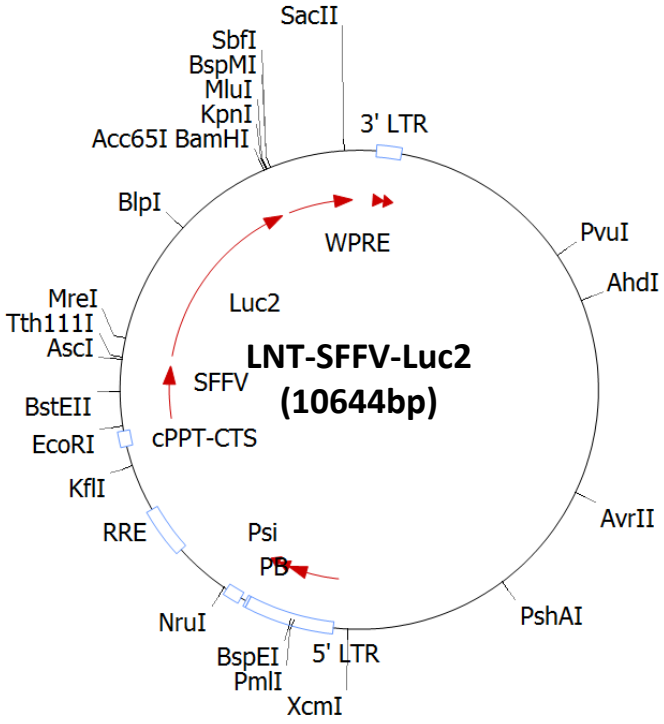

LNT-*d*PBS-Luc2 – Lentiviral genomic construct modified to be unable to undergo reverse transcription by deletion of the primer binding site and other genomic modifications, Luciferase transgene, Generated in 3.2.1

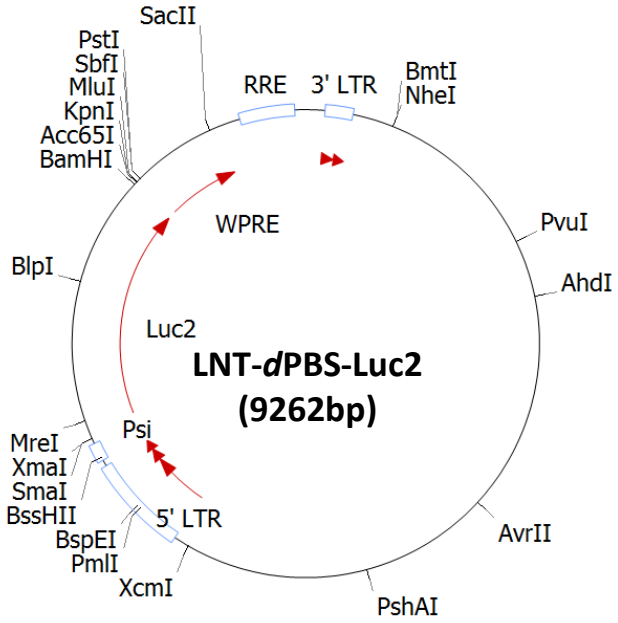

pd10-pst2.2 – AAV genomic construct based on AAV2/2 ITRs, eGFP transgene under the control of CMV promoter. Used to generate all AAV vectors suffixed with: -CMV-eGFP

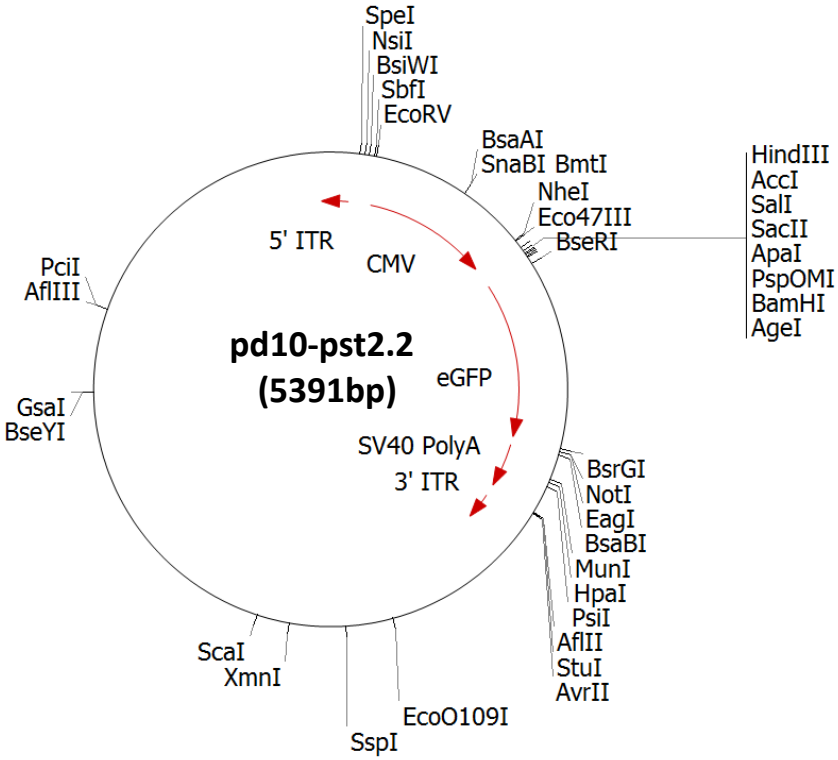

pd10-CMV-IL10-IRES-eGFP – AAV genomic construct based on AAV2/2 ITRs, murine IL10 transgene under the control of CMV promoter. Also contains internal ribosome entry site sequence (IRES) driving eGFP expression. Used in Chapter 4.

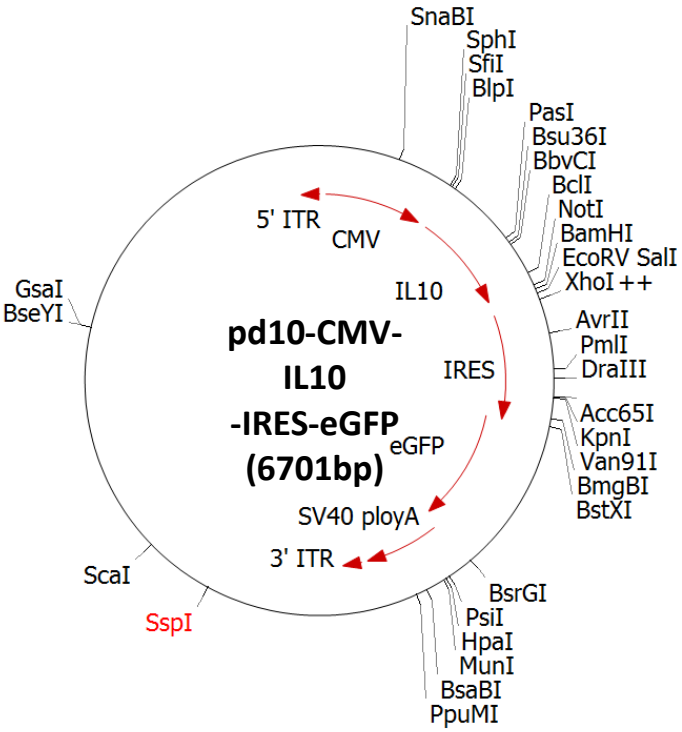

pd10-CMV-musFlt1 – AAV genomic construct based on AAV2/2 ITRs, murine sFlt1 transgene under the control of CMV promoter. Used to generate all AAV vectors suffixed with: -CMV-musFlt1. Used in Chapter 5.

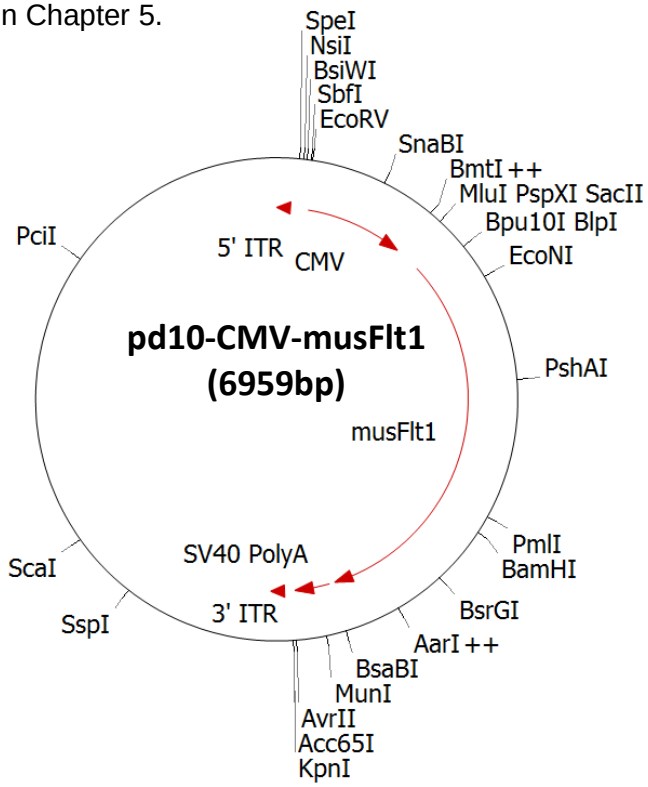

pd10-NULL – AAV genomic construct based on AAV2/2 ITRs, No promoter, contains truncated version of RPGR gene with no start codon. Used to generate all AAV vectors suffixed with: -NULL. Used in Chapter 5.

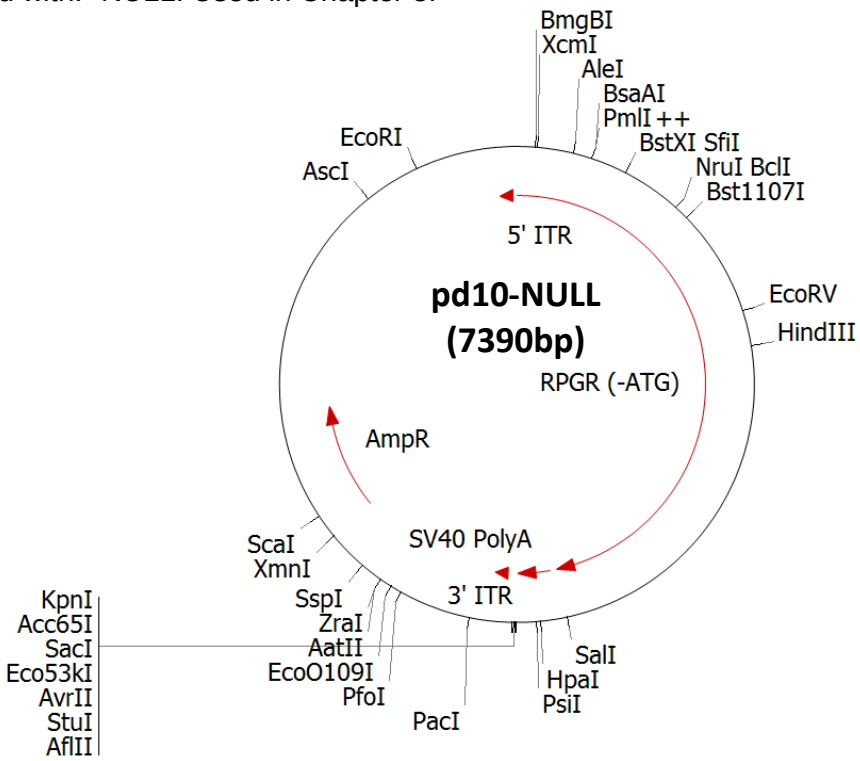

9.2 Appendix 2 – Full SLO data of all 3 limbal-intraepithelially injected cohorts to 52 weeks

9.2.1 Cohort 1, Cage 1

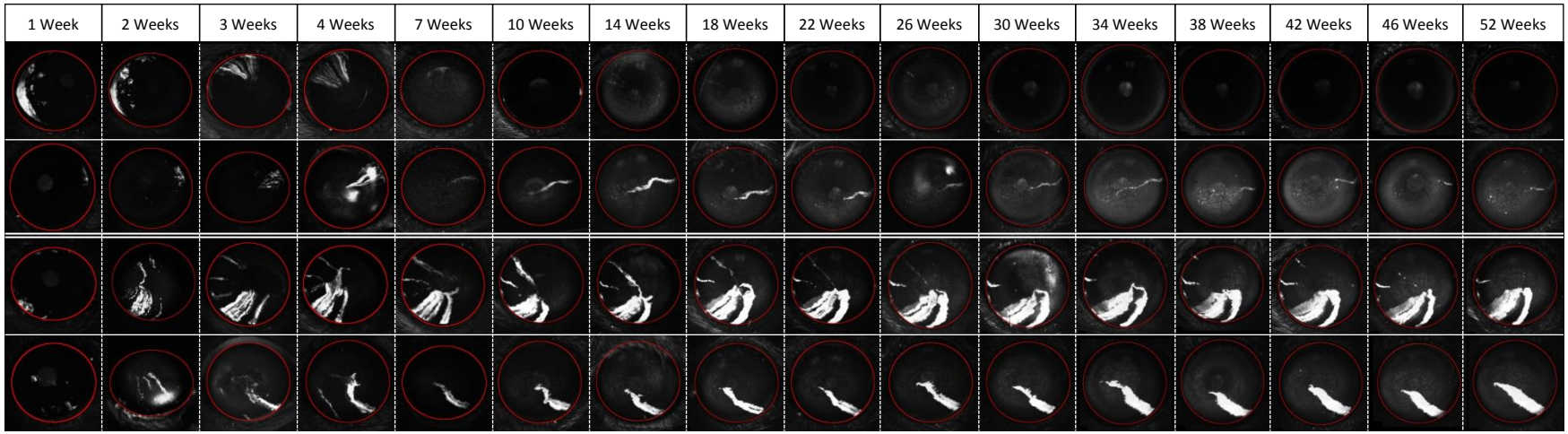

Appendix 2 Key

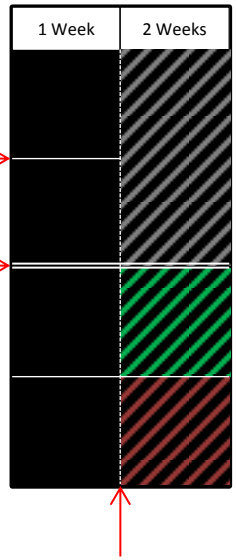

Solid line separates eyes within the same animal

Double line separates animals

Dotted line separates time points

Grey Hash indicates animal was culled for reasons of stock control, no visible expression, or histological analysis.

Green Hash indicates complications leading to eye not imaged at this time point. Animal remains alive.

Red Hash indicates animal died during or shortly after procedure.

9.2.2 Cohort 1, Cage 3

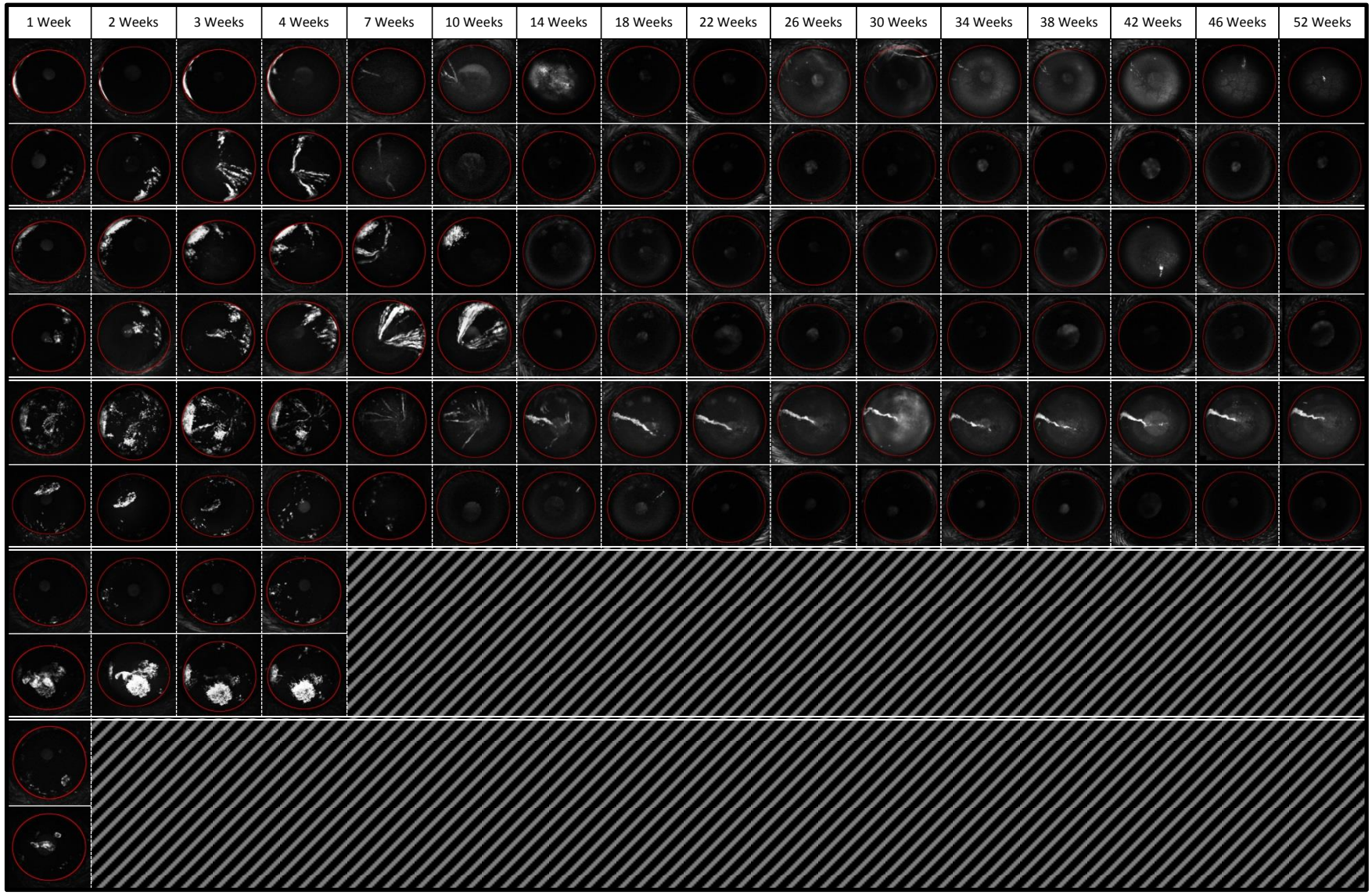

9.2.3 Cohort 2, Cage 1

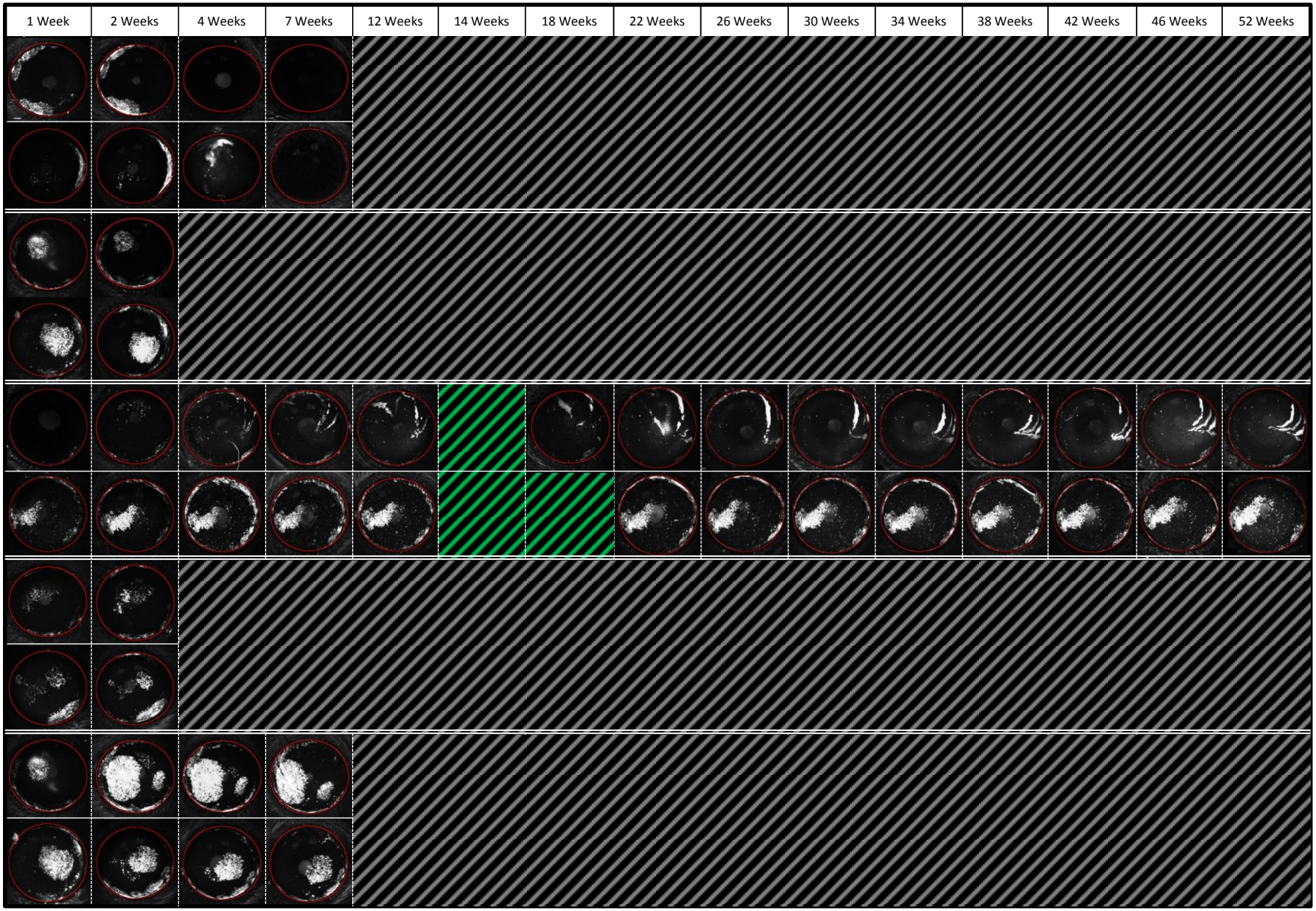

9.2.4 Cohort 2, Cage 2

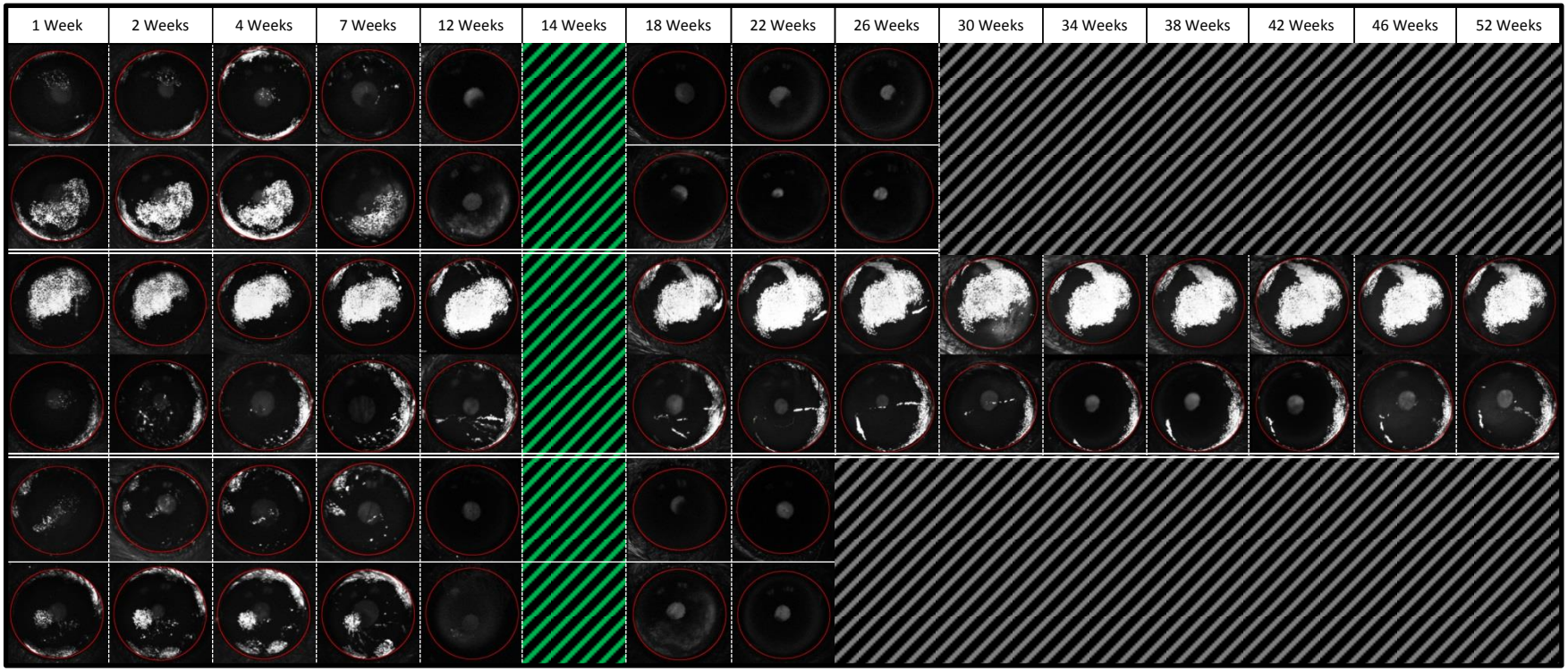

9.2.5 Cohort 2, Cage 3

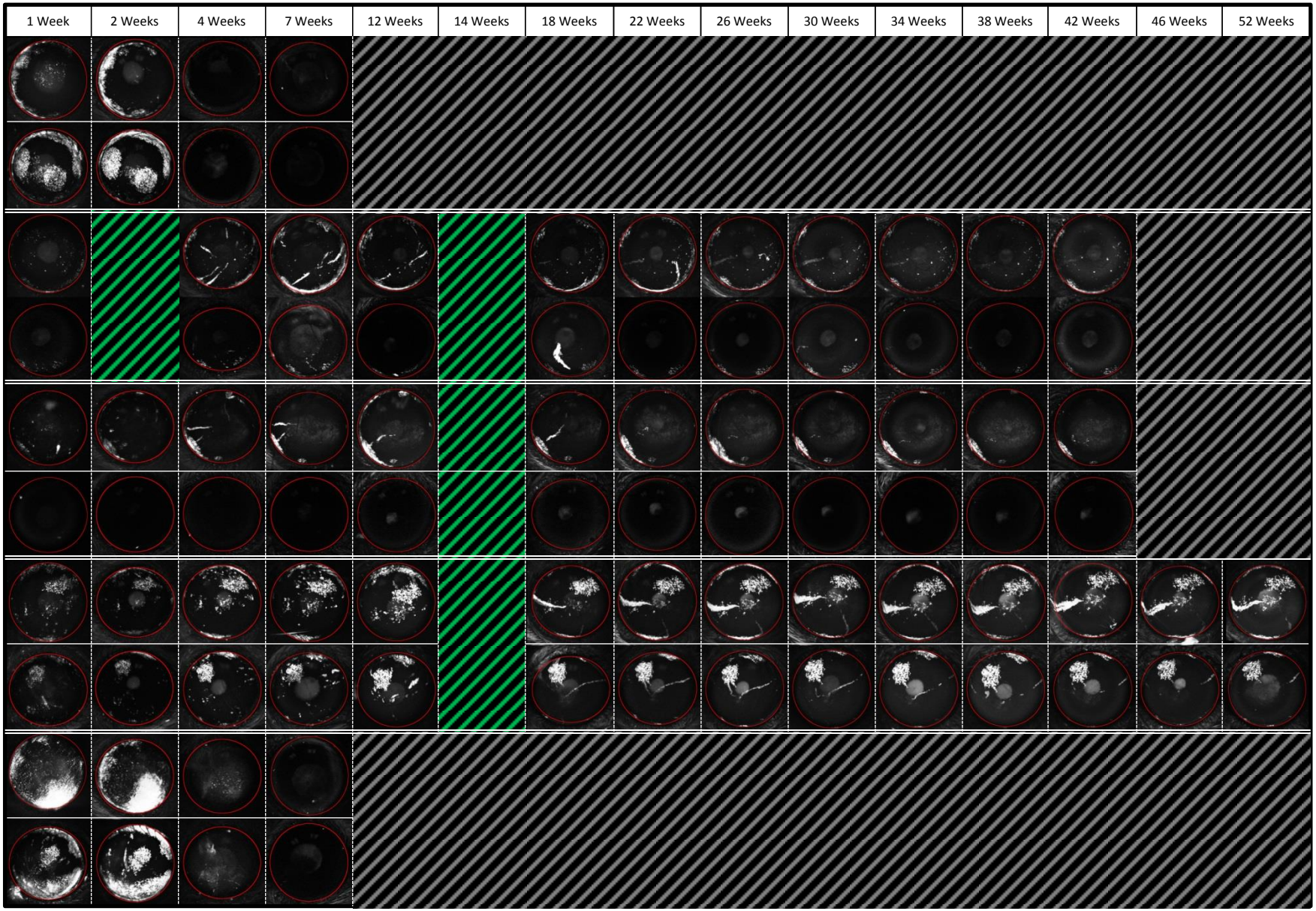

9.2.6 Cohort 2, Cage 4

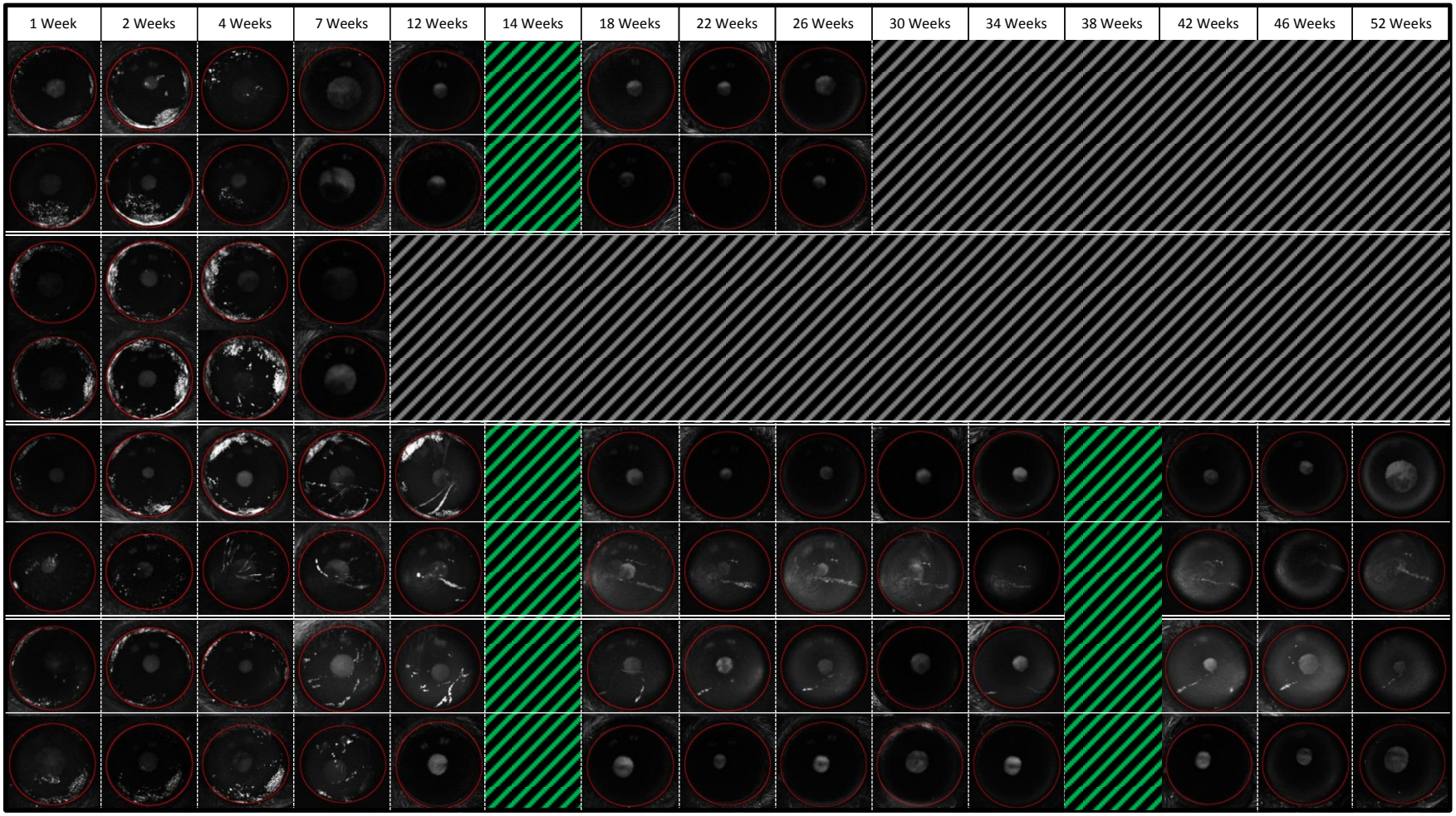

9.2.7 Cohort 2, Cage 5

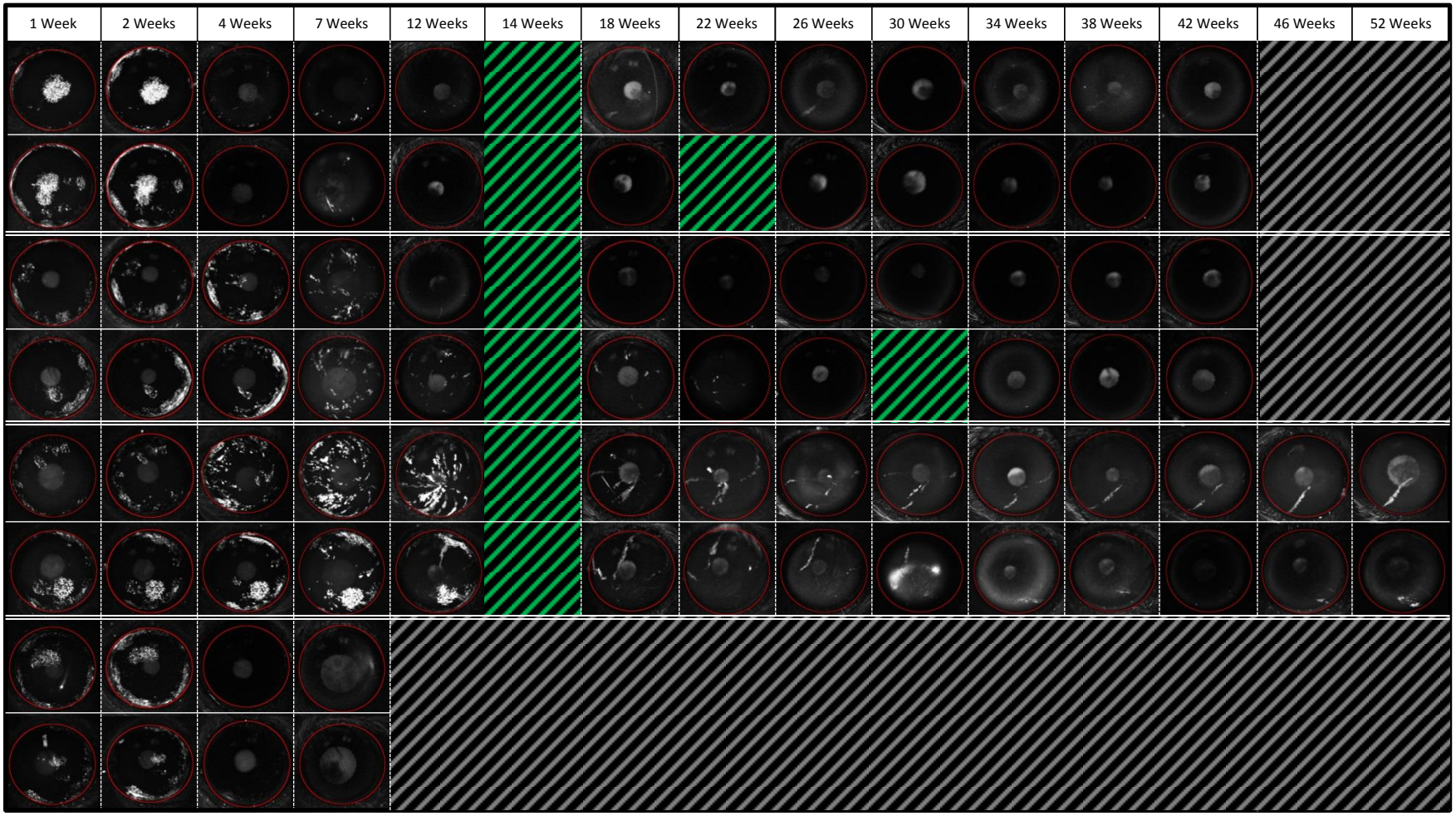

9.2.8 Cohort 3, Cage 1

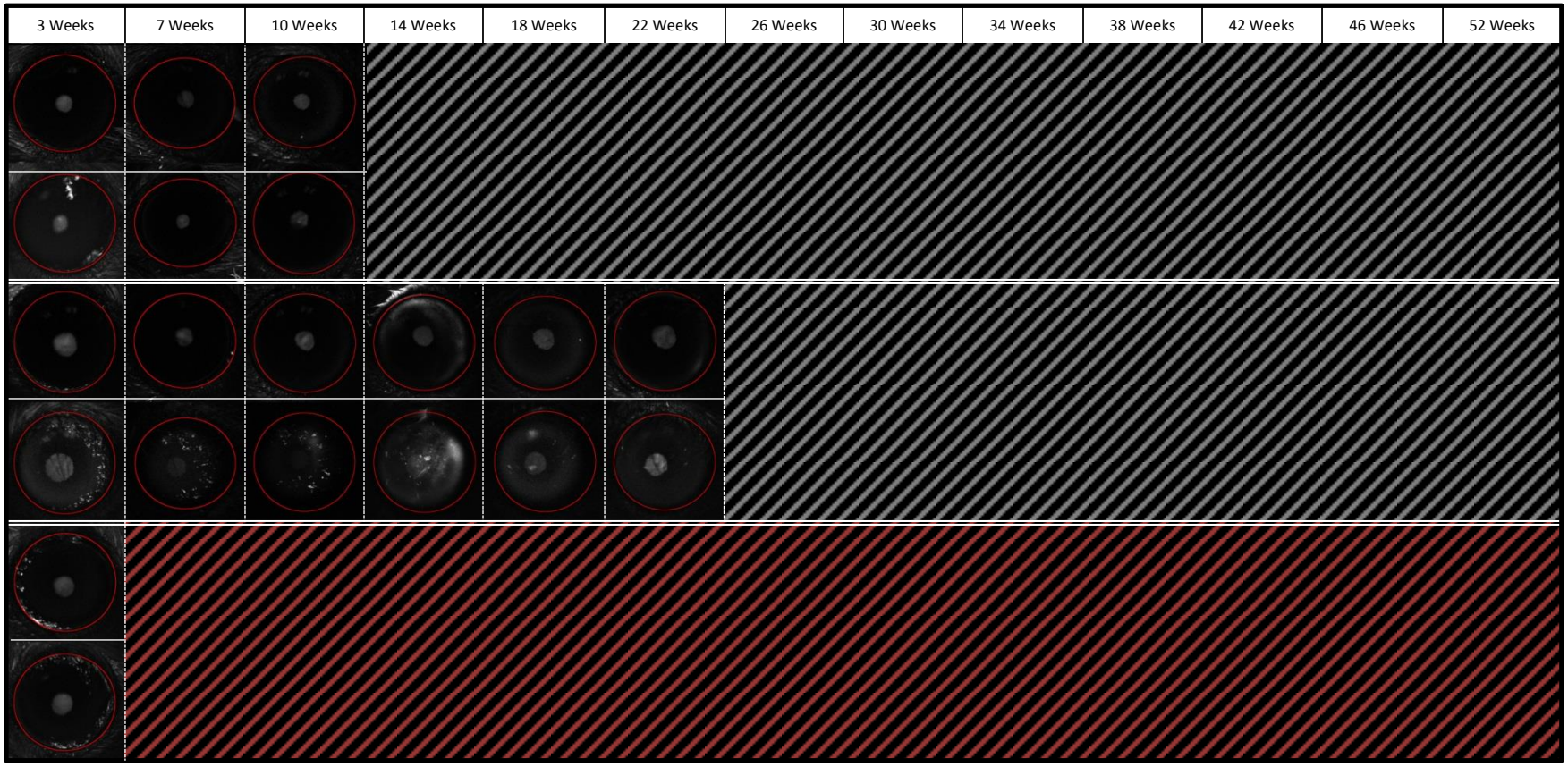

9.2.9 Cohort 3, Cage 2

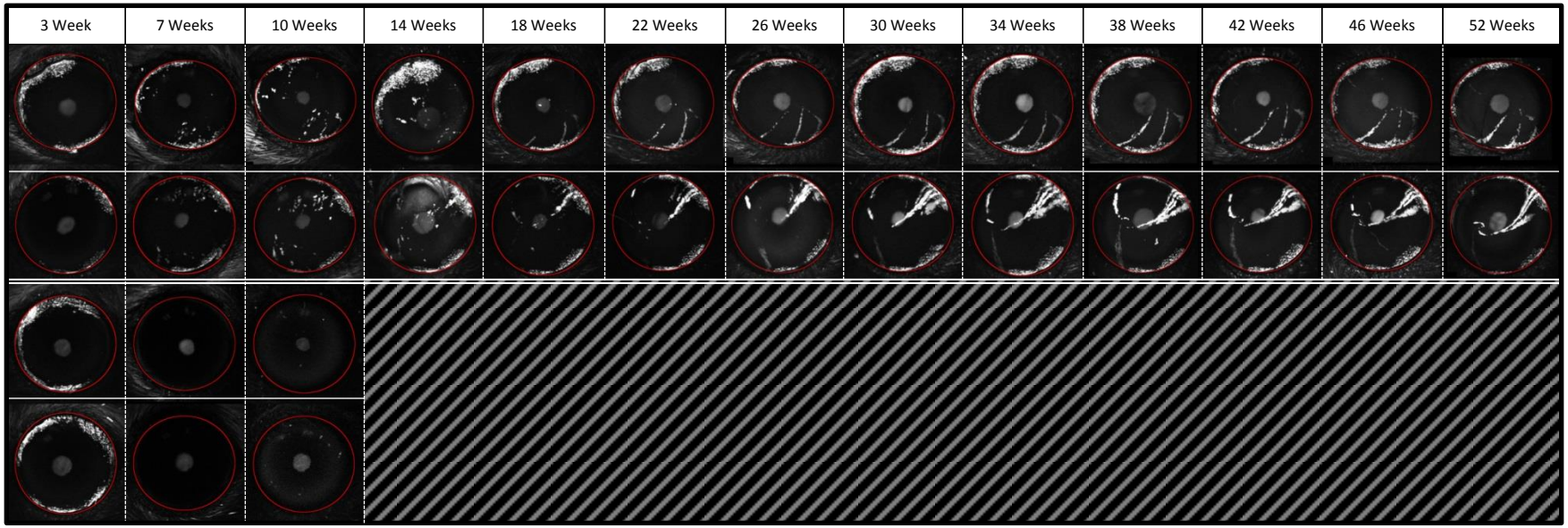

9.2.10 Cohort 3, Cage 3

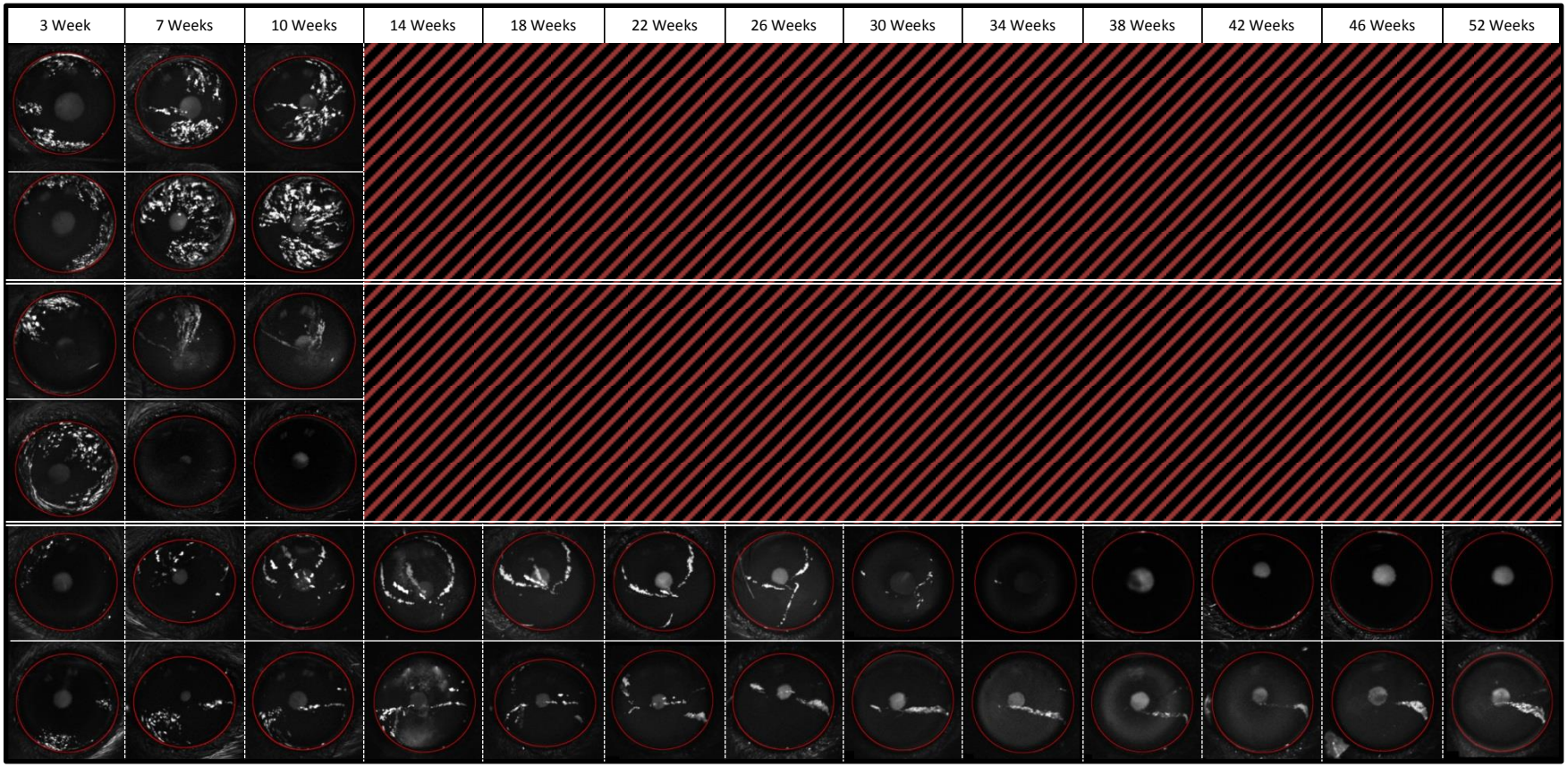

9.2.11 Cohort 3, Cage 4

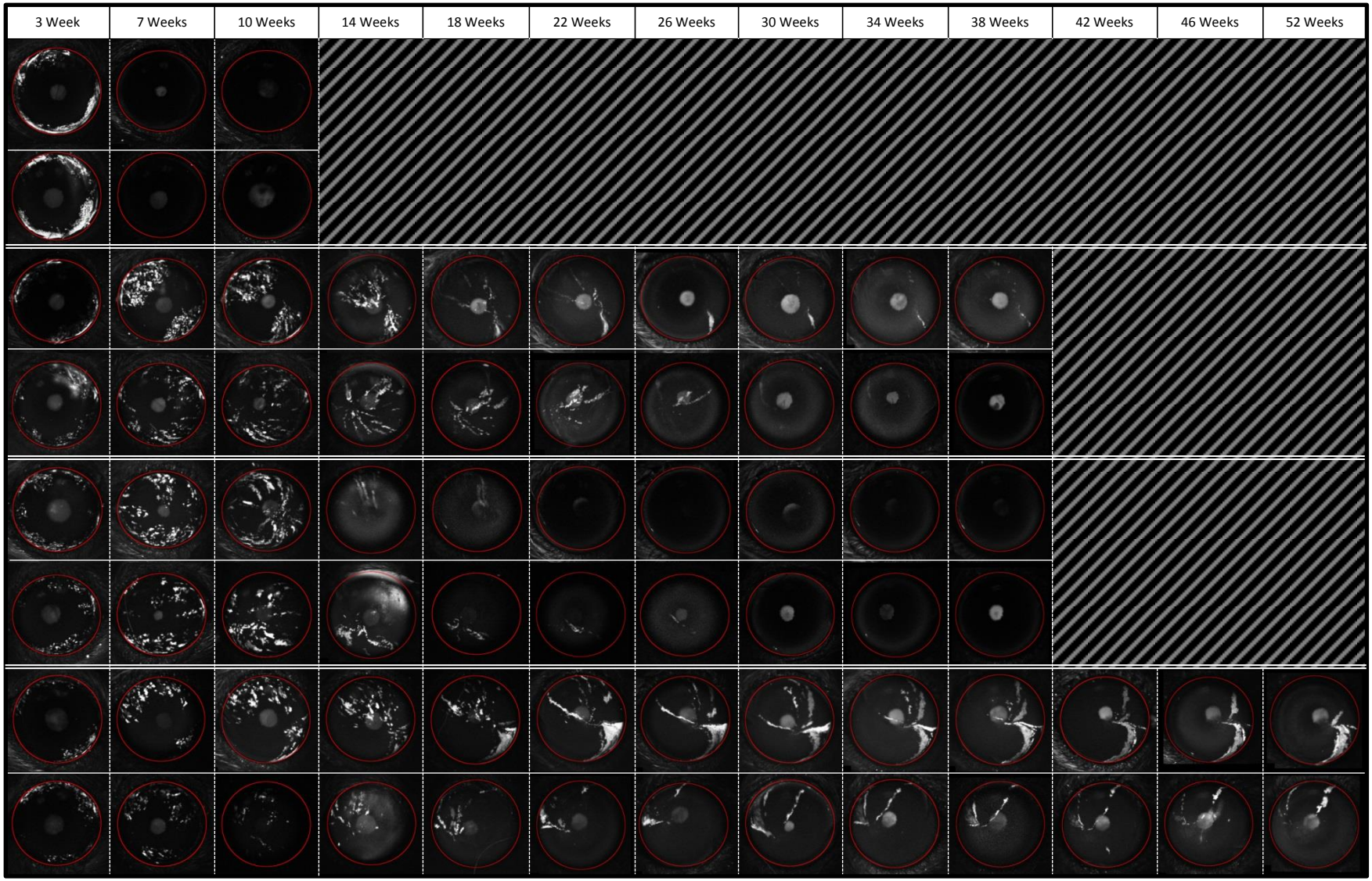

9.2.12 Cohort 3, Cage 5

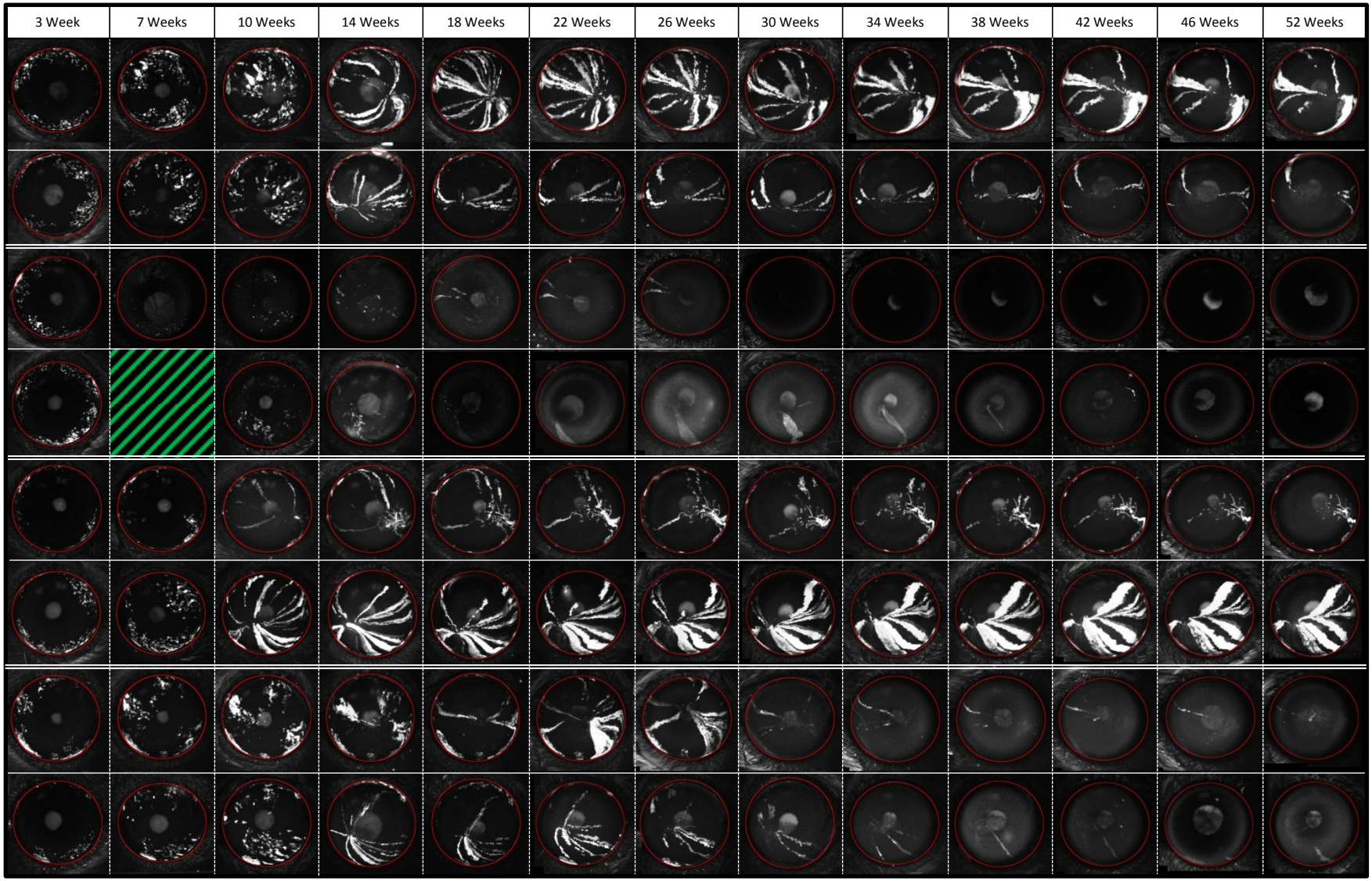

9.2.13 Cohort 3, Cage 6